Design, Synthesis and Evaluation of Pyrrolo[2,1-c][1,4]benzodiazepines (PBDs) Pyrrole/Imidazole polyamide conjugates

Arnaud Tiberghien

A Thesis Submitted in Partial Fulfilment of the Requirements for the Degree of Doctor of Philosophy

School of Pharmacy
University of London

2007

Supervisors: Dr P. W. Howard
And Prof. D. E. Thurston

ProQuest Number: 10104194

ProQuest 10104194

ABSTRACT

The aim of the project presented in this thesis, was to design and synthesise DNA binding agents with superior sequence selectivity. Ultimately, the challenge was to be able to make compounds with the potential to bind specifically to predetermined DNA sequences. Molecules with such properties could be used to knock-out oncogenes with minimal damage to healthy DNA.

Pyrrole/imidazole polyamides are extensively studied small oligomers which bind non-covalently to DNA with high selectivity. Pyrrolo[2,1-c][1,4]benzodiazepines (PBDs) are naturally occurring antitumour antibiotics which bind preferentially to AGA DNA sequences through an aminal bond. There is currently great interest in studying the beneficial interactions that can be gained from tethering the two types of molecules together. To this end, new PBD capping units were designed and synthesised. Crucially, base driven racemisation problems at C11a were resolved by protecting the C11-hydroxy position. The pyrrole and imidazole building block syntheses were successfully optimised. Seven PBD dimers, featuring pyrrole/imidazole polyamides in their core were synthesised, as well as eleven PBD pyrrole/imidazole "hairpin" conjugates.

The majority of conjugates were more active than either of their constituent moieties in the National Cancer Institute 60 cell lines *in vitro* cytotoxicity assay. The dimers were found to crosslink DNA efficiently in the whole cell "comet" assay. The selectivity of the compounds was evaluated by DNase I footprinting assay. Clear footprints were observed at discrete locations in Bcl-2 and AR fragments, although not always in a predictable fashion.

CONTENTS

3. Sequence Selective Minor Groove DNA Binders: Strategic Overview

ACKNOWLEDGMENTS

ABBREVIATIONS

AcOH   — Acetic acid

Ac$_2$O   — Acetic anhydride

All   — Allyl

Alloc   — Allyloxycarbonyl

AR   — Androgen receptor

BAIB   — Iodobenzene Diacetate

Bn   — Benzyl

BOC   — tert-butyloxycarbonyl

BOC$_2$O   — di-*tert*-butyl dicarbonate

CBI   — 1,2,9,9*a*-tetrahydrocyclopropa[c]benz[e]indol-4-one

CBz   — Benzyloxycarbonyl

CPI   — cyclopropylpyrroloindole

CR-UK   — Cancer Research UK

CT-DNA   — Calf Thymus DNA

DBU   — 1,8-Diazobicyclo[5.4.0]undec-7-ene

DCC   — Dicyclohexyl Carbodiimide

DCM   — Dichloromethane

DEAD   — Diethyl Azodicarboxylate

DHP   — Dihydropyran

DIAD   — Diisopropyl Azodicarboxylate

DIPEA   — Diisopropylethylamine

DMAP   — 4-Dimethylaminopyridine

DMF   — *N,N*-Dimethylformamide

DMSO   — Dimethylsulfoxide

DNA   — Deoxyribonucleic Acid

Dst   — Dystamycin

ES   — Electrospray

EDCI   — 1-Ethyl-3-(3-Dimethyl-Aminopropyl) Carbodiimide

FAB	—	Fast Atom Bombardment
Fmoc	—	9-Fluorenylmethyloxycarbonyl
GDP	—	Guanosine Diphosphate
GTP	—	Guanosine Triphosphate
HOBt	—	1-Hydroxybenzotriazole Hydrate
HPLC	—	High Performance Liquid Chromatography
HRMS	—	High Resolution Mass Spectrometry
IR	—	Infrared
KOtBu	—	Potassium *tert*-butoxide
LDA	—	Lithium Diisopropylamide
LiHMDS	—	Lithium Bis(trimethylsilyl)amide
MeOH	—	Methanol
MEM	—	Methoxyethoxymethyl
MOM	—	Methoxymethyl
MS	—	Mass Spectrometry/Molecular Sieves
MTT	—	3-(4,5-Dimethylthiazolyl)-2,5-diphenyltetrazolium Bromide
NCI	—	National Cancer Institute
Net	—	Netropsin
NMO	—	*N*-Methylmorpholine *N*-Oxide
NMR	—	Nuclear Magnetic Resonance
PBD	—	Pyrrolobenzodiazepine
PDC	—	Pyridinium Dichromate
PTSA	—	*para*-Toluenesulfonic acid
Py	—	Pyridine
pH	—	Potential of Hydrogen
pKa	—	Negative Logarithm of the Acid Ionization Constant (K_a)
Q-PCR	—	Quantitative Polymerase Chain Reaction
RCM	—	Ring Closing Metathesis
RNA	—	Ribonucleic acid
SEM	—	Trimethylsilylethoxymethyl
TBAF	—	Tetrabutylammonium Fluoride
TBDMS	—	*tert*-Butyl-dimethylsilyl

TBS	— *tert*-Butyl-dimethylsilyl
TEA	— Triethylamine
TEMPO	— 2,2,6,6-Tetramethyl-1-piperidinyloxy (free radical)
Teoc	— Trimethylsilylethoxycarbonyl
TFA	— Trifluoroacetic Acid
TFO	— Triple helix forming oligonucleotides
THF	— Tetrahydrofuran
THP	— Tetrahydropyran
TIPS	— Tri-isopropylsilyl
TPAP	— Tetra-n-propylammonium Perruthenate
TPP	— Triphenylphosphine
Troc	— 2,2,2-Trichloroethoxycarbonyl
UCL	— University College London

Foreword

This thesis presents efforts made to selectively target cancer through the genetic aberrations that give rise to the disease.

Since the beginning of cancer therapy, clinicians have been using various types of "mass destruction" to try and kill the cancer. It involves surgery with a straightforward tumour extraction, which works well as long as the cancer does not spread as metastasis. In that latter case, very potent and toxic methods are used, such as high-energy rays or cytotoxic chemical agents. Their toxicity and poor differentiation between normal and cancerous cells limits their dosages and often prevent a successful cure. An analogy can be drawn with the development of aerial bombing campaigns in the Second World War when targeting specific installations was eschewed in favour of indiscriminate area bombing. In more recent wars "smart bombs" have been employed to hit selected targets, thus limiting the extent of collateral damage to civilian areas.

The key question is: how can we kill or disable the cancerous cells with no toxicity to the normal cells?

As described in the first chapter of this thesis, cancer is an extremely complex disease, with an accumulation of causes. They have essentially genetic origins and therefore, it makes sense to try and treat it at a genetic level.

The latter chapters describe efforts to conceive and synthesise DNA binding agents hybrids of performing and recent molecules: The PBDs (Pyrrolo[2,1-c][1,4]benzodiazepines), and pyrrole/imidazole polyamides. The goal is to combine their strengths to allow specific recognition of targeted oncogenes.

1. Cancer is a genetic disease

1.1 Introduction

This section will focus on the genetic origins of cancer rather than the epidemiological and statistical data. However, cancer is the second biggest killer in the UK, and one out of three people is expected to develop the disease.

1.2 General Considerations

Cancer differs from other diseases caused by infectious agents such as viruses and bacteria because it arises from the body's own cells.

It may naively be thought that a single mutation event in a single cell can cause cancer; in reality cancer is a very difficult disease to trigger in humans. Millions of mutations occur every day in cells but fortunately the vast majority of those mutations do not promote a tumour phenotype. Complex organisms have evolved a number of mechanisms, which detect and correct DNA damage.

This is not to deny that cancer occurs very frequently in the population, but to make the point that it is a statistically very rare event compared to the huge number of mutations that occur in cells each day.

In fact, the genome is so well defended that it can take up to seven cumulative steps to progress from a normal cell to an invasive metastatic tumour (Hanahan and Weinberg, 2000). It therefore takes a considerable time to accumulate sufficient mutations to affect all seven critical functions, and cancer is most prevalent in people over sixty.

The seven steps are:

- Mutations in the growth control system (for example a mutant RAS protein continually switched on, sending signals ordering growth and division).

- In addition, cancer cells must become insensitive to anti-growth signals.
- Mutations in DNA repair systems, especially the tumour suppressor genes such as P53 (dubbed the genome guardian).
- A reactivation of the telomerase enzyme. Normally, the non-coding ends of the chromosomes, the telomeres, shorten during each division. Eventually, for example after 20 divisions, the telomeres are too short, the cell cannot replicate, and enters senescence. Cancer cells inappropriately express the telomerase enzyme, which can replace the telomeres indefinitely. This is why, contrary to normal cells, cancer cells are practically immortal and can be cultured indefinitely in a lab.
- A growing nutrients supply. Under hypoxic stress, cells acquire the capability to attract blood vessels and make them grow toward and around them. Thus, the tumour as a whole recruits the continuous supply of oxygen and nutrients it needs to sustain growth.
- Mutations to change membrane properties. An invasive, metastatic tumour cell has to lose its cell-cell, or cell-matrix adhesion in order to detach and travel in the body.
- Genomic instability: Loss or impairment of mechanisms that prevent mutations arising during and after DNA replication increase the rate of mutation. Cells thus impaired display a mutator phenotype and suffer genomic instability.

Tumour development is therefore a long and complex process, with many opportunities for therapeutic intervention.

Many of the steps cited above involved mutations in critical regulatory genes. The accumulation of mutations triggers the disease as we know it.

Normal genes whose cellular functions are activated or enhanced by mutation are called proto-oncogenes. The mutant form of a proto-oncogene is called an oncogene and the protein product of an oncogene is called an oncoprotein. In short, oncogenes are mutant genes that cause cancer.

1.3 Mutations and cancer

Cancer promoting mutations can be divided into four separate classes (Stratton, 1996)

- Point mutations
- Translocations (gene rearrangement)
- Gene amplifications
- Deletions

1.3.1 Point mutation

The term point mutation describes the substitution of one base pair of a DNA sequence by another, for example, substitution of a G:C base pair by an A:T. This event has different consequences depending upon its position.

The mutation may result in the substitution of one amino acid for another (a missense mutation), resulting in a protein identical to the wild type except for the single amino acid change.

If that amino acid is situated critically at the active site of the protein, it can have dramatic effects on its activity. One prominent example of this kind of mutation occurs in the RAS gene.

RAS proteins are composed of 188 or 189 amino acid residues. Normally, they undergo a cycle of activation and inactivation associated with the hydrolysis of GTP to GDP. Mutated RAS proteins in human tumours, however, are fixed in the activated conformation. When glycine 12 is affected by mutation and replaced by any other amino acid, the new side chain prevents the enzyme responsible for the hydrolysis of GTP to GDP from accessing its target, and therefore, prevents hydrolysis. (Friday and Adjei, 2005).

As the Ras protein is an integral part of cellular growth signalling cascades, it is crucial in cancer development, and mutant versions are very frequently found, particularly in colon and pancreatic carcinoma.

1.3.2 Translocation

In a translocation, part of one chromosome is joined to another. The outcome is a hybrid chromosome detectable by cytogenetic analysis of tumour cells. At the molecular level, a gene located at or near the breakpoint in one of the two chromosomes is fused to sequences from the other chromosome. This can have important consequences such as deregulated gene expression:

A gene silenced during normal cell differentiation may come under the influence of strong transcriptional promoters and enhancers, resulting in deregulated expression of the translocated gene. For example the bcl2 gene is switched off in most B-Cells within the germinal centre, thereby allowing programmed cell death, or apoptosis to occur. However, placement of the bcl2 gene next to the IG locus, which contains a B-cell specific transcriptional enhancer, results in deregulated bcl2 expression and prolonged B-cell survival.

If the breakpoint occurs within introns of the two genes, then translocation results in the formation of novel hybrid or fusion gene containing components of the two. The resulting protein will consequently have unique properties. The most well known example of this type of mutation is the bcr-abl fusion gene. The bcr-abl fusion protein has an elevated tyrosine kinase activity and its relocation from the nucleus to the cytoplasm contributes to its oncogenic action.

1.3.3 Gene amplification

The diploid genome of each eukaryotic human cell normally carries two copies of each gene, one originating from each parent (genes on X and Y chromosomes are exceptions). Under certain circumstances one copy may be multiplied to up to several thousand-fold, a phenomenon known as gene amplification. Amplified genes can form two types of microscopically abnormal chromosomal configurations known as double minutes and homogeneously staining regions.

Many types of oncogenes are activated by gene amplification. These include the genes for growth factors receptors (e.g. epidermal growth factor receptor in malignant gliomas) and nuclear oncogenes such as N-myc in neuroblastoma.

Gene amplification is usually a late and hence progressive step in oncogenesis rather than an initiating or early event.

Interestingly, the gene amplification process was first characterized as a common mechanism by which mammalian cells acquire resistance to metabolic inhibitors and is often seen in tumour cells that have become resistant to a chemotherapeutic agent.

For example, methotrexate is a commonly used drug in cancer chemotherapy. It inhibits the enzyme dihydrofolate reductase. When the corresponding gene is amplified and increased levels of enzyme are produced, effective inhibition by methotrexate is no longer achieved.

1.3.4 Deletion

DNA deletions are frequent in tumour cells. They can be as large as an entire chromosome or as small as a base pair deletion. Large deletions are likely to result in inactivation or production of structurally abnormal proteins.

If the removed fragment is a multiple of 3 base pairs coding for an amino acid, then only this amino acid will be absent from the protein. This can have a variety of effects depending upon the functional properties of this segment in the normal protein.

However, if the deleted fragment is not a multiple of three base pairs, then a frame shift will be introduced. In those cases, it is possible that the new sequence will code for a premature stop codon and the protein will be non functional.

As deletion often results in inactivation of the concerned protein, they become a serious problem when they affect tumour suppressor genes such as P53. The P53 protein exerts a wide variety of properties, ranging from cell cycle regulation, induction of apoptosis in cells with highly damaged DNA, to regulation of angiogenesis. In this respect, P53 is known as the "guardian of the genome".

Genetically engineered mice without P53 genes are able to grow normally and even reach maturity. However, they are very likely to develop cancer at a young age, thus demonstrating the tumour suppressor properties of the P53 gene.

These findings revealed that once the p53 protein is not present or able to control DNA abnormalities, cancers are likely to emerge. (Cooper, 1995)

It is noteworthy that because human cells are diploids, tumour suppressor genes must be disabled on both alleles in order to completely suppress the production of corresponding proteins. In contrast, dominantly acting oncogenes such as the mutant Ras, need to be activated in only one of the two alleles to produce a significant amount of the rogue protein.

1.4 Conclusion

To summarize, it can be said that cancer arises from the mutation of critical regulatory genes. These mutations produce unique DNA sequences, which could be recognised by DNA targeting agents. If selective enough, those agents could disable dominant oncogenes and re-establish regulation.

As mutations are so frequent in cancerous cells, it should be easy to target at least one of them, (the easiest or the most important to target), or even many of them at the same time.

It is with these ideas in mind that we hope to design more selective DNA binding agents, with the ultimate goal to deactivating oncogenes at will.

2. The Pyrrolo[2,1-c][1,4]benzodiazepines (PBDs)

21

2.1. Introduction

PBDs are naturally occurring antibiotics, which possess unique DNA interactive properties, combining selectivity for AGA sequences with covalent binding. This last characteristic qualifies them for coupling with non-covalent specific DNA binding agents. The PBD nucleus could provide an anchor point for the resulting hybrid molecule and would actively participate in the DNA recognition process.

This chapter is designed to review the most important features of the PBD molecules including mode of action and structure activity relationship.

2.2 PBD Basics

2.2.1 Natural product family
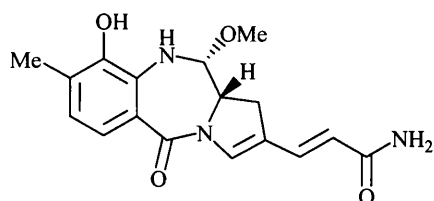
1
Anthramycin methyl ether
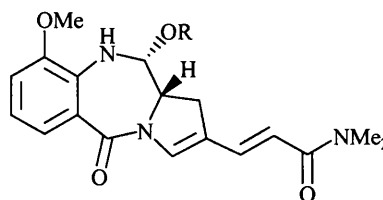
2 Porothramycin A: R = H
3 Porothramycin B: R = Me
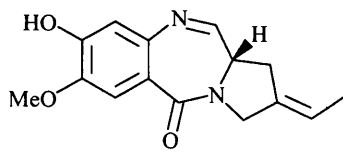
4
Tomaymycin
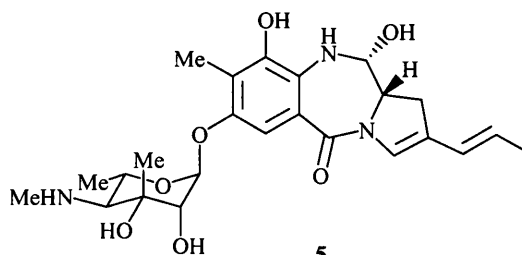
5
Sibiromycin
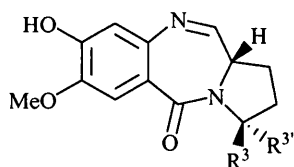
6 Neothramycin A: R³ = H, R³' = OH
7 Neothramycin B: R³ = OH, R³' = H
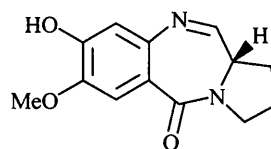
8
DC-81

Figure 2.2a: Some well-known naturally occurring PBDs.

Following the isolation of anthramycin, a variety of naturally occurring antitumour antibiotics agents of similar structure have been discovered (**Figure 2.2a**) (Thurston, 1999). Amongst them, anthramycin, sibiromycin and neothramycin have undergone clinical trial against human cancers. (Hurley, 1988b).

2.2.2 PBD ring system and numbering

The basic structure of these natural products is a highly conserved tricyclic skeleton comprising a benzene (A-ring), a diazepine (B-ring) and a pyrrole (C-ring) (**Figure 2.2b**).
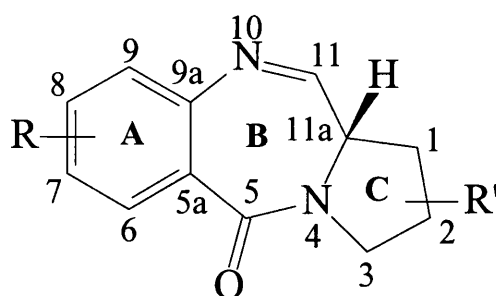
Figure 2.2b: PBD ring system and numbering.

2.2.3 PBD interconvertable forms

These natural products all feature (*S*)-stereochemistry at the chiral C11a-position. The N10-C11 functionality is typically drawn as an imine bond. In fact, this bond is at the center of a dynamic equilibrium depending on the ambient medium. For exemple, a PBD dissolved in an anhydrous and non-nucleophilic solvent such as chloroforom will be able to exist as an imine. However, if the same molecule is kept in the presence of water or a nucleophilic solvent such as methanol, the equilibrium will be driven towards the formation of carbinolamine or carbolamine methyl ether adducts (**Figure 2.2c**) (Leimgruber *et al.*, 1965a and b; Thurston *et al.*, 1986)

carbinolamine   imine   carbinolamine methyl ether
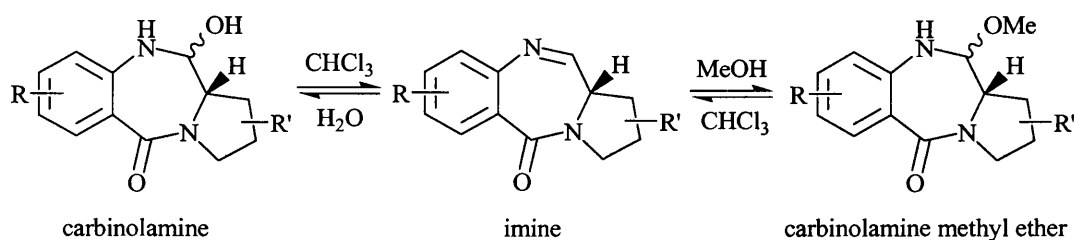
Figure 2.2c: PBD interconvertable forms.

It is important to realise that the same equilibrium will exist in biological systems, with the molecule existing as a carbinolamine in the aqueous plasma, but with the possibility of reverting back to the imine in hydrophobic systems such as the DNA minor groove.

2.2.4 PBD mode of action

2.2.4.1 Generalities
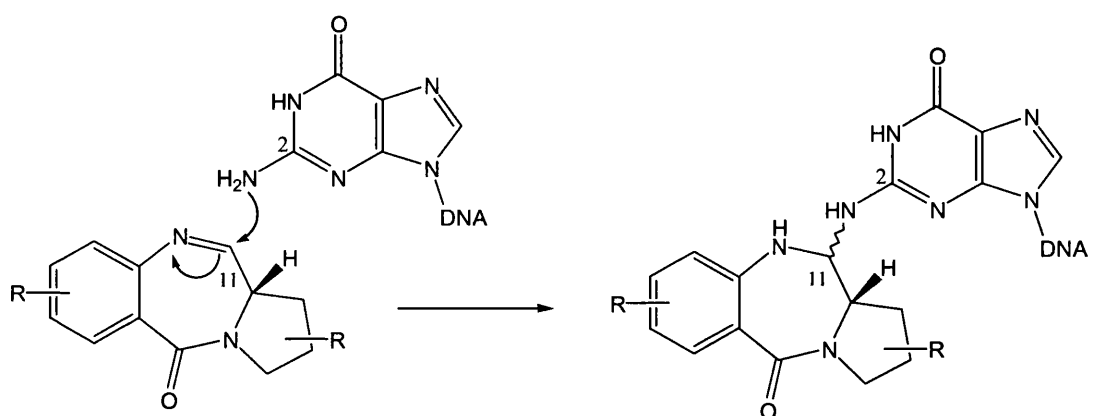
Imine-based mechanism
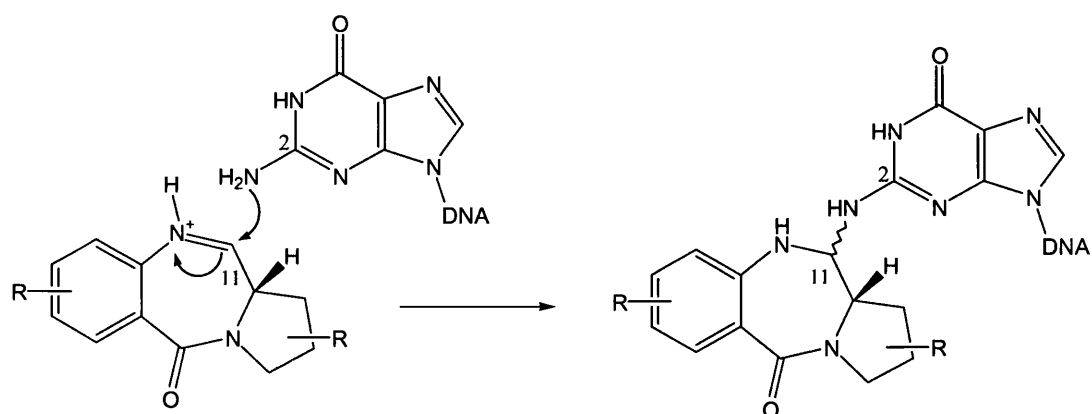
Iminium-based mechanism

Figure 2.2d: Proposed mechanisms for the reaction of PBDs with DNA.

PBDs were found to specifically alkylate the exocyclic amino group of guanine in the minor groove of DNA through an aminal bond (Kopka *et al.*, 1994). The alkylation

reaction is catalysed by acid, but can be reversed below pH 3 (Kohn and Spears, 1970). An important feature of the PBD-DNA bond (or more generally any PBD-nucleophile bond) is its reversibility. For example, the molecule is released intact if the DNA is digested by DNase I and snake venom phosphodiesterase. (This finding even prompted Hurley *et al.* to consider DNA-PBD complexes as prodrugs. *Hurley et al.,* 1979) In fact, the relative weakness of the PBD-nucleophile bond bestows the molecule with its remarkable selectivity for guanine in the minor groove of B-DNA, through a simple thermodynamic equilibrium. The tricyclic structure of the PBD is complementary to the minor groove of B-DNA and the complex is further stabilised by two to three hydrogen bonds. (see **Figure 2.2e** below).

Once in this stable position, the PBD molecule inhibits RNA and DNA synthesis, ultimately resulting in cell death (Kohn *et al.,* 1968). Although excision and repair mechanisms induce DNA strand breaks, the non-removal of PBDs from the DNA appears to be detrimental to cell survival (Petrusek *et al.,* 1982, reaction of anthramycin with DNA)

2.2.4.2 Mechanism of alkylation

There has been a long-running investigation to determine which species was responsible for guanine alkylation. The carbinolamine was a favoured candidate as aqueous biological environment should favour its formation (Hurley *et al.,* 1977). However an imine/iminium based mechanism explains most experimental observation, including the proportion of the two conformational forms of tomaymycin on DNA (11S and 11R adducts) compared with the proportion of the two carbinolamine diasteroisomers. (Barkley *et al.,* 1986*).* Consistent with an acid-catalysis mechanism, the imine can be protonated to provide the highly electrophilic iminium species which reacts with guanine. (**Figure 2.2d** above). Interestingly, some tumour regions having a more acidic pH than average (hypoxic metabolism) could be preferentially targeted by PBDs, therefore conferring a degree of selectivity to the molecule.

2.2.4.3. Sequence selectivity

DNA footprinting techniques allowed the determination of preferred PBD binding sequences. In 1986, Hertzberg *et al.* demonstrated that PBDs will preferentially alkylate

purine-guanine-purine motifs in preference to other sequences. (purine-G-purine > purine-G-pyrimidine ~ pyrimidine-G-purine > pyrimidine-G-pyrimidine). An exhaustive analysis by Pierce *et al.* (1993), in accord with computational calculation (Kopka *et al.*), further defined a clear ranking in binding preferences among 5'-X-G-X-3' triplets as follows: A-G-A > A-G-G > G-G-A> G-G-G.

This last characteristic could allow PBDs to play an active role as part of a gene targeting strategy.
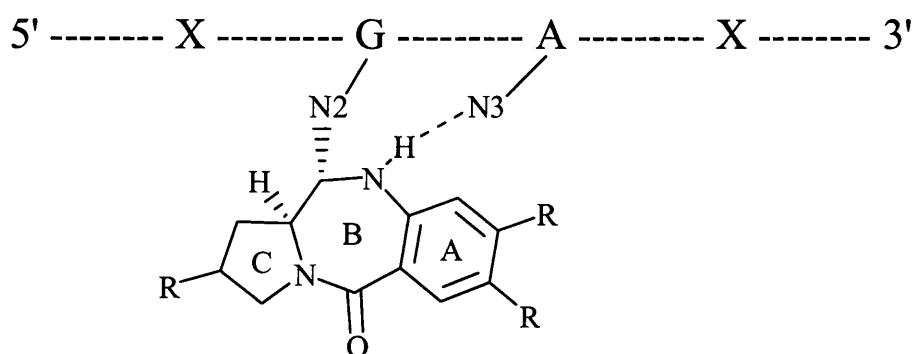
Figure 2.2e: Proposed model of PBDs binding to 5'-XGA sequence of DNA.

2.3 Structure-Activity Relationships (SARs)

Biological evaluation of a large numbers of synthetic PBD have helped to determine which essential features and functionalities control the activity of the molecules. Amongst them, electron-donating groups in the A-ring, stereochemistry in the B-ring, and unsaturation in the C-ring were found to be critical.

2.3.1 A-ring SAR

2.3.1.1 Introduction

The A-ring SAR is dominated by electronic factors. Electron donating groups such as hydroxy and methoxy enhance the biological activity of the molecule whereas electron withdrawing groups such as nitro, decrease or even abolish it. (Hurley and Boyd, 1988;

Guitto *et al.,* 1998; Thurston *et al.,* 1999). Attempts to substitute the benzenoid A-ring by electron deficient ring such as a pyridine failed to provide active compounds. To our knowledge, no electron-rich heterocyclic A-ring (such as a pyrrole) PBD hybrid has been synthesised.

These findings are consistent with an acid-catalysed iminium alkylation mechanism. Indeed, the more electron density from the A-ring is fed to the N-10 nitrogen, and the more basic it becomes. The pKa of the imine increases, and so does the likelihood of it being present as the activated iminium in the minor groove. Interestingly, electron withdrawing groups are known to stabilise the carbinolamine form of the molecule, in contrast to electron-donating groups favouring dehydration to the imine form.

- C8 and C7 positions

C8-hydroxy alkylation was found to decrease DNA binding affinity, but allows correct positioning of linkers along the minor groove, an important factor in the design of PBD-heterocycles conjugates. It should be noted that, in contrast to the C8 position, C7 substituents point out of the minor groove. The C7 position is therefore not an optimum point of attachment for DNA recognising agents. It is, however, a privileged position to introduce pharmacologically enhancing groups such as sugar moieties (i.e. siboromycin).

2.3.1.2 C9-hydroxy group and cardiotoxicity

Despite being involved in a stabilising hydrogen bond with DNA, the C9 hydroxy group found in anthramycin and other members of the PBD group, is responsible for dose-limiting cardiotoxicity and withdrawal from clinical trials. (Thurston and Hurley, 1983). The toxicity of anthramycin mimics very closely that produced by the anthracyclines adriamycin and daunomycin, which feature a *para* quinone ring. Anthramycin can oxidise or tautomerise to form the related quinoneimines. (**Figure 2.3a**). The fact that co-enzyme Q10 or vitamin E can offer protection against this type of cardiotoxicity further supports this theory.
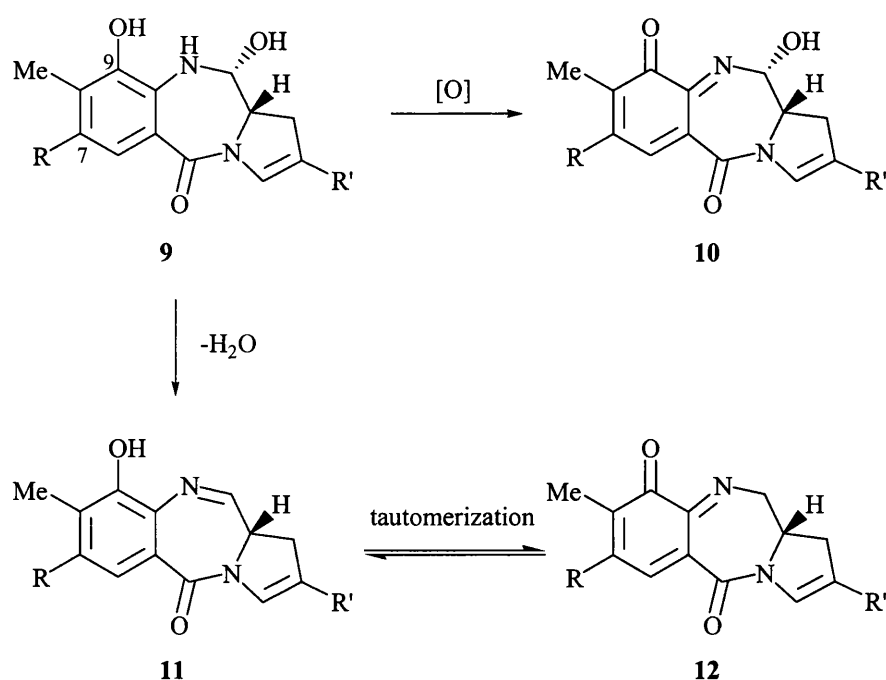
Figure 2.3a: Proposed mechanisms for the formation of cardiotoxic quinoneimines.

2.3.2   B-Ring SAR

2.3.2.1 C11a stereochemistry

As discussed previously, the electrophilic functionality at N10-C11 is responsible for the irreversible covalent binding between PBDs and the DNA (Hurley, 1977). An (S)-configuration at C11a provides the molecule with a right-handed twist when viewed from the C-ring toward the A-ring, which allows it to fit snugly within the minor groove of DNA. However, compounds possessing the (R)-configuration do not interact with DNA and exhibit significantly less cytotoxicity compared to the corresponding (S)-isomers (Hurley et al., 1988a).

2.3.2.2. N10-C11 functionality, covalent versus non-covalent binding.

From all the elements described previously, it is clear that the imine/carbinolamine moiety of the PBDs is responsible for covalently binding the DNA. Compounds lacking this functionality are interesting since they reveal the importance of non-covalent

interactions with duplex DNA. Several compounds of this type have been synthesised. They include PBD dilactams, amidines and secondary amines.

In 1990, Jones *et al.* have shown that certain dilactams bearing hydroxyl or acetoxyl group at their C2 and C8 position, elevate the melting point of CT-DNA by a significant 3°C. More recently, Kamal *et al.* (2002) have shown that mixed imine/dilactams PBD dimers can elevate the helix melting point by up to 17°C, which is more than the imine/imine dimer DSB-120 (15.4°). This is a remarkable demonstration of the strength of the non-covalent component of the PBDs.

In 2004, the same group (Kamal *et al.*) reported the properties of mixed amine/imine dimers and found that they could also elevate the DNA melting point (up to 11°C), but to a lesser extent than mixed dilactam-imine dimers. This could show the importance of the carbonyl group for non-covalent interactions.

Eleven amidines PBD monomers (Foloppe *et al.*, 1996) were also reported, but their slight DNA melting elevation (0.7 °C) was non selective and could be due to non-specific interaction with the amidine moiety.(**Figure 2.3c**)
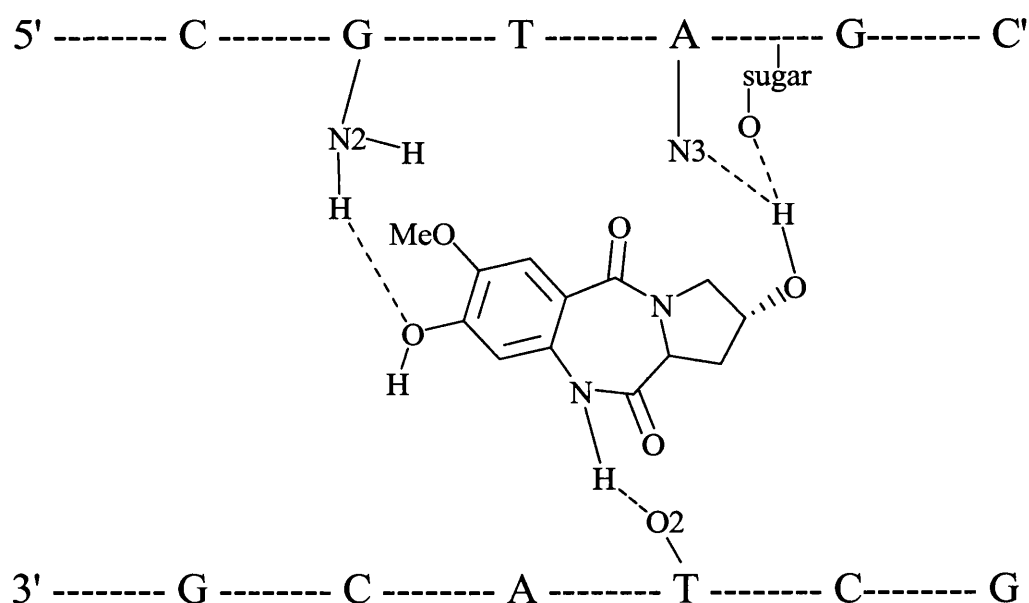
Figure 2.3b: Proposed model of non-covalent binding between dilactam and DNA.

DC-81, $\Delta T_m = 0.7\ °C$

13, $\Delta T_m = 3.0\ °C$

14, $\Delta T_m = 0.7\ °C$

DSB-120, $\Delta T_m = 15.4\ °C$

15, $\Delta T_m = 17.0\ °C$

16, $\Delta T_m = 11.0\ °C$
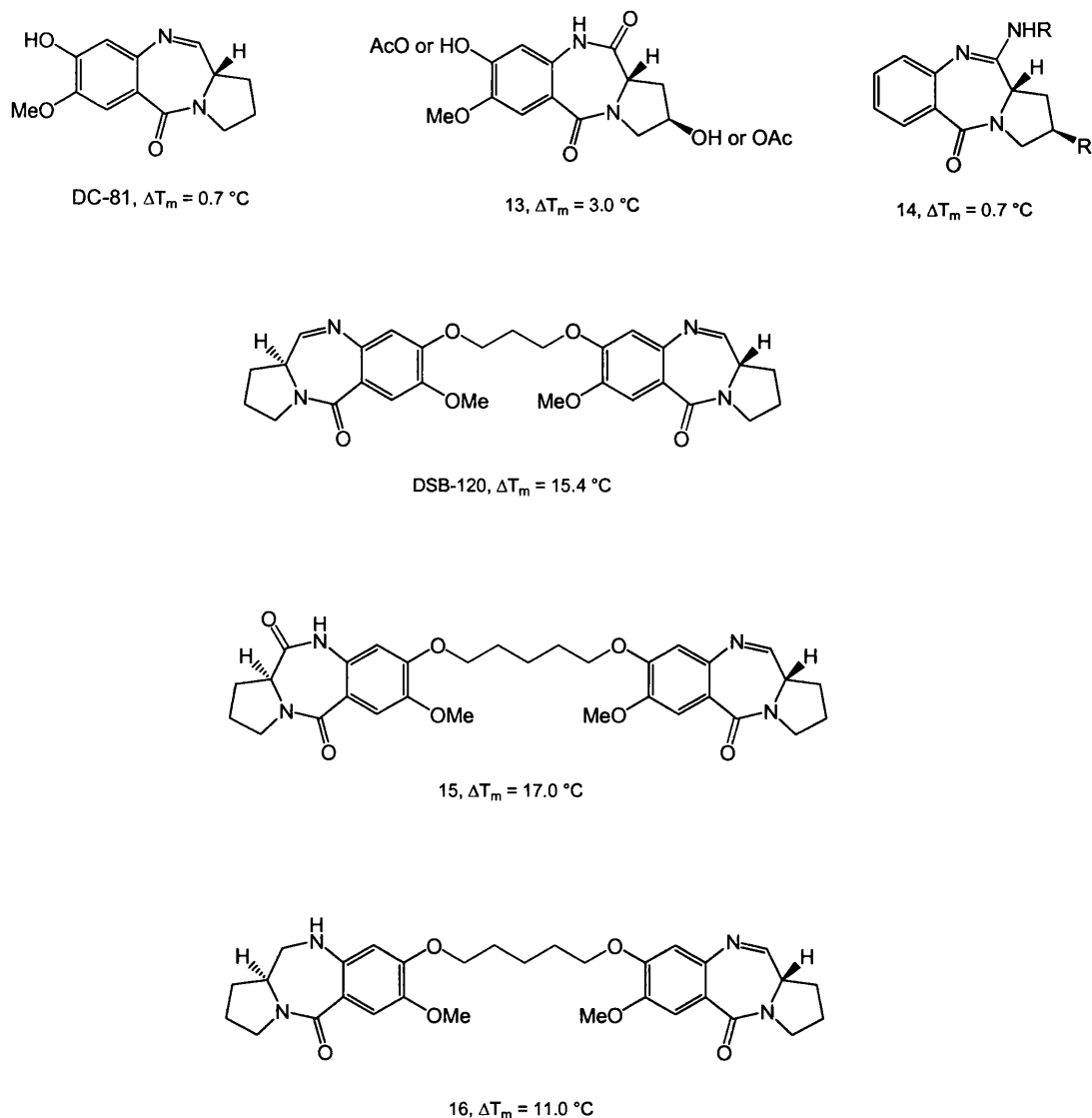
Figure 2.3c: Effect of PBD Imine, dilactams, amines and amidines on thermal denaturation of CT-DNA. Effects on DNA binding affinity as measured by elevation of melting point of CT-DNA after 18h of incubation at 37°C.

2.3.2.3 N10 position and PBD prodrugs.

The PBD molecules are particularly well suited to a prodrug approach. Molecules substituted at their N-10 position are not cytotoxic. N-10 protecting groups can be designed to be removed under specific conditions than can bring a greater degree of selective tumour targeting (**Figure 2.3d**). For example, they could be activated under acidic conditions, or reductive conditions (Berry *et al.*, 2002). Another approach is the use of enzyme as part of an ADEPT strategy (Sagnou *et al.*, 2000). This concept is very

promising, and it is conceivable to achieve 100 fold higher concentration of active drug in the tumour as compared with healthy tissue.
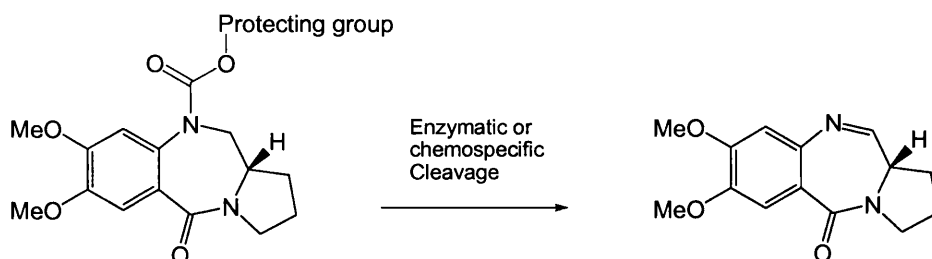
Figure 2.3d: The N-10 position is particularly suitable for prodrug design.

2.3.2.4 Bisulphite adducts

The product of reaction of sodium bisulphite with an aldehyde (or in certain cases, a ketone or an imine) is usually known as a bisulphite addition compound. (**Figure 2.3e**).
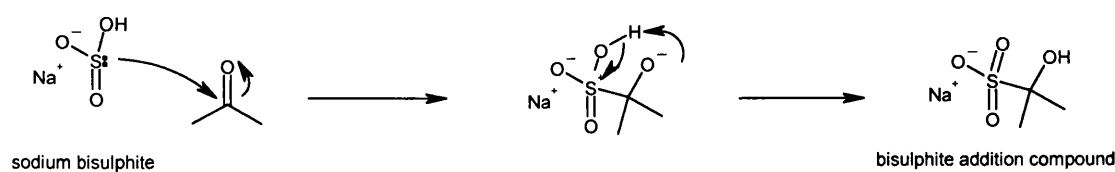
Figure 2.3e: Bisulphite adducts formation

These products are valuable for a number of reasons, including water solubility and stability. Additionally, the reaction is reversible in dilute acid or base, making the bisulphite compounds useful intermediates in chemistry and medicinal chemistry.

The antileprosy drug Dapsone is insoluble in water, and as such, can not be administered easily. However, its formaldehyde bisulphite adduct is water-soluble. As the reaction is reversible, the drug Dapsone is eventually released under physiological conditions. (**Figure 2.3f**) (Clayden *et al.*, 2001).

Dapsone, antileprosy drug
unsoluble in water

formaldehyde bisulphite adduct

water-soluble prodrug
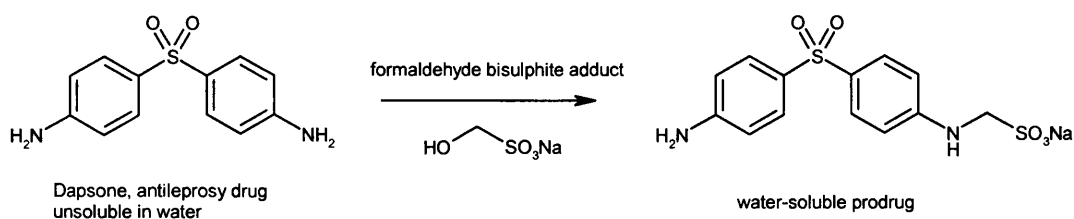
Figure 2.3f: Formation of a water-soluble prodrug adduct of Dapsone

Interestingly, the same methodology can be applied to PBDs. Their imine functionality reacts with sodium bisulphite to form stable, water-soluble adducts.

One of the first PBD-bisulphite adducts was reported by Kaneko *et al.* (1985) and this water soluble molecule (17) displayed significant *in vivo* anti-tumour activity against the P388-leukaemia model (**Figure 2.3g**).

17

18

19
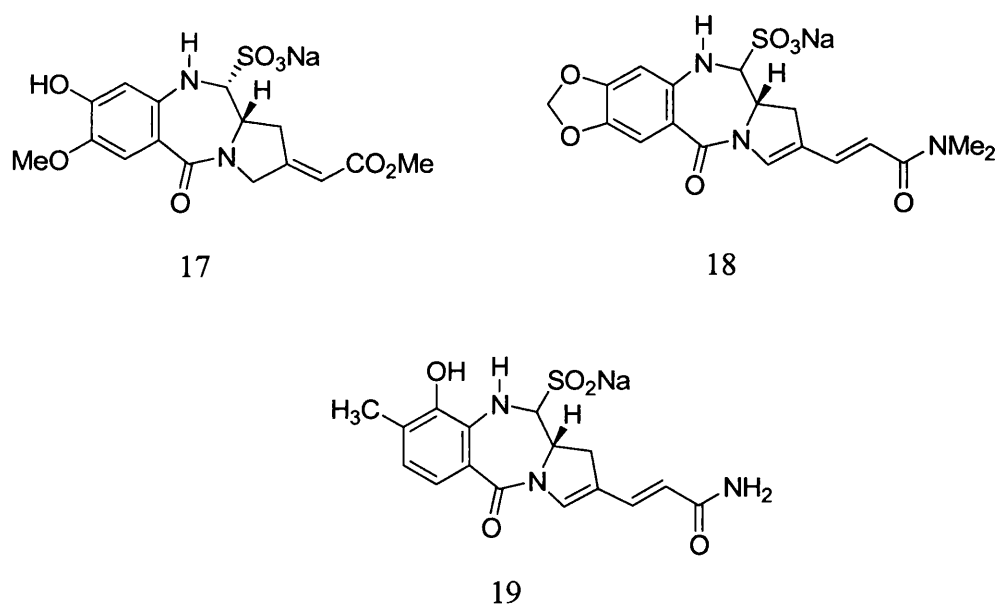
Figure 2.3g: Known PBD Bisulphite adducts.

Kaneko also mentions spadicomycin (19), an anthramycin sodium sulphino adduct (Ueda *et al.*, 1979) which entered clinical trial in the mid-1980s. Spadicomycin, which was developed by Mitsubishi Pharma, reached phase III clinical trial in Japan and was much less cardiotoxic than the parent PBD anthramycin. However, the molecule was withdrawn due to dose-limiting toxicity caused by hepatic and renal dysfunction. More recently, Langlois and co-workers (2001) reported the synthesis and cytotoxic evaluation of a bisulphite adduct of 7,8-methylenedioxy-porothramycin (18).

Significantly, this water soluble derivative retained the *in vitro* cytotoxic potency of the parent molecule in the various cell lines tested.

Additional work carried out in our laboratories (Dr Stephen J Gregson, unpublished results) concluded that PBD bisulphite adducts are resistant to interconversion through hydrolysis, methanolysis or dehydration. They are also stable in one diasteromeric form and can be isolated by lyophilisation. (More information is given in Appendix A)

This method was therefore applied to a few final compounds described in this thesis, as a way of enhancing their formulation and stability.

2.3.2 C-Ring SAR

2.3.3.1. Effect of an *sp2* carbon at the C2 position:

The structural analysis of naturally occuring PBD's showed quite early that an *sp2* carbon at the C2 position was the key to superior biological activity. An exhaustive synthetic campaign by Howard and Thurston further reinforced this discovery by providing an array of analogues (see **Table 2.3a** further down).

4
Tomaymycin

1
Anthramycin

8
DC-81

20
DRH-417
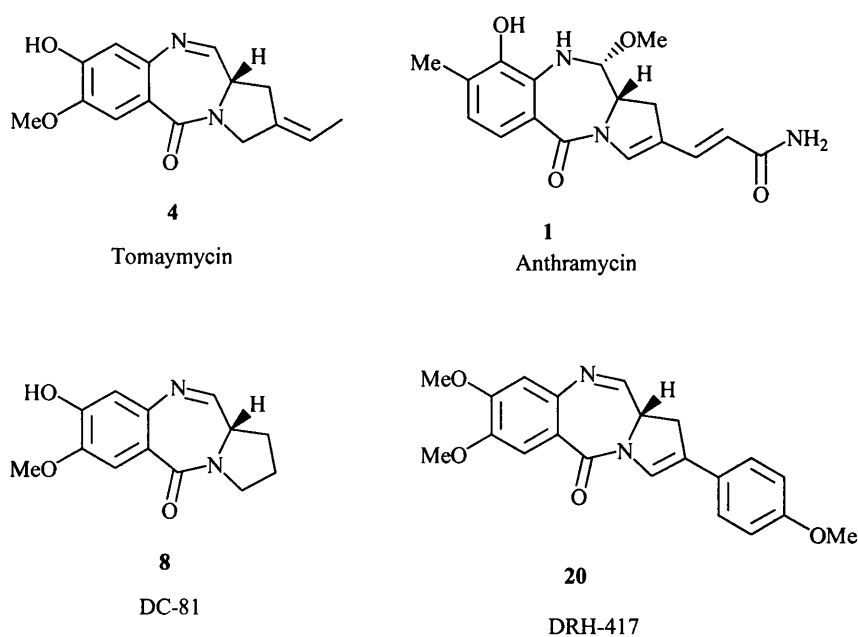
Figure 2.3h: Examples of saturated, *exo*, *endo-exo*, and C2-aryls PBDs: Tomaymycin, DC-81, Anthramycin and DRH-417.

33

C2-unsaturated PBDs bind with better affinity to DNA, are more cytotoxic *in vitro*, and are more active *in vivo* than their saturated counterpart. This remarkable gain of activity has been attributed to a combination of factors:

a) The overall shape of the molecule

The flattening of the C-ring and the different torsion angles between the C-ring and the B-ring makes unsaturated PBD a better fit to the DNA groove. The molecule is immersed more deeply in the minor groove than saturated PBD and therefore remains invisible to repair enzymes. It is thought that this causes the adduct to remain undetected for a longer length of time. (Gregson *et al.*, 2001b)

b) The possibility of C2 substitution

C2 substituents in unsaturated PBD are projected directly along the groove, in an optimal position to pick up favourable electrostatics or hydrogen bonding interactions (anthramycin). This was dramatically demonstrated when C2-aryl substituents synthesised by Cooper *et al.* (2002) revealed an outstanding antitumour profile in the NCI 60 cells lines assay.

c) A reduced reactivity towards scavenging thiols and proteins.

In vivo toxicity and lack of efficacy (narrow or non-existing therapeutic window) of a number of saturated PBDs can be attributed to protein alkylation and scavenging by cellular thiols prior to reaching the tumor site. Interestingly, C2 unsaturation can lead to lower electrophilicity at the N10-C11 position (Morris *et al.*, 1990) and reduce the collateral damage occasioned by this type of nucleophilic attack.

In summary, C2 unsaturated PBD are more specific for DNA than their saturated counterparts and therefore, more efficient.

2.3.3.2. *Endo*, *exo*, and *endo-exo* unsaturated PBDs

In general, the double bond at the C2 position in unsaturated PBDs has a tendency to position itself inside the C-ring (*endo*) to benefit from a conjugation effect with N-4 nitrogen. This behaviour is reinforced if there is a possibility of conjugation with the C2-substituents (anthramycin side chain, C2-aryl PBDs) (*endo-exo* unsaturated

compounds). On rare occasions however (methylidene, ethylidene substitution) the double bond can remain outside the ring (*exo*) as seen in tomaymycin and SJG-136 (see later).

NB: Some *endo* unsaturated PBDs are susceptible to C-ring aromatisation under relatively mild heating or acidic conditions. This has to be avoided at all cost since the fully aromatic compounds are inactive. In the early literature, the structure of sibiromycin was wrongly interpreted as the fully aromatic/inactive compound and this resulted in misleading assumptions about the reactivity of the N10-C11 imine.
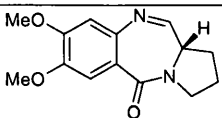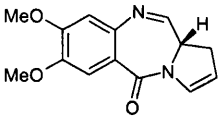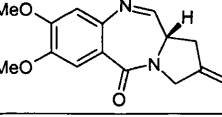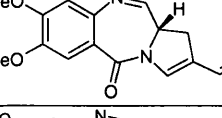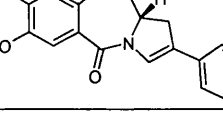
Compound	Biological activity (mean GI50) NCI 60 cell lines panel (2004)
21	2.39 µM
22	1.28 µM
23	0.309 µM
24	0.123 µM
20	< 0.01 µM

Table 2.3a: Effect of *endo* and *exo* unsaturation on biological activity.

2.3.3.1 Summary

A summary of structure-activity relationships originally derived by Thurston *et al.* (Thurston, 1993) is illustrated in **Figure 2.3i**.

Bulky substituents at N10 (e.g. acetyl, carbamate, hemiaminal) inhibit DNA binding affinity and cytotoxicity.

Electron-donating substituents required at position 7,8 or 9 of the A-ring.

An imine, carbinolamine or carbinolamine methyl ether required at N10-C11 position.

S-Stereochemistry required at C11a.

Replacement of C1 with an oxygen maintains cytotoxicity.

Sugar moiety at C7 enhances DNA binding affinity and cytotoxicity in some cell lines.

Endocyclic and exocyclic unsaturation at C2 enhances cytotoxicity and *in vivo* antitumour activity. Fully unsaturated C-ring leads to complete loss of DNA binding affinity and cytotoxicity. C2-C3-*endo* unsaturation in combination with an aryl group at C2 significantly enhances *in vitro* cytotoxicity.

Small substituents (e.g. OH), tolerated at C3 in fully unsaturated C-ring compounds.

Figure 2.3i: Structure-activity relationships of the PBD ring system.

2.4 PBD Dimers

2.4.1 Introduction

At the end of the 1980s, two groups began investigating the idea that linking two PBD units together would form a bis-alkylating molecule capable of forming DNA interstand crosslinks. This cellular event is known to disrupt DNA replication in rapidly dividing cells and is the basis of action for widely used anticancer drugs such as chlorambucil or cisplatin.

The Suggs's group joined two PBDs through an amino C7 linker, the resulting dimer was found to be a moderate DNA binder, but vulnerable to pH changes. However, linking two PBDs, along the minor groove, through their C8 hydroxy group (as in DC-81), was found to be more efficient and generated the dimer DSB-120 (see below). The resulting DNA crosslink adducts were found to be considerably more stable than those produced by PBD monomers. In thermal denaturation assays, DSB-120 elevated the DNA melting by a significant 15.1°C.

25

DSB-120

26
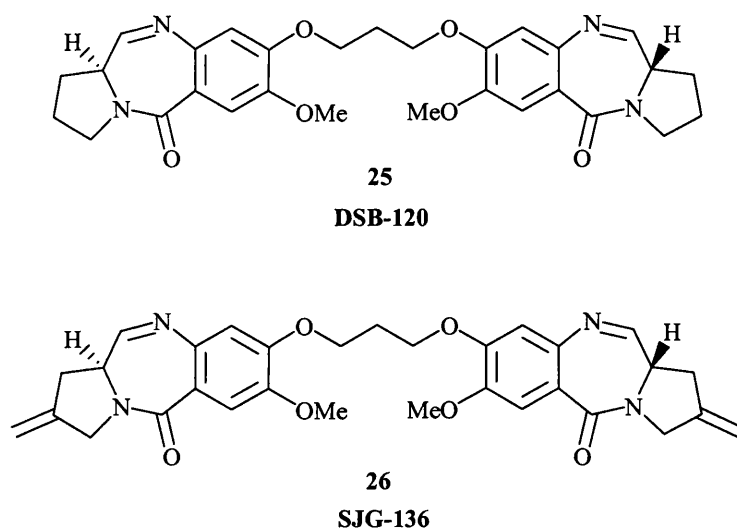
SJG-136

Figure 2.4a: DSB-120 and SJG-136.

37

2.4.2 *In vitro* and *In vivo* biological evaluation.

DSB-120 was found to be a hundred to a thousand fold more active in cytotoxicity assays *in vitro* than the monomer DC-81. Unfortunately, the molecule displayed a poor *in vivo* profile in the NCI hollow fiber assay and xenografts assays. This was interpreted to be linked to the low therapeutic index of saturated C-ring PBDs. (See C-ring SAR, in the previous section).

Thurston and Howard remedied this problem by designing and synthesising a C2 *exo*-unsaturated PBD dimer, SJG-136. The molecule featured all the key benefits conferred by C2-unsaturation: higher DNA binding affinity (stabilising DNA during thermal denaturation by 33.6°C), higher antitumour activity in the NCI 60 cell lines assays, a lower level of inactivation by intracellular thiol containing molecules, lower binding levels to plasma proteins and most importantly, a significantly improved *in vivo* therapeutic index as verified in a number of xenografts assays. (Wilkinson; Alley; Hartley; 2004). As a result of this encouraging profile, SJG-136 is now undergoing phase I clinical trials in the United States and the United Kingdom.

2.4.3 Sequence selectivity and gene targeting

Molecular modelling studies predicted that DSB-120 and SJG-136 would preferentially crosslink PuGATCPy sequences. This was later verified by footprinting and enzyme inhibition studies (Martin *et al.*, 2005) raising the possibility of using PBDs dimers as part of a gene targeting strategy.

In 1994, Neidle *et al.* attempted to correlate the sequence selectivity of DSB-120 (or SJG-136) with their biological activity. The authors screened oncogene databases for the target 5'-PuGATCPy sequence. Surprisingly, the sequence was not as randomly spread as expected. In fact, it was overexpressed in a number of oncogenes (3.8 times more than expected in v-src) and not expressed at all in others (abl, Ha-ras1, Blym-1, and bcl-2. It would now be interesting to conduct a study to verify if tumours cell lines sensitive to SJG-136 possess oncogenes with elevated frequencies of GATC compared with unsensitive cell lines. The fast developing field of gene array technologies should provide some answers to this question in the near future.
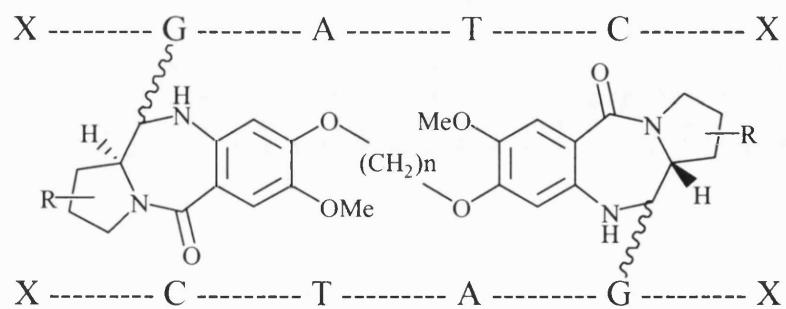
Figure 2.4b: DNA sequence selectivity and interstrand cross-linking of PBD dimers.
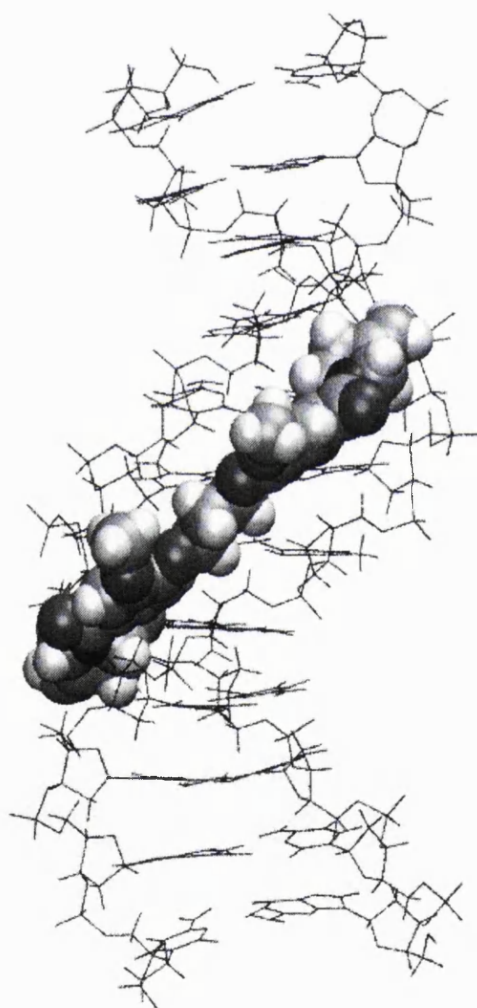
Figure 2.4c: Molecular modeling of interstrand cross-link formation by SJG-136.

(Dr David Evans, Spirogen, School of Pharmacy, London).

3 Sequence selective minor groove DNA binders: Strategic overview.

3.1 Introduction

DNA is the blueprint of all living organisms; it can be considered as the book of life containing all the instructions for synthesising the building blocks of living matter. This manufacturing process can be summed up to two steps: Initially, a messenger RNA strand is synthesised by transcription of its corresponding DNA sequence. Secondly, a protein is synthesised from this RNA in a second step called translation. (See **Figure 3.1a**). (http://fig.cox.miami.edu/~cmallery/150/gene/mol_gen.htm).
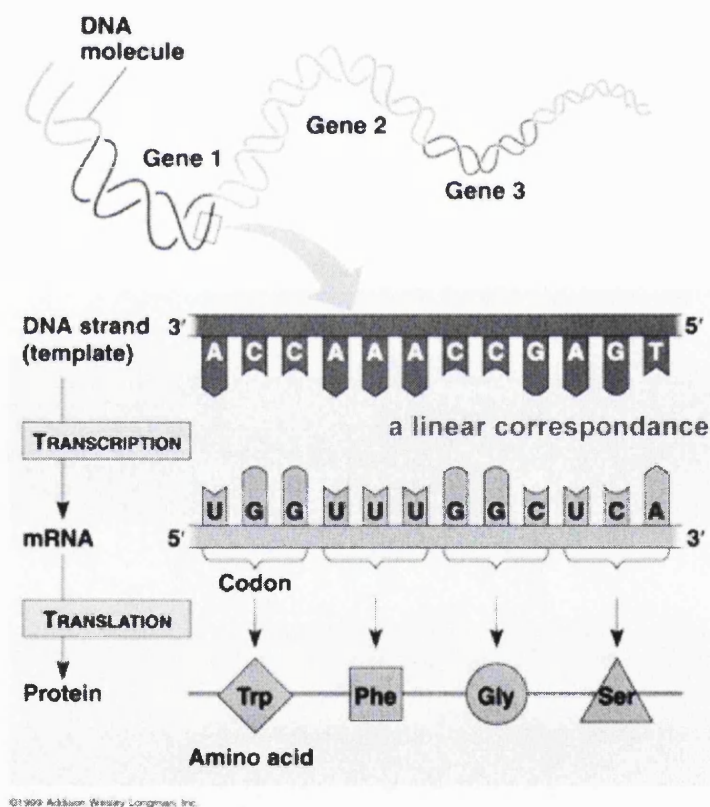
Figure 3.1a: Schematic representation of protein synthesis from DNA

Diseases (especially cancer) are often caused by overexpression of healthy or mutant proteins. A classical solution to this problem would be to disable these proteins by allowing a ligand to bind in their active site. This approach usually requires chronic

administration of drugs, as it takes at least one drug molecule to neutralize one copy of the protein. The binding is usually reversible and the drug is metabolised and excreted relatively quickly, thus requiring administration of more drugs.

Therefore, it would make sense to prevent protein production one or two levels before (RNA or DNA), instead of trying to disable them once they have been already manufactured. Targeting RNA is an interesting idea in its own right, but disabling precisely and definitively the gene (the DNA sequence) responsible for rogue protein production would be the ultimate expression of this strategy. In theory, it would take a single molecule of DNA binding drug per gene to prevent undesired protein production. In short, addressing rogue proteins at the DNA level would be attacking them at their source.

3.1.1 DNA targeting strategies: the choice of small ligands.

A number of DNA targeting approaches have been explored to date. They include triple helix forming oligonucleotides (TFOs), zinc finger proteins, peptide libraries and small ligands. (Thurston, 1999b). Triple helix forming oligonucleotides are made of backbone-modified sequences of single-stranded DNA. They bind in the major groove of the DNA through hydrogen-bonding interactions to form a triple helix structure. The main problems associated with this approach are stability, delivery, cell membrane penetration and pharmacokinetics. Zinc fingers and peptide libraries share the same problems as they are essentially small modified proteins. These difficulties arise from their relatively high molecular weight and also from their structure, which, being too close to naturally occurring biological building blocks (amino acid, nucleotides), are subject to metabolic degradation. Using small "drug-like" molecules, devoid of biologically labile chemical bonds or any other features vulnerable to enzymatic degradation, could circumvent these issues.

3.1.2 Netropsin / Distamycin and the DNA minor groove

This concept was first exemplified by the discovery of two naturally occurring antiviral antibiotics netropsin (Net) and distamycin (Dst). These crescent-shaped molecules made of two or three pyrrole units (see **Figure 3.1b**), bind to A, T sequences in the minor groove of the DNA as 1:1 or 2:1 ligand-DNA complexes. (Bu-Daya *et al.*, 1995).

3.1.2.1 Netropsin and Distamycin structures

Netropsin, 27   Dystamycin, 28
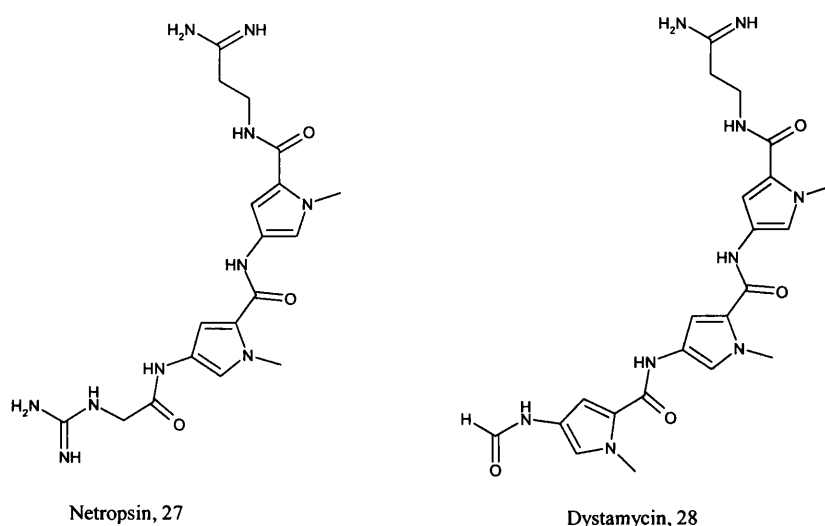
Figure 3.1b: Chemical structure of Netropsin (Net) and Distamycin (Dst).

3.1.2.2 DNA topology

An understanding of the topology of the B-form (generally accepted as the most common form) of the DNA helps to understand how these molecules work. The DNA B-form structure is comprised of two strands of Watson-Crick bases attached to a phosphodiester backbone. The two strands coil around each other in a double helical structure separated by two unequal indentations: the major and the minor groove. (See **Figure 3.1c**).

© 1999 Addison Wesley Longman, Inc.
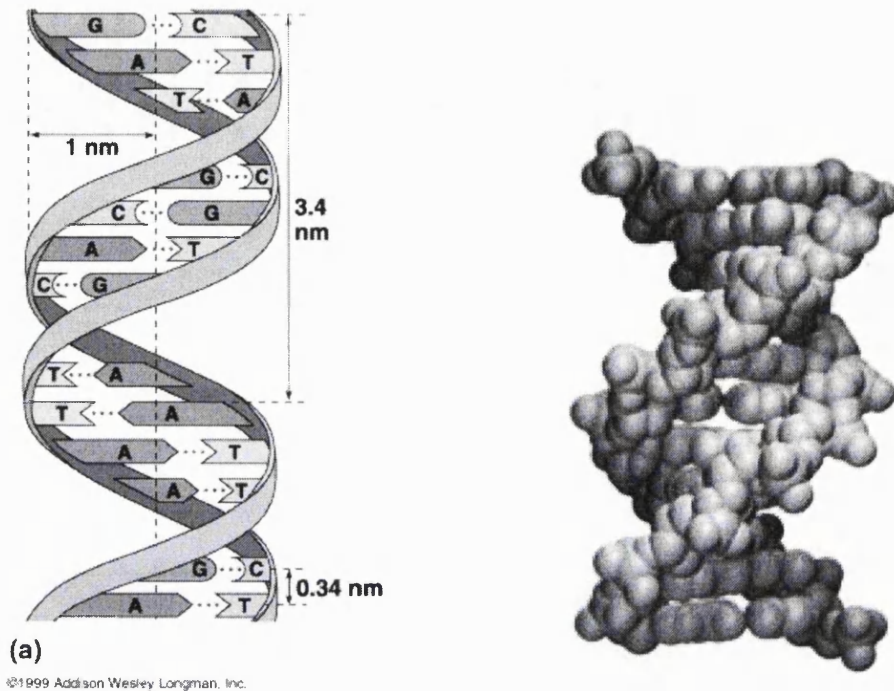
Figure 3.1c: Schematic representation and molecular model of B-form double stranded DNA. Minor and major grooves are clearly visible.

The dimensions of the grooves are:

- Major groove: Width 11.6 Å; Depth 8.5 Å.
- Minor groove: Width 6.0 Å; Depth 8.2 Å. (Neidle, 2001).

It is noteworthy that although the groove's depths are nearly equal, their widths are very different. This factor is of critical importance when designing DNA interactive molecules.

3.1.2.3 DNA base pairing

Of course these are average figures and the groove dimensions tend to vary depending on the base sequence. Indeed, minor groove widths for non-alternating runs of A:T base pairs have been reported in the range of 3-4 Å. On the other hand, runs of sequence with a high proportion of G:C base pairs tend to have widened minor groove. (Neidle, 2001).

43

Major Groove

Major Groove
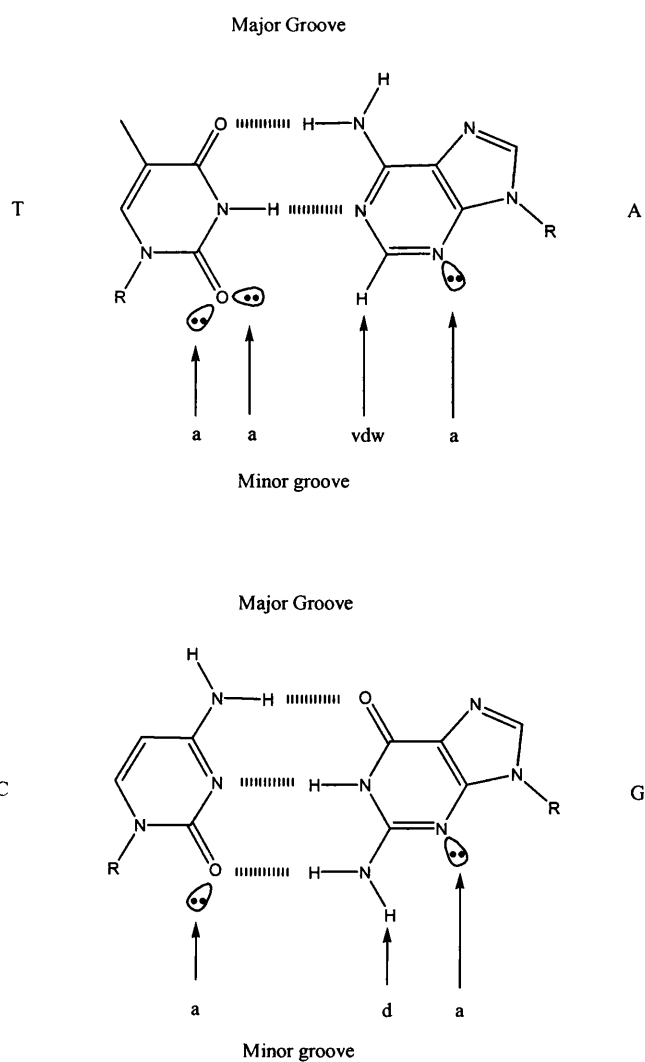
Figure 3.1d shows the structure of the Watson-Crick base pairs. Arrows indicate possible interactions point in the grooves. a= acceptor, d= donor, vdw= van der waals.

3.2 Factors to consider when designing DNA recognising agents

3.2.1 Introduction

Binding in the groove of the DNA is successful if enough favourable interactions are created to overcome the entropic cost of immobilizing the hitherto free ligand, as well as the disruption of the spine of hydration. (Bailly and Chaires, 1998).

Favourable interactions consist of:

- Van de Waals contact with the floor and walls of the groove (hydrophobic interactions)

- Hydrogen bonding with the bases (see **Figure 3.1d**)

- Ionic interaction between the cationic ligand and the anionic phosphate backbone.

3.2.2 Isohelicity

Of course, maximising favourable interactions requires shape complementarity between the ligand and the groove. This has given rise to the concept of isohelicity as exemplified in **Figure 3.2b** (Dervan and Edelson, 2003). Only a few ring system posses the correct curvature and size to be joined together in a small isohelical ligand. For instance, although slightly too long, the benzimidazole unit found in Hoechst 33258 is isohelical with the groove (Goodsell and Dickerson, 1986), whereas a furan heterocycle induces substantial curvature when included in distamycin analogues (**Figure 3.2a**). It is fortunate that isohelicity can largely be calculated by molecular modelling. Likewise, optimum binding affinity requires the polymeric ligand to be perfectly in register with the hydrogen-bonding pattern in the groove.
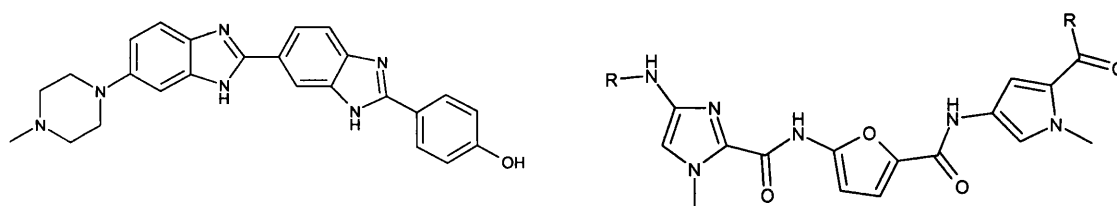
Figure 3.2a: The bisbenzimidazole unit found in Hoechst 33258 (on the left) possess complementary curvature with the DNA minor groove. The central furan amino acid found in the above lexitropsin causes an overcurvature of the overall structure. (As illustrated in the figure below).
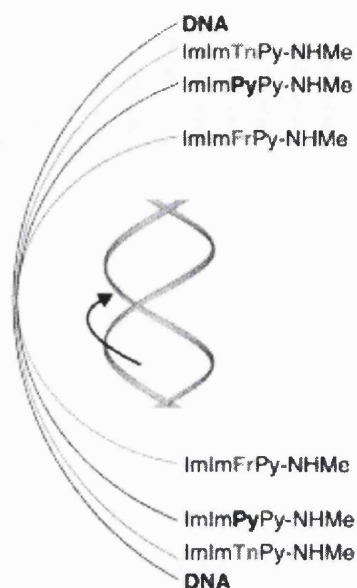
Figure 3.2b: Isohelicity of a variety of lexitropsins (Dervan and Edelson, 2003).

3.2.3 Base pairs registry; length of the ligand

Unfortunately, the pyrrole carboxamide unit found in lexitropsin and distamycin is approximately 20% longer than required to match perfectly the base pair rise in the minor groove. This is why a maximum of six Py (pyrrole unit) can be joined whilst retaining binding but four Py is the generally accepted upper limit for retention of base pair recognition.

The flexible β-alanine unit can be inserted between two heterocycles to relax the structure and allow it to be kept in phase with the groove pattern (Wang *et al.*, 2001).

3.2.4 Shape complementarity and exocyclic guanine NH$_2$

Shape complementarity also helps to explain why distamycin and netropsin (as well as the majority of small minor groove binders) are selective toward A:T base pairs. Whereas the floor of continuous A:T tracks can be approximated by a single smooth curve, the protruding position of the exocyclic guanine NH$_2$ is of critical importance. Not only does it represent the only H-donor in the minor groove, but it can also be thought of an obstacle in the way of small molecular ligands.

Distamycin and Netropsin binds selectively to A:T rich sequences of DNA because these somewhat tighter tracks provides better van der walls contact on their walls and their floor are devoid of the protruding guanine-NH_2 irregularity.

The only ligands capable of binding to sequences including G:C base pairs possess a hydrogen acceptor (typically an aromatic nitrogen as found in pyridine). For example the bithiazole moiety of the antitumour drug bleomycin shows selectivity for G:C sites. (Bailly *et al.*, 1992). **Figure 3.2c** below
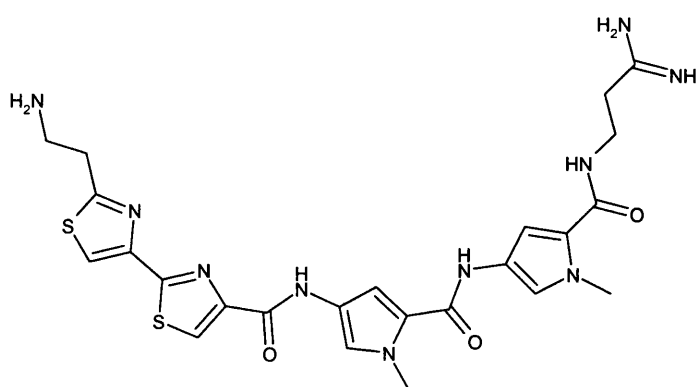
Figure 3.2c: Lexitropsin featuring the G/C selective bithiazole moiety of Bleomycin

In fact, Distamycin analogues (known as lexitropsins) including heterocycles with a hydrogen acceptor heteroatom in the correct position (pyridine, imidazole, thiazole, furan…) are capable of tolerating or even recognising a G:C base pair. **(Figure 3.2d)** (Bailly and Chaires, 1998).

thiazole
S inward

furan

Pyrazole

thiazole
N Inward

NH$_2$
C$_2$

H$_2$N C$_2$

Imidazole

thiophene

G
G
G

G
G
G

NH$_2$
C$_2$

Triazole

H$_2$N C$_2$

oxazole

H$_2$N C$_2$

NH
R

C$_2$
NH$_2$
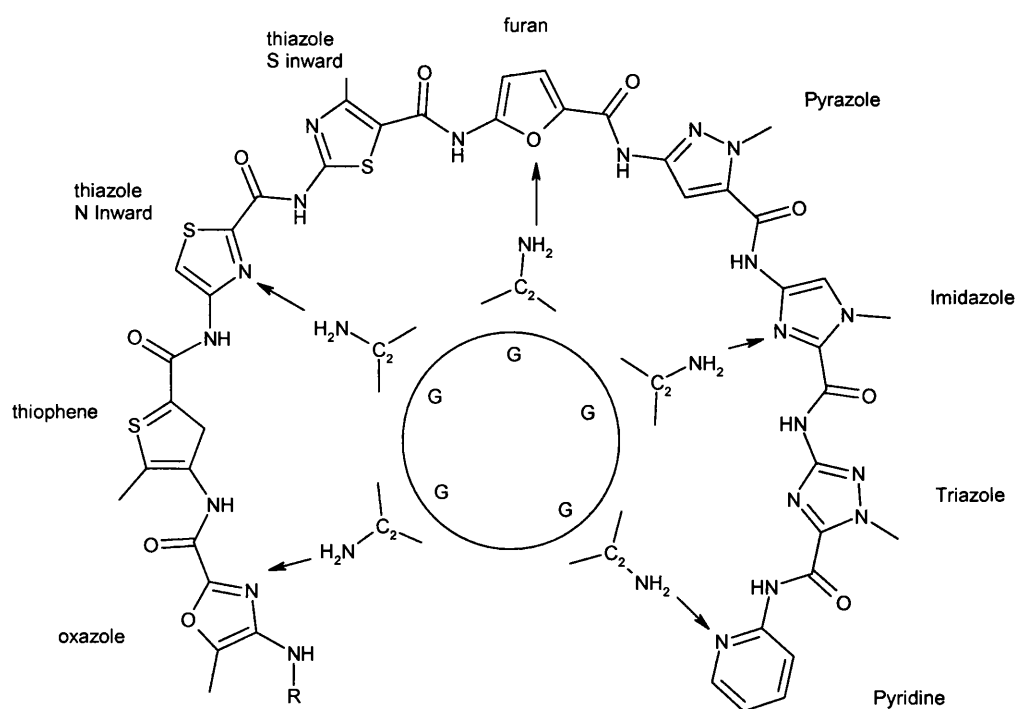
Pyridine

Figure 3.2d: Representation of a hypothetical lexitropsin featuring H bond acceptor heterocycles such as pyridine and imidazole. These heterocycles are able to bond with the exocyclic guanine amino group as depicted by the dotted arrows.

3.2.5 The 2:1 binding mode

Selectivity and binding affinity varies depending on the number and position of heterocycles in the lexitropsins. It is fascinating that some lexitropsins possess remarkable selectivity for some short DNA sequences. It was discovered in 1989 (Pelton and Wemmer, 1989) that the minor groove is just wide enough to accommodate two stacked ligands. The very tight fit thus provided renders the complex thermodynamically stable and allow each ligand to recognise one strand of DNA (with again an H bond acceptor unit such as Imidazole being able of interacting with guanine's exocyclic amino group.

The lexitropsin ImPyPy (dyst analogue) was observed to stack in an antiparallel fashion and to recognise the G(A/T)C sequence. These results generated the first pairing rules for DNA recognition: an imidazole stacked on top of a pyrrole targets a G:C base pair (with the guanine on the imidazole side), whereas pyrroles stacked on each other are selective for A:T base pairs.

Py / Im targets C•G

Py / Py targets A•T and T•A

Im / Py targets G•C
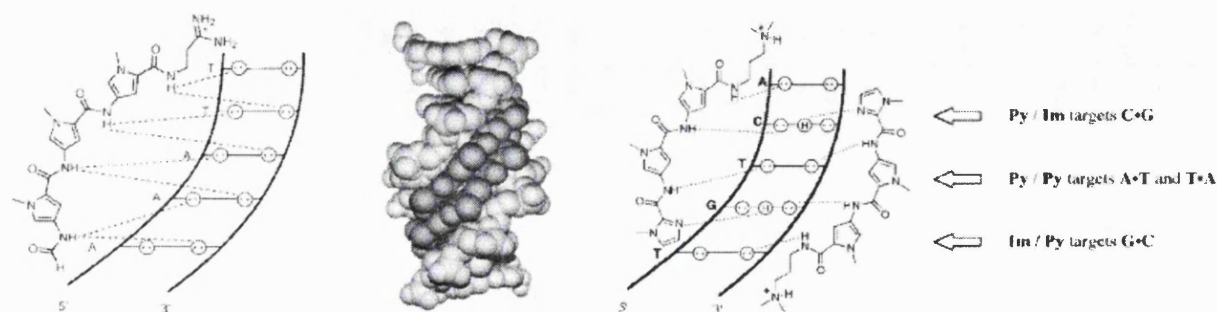
Figure 3.2e: Distamycin (left) binding in the 1:1 binding mode. Lexitropsin ImPyPy (right) binds in the 2:1 mode within a set of rules. The imidazole binds on the guanine side through an additional hydrogen bond. (Melander *et al.*, 2004).

It can be seen in **Figure 3.2e** that the N-methyl groups of the pyrroles and imidazole point out of the groove. The ring nitrogen thus offers a potential site of attachment for auxiliary moieties, that could improve the physico-chemical properties of the polyamides. For example an isopropyl group increases hydrophobic interactions and enhance activity (James *et al.*, 2004), whereas branching of a sugar group at this position afford water-soluble compounds with improved biological properties (Kumar and Lown, 2003). This position can also be considered when designing covalently linked polyamides. This latter possibility will be discussed further in this thesis.
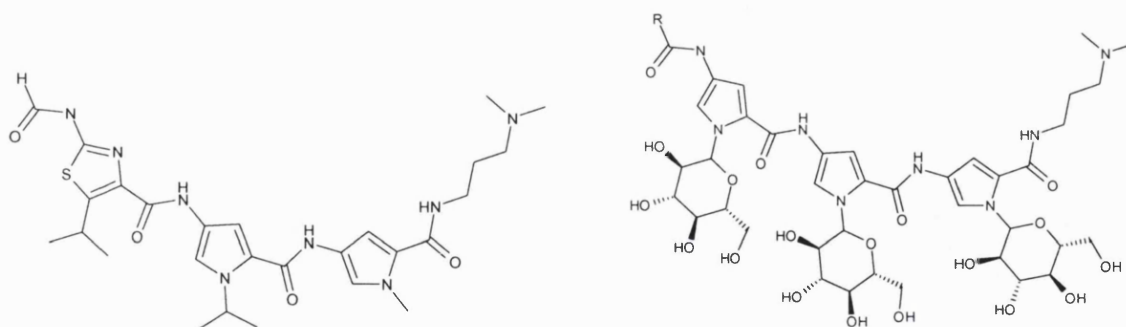
Figure 3.2f: A lexitropsin containing a N-isopropyl pyrrole and the more liphophilic thiazole equivalent (left). A glycosylated distamycin analogue. The sugar moiety confers enhanced water solubility.

These discoveries triggered a sharp rise of interest in small molecule DNA recognition, but so far, only a few groups have actively pursued a systematic exploration of the possibility offered by these ligands.

3.3 Rational for Coupling an Alkylating Moiety to a DNA Recognising unit: the Role of the Alkylating Moiety.

3.3.1 Knocking out an oncogene with a non-alkylation moiety: advantages and disadvantages.

When considering the different strategies for optimum gene recognition, it is useful to approach the problem from a medicinal chemistry perspective: the primary aim is to create a drug that will selectively disable an oncogene whilst causing the least toxicity to healthy tissue.

All of the interactions listed previously (van der waals, H-bond, ionic...) are relatively weak and above all: reversible. The only way one of these ligands could stop an oncogene expression is by binding to its promoter with a superior affinity than the transcription factors themselves. For an optimum result, two or three of these ligands should be used in conjunction as there are usually more than one transcription factor binding sites within the promoter.
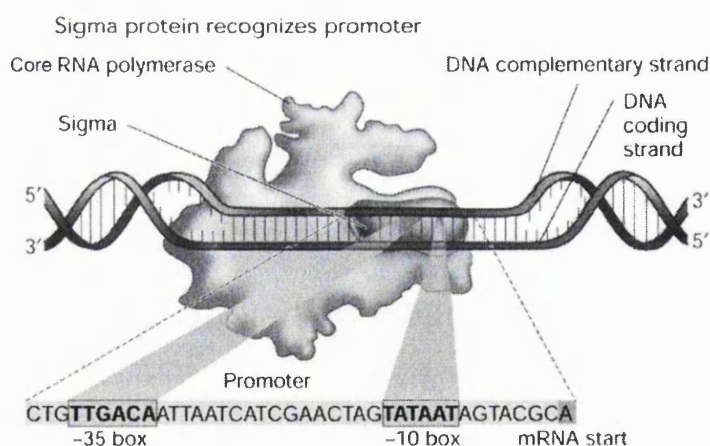
Figure 3.3a: This picture shows how gene transcrition is initiated by binding of a protein (transcription factor) to a promoter. Some short sequences (bold) in the promoter are critical as they are recognised by the transcription factors. These short sequences can be targeted by polyamides to prevent transcription. (http://fig.cox.miami.edu/~cmallery/150/gene/sf13x5a.jpg)

50

In addition, the combination of three of these small recognising elements binding to three promoter regions would probably be unique (or at least, highly selective) and would not cause disruption of the rest of the genome. It would therefore be unlikely to cause any significant toxicity.

However, this approach entails several limitations due to the reversibility of the binding.

First, the strategy does not work when targeted at the transcribed region of the gene as the ligands are easily displaced by the transcription machinery. This poses a serious problem when targeting a gene where a mutation has occurred in the transcribed region (disabling the promoters would also prevent transcription of the healthy, non-mutated, genes). As described earlier, the transcription factors binding sites are separated and cannot be all covered by a single small molecule. In contrast, a single ligand covering 16 contiguous base pairs in the coding region of the gene would be able to provide specificity. This conveys an advantage, as it is simpler for a drug company to submit a single molecule, rather than a mixture of three different compounds, to the regulatory agencies.

Second, because the ligand does not stay covalently attached in the groove, it can eventually escape to be metabolised and excreted. A constant supply of fresh binder would therefore be necessary to permanently deactivate the oncogene.

3.3.2 Project objectives: an alkylation moiety coupled to a DNA recognising moiety.

As a result, it would be extremely attractive to attach the gene recognising moiety to a covalent binder (a molecule capable of reacting chemically with the DNA and form a covalent bond with one or more of its bases, see **Figure 3.3b**) such as a mustard (Wurtz and Dervan, 2000), a CPI (Shinohara *et al.*, 2004; Chang and Dervan, 2000) or as it is the case in this project: a PBD.

Recognition unit   Alkylating moiety

G   G   T   A   C   T   G   A   G   A

Mutation region
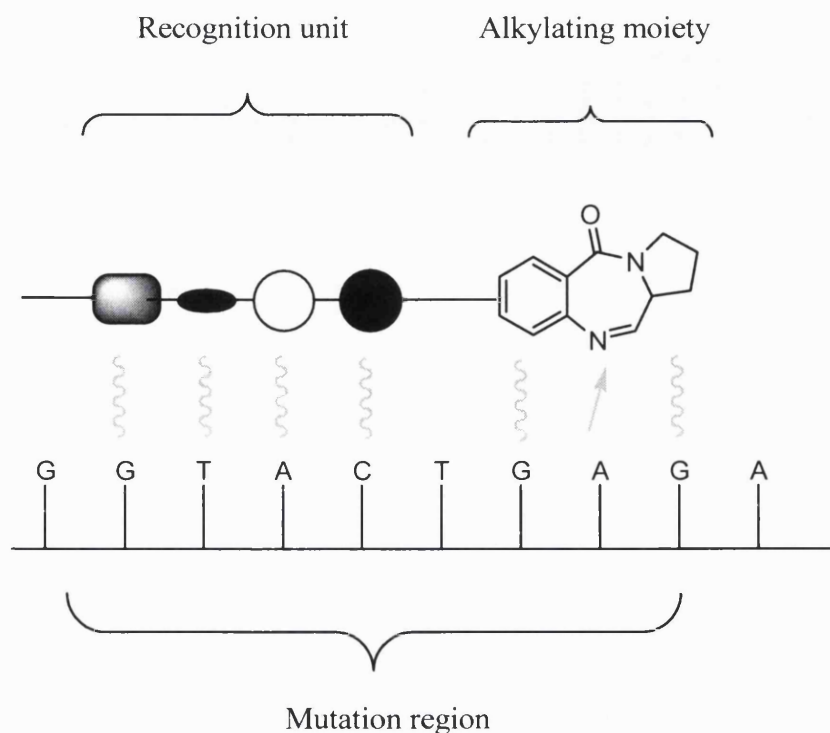
Figure 3.3b: Chimera concept (above). The heterocyclic polyamide recognises target DNA, followed by covalent binding by the alkylating moiety. Some alkylating agents are shown below: PBDs are G/C specific whereas CPI are A/T specific. Nitrogen mustards historically have been amongst the most widely used alkylating agents in cancer treatment.

a PBD   a CPI   a nitrogen mustard
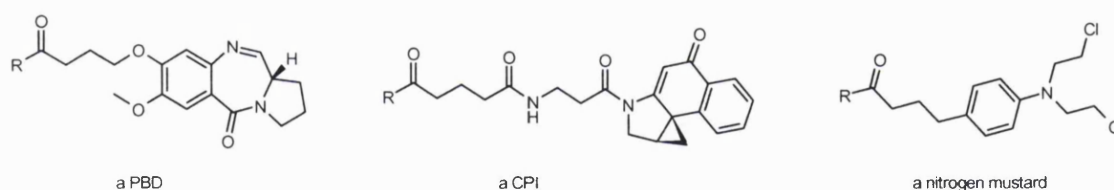
Figure 3.3d: Alkylating and binding agents suitable for conjugation with DNA recognising moieties.

Additionally, the alkylating moiety can affect the pharmacokinetic properties of the hybrids by conferring improved membrane permeability and water solubility. Naturally occurring covalent binders may be capable of sharing their active transport properties with the rest of the molecule.

However, introduction of a covalent binding moiety, would almost certainly increase the cytotoxicity of the hybrid molecules. It is also possible that the inherent cytotoxicity of the molecules could mask any gene specific effects:

It may nevertheless not be absolutely necessary to target alkylating damage to a single lesion on an oncogene to achieve therapeutic benefits.

3.4 Different strategies for discovering sequence selective DNA therapeutic agents.

Historically much of the research into sequence selective DNA binders has revolved around naturally occurring molecules (e.g. Distamycin) or individual synthetic compounds such as Hoechst 33258. (Buchmueller *et al.*, 2005a and 2005b ; Khalaf *et al.*, 2004; Anthony *et al.*, 2004; Baraldi *et al.*,2000 and 2004).

However, it should prove fruitful to apply a more systematic approach to this developing field. There are at least three different possible strategies to allow the discovery of new and more selective DNA binding drugs.

3.4.1 The Boger approach: High throughput screening of DNA binding agent libraries.

Statistical analysis of the human genome suggests that there is a high probability that any given 16 bp sequence would be unique in the genome. A smaller molecule targeting a shorter DNA sequence (8 bp) with sufficient affinity and an adequate pharmacological profile could bind preferentially to oncogenic DNA rather than non-oncogenic DNA. (Discrimination by a factor of 10 would already make a significant difference). This would be superior to today's anticancer DNA binding drugs and sufficient to bring patient benefits.

In this case, a high throughput approach can be applied, screening libraries (small or large) of low molecular weight DNA ligands against target oncogenic DNA or cancer cells.

In a key paper (Boger *et al.*, 2000b), Dale Boger laboratory described the synthesis of 2640 distamycin analogues using a solution phase approach, in conjunction with high-throughput screening to determine relative DNA binding affinity or DNA binding sequence selectivity.

Both the synthesis and screening are of interest in terms of strategy. Simplicity is the key for success in high-throughput screening. First, the ligands were designed to be relatively short and cover only five base-pairs. This can be achieved by linking only three heterocycles together. The chemistry was designed in such a way as to avoid the use of complicated reactions and chromatography. Purification was achieved through acid base liquid-liquid extraction. Determination of sequence selectivity was not achieved by lengthy footprinting experiments, but by an ethidium bromide displacement assay (see **Figure 3.4a** below).

96-well plate containing a library of hairpin deoxyoligonucleotides. Each well contains one of all possible sequences

Addition of ethidium bromide or thiazole orange

nonspecific intercalation

Addition of DNA binding compound

DNA affinity is measured as a decrease in relative fluorescence (displacement of ethidium bromide or thiazole orange)

Define rank order binding and establish DNA sequence selectivity of an agent

5'-CGXXXXC $^{A\ A}$ $_A$ 5'-CGXXXXC $^{A\ A}$ $_A$
3'-GCXXXXG $_{A\ A}$ 3'-GCXXXXG $_{A\ A}$

4 base pair hairpin   5 base pair hairpin

X = A, T, G, C

Figure 3.4a: Dale Boger's high throughput screening approach.

Affinity is directly correlated to a decrease in fluorescence. Of course, cytotoxicity can be determined similarly, in a high-throughput fashion. Thus, a small molecule drug candidate can rapidly be discovered, with high DNA binding affinity against oncogenic sequences.

3.4.2 The rational approach to sequence recognition using heterocyclic polyamides.

Dervan et al. have adopted a different approach to sequence targeting. Focusing on a hairpin polyamide template that interacts with DNA in a 2:1 fashion, Dervan has compiled a set of rules, which, in principle, would allow the rational targeting of any selected DNA sequence.

3.4.2.1 The first hairpins

Capitalizing on Wemmer's landmark discovery of the 2:1 binding mode and the pyrrole/imidazole: C/G rule of recognition motif, Dervan constrained two lexitropsins to adopt a 2:1 binding mode by joining them together with an aminobutyric acid linker. The molecules thus form a hairpin when inserted in the minor groove. (Mrksich *et al.*, 1994). **Figure 3.4c**, further down.

3.4.2.2 3-Hydroxypyrrole and recognition of T/A *versus* A/T.

The early polyamides were capable of recognising a G or a C, yet were not capable of breaking the degeneracy between a T/A bp and an A/T bp. A third building block was required to recognise the asymmetric cleft on the thymine side. Molecular modelling studies concluded that the addition of an hydroxy group in the pyrrole 3-position would be selectively destabilizing towards adenine for steric reasons, but favourable towards thymine thanks to the possibility of one or more hydrogen bonds to the lone pairs electrons of O(2) of T. (White *et al.*, 1998; Urbach *et al.*, 1999). **Figure 3.4b**
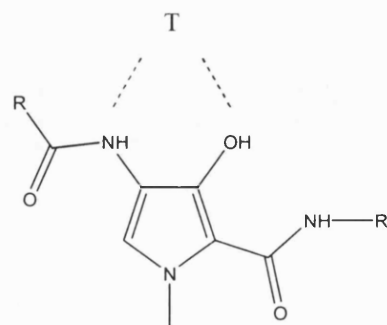
Figure 3.4b: Stucture of hydroxypyrrole. Possible hydrogen bonding with Thymine are shown in dotted lines.
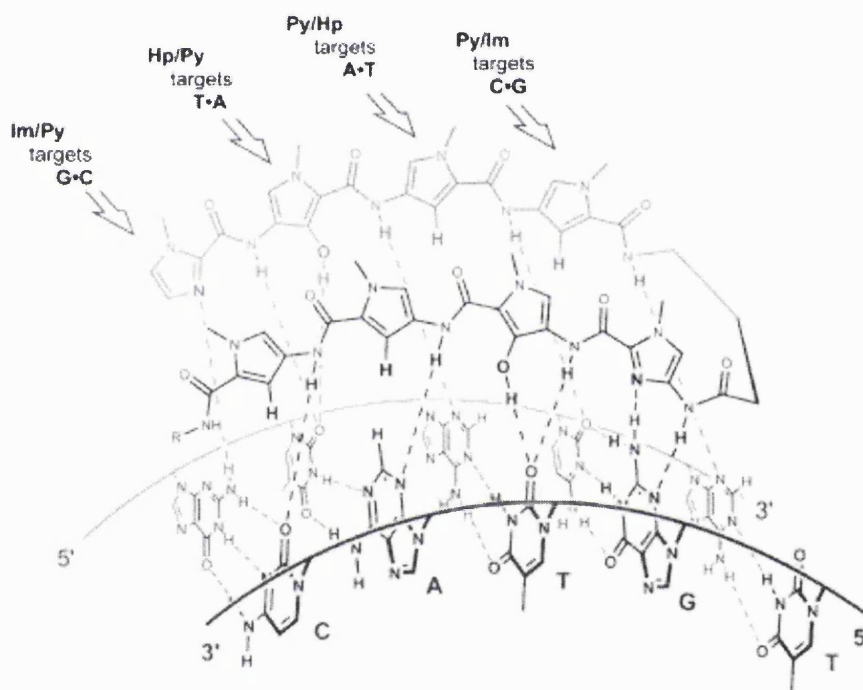
Figure 3.4c: Perspective view of a hairpin binding in the minor groove. Hydrogen bonds are clearly visible (dotted lines). Hydroxypyrrole recognises T through two hydrogen bonds. (Dervan and Edelson, 2003).

The synthesis and footprinting of hairpin polyamides containing imidazole/pyrrole pair, the hydroxypyrrole/pyrrole pairs allowed Dervan to formulate a set of rules allowing the rational targeting of short DNA sequences.

Table 3.4a: 2:1 binding mode rules of recognition

Pair	G•C	C•G	T•A	A•T
Im/Py	+	-	-	-
Py/Im	-	+	-	-
Hp/Py	-	-	+	-
Py/Hp	-	-	-	+

In theory, these hairpin polyamides are capable of recognising any 4 bp DNA sequences sandwiched between two degenerate A/T base pairs (e.g. (A/T)GACT(A/T)). The flanking A/T sequences arise from interactions with aminobutyric acid derived loop and the dimethylaminopropyl tail.

Figure 3.4d: Drawing of a typical hairpin. Tail and loop region recognise A/T in a degenerate fashion.

Tail: A/T degenerate   Core: Precise targeting   Loop: A/T degenerate
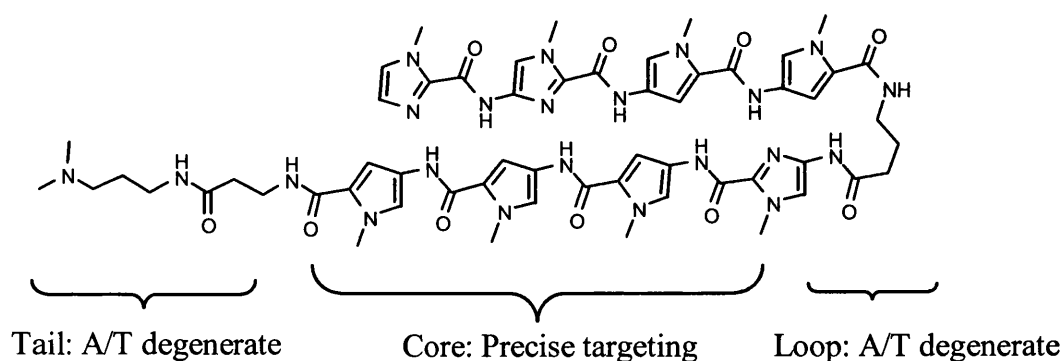
3.4.2.3 Hydroxybenzymidazole, β-alanine and other building blocks

As the hydroxypyrrole is relatively unstable, it can be replaced by a 3-hydroxybenzimidazole building block, although it has to be introduced as a dimeric unit. Likewise, the imidazopyridine (Ip) building block can replace imidazole when coupled to a pyrrole. This allowed the formulation of new set of rules (Renneberg and Dervan, 2003):
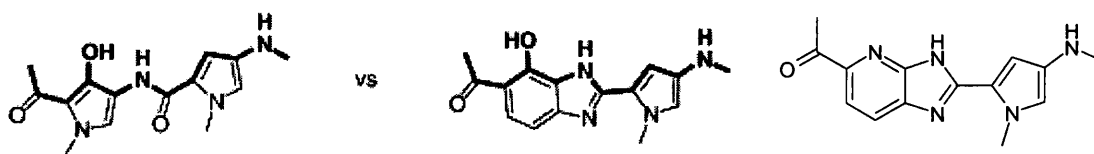
Figure 3.4e: Hydroxybenzimidazole versus hydroxypyrrole (left). Imidazopyridine (right).

Table 3.4b: 2:1 Pairing code for Hz and Ip

Pair	G•C	C•G	T•A	A•T
Ip/Py	+	-	-	-
Py/Ip	-	+	-	-
Hz/Py	-	-	+	-
Py/Hz	-	-	-	+

The role of β-alanine as a flexible linker, allowing the polyamide to keep in register with the minor groove structure has already been mentioned. Later, it was discovered (Turner *et. al.*, 1998) that substitution of pyrrole by β-alanine can be dramatically beneficial, even in relatively short hairpins (8 heterocycles).

For example, the pyrrole in ImPyImPy-γImPyImPy-βdp can be advantageously replaced by β-alanine to give ImβImPy-γImβImPy-βdp. This β-alanine substitution is very important at positions next to an imidazole (and especially between two imidazoles) as it resets the imidazoles in phase with the guanine amino group. The β-ala unit can be used to replace Py to give another set of rules.

Table 3.4c: 2:1 pairing code for β-alanine.

Pair	G•C	C•G	T•A	A•T
Im/β	+	-	-	-
β/Im	-	+	-	-
Py/β	-	-	+	+
β/Py	-	-	+	+

3.4.2.4 Additional features of Dervan's hairpin design: Loop, tail, terminal heterocycle.

- The loop:

Hairpin affinity has been enhanced by the substitution of amino butyric acid by R-2-4-diaminobutyric acid. The free chiral amino group can be left uncapped or provides a handle to attach alkylating agents or further DNA recognising units (as in tandem hairpins). It is noteworthy that, in contrast to the S isomer, the R isomer respects the natural twist of the DNA and has a much higher binding affinity. (Herman *et al.,* 1998).

- The tail:

If no alkylating moieties are present in the molecule, a cationic charge (as provided by a charged amino group at physiological pH) has to be introduced to enhance binding by ionic interactions. A charged tail was present in the form of an amidine or a guanidine in netropsin and distamycin, but has been replaced in hairpin by a simpler tertiary amine. There still is some debate whether the tertiary amino group is optimum for binding activity, but it is certainly much easier to introduce chemically. Indeed, since Dervan's team turned to solid phase chemistry (see solution versus solid phase chemistry, appendix section), the tail depends on the resin and chemistry used. Typically, cleavage off the resin involves aminolysis with dimethylaminopropylamine on a β-ala linker. (Swalley *et al.,* 1999).

It is interesting that this design precludes accurate DNA recognition both at the loop and tail level as both moieties show fail to discriminate between A/T and T/A base pairs.

- The terminal heterocycle:

It is quite striking that until recently, Dervan's group has only reported hairpin polyamides with an imidazole in the terminal position, therefore biasing their choice of target sequence to those exhibiting a G/C at this particular position (see **Figure 3.4e**). Indeed, it was not possible to target the opposite sequence (C/G) with a pyrrole in terminal position until the introduction of a β-ala next to the imidazole (Wang *et al.*, 2001).

Likewise, hydroxypyrrole at the terminal position is not very efficient at recognising T/A. The lack of recognition was attributed to the freedom of rotation inherent to the terminal position. 3-methoxy and 3-chlorothiophene are being investigated as more efficient substitutes. (Foister *et al.*, 2003).
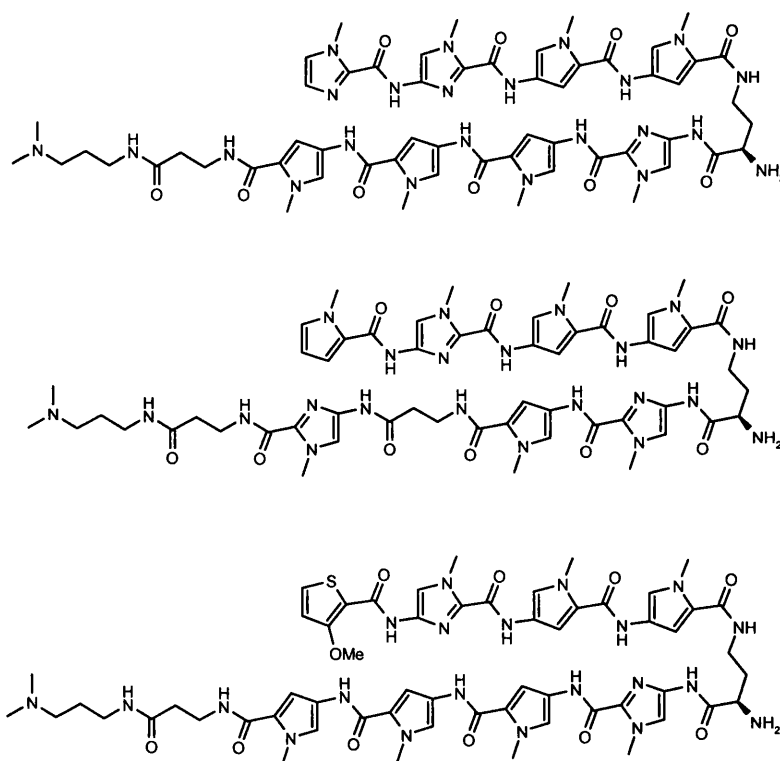
Figure 3.4e: Terminal position occupied by an imidazole (top). It is now possible to reverse the terminal pair and recognise the desired C/G bp by inserting a β-ala next to the imidazole (middle). The terminal position is not well suited for hydroxypyrrole because of its high rotation freedom. Studies performed on methoxythiophene (bottom) suggest this moiety could be suitable for T/A recognition.

Interestingly, in 2005, Buchmueller *et al.*, (2005c) initiated the use of 3-methylpicolinic acid as a terminal heterocycle. This acid is more convenient and couples in better yield than its imidazole counterpart, but retains its specificity for guanines.

3.4.2.5 Other designs investigated by Dervan's team.
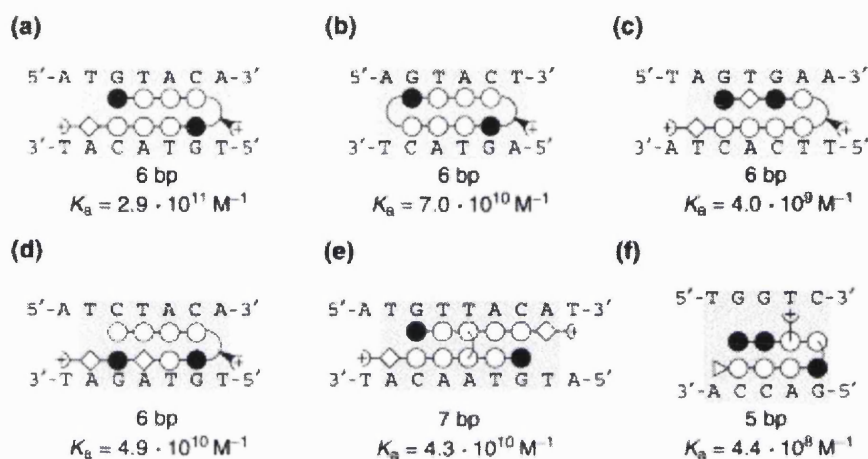
Figure 3.4f: Summary of Dervan's short designs. A) Standard Design. B) Cyclic polyamide. C) β-ala between a pair of imidazoles. D) β alanine next to a terminal imidazole on the C strand. E) Crosslinked "H-pin". F) Crosslinked "U-pin".

Figure 3.4f presents some additional exemples of polyamides designed by the Dervan's group. Design b) is a cyclic polyamide. Although more challenging to synthesise, these polyamides show higher affinity than non-cyclised analogues with the same number of cationic groups. (Cho *et al.,* 1995; Herman *et al.,* 1999b).

Design e) and f) are respectively named H-pin and U-pin because of their shape. They show higher affinity than non-linked analogues. However, H-pin are usually symmetrical for synthetic reasons and are therefore limited to palindromic DNA sequences (Greenberg *et al.,* 1998). The U-pin design (Heckel and Dervan, 2003) is interesting as it represents a way of abolishing the loop present in a standard hairpin design. Indeed, the loop is not a DNA recognizing element in its own right and is not useful in this respect. A pyrrole and an imidazole can be linked together at the bottom of the U-pin and precisely recognize a G:C.

(a)

5′-A A G G G A A T C C C T T-3′

3′-T T C C C T T A G G G A A-5′

11 bp

$K_a = 1.4 \cdot 10^{10} \, M^{-1}$

(b)

5′-A G C A G C T G C T-3′

3′-T C G T C G A C G A-5′

10 bp

$K_a = 1.9 \cdot 10^8 \, M^{-1}$

(c)

5′-A T G G C A T A C C A T-3′

3′-T A C C G T A T G G T A-5′

10 bp

$K_a = 7.5 \cdot 10^{10} \, M^{-1}$

(d)

5′-A A G T G A A G T G A-3′

3′-T T C A C T T C A C T-5′

10 bp

$K_a = 3.2 \cdot 10^{10} \, M^{-1}$
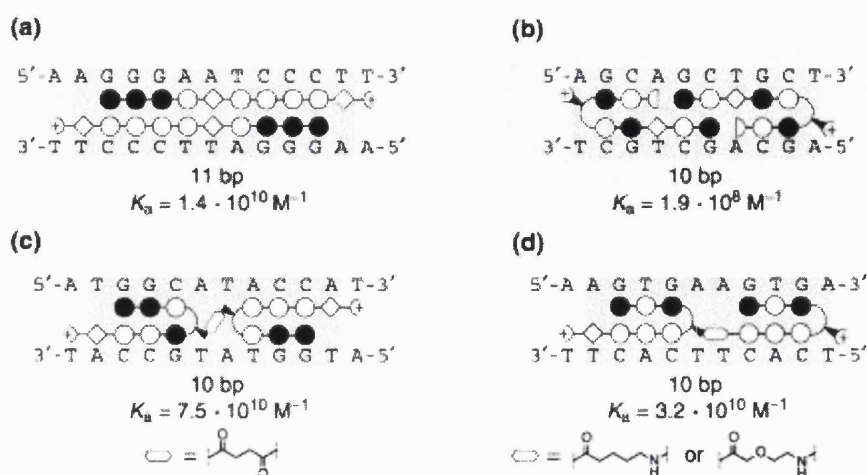
Figure 3.4g: A) fully overlapping homodimers. B) cooperative dimers. C) and D) tandem hairpins.

Figure 3.4g presents some of the longer polyamide designs published by the Dervan's group. Fully overlapping dimers (a) is suitable for palindromic DNA sequences. Cooperative dimers (b) seek to extend the recognised DNA length with the aid of a cooperative region. However, the target DNA has to be symmetrical and the binding affinity poorer than for most hairpin.

Tandem hairpins (c) and (d) solved the problem and recognise recognise long DNA (c 12 bp) sequences with good specificity and excellent binding affinity. (Herman *et al.*, 1999a; Kers and Dervan 2002).

3.4.2.6 Biological effects

As Dervan's approach is systematic and grounded in rational design, initial biological experiments were mostly performed on naked DNA (plasmid), typically in footprinting assays. This allowed Dervan's team to focus on DNA binding affinity and apply relevant data to inform molecular modelling studies. However, this did not allow routine investigation of the cellular activity. Therefore, cell-based experiments were required to assess *in vivo* behaviour in greater depth. In particular, Py-Im polyamides were known to be cell permeable but failed to penetrate the nucleus in most cell lines, with the exception of some lymphoid cells (Belitsky *et al.*, 2002). However, in a recent and extensive investigation with polyamide-dye conjugate, (Best *et al.*, 2003) concluded "nuclear localization is a property of polyamide composition, molecular weight, ring sequence, location, and identity of the fluorophore and composition of the dye ring linker" (NB: it is necessary to attach a fluorophore to the polyamide for nuclear localization studies).

In other words, when synthesizing a polyamide with a therapeutic goal, one can never be certain of its nuclear penetration capabilities. Even if the hairpin did penetrate, it is not guaranteed that the target DNA sequence will actually be available for binding. Instead, the target DNA sequence may be rendered inaccessible by histone binding or folded deep into the chromatin structure. Thus, the polyamide could fail in whole cells or *in vivo*, even if it binds successfully to the target DNA sequence in naked DNA.

3.4.2.7 Summary of the fundamental approach used by Peter Dervan.

Dervan and his team have developed an elegant, systematic and rational approach. This approach allowed the discovery of new building blocks and designs to improve DNA binding and selectivity. *In fine*, the research group formalised a set of rules to use these building blocks and designs.

However, this approach also entails several limitations: The necessary iteration loops between chemists, biologists, molecular modellers and crystallographers can be rather lengthy. The biological activity can be disappointing *in vivo* due to poor absorption or poor accessibility of target DNA. The choice of targeting the longest possible sequence (up to 16 bp) requires the design of long and complex molecules (tandem hairpins). It is complicated, long, and expensive to synthesise, with added flaws like non-recognising linkers and loops.

3.4.3 From cell screening to DNA target sequence:

Initially, Dervan and co-workers investigated binding to simple naked DNA sequence. However, the approach did not accurately predict activity in more complex systems and such as whole cells. More recently Gottesfeld and Dervan have taken the opposite approach, conducting their primary screening studies on whole cells.

In a recent study (Dickinson *et al.*, 2004), Gottesfeld and his team have screened a small library of hairpin polyamide-chlorambucil conjugates (a ligand with covalent binding capabilities, as in our studies with pyrrolobenzodiazepines) against a human cancer cell line. One molecule, 1R-Chl, (**Figure 3.4h**) induced growth arrest and morphological changes. Subsequent investigation including the use of DNA microarrays, led to the identification of one gene (coding for histone H4c), being particularly down regulated.
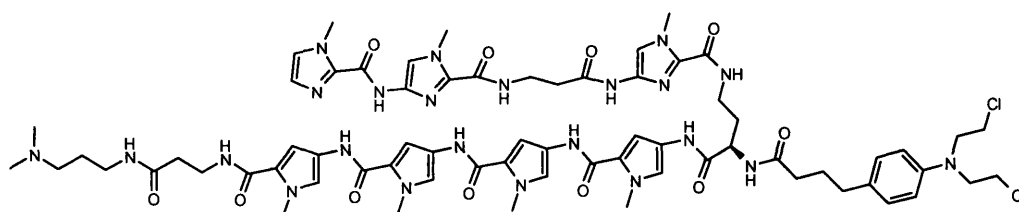
Figure 3.4h: A pyrrole/imidazole nitrogen mustard hybrid. This molecule recognises and alkylates selectively a 6 bp long DNA sequence in the H4c gene, stopping SW60 cancer cells proliferation with no obvious toxicity.

Histone H4c is a key component of cellular chromatin and is up regulated and indispensable for the proliferation of certain cancers. H4c was then validated with matching SiRNA, which induced the same morphological changes than 1R-Chl. A H4c DNA fragment including four match sites was used in DNase I footprinting studies. Two match sites were well bound ($K_{d\ s}$= 0.3 and 0.7 nM). The two other match sites were polypurine tracts, which are known not to be bound by hairpin polyamides. (Dervan and Edelson, 2003). Ligation mediated PCR further demonstrated direct binding and alkylation of the H4c gene by 1R-Chl in live SW620 cells.

The discovery approach adopted by Gottesfeld and co-workers is initiated by morphological and cytostaticity screening on live cells and only latter focus on gene targeting and footprinting studies. This strategy allows the discovery of molecules, which are found active in cells whatever their possible targets. The reverse approach risks failure by poor nuclear penetration in the later stages of the discovery process.

In conclusion, not only did this approach led to the discovery of one molecule blocking cancer cell proliferation, but it also helped to understand the influence of one gene and its protein on biocellular mechanisms.

3.5 Conclusion and Project aims

This chapter was written in such a way as to provide the reader with a sense of what is possible to achieve with small molecule DNA binders, and to describe a variety of strategies on how to achieve it. The project presented in this thesis aims at synthesising anticancer DNA binding agents using all of the aspects of the above strategies, within the laboratory capabilities: i.e.: fundamental research on molecule design, small library synthesis, and biological investigation in cells and using high-throughput assays.

As we think it may be necessary to endow the DNA recognising molecule with an alkylating moiety, our molecules will be composed of pyrrole-imidazole polyamides, linked to a pyrrolobenzodiazepine capping unit. To our knowledge, no PBD has ever been coupled with a polyamide capable of interacting with DNA in the 2:1 binding mode (such as hairpin polyamide). Hybrids studied until now were always relatively short and never forced in the 2:1 binding mode (and therefore, of limited selectivity). Examples provided by Dervan and Sugiyama using polyamides coupled to nitrogen mustards and CPI are extremely encouraging and stimulating as they are putting the theory into practice. It will be of great interest to discover all the new properties conferred by the PBD, on the biological activity of the polyamide. (DNA targeting, active transport system, nuclear membrane penetration...).

4 Synthetic Strategy and Building Blocks

4.1 Introduction

A modular strategy employing a small number of key building blocks has been adopted to synthesise the molecules described in this thesis. Linking these building blocks together does not only rely on modified peptide coupling chemistry, but most importantly on the judicious choice of protecting groups to cap reactive functionalities.

Building blocks synthesized during the course of the project can be divided in three families: First and foremost, the PBD capping units. At least 5 discrete syntheses of PBD capping units have been completed during the project. Although the same PBD ring system has been conserved, the protecting groups, the linker, the reactive functionality and the degree of unsaturation have been varied. Additionally, the syntheses of pyrrole and imidazole building blocks are also described. Although the pyrrole synthesis was relatively straightforward and remarkably well described in the literature, the imidazole synthesis required the investment of some time and effort before being of practical value. Remaining building blocks such as linkers and loops could be purchased from chemical suppliers.
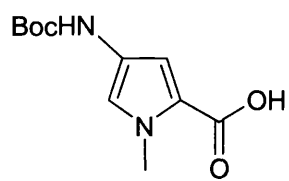
Boc pyrrole amino acid
86
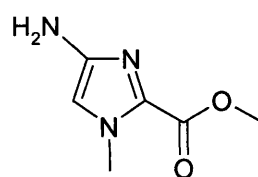
Imidazole amino ester
98
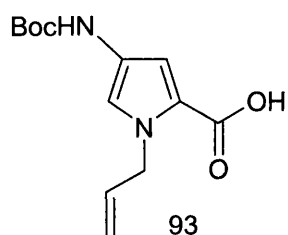
Boc Allyl-pyrrole amino acid
93
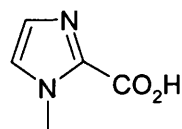
1-Methyl-2-imidazole acid
100
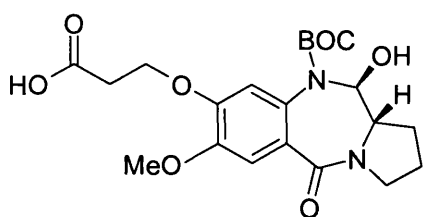
3C Boc PBD acid
37
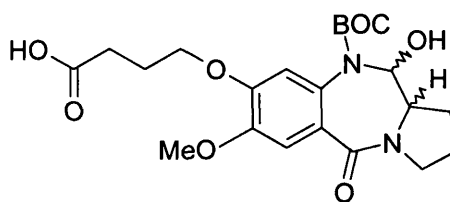
4C Boc PBD acid
46
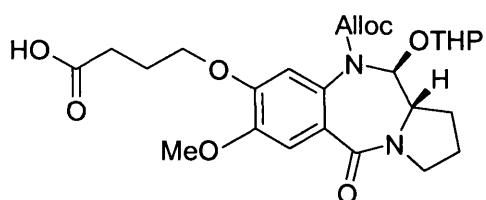
4C Alloc THP PBD acid
57
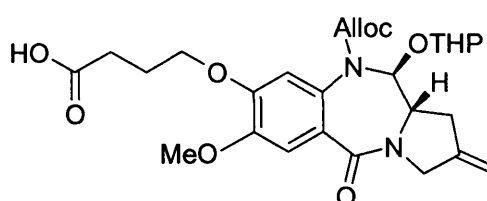
4C Alloc THP C2 exo unsaturated PBD acid
77
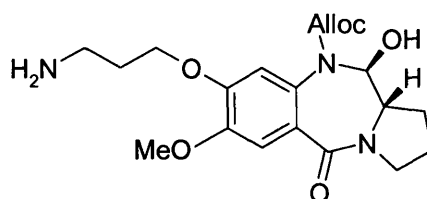
3C Alloc PBD amine
66

Figure 4.1a: A selection of the main building blocks synthesised during the project

67

4.2 PBD building blocks: Synthesis

4.2.1 Introduction

The five PBD building blocks shown in the previous figure are the result of a continuous review of syntheses and biological activity. The global group strategy required the building blocks to be versatile enough to be used on solid phase or in solution. It also required the synthesis to be practical on a large scale. This, in turn, determined what sort of chemistry could be used.

The key consideration in the synthesis of PBD capping units is the nature of the N10 protecting group. Being removed in the last step, it needs to resist the variety of conditions experienced in the prior steps. The deprotection step must proceed smoothly, in high yield, as the compounds are extremely precious and sensitive at this final stage of the synthesis. Once the N10 protecting group has been chosen, an orthogonal side chain ester must be selected to mask the terminal carboxylic acid (or amino group). Three combinations previously used are shown below.
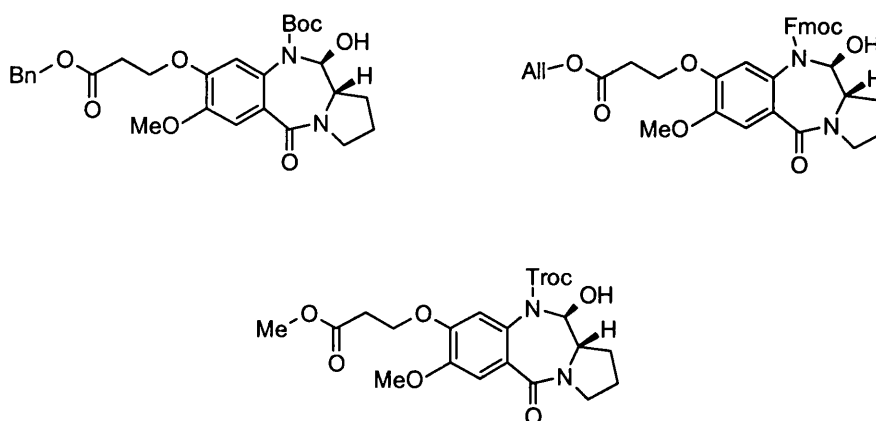
Figure 4.2a: Protecting groups combinations previously used in the research team.

The initial Troc protected capping unit required the use of toxic reagents (e.g. cadmium) to remove the protecting group and is inconvenient for solid phase work.

The second, Fmoc protected capping unit, was found to be convenient for solid phase synthesis but required tedious chromatography (prohibitive on a large scale) after palladium catalysed (expensive) removal of the allyl ester.

The latter Boc protected capping unit was considered ideal for solid phase synthesis and could be prepared on a large scale. It can be used orthogonally with a benzyl ester, which can be easily removed by hydrogenolysis. The free acid does not require chromatographic purification and can be used directly in subsequent steps. The project therefore started with the synthesis of acid PBD capping unit **37** using this combination of protecting groups. Although no inventive steps were introduced during this initial synthesis, it provided a reference against which subsequent strategies could be compared. The synthetic route had been developed and optimised by a number of chemists and was reasonably practical on a large scale, however a few remaining challenges were identified.

4.2.2   3C-Boc protected PBD acid: (Synthesis by the traditional route)
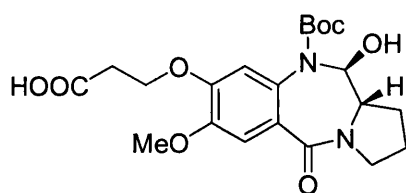
The synthesis commenced with ether bond formation on the aromatic A-ring. Etherification was performed under classical conditions, the phenoxide nucleophile displacing the bromine from 3-bromopropanol acid to afford the product in 71% yield. Treatment of ether **30** with concentrated nitric acid (70% in water) allowed two steps to be performed in one-pot, both oxidation of the aliphatic alcohol to a carboxylic acid, and introduction of a nitro group at the 2-position of the aromatic A-ring occurring simultaneously. A first crop was obtained by direct filtration, and a second by extraction. However, it was decided to discard the extracted batch because it was impure and hazardous to retrieve. Indeed, the ethyl acetate used in the extraction can occasionally react violently with the residual nitric acid.

Chemoselelective esterification of the aliphatic acid with benzyl alcohol provided the desired monoester **32** in 60 % yield. Forcing conditions such as a dean stark approach failed to improve the yield, and instead, led to diester formation. (Dr Luke Masterson, unpublished work).
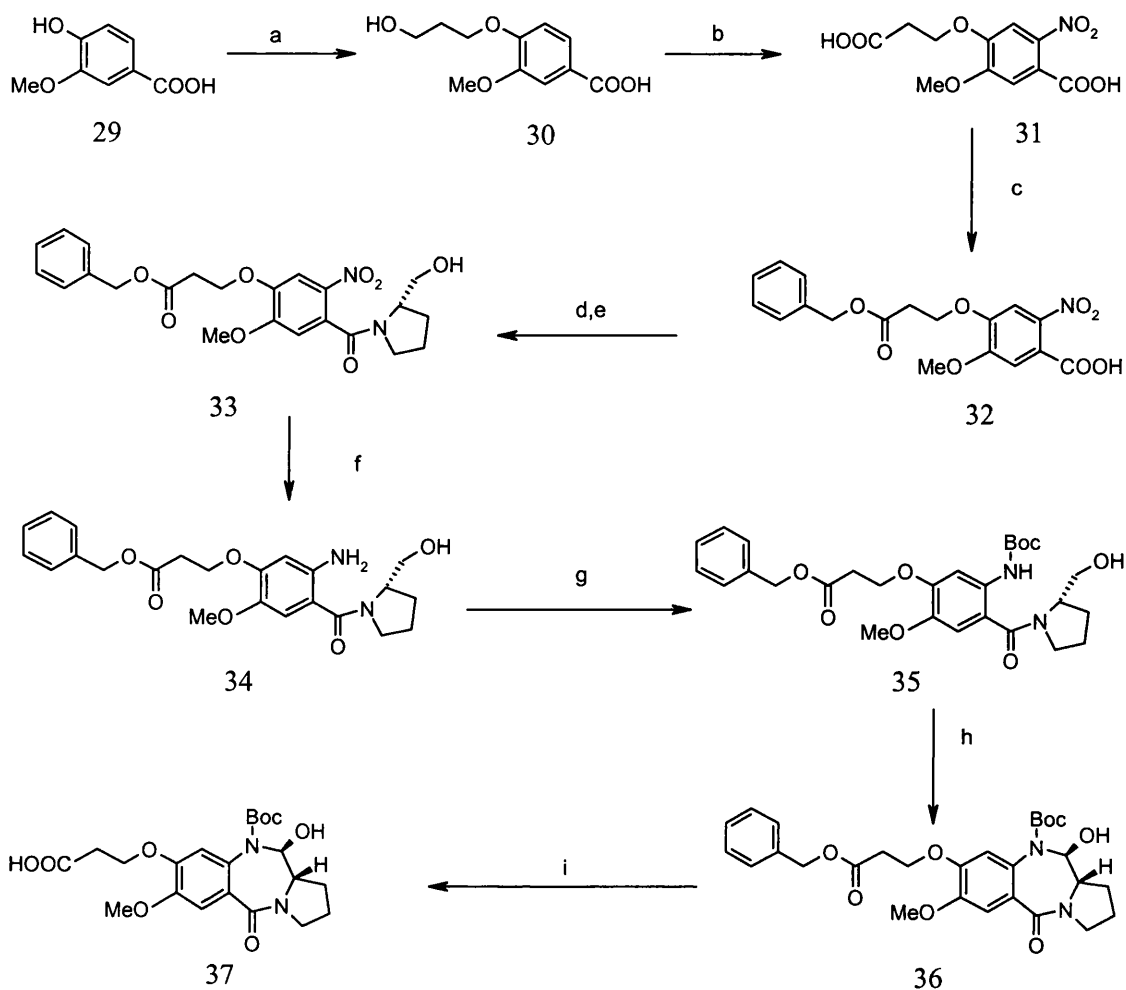
Reagents: (a) 3-bromopropanol, aq. NaOH, reflux, (71%); (b) 70% HNO₃, (60%); (c) benzyl alcohol, PTSA (56%); (d) oxalyl chloride/DMF, dry CH₂Cl₂; (e) 2(S)-(+)-pyrrolidinemethanol, Et₃N, dry CH₂Cl₂, (98%); (f) SnCl₂.2H₂O, MeOH, (98%); (g) (Boc)₂O, THF, (99%); (h) pyridinium dichromate, 4A mol seives, dry CH₂Cl₂, (35%); (i) 10% Pd/C, EtOH, (100%);

Scheme 4.2a: 3-C BOC PBD acid synthesis.

The aromatic acid **32** was then activated by treatment with oxalyl chloride, and coupled with 2(S)-(+)-pyrrolidinemethanol. Here, another difficulty was encountered, in the form of the pro-C11 primary alcohol off the five-membered ring. Although less nucleophilic than the secondary amine, it would still be capable of reacting with the acid chloride to provide an ester. Aside from protecting the alcohol, the only way to prevent this side reaction is through careful control of reaction conditions. A limited quantity of acid chloride was added dropwise over a long period, at low temperature affording the amide in quantitative yield.

70

The amide coupling reaction therefore constitutes a limiting step in the scale up process, and must be repeated in order to provide large quantities of intermediates.

The next step involved reducing the nitro group to the amine required for the B-ring formation. Although hydrogenation is usually considered the method of choice, the presence of a benzyl ester precluded its use. Instead, the nitro group was reduced with tin (II) chloride in quantitative yield. After work up, the sensitive amino group **34** was quickly protected as a carbamate with Boc dicarbonate.

With the N10 group protected it was now possible to attempt the B-ring cyclisation. The reaction involves the oxidation of the primary alcohol to an aldehyde, followed by cyclisation in one-pot. As the product of ring closure is a carbinolamine, overoxidation to the dilactam is possible and a number of oxidation methods have been investigated. There are many methods of closing the PBD B-ring, and each approach has its advantages and drawbacks. Swern oxidation is usually the method of choice. The reagents are cheap and although malodorous by-products are formed, the reaction avoids the use of environmentally harmful metals.

However, the reaction requires careful control of the reagent addition to avoid dilactam formation and this can lead to prohibitive reaction times on a large scale. Moreover, this approach is not compatible with the final hydrogenolysis step. Sulphur species produced in the Swern reaction are known, from experience, to poison the catalyst and prevent hydrogenolysis. Ring closure can also be achieved with pyridinium dichromate although some loss in yield is caused by entrapment of product in the chromium by-product. This method was eventually adopted for its convenience and the cyclised compound **36** was isolated in 35% yield.

Finally, benzyl ester deprotection by hydrogenolysis afforded the Boc protected acid capping unit **37** in quantitative yield. The overall yield was 7.6% over 8 steps.

4.2.3 4C-Boc protected PBD acid: (New route)

More recently, molecular modelling studies revealed that a four-carbon linker would be superior compared to the 3-carbon linker, when linked directly to a pyrrole/imidazole polyamide. As demonstrated in **Figure 4.2b**, the span of two methylenes groups is not long enough to allow the heterocyclic chain to fit snugly in the minor groove without clashing with the PBD moiety. The first heterocycle is flipped out of the minor groove, thus preventing it from binding. (Dr Charlie Laughton, Zara Sands, University of Nottingham).
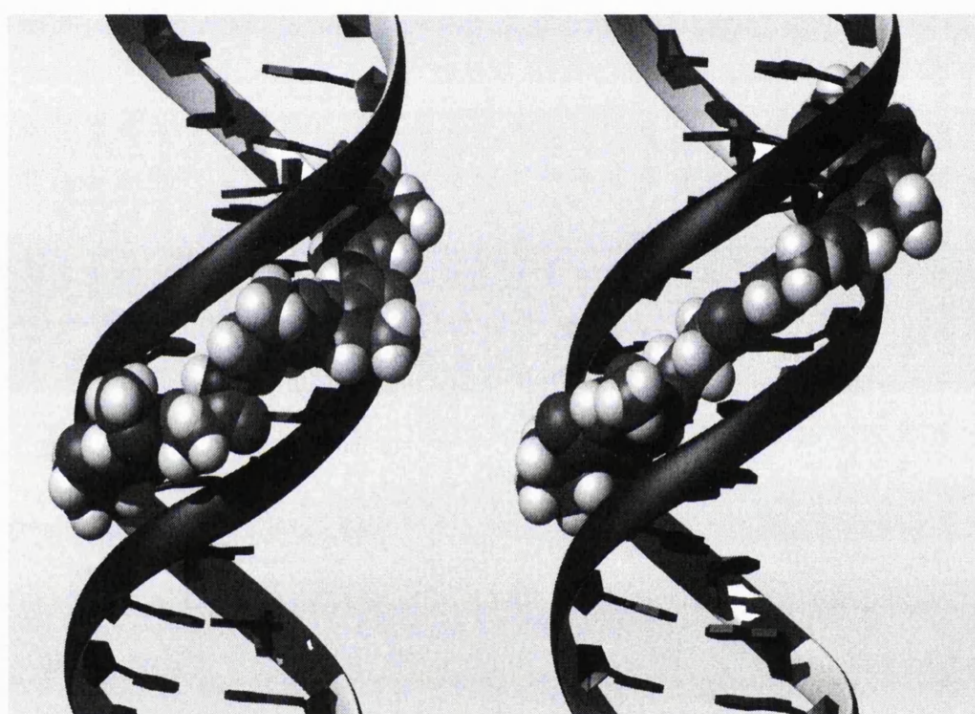
Figure 4.2b: 4C PBD polyamide conjugate (right) shows superior binding affinity to 3C PBD polyamide conjugate (left).

It was therefore decided to synthesize a 4-carbon linker BOC-protected-PBD-acid building block. This provided the opportunity to revisit and improve the synthesis by removing difficult or inefficient steps. For example, the nitration reaction was inconvenient and slightly hazardous, the benzyl ester formation occurred in unsatisfactory yields due to inefficient chemoselectivity, nitro reduction could not be achieved by hydrogenation because of the benzyl ester and the final oxidation could not

use the Swern procedure because the sulphur by-products poison the Pd/C catalyst needed for the benzyl ester deprotection.

Clearly, benzyl ester substitution by the simpler methyl ester should circumvent, if not eliminate, most of these problems. The initial steps of the synthesis are described in the literature, whereas new compounds are described from the pyrrolidine-methanol coupling.
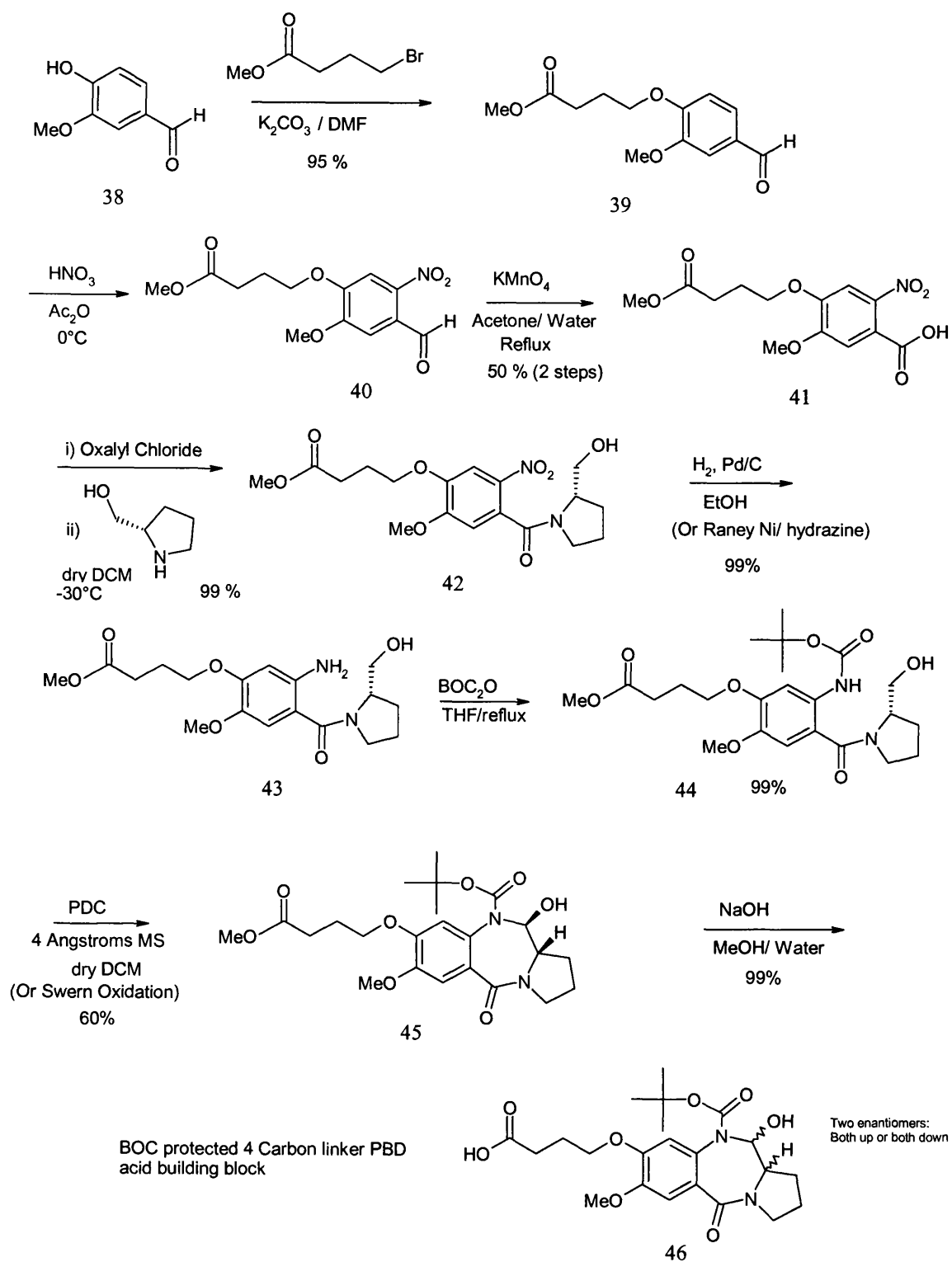
Scheme 4.2b: 4C-Boc protected PBD acid synthesis

Vanillin was alkylated with methyl bromobutyrate in DMF at room temperature, overnight. High yields of product (95%) were easily retrieved by filtration after precipitation in water.

Nitration of ester **39** with nitric acid in acetic anhydride proceeded smoothly and without incident. The product precipitated efficiently from ice-water (unlike the nitro substituted diacid formed in the C3 synthesis, which was partially soluble in water) obviating the need for extraction. However it was observed that if the precipitate was allowed to remain in the diluted reaction mixture overnight, some ester hydrolysis occurred.

Treatment of nitro aldehyde **40** with aqueous potassium permanganate afforded the required acid. During the work up, sodium thiosulphite was used to remove manganese impurities and addition of HCl triggered the product precipitation. (50% over the two last steps).

The C-ring was installed by the same method described in the previous section. However, the reaction temperature was lowered from –20°C to below –30°C in order to prevent any side reaction with the primary alcohol on pyrrolidinemethanol. The pure product **42** was obtained on a large scale and in quantitative yield.

It was then possible to reduce the nitro group by catalytic hydrogenation, to afford amine **43** in quantitative yield. Alternatively, the nitro group could be reduced with Raney nickel and hydrazine hydrate. However, care was required when performing this reaction due to the pyrophoric nature of the Raney nickel. As in the previous synthesis, Boc anhydride protected the free amino group smoothly in quantitative yield.

Two methods were investigated in order to oxidise the primary alcohol and promote B ring closing. Previously, a pyridinium dichromate mediated oxidation reaction had been employed to close the PBD B-ring. Apart from the convenient nature of the method, it had been chosen because the alternative Swern reaction could not be used, as it leads to poisoning of the catalyst in the subsequent hydrogenation reaction.
With a simple methyl ester replacing the benzyl group, Swern oxidation provided the ring-closed product **45** in 60% yield. (instead of 35% with the PDC method).

The methyl ester was hydrolysed with aqueous sodium hydroxide in methanol. The reaction proceeded slowly at room temperature to afford the pure material in quantitative yield. Raising the reaction temperature to 70°C increased the reaction rate, but at the expense of the overall purity.

The acid building block **46** was thus isolated in very good yield (30% overall, 4 times better than the old route) using standard procedures. The product was obtained as a crystalline solid allowing the possibility of purification through recrystallisation rather than chromatography.

Although this synthesis marked a significant improvement in yield and practicality over the previous route, some problems came to light when the capping unit was used in the development phase of PBD-polyamide hybrid synthesis. Firstly, although the N10 BOC protecting group was ideally suited for solid phase methods, the necessarily strong acidic conditions can trigger side reactions and have to be stringently controlled. On the longer substrates, this can become a significant challenge, causing arduous purification and loss of yield. Secondly, preliminary coupling experiments with short polyamide chains produced a significant amount of side product. Indeed, the secondary alcohol found at the C11 position of the PBD capping unit was found sufficiently nucleophilic to react with activated species. (*i.e.* esterification). Finally, optical rotation values dropped to zero after saponification (**Chromatogram 4.2a**). Interestingly, Tercel *et al.* (2003) encountered the same problem during the synthesis of a related PBD capping unit: again, racemisation seemed to occur during saponification. They resolved this problem by substitution of the simple methyl ester, by a trichloroethyl ester that can be removed with zinc in formic acid.

Auto-Scaled Chromatogram
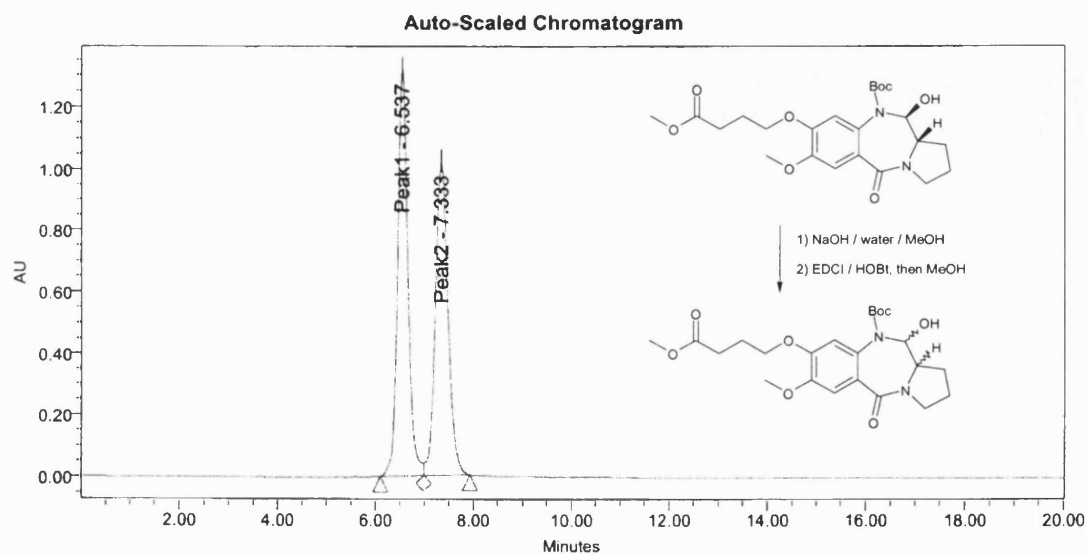
Chromatogram 4.2a: Racemisation at C11a during NaOH driven methyl ester hydrolysis.

4.2.4   4C-Alloc THP protected PBD acid

The capping unit synthesis was revisited in order to address the poor coupling and racemisation problems. The BOC protecting group was replaced by ALLOC to allow smooth and high yielding deprotection in the final step of target synthesis. As drops in optical rotation seemed to occur only in the presence of strong bases, the following potential mechanism of racemisation was proposed (see **Scheme 4.2c**).
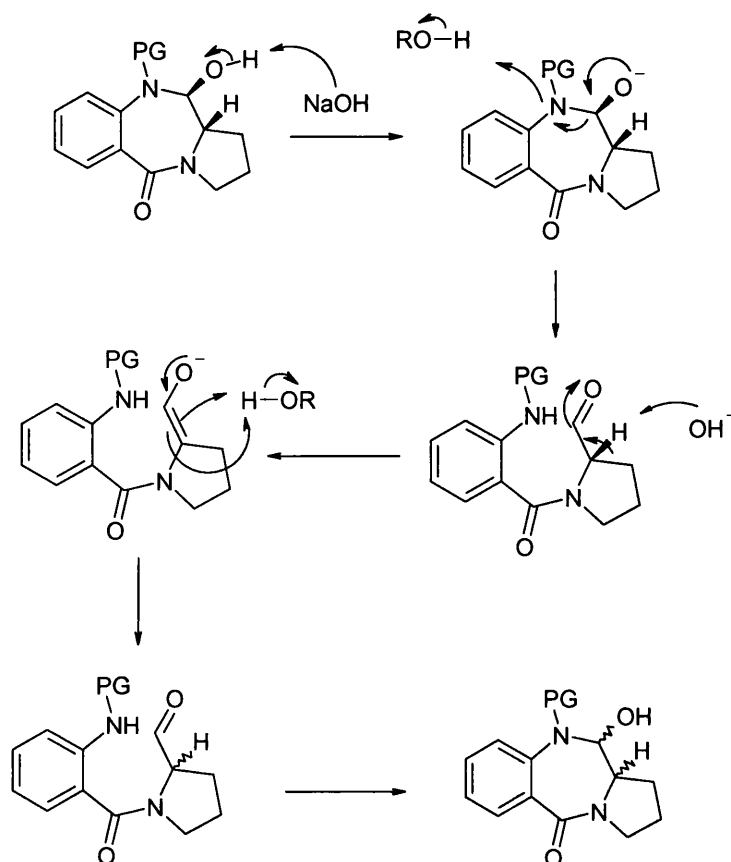
Scheme 4.2c: Possible mechanism of racemisation

Deprotonation of the 11-hydroxy group could trigger a Grob like fragmentation to open the B-ring and regenerate a transient aldehyde species. This aldehyde could enolise by abstraction of the acidic H-11a under basic conditions, abolishing chirality at this critical position. Subsequent equilibration back to the aldehyde followed by ring closure would afford the, now racemic, protected carbinolamine.

Based on this mechanism, it seemed that protecting 11-hydroxy group should prevent base mediated ring opening and racemisation. As an added bonus, it would also prevent side reaction from occurring during peptide coupling. Therefore, considerable effort was invested into finding the ideal 11-hydroxy protecting group. The method of introduction had to be suitable for large scale (*i.e.* no chromatography, ease of reaction) synthesis and avoid strong bases. A chiral HPLC column was purchased to complement optical rotation measurement and to monitor any racemisation (or the absence thereof) taking place.

A number of standard protecting groups and methods were investigated (see **Scheme 4.2d**). As mentioned above, conditions employed had to be only mildly basic, which meant that the alcohol itself (and not its anion) had to be the nucleophilic species. Vigorous heating or strongly acidic conditions were also proscribed.
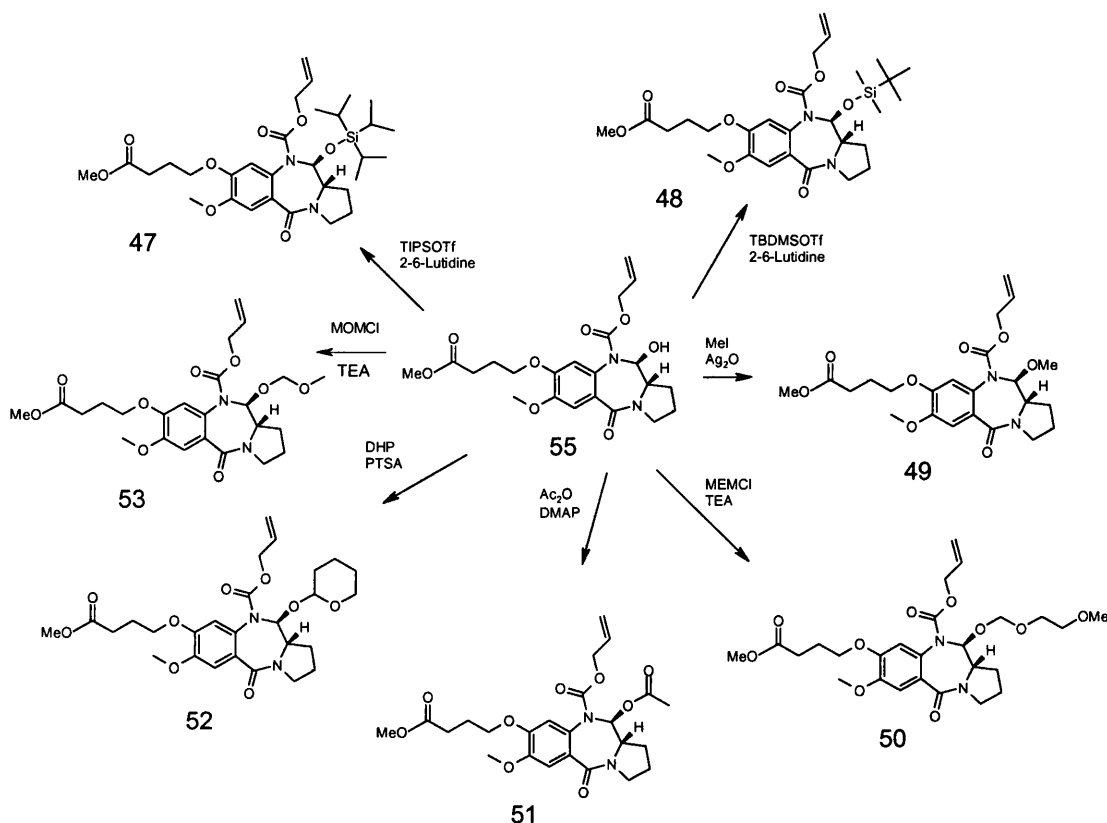
Scheme 4.2d: C11-hydroxy protection reactions

TBDMS protection using TBDMS triflate and 2,6-lutidine was successful and relatively clean. However, It still required chromatographic purification. Acetate protection was relatively easy to achieve, but was inappropriate on this methyl ester building block. Methylation was ideally suited for this purpose, as it would provide strong, orthogonal protection, and clear analytical data. A number of conditions were investigated, and the most promising was found to be MeI/ silver oxide in DCM. The reaction proceeded smoothly and optical rotation values were encouraging, however analysis by chiral HPLC revealed that partial racemisation had occured and produced 10% of the biologically inactive enantiomer. (**Chromatogram 4.2b**)
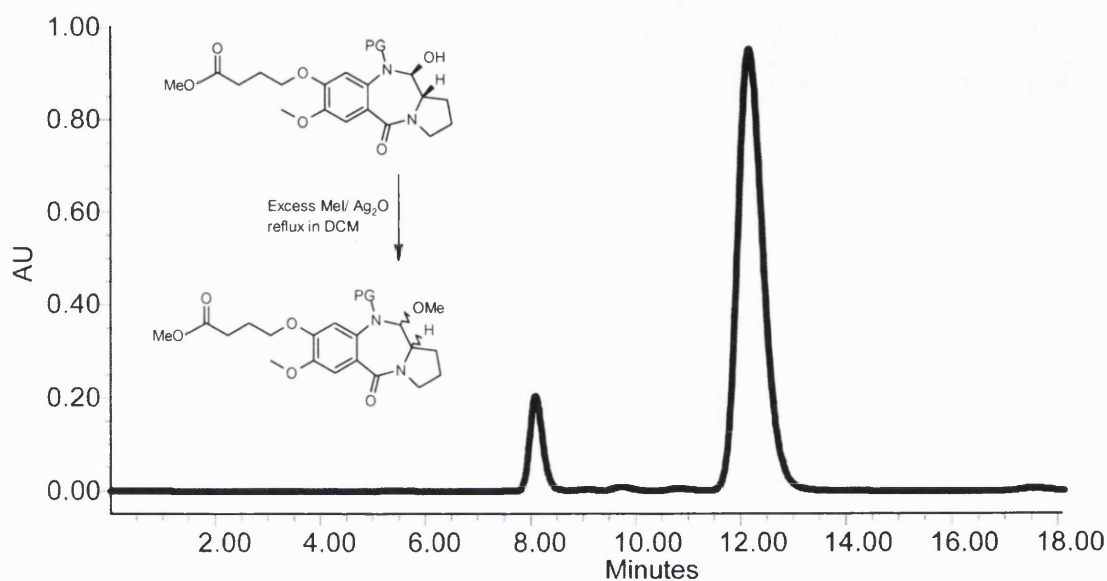
Chromatogram 4.2b: MeI/ Ag$_2$O driven protection produces 10% of undesired R-stereoisomer.

Although this represented a setback, further analysis revealed that the protected compound was now resistant to further racemisation during base treatment, thus providing important clues to confirm the mechanism of racemisation. Indeed, silver hydroxide is produced during the methylation catalysed by silver oxide. This hydroxide anion is then in position to initiate the racemisation mechanism, but only on the unprotected population. This explains the small proportion (10%) of R isomer produced during this reaction.

$$Ag_2O + ROH + MeI \rightarrow ROMe + AgI + AgOH$$
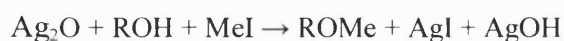
In retrospect, one way of preventing this partial racemisation from occurring would be to employ a silver catalyst producing non-basic (or weakly basic) species. Silver carbonate or silver nitrate may deserve consideration in any further investigation.

However, the most compatible protecting group with the chosen synthetic strategy was THP. Its introduction was fast and clean, with no need for further purification. It is base resistant, and thus, compatible with sodium hydroxide saponification. The complex NMR spectrum generated by introduction of THP did not represent an insurmountable problem, as the protecting group is only present for two additional steps in every target

80

synthesis. Optical purity was demonstrated by saponification, re-esterification, THP removal and analysis by chiral HPLC. Gratifyingly, as will be seen in subsequent chapters, peptide coupling using the protected capping unit were relatively clean, as a result of the absence of competition by hydroxy 11.

Protection Method	Clean TLC / Yield	Optical purity	Base resistance	Acid resistance
MeI /Ag$_2$O	Yes / 100 %	90 % S	Strong	Strong
Ac$_2$O/ DMAP	Yes / 100 %	100 % S	Weak	Medium
TBDMS/ Lutidine	Chromatography / 80 %	100 % S	Medium	Weak
DHP/PTSA	Yes / 100 %	100 % S	Strong	Weak

Table 4.2a: C11- hydroxyl protection methods summary.

Interestingly, the choice of 11-OH protecting group does not seem to affect imine formation following N10 deprotection (**Scheme 4.2e**). For example, TBDMS ethers are known to be stable to Pd(0)/pyrrolidine mediated Alloc deprotection conditions. However, exposure of **48** to these conditions resulted in formation of the imine rather than the silyl protected carbinolamine. This observation confirms the view that PBDs with electron donating substituents prefer to exist in the imine rather than the carbinolamine form.
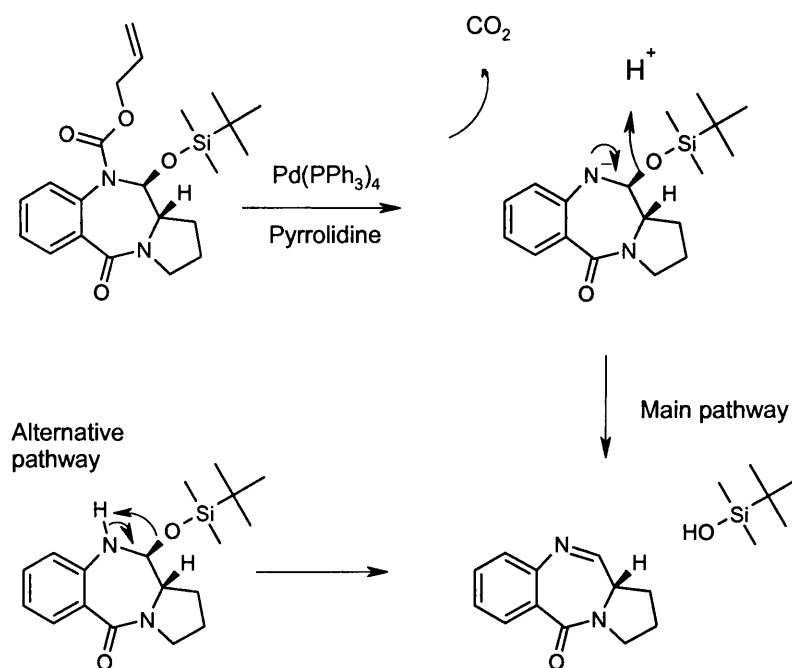
Scheme 4.2e: The nature of hydroxy 11 protecting group has no influence on the final N10 driven deprotection step.

Another improvement in the synthesis came with the introduction of TEMPO/BAIB mediated ring closing oxidation. The method is practically more convenient than the Swern procedure with equals or improved yields. (Masterson *et al.*, 2006). **Scheme 4.2f** shows the latter stages of 4C Alloc PBD acid capping unit synthesis.
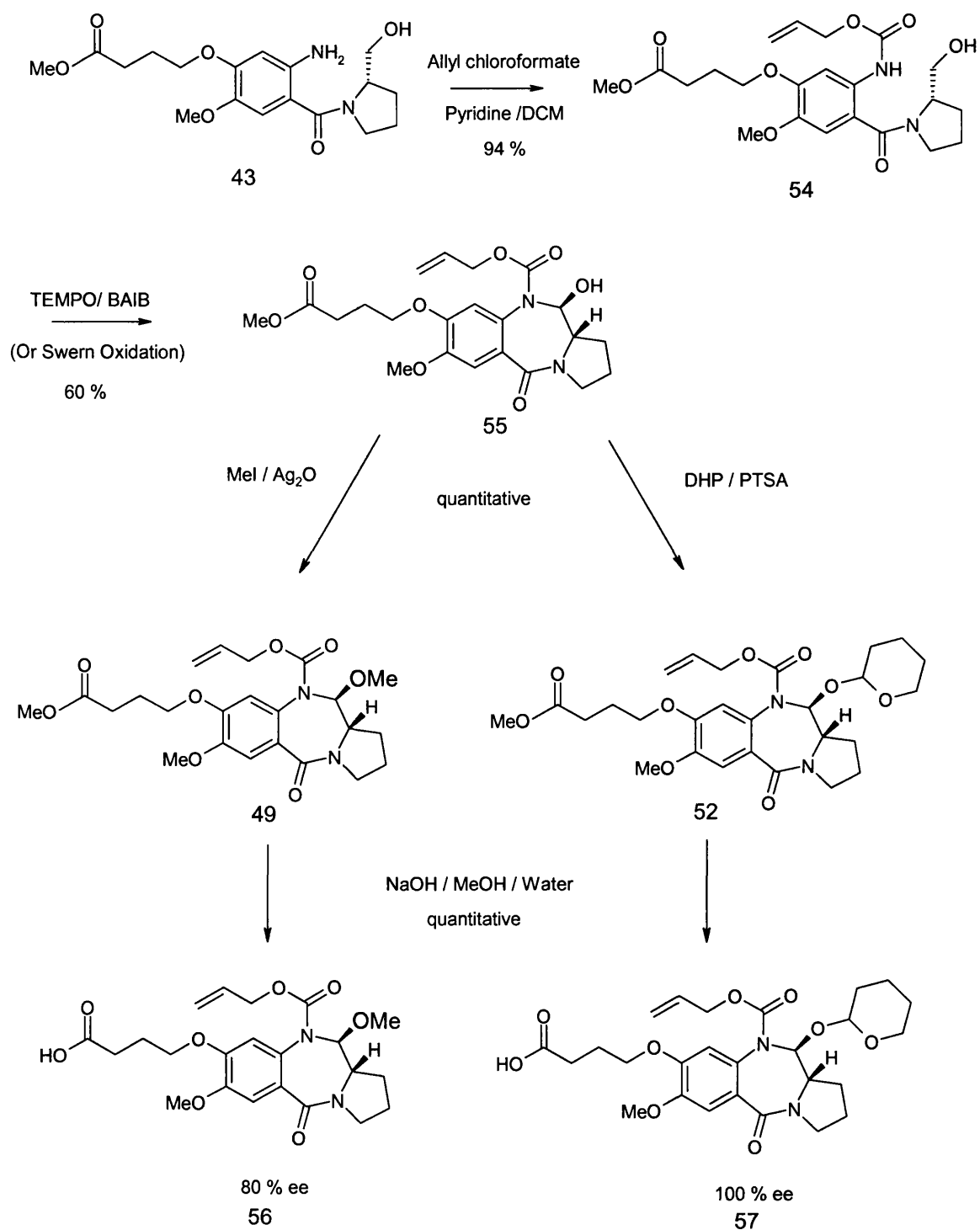
Scheme 4.2f: Enantioselective synthesis of 4C Alloc THP PBD acid. (final steps).
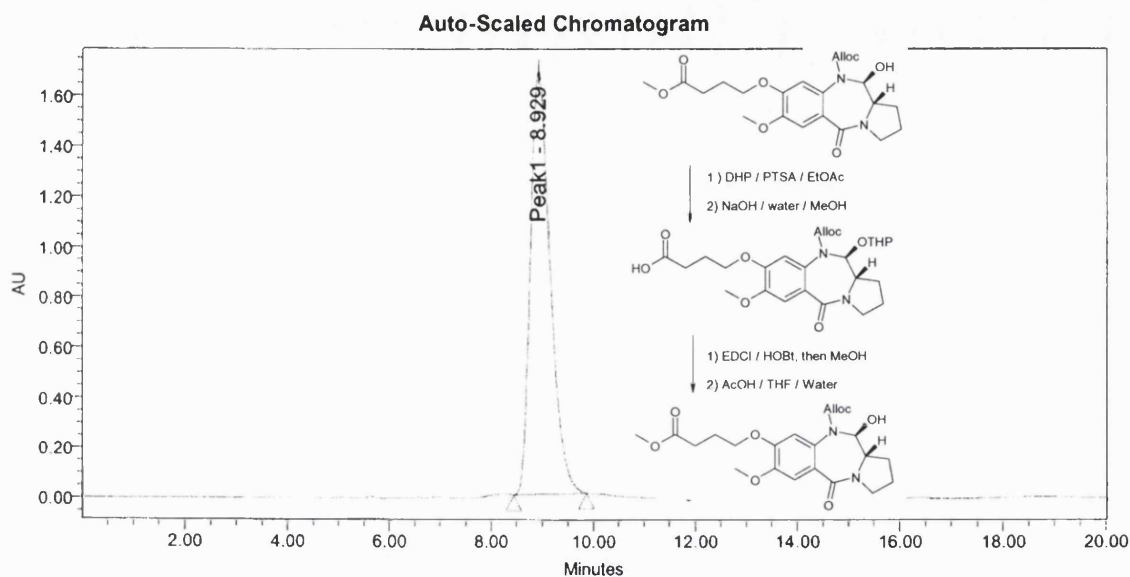
Chromatogram 4.2c: The scheme and the chromatogram demonstrate that THP protection prevents base-driven racemisation and that the 4C Alloc-THP PBD acid capping unit **57** is chirally pure. (the acid was reesterified in order to run in the column, and the THP removed for clarity)

4.2.5 3-C N10 Alloc, amino PBD capping unit

The PBD acid capping units were designed for coupling to the N-termini of heterocyclic polyamides. It would also be highly desirable to possess the capability to couple PBDs to the C-termini of heterocyclic polyamides as well. A PBD amino capping unit was therefore designed and synthesised to meet this need.

The 10 step synthesis of 3-C amino PBD capping unit is shown in **Scheme 4.2g**. The nitrophenol intermediate **60** was synthesised as previously published on a 50 g scale. The aliphatic BOC amino side chain was introduced by Mistunobu phenol etherification and the aldehyde was oxidised with potassium permanganate, as previously described (Fukuyama *et al.*, 1990). Impurities were removed by solvent trituration and acid/base liquid extraction.

In contrast to previous synthesis, the acid chloride coupling method was abandoned in favour of the milder EDCI/ HOBt coupling method. This allowed retention of the BOC protecting group, by avoiding the acidic conditions associated with acid chloride

84

formation. Hydrogenation of the nitro group in **63** was followed by immediate Alloc protection of the resulting amine. Ring closing oxidation was mediated by the TEMPO/ BAIB system as described in the acid PBD capping unit synthesis. The crude material was then subjected to the first and only chromatographic purification of the synthetic route to yield the protected capping unit **65**.

The final BOC deprotection required investigation of a range of conditions, as the resulting amine was relatively unstable. 4N HCl in dioxane was found to be too vigorous for this deprotection, but a mixture of TFA/DCM/water, 47/47/6, efficiently removed the BOC group in twenty minutes at room temperature. A DCM/ sat aqueous NaHCO$_3$ work-up was ineffective in extracting the free base, in contrast to a CHCl$_3$/conc aqueous ammonia system. Pure amino PBD capping unit **66** was thus retrieved as a white foam in a global yield of 10% (10 steps).

Chiral HPLC analysis (**Chromatogram 4.2d**) confirmed the optical purity of the capping unit, thereby demonstrating that an extraction with concentrated aqueous ammonia does not trigger the racemisation mechanism. (NB: only non-polar compounds could run in the chiral HPLC system, so the amino capping unit had to be re-protected with BOC). As the aliphatic amine is a good nucleophile, the 11-hydroxy group does not efficiently compete in peptide coupling and does not require protection. It was therefore possible to use the amino PBD capping unit as such in subsequent PBD-polyamide conjugate synthesis.
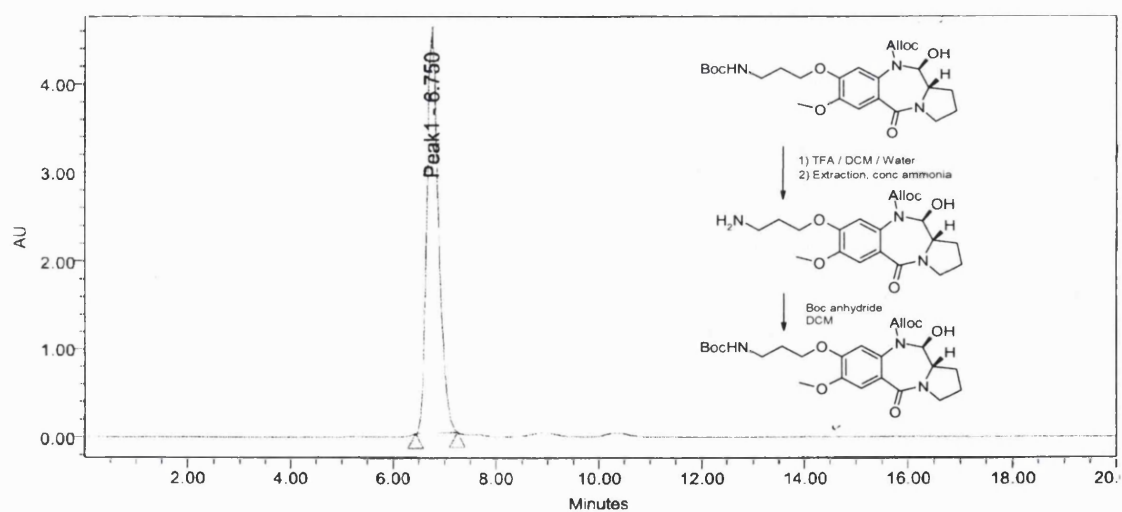
Chromatogram 4.2d: The 3C Alloc amino PBD capping unit is chirally pure and resistant to treatment with TFA or ammonia.
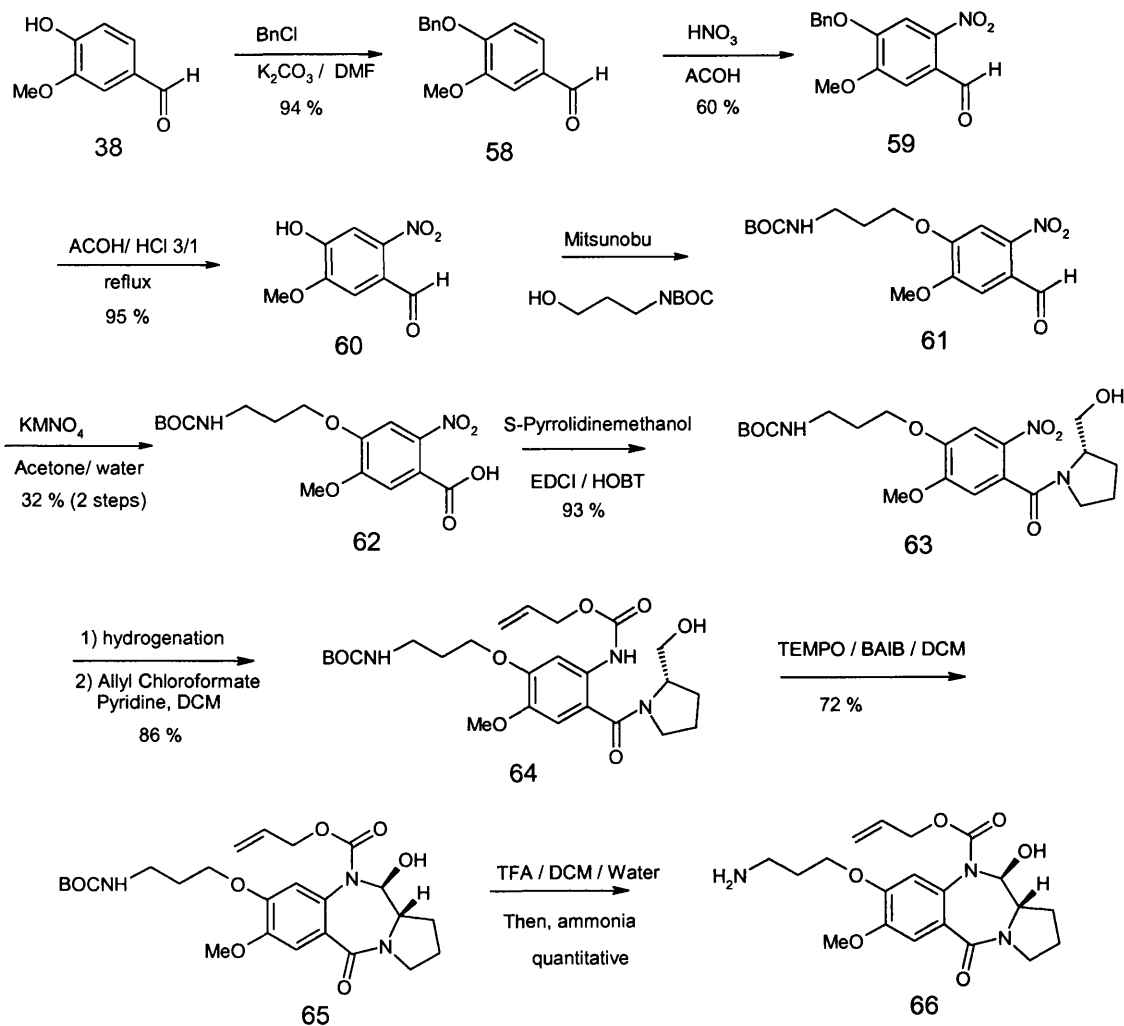
Scheme 4.2g: 3C amino PBD capping unit

4.2.6 4-C Alloc THP C2 exo-unsaturated acid PBD capping unit

The importance of the C2 unsaturation has already been discussed in chapter 2. Introduction of C2 *exo*-methylenes in DSB-120 lead to a significant (i.e. from two to three order of magnitude) increase in *in vitro* potency toward A2780 and A2780*cis*R cell lines (Gregson *et al.*, 2001), and a highly improved *in vivo* activity, as demonstrated by the high score of SJG-136 in NCI hollow fibers assay (SJG-136 is in the top 5% of the most active compounds tested in this assay to date) (Hartley *et al.*, 2004).

DSB 120

25

SJG 136

26
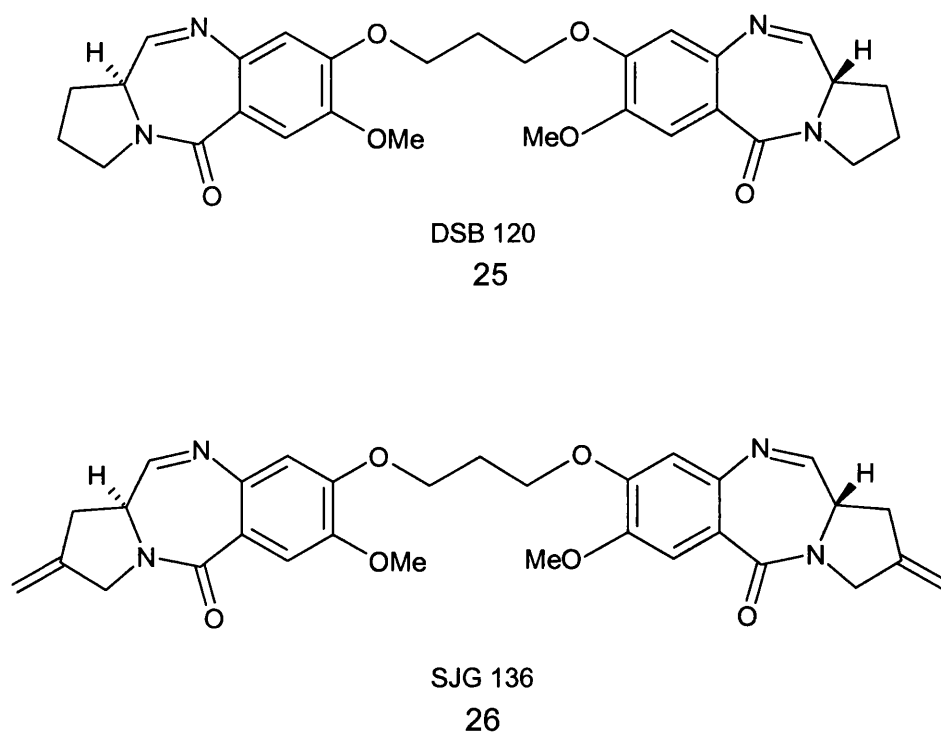
Figure 4.2c: The introduction of C2 *exo*-unsaturation in SJG-136 lead to enhanced *in vitro* and *in vivo* biological activity, and the initiation of phase I clinical trials.

When the polyamide-PBD hybrid project was initiated, it was decided to work with a fully saturated C-ring PBD, as in DSB 120. This was motivated by a number of reasons, the most important being:

- DNA sequence selectivity being the main objective of the project, it was feared that the highly potent unsaturated PBD would rapidly alkylate DNA, regardless of its sequence selective side chain. A presumably less reactive saturated PBD

would only alkylate if its side chain were in a thermodynamically stable position in the minor groove (*i.e.* on a specific target sequence).

- Synthesis of an unsaturated PBD capping unit would require a new, unproven synthetic strategy, considerably longer and more expensive than for a saturated PBD.

Therefore, every target synthesised in this project, but one, bears a saturated C-ring PBD. However, it would be particularly interesting to compare the same hybrid molecule with and without an *exo*-methylene functional group.

It was therefore decided to design and synthesise a C2-*exo*-unsaturated PBD capping unit to address these issues. Previous synthetic efforts provided the necessary key intermediates and knowledge for such an attempt. For example, the protection strategy methyl ester/N10 Alloc/11-hydroxy THP was used again, allowing the A ring intermediate **41** to feature in both saturated and unsaturated synthesis. C-ring intermediate **68** is routinely used for C2 derivatisation studies, by Wittig, Suzuki, Heck or Stille reactions (Gregson *et al.*, 2000). Its synthesis is already optimised, and allowed production of the required batch without any problems.
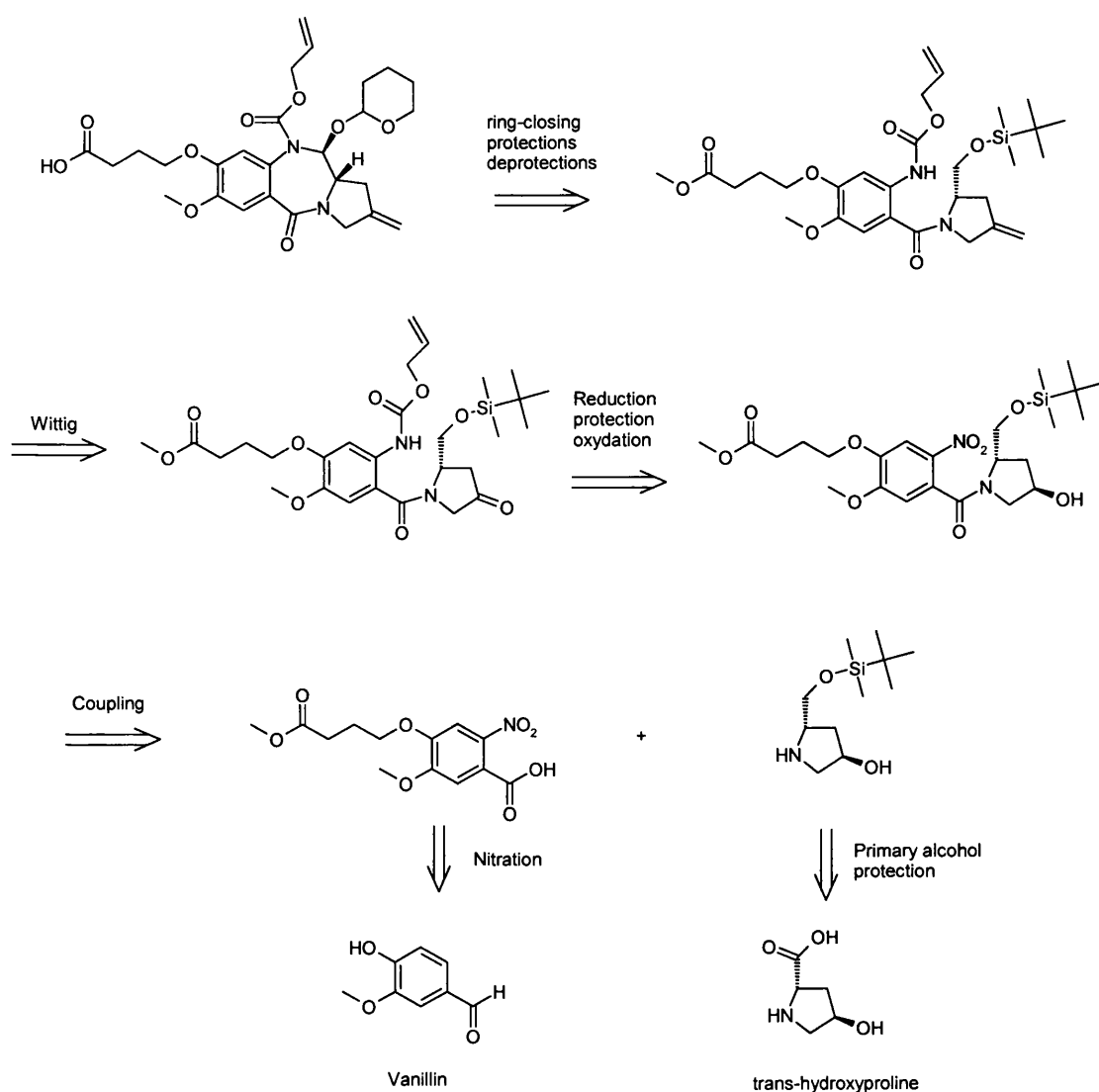
Scheme 4.2h: Retrosynthetic analysis of C2 exo unsaturated PBD acid capping unit

The A to C ring coupling was disappointing, possibly because of C2-secondary alcohol competition, providing the desired amide **69** in a modest 35% yield after chromatography. Reduction of the nitro group by hydrogenation, followed by allyl chloroformate protection was straightforward, as in previous synthesis. C2 alcohol oxidation by TEMPO/BAIB was disappointing, furnishing the desired ketone **72** in 38% yield, and it is possible that PDC or Swern oxidation would have been more efficient on this substrate. Olefination of the C2 ketone was performed under Wittig conditions, as it was feared that the methyl ester might not survive such reaction conditions, care was taken to rigorously exclude moisture. Column chromatography afforded the desired product **73** in a satisfactory 58 % yield.

After TBAF mediated TBDMS deprotection, the TEMPO/BAIB method was again found to be remarkably efficient at forming the B-ring, thus confirming its usefulness at this stage of the synthesis (71% yield). THP protection followed by saponification provided the C2 unsaturated PBD acid capping unit **77** in quantitative yield.

At the time of writing, this remarkable capping unit has been coupled only once. For the sake of simplicity, it was decided to use the tripyrrole moiety found in distamycin, as it allowed a comparison in biological activity to be drawn with its saturated analogue GWL-79. (see chapter 9).

The coupling reaction itself, as well as the final deprotection were performed without problems using the general methods described in the following chapter and do not deserve any particular comments. However, it should be noted that the total synthesis of AT-355 required 29 separate chemical steps from commercially available material, but only 13 steps starting from intermediates generated from previous syntheses. In fact, only this synergistic exploitation of intermediates allowed AT-355 to be synthesised during the course of this project.
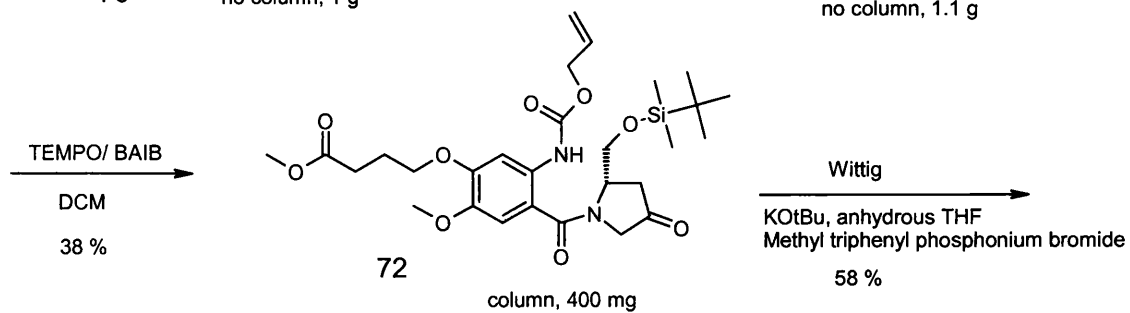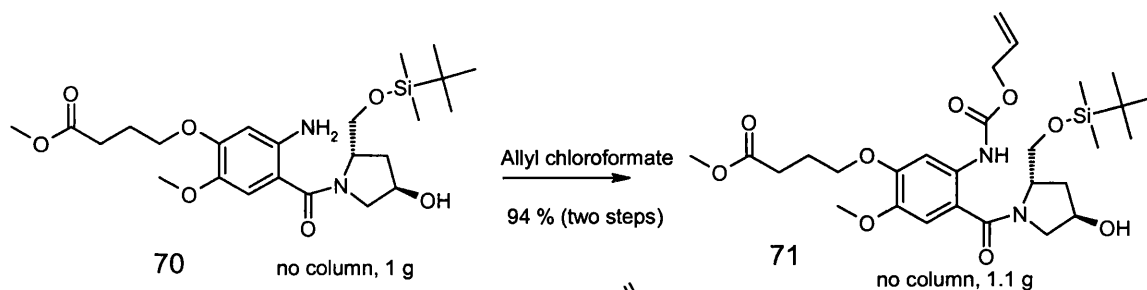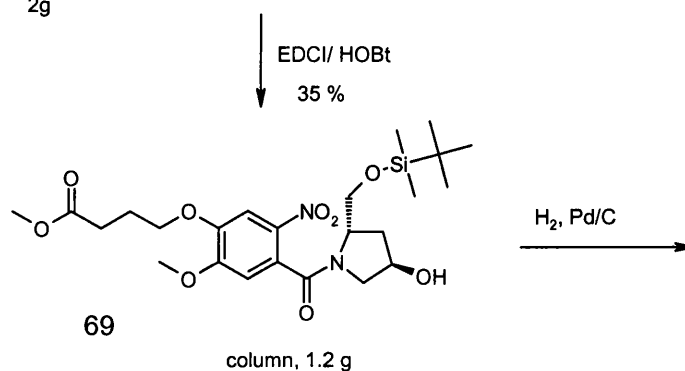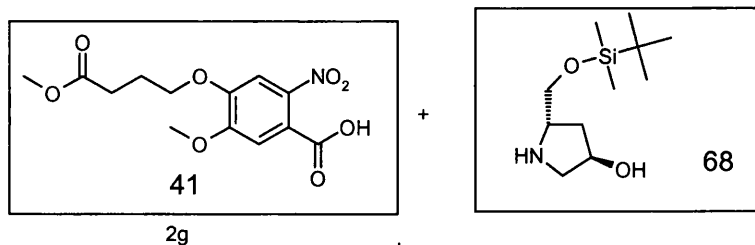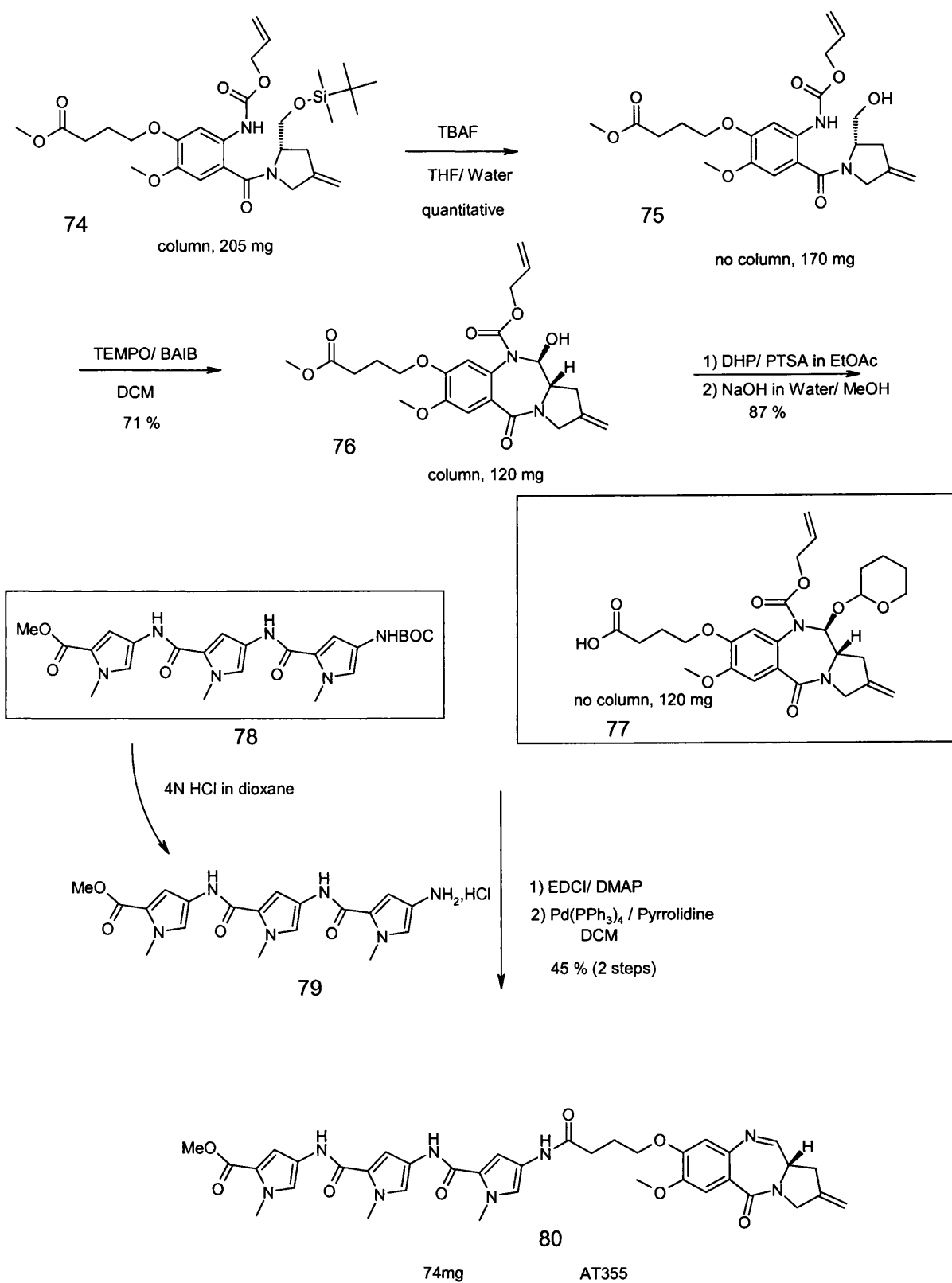
Scheme 4.2i: Synthesis of 4-C Alloc THP C2 *exo*-unsaturated acid PBD capping unit and tripyrrole derivative AT355

92

Sample Ref AT353
PROTON CDC13 {D:\u} atl 55
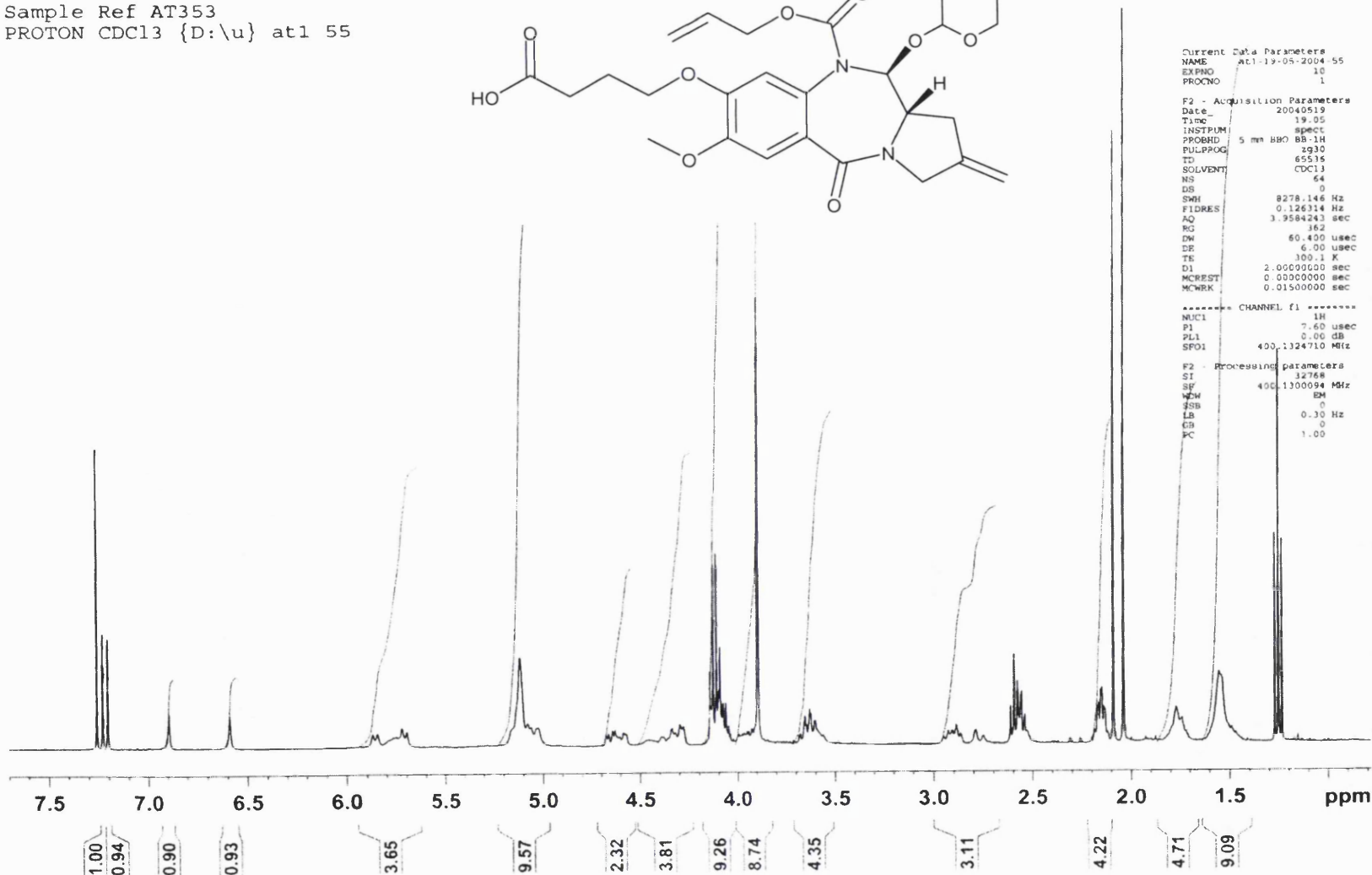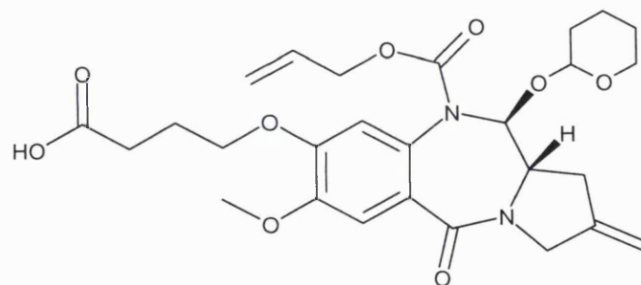
Current Data Parameters
NAME   atl-19-05-2004-55
EXPNO   10
PROCNO   1

F2 - Acquisition Parameters
Date_   20040519
Time   19.05
INSTRUM   spect
PROBHD   5 mm BBO BB-1H
PULPROG   zg30
TD   65536
SOLVENT   CDCl3
NS   64
DS   0
SWH   8278.146 Hz
FIDRES   0.126314 Hz
AQ   3.9584243 sec
RG   362
DW   60.400 usec
DE   6.00 usec
TE   300.1 K
D1   2.00000000 sec
MCREST   0.00000000 sec
MCWRK   0.01500000 sec

======== CHANNEL f1 ========
NUC1   1H
P1   7.60 usec
PL1   0.00 dB
SFO1   400.1324710 MHz

F2 - Processing parameters
SI   32768
SF   400.1300094 MHz
WDW   EM
SSB   0
LB   0.30 Hz
GB   0
PC   1.00

7.5   7.0   6.5   6.0   5.5   5.0   4.5   4.0   3.5   3.0   2.5   2.0   1.5   ppm

1.00 0.90 0.93   3.65   9.57 2.32 3.81 9.26 8.74 4.35   3.11   4.22   4.71 9.09
0.94

Sample Ref AT355
a weekend after the column 6%MeOH/DCM
PROTON DMSO {D:\u} at1 46

Current Data Parameters
NAME   at1-21-05-2004-46_2
EXPNO   10
PROCNO   1

F2 - Acquisition Parameters
Date_   20040524
Time   9.01
INSTRUM   spect
PROBHD   5 mm BBO BB-1H
PULPROG   zg30
TD   65536
SOLVENT   DMSO
NS   64
DS   0
SWH   8278.146 Hz
FIDRES   0.126314 Hz
AQ   3.9584243 sec
RG   1290.2
DW   60.400 usec
DE   6.00 usec
TE   300.1 K
D1   2.00000000 sec
MCREST   0.00000000 sec
MCWRK   0.01500000 sec

======== CHANNEL f1 ========
NUC1   1H
P1   7.60 usec
PL1   0.00 dB
SFO1   400.1324710 MHz

F2 - Processing parameters
SI   32768
SF   400.1300000 MHz
WDW   EM
SSB   0
LB   0.30 Hz
GB   0
PC   1.00

=CH2

(H2O)

CH3

H18

C1

10.0 9.5 9.0 8.5 8.0 7.5 7.0 6.5 6.0 5.5 5.0 4.5 4.0 3.5 3.0 2.5 2.0 ppm

3.00

0.71 1.02 0.71 1.19 1.01 1.14 1.02 0.99 0.73

1.55

2.41 1.74 12.36 3.52

1.42

2.16

2.06
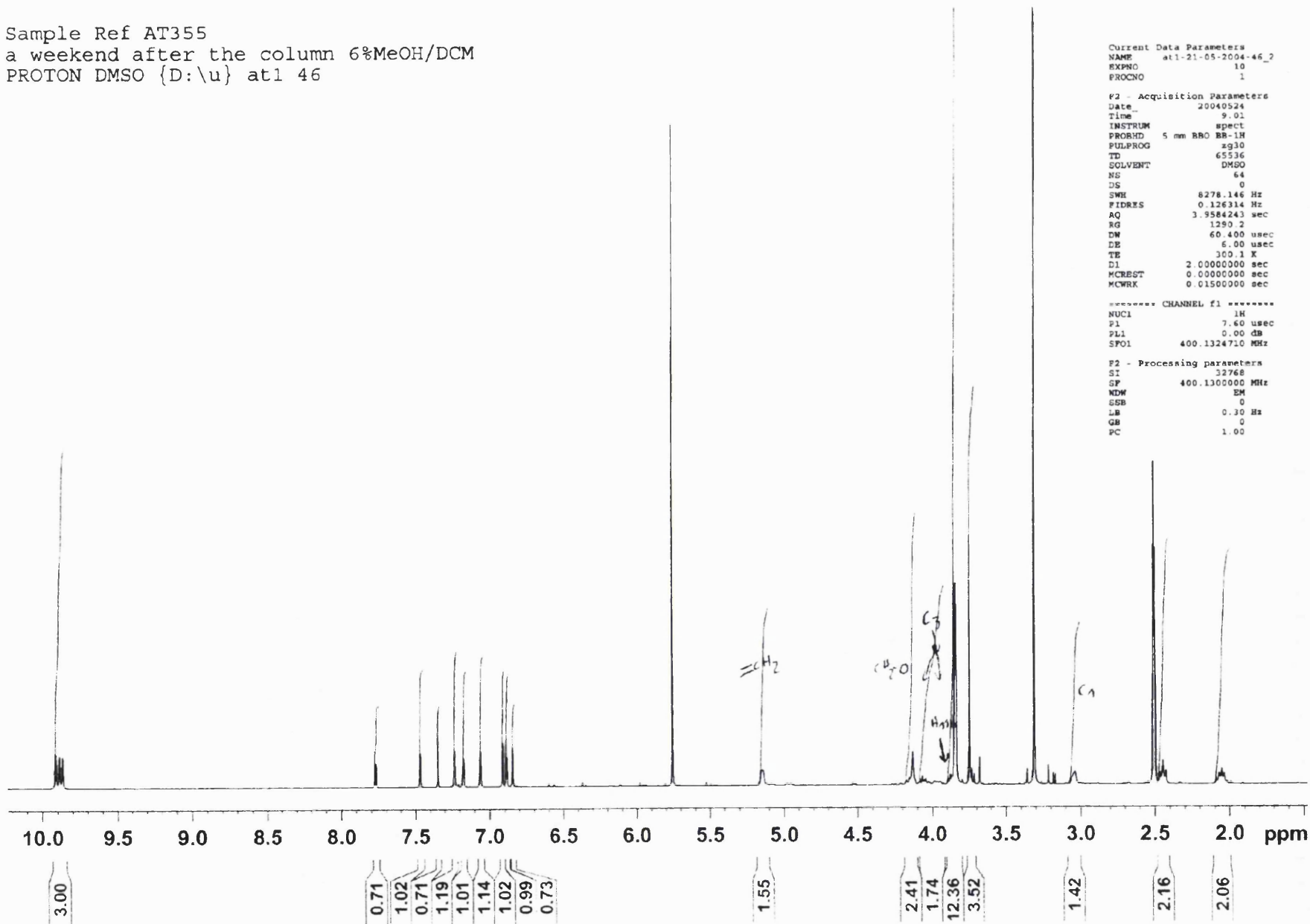
4.3 Polyamides building blocks

Pyrrole/imidazole polyamide required for coupling to the PBD capping units described in the previous sections were assembled from Boc protected building blocks. These building blocks themselves were already known in the litterature (see synthetic section). In particular, the BOC pyrrole acid building block did not necessitate any research effort, since it is particularly well described (Baird and Dervan, 1996). In contrast, synthesis of the imidazole building block on a useful scale required some effort. This section, therefore describes the different building block syntheses, and adds some useful observations to the published literature. Minor, but important alterations are also reported.

4.3.1 Synthesis of the Pyrrole amino acid building block

A single, 125 g batch of pyrrole building block was successfully prepared following the method of Baird and Dervan (1996) shown below (**Scheme 4.3a**). The synthesis was relatively straightforward to follow and did not require any chromatographic purification.

The first step was an indirect introduction of a carboxylic acid unit to the pyrrole nucleus. This presents some important advantages compared with a more direct approach with methyl chloroformate. First, the trichloro product **82** is crystalline and easy to isolate. Secondly, the trichloroacetyl group greatly helps in the following nitration reaction, by deactivating the pyrrole, directing the subsequent nitration, and providing the crystalline product **83**.

Conversely the methyl ester would require purification by distillation under high vacuum, and lead to a low yielding nitration step.
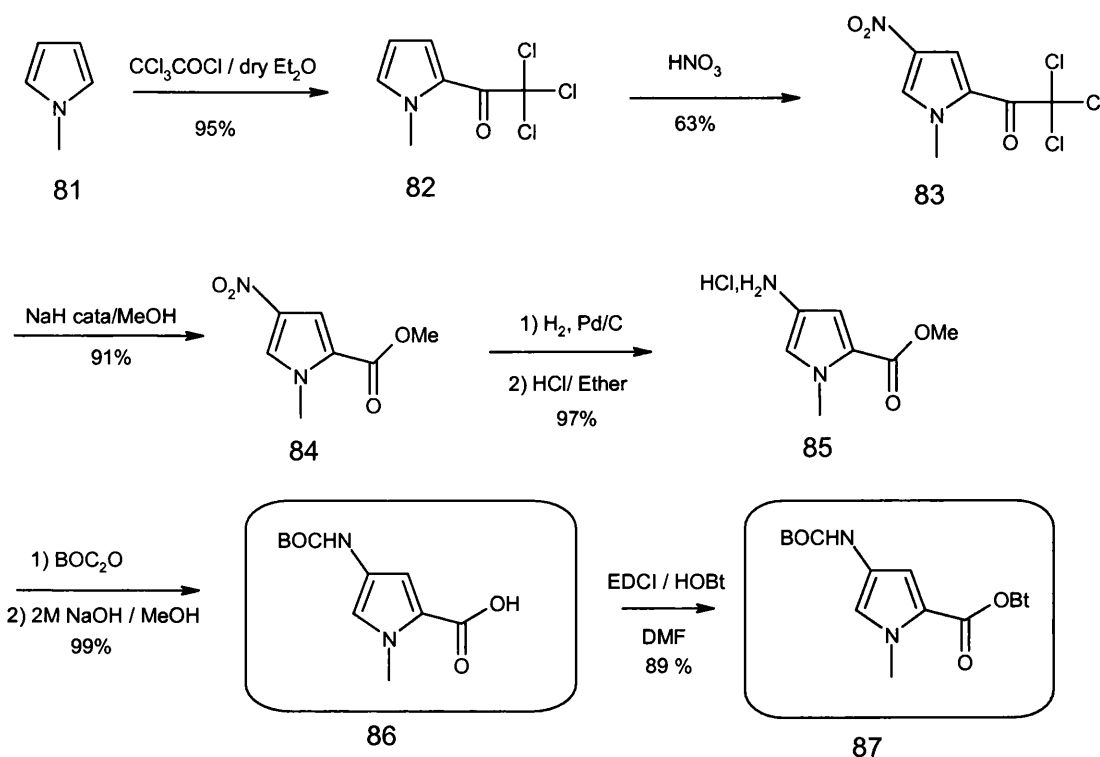
Scheme 4.3a: Synthesis of BOC-4-Amino-1-methyl-1H-pyrrole-2-carboxylic acid

Once the nitro group was successfully installed, methanolysis afforded the required ester **84**.

The nitro group was reduced to the amine by catalytic hydrogenation. Despite being exothermic on large scale, it was a very clean and efficient method. The resulting amine was quite unstable, and air-sensitive, and was therefore isolated as its chloride salt using a solution of HCl gas in ether. Interestingly, completion of the salt formation coincided with a colour change from pink to grey, providing a useful indicator for the reaction. The amine salt was then converted to the Boc carbamate under slightly basic conditions with di-*tert*-butyl dicarbonate. (The amine salt is useful for storage purposes and allows a large batch of pyrrole amine to be prepared and kept for later use. However, this procedure is not always required and can actually be time-wasting. For exemple, when preparing the BOC allyl pyrrole building block, the hydrogenation filtrate was immediately treated with BOC anhydride to yield pure protected amine.)

Finally, the acid group was unmasked by hydrolysis with sodium hydroxide to provide the BOC pyrrole acid building block **86**. Reaction with EDCI and HOBt in DMF

yielded the extremely useful and convenient OBt activated ester **87**, which can be isolated and stored at room temperature as a white powder.

4.3.2 N-allyl, BOC pyrrole amino acid

A slightly modified pyrrole amino acid was required to perform ring-closing metathesis of polyamide chains. Its synthesis was very similar to the conventional N-methyl pyrrole amino acid, and already documented by Olenyuk *et al.* (2003). Some difficulties were encountered at the N-alkylation step as the substrate **91** was relatively unreactive. It would have been easier to perform on an electron-deficient heterocycle (substituted by a nitro group), but this strategy would have precluded the use of reductive hydrogenation.

A variety of reaction conditions were investigated (including KOtBu/18-crown-6, or LiHMDS) but only allyl bromide alkylation catalysed by TBAI and potassium carbonate in DMF proved satisfactory. Butenyl bromide was found to be unsufficiently reactive under these conditions and attempts to synthesise the N-butenyl analogue were not pursued. Once again, sodium hydroxide hydrolysis provided the necessary BOC-allyl-pyrrole amino acid **93**. (**Scheme 4.3b**)
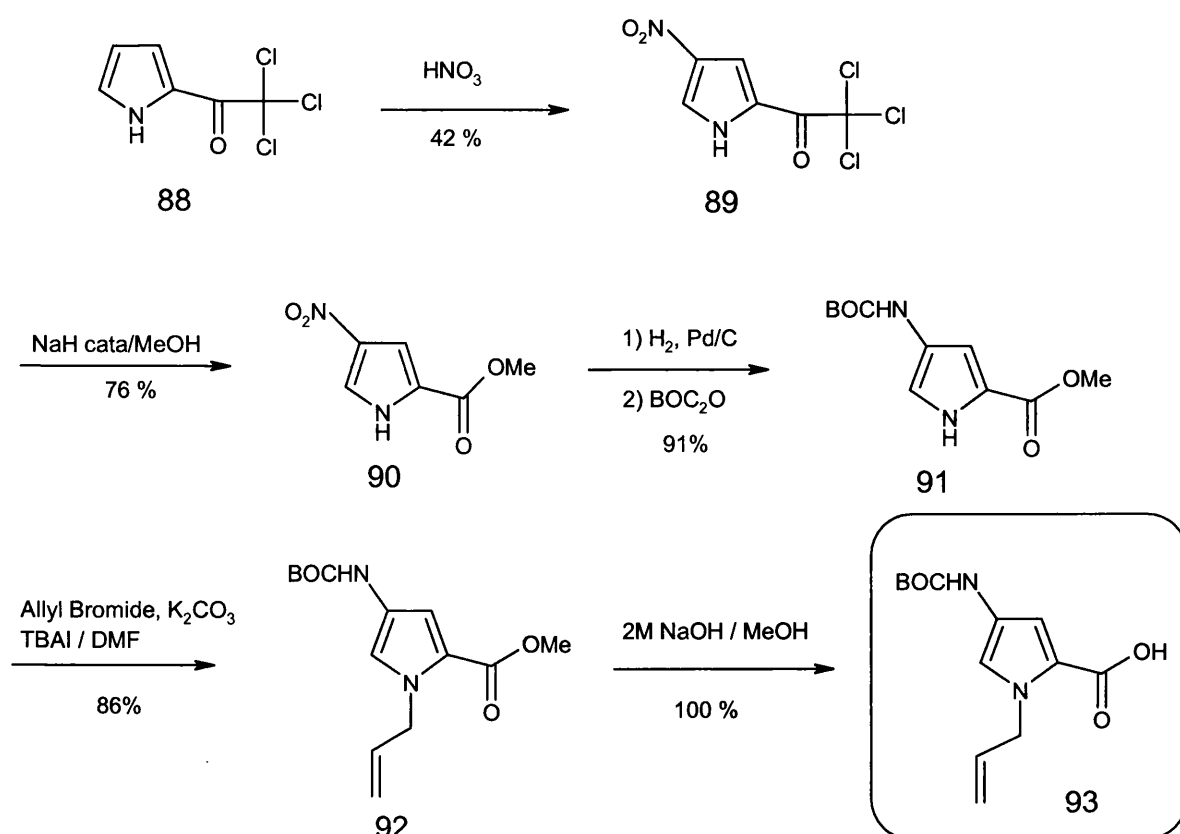
Scheme 4.3b: Allyl pyrrole BOC amino acid synthesis

4.3.3 BOC Imidazole amino acid

Boc imidazole amino acid   N-methyl-2-imidazole acid
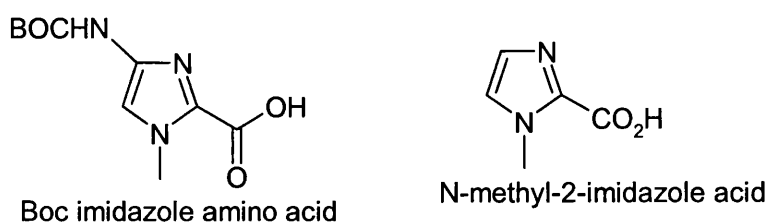
Figure 4.3a: Boc imidazole amino acid and N-methyl-2-imidazole acid

The imidazole building block was initially prepared by Dr G Wells according to the method of Dervan (Baird and Dervan, 1996). However, the synthesis proved impractical and included several problematic reactions. The ester was introduced directly with ethyl chloroformate but required distillation. More importantly, the nitration method required the use of refluxing nitric acid, followed by a complex recrystallisation to obtain the required isomer, in very poor yield (22% as quoted in Baird and Dervan, 1996).
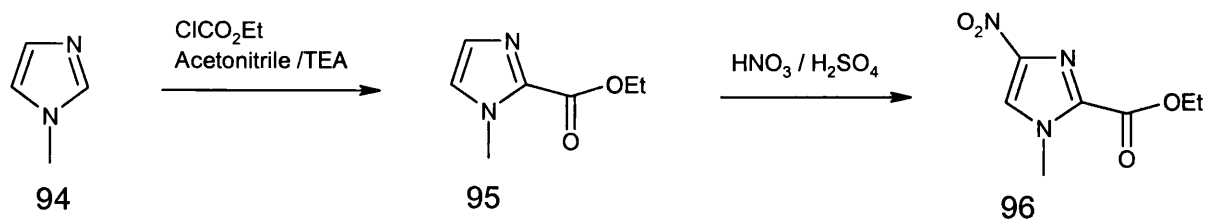
Scheme 4.3c: Preparation of the nitroimidazole precursor *via* the ethyl ester route

It was therefore decided to use a similar approach to the one applied to the BOC pyrrole building block, employing a trichloroacetylation reaction, as described by Nishiwaki *et al.* (1988).
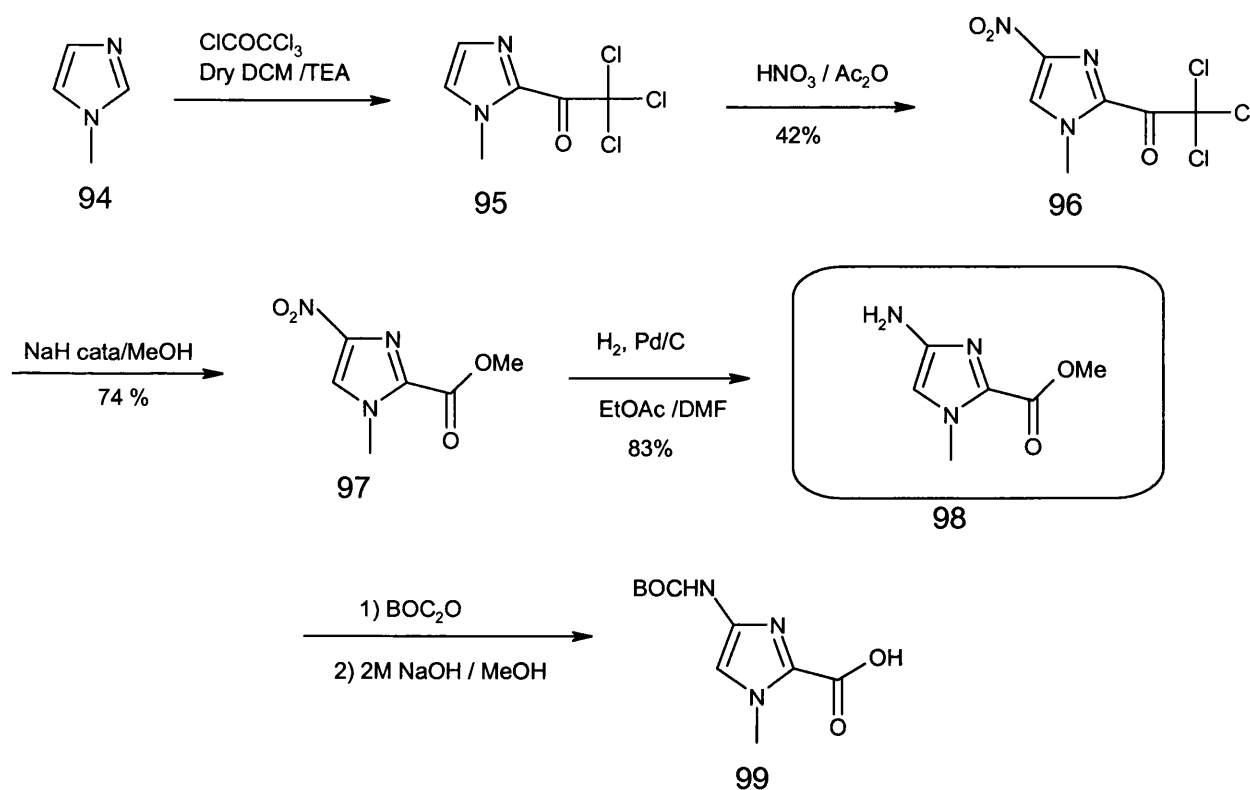
Scheme 4.3d: Synthesis of the BOC-Nitroimidazole acid.

In our hands however, the first two steps (trichloroacetylation and nitration) were not as straightforward as described in the literature, especially when performed on a large scale (200 g and over). The trichloroacetyl imidazole **95** was heavily contaminated with triethylamine hydrochloride and found very unstable to heating. Additionally, the nitration was relatively hazardous on a large scale, with unpredictable and violent

exotherms occuring during the overnight reaction. As a result, extraction of the product from the reaction mixture with chloroform on this scale was not an attractive prospect.

Careful timing, temperature control, and replacing chloroform with dichloromethane allowed pure trichloroacetyl imidazole **95** to be retrieved after filtration through a pad of silica gel. Although not entirely optimized, the nitration was rendered safer and more practical by a few modifications. The reaction mixture was allowed to react at 10°C and then poured into trays at room temperature where the product could safely crystallize overnight. The crystals were neutralized with saturated aqueous NaHCO₃, collected by filtration and dried. These steps are important as batches of acidic and slightly wet product (non neutralized and not properly dried) were reported to decompose slowly when stored at room temperature. The trichloroacetyl-nitro-imidazole **96** thus obtained is an extremely useful building block in its own right. It can be used as an activated acid, through haloform reactions. As can be seen in **scheme 4.3e**, the imidazole analogue is more reactive than the pyrrole, and makes these reactions very practical and clean.
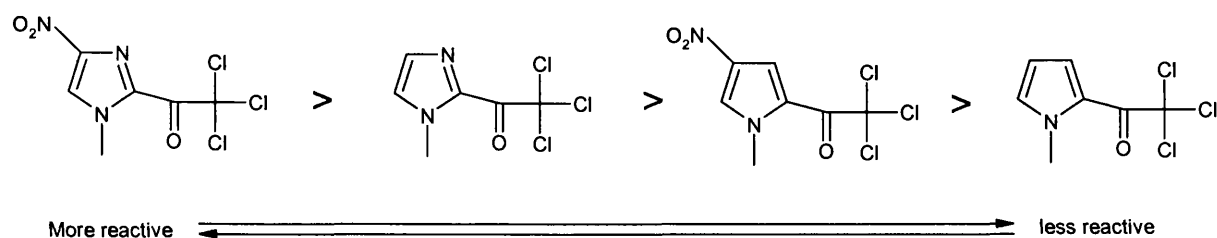
Scheme 4.3e: Chart of reactivity from Xiao *et al.*, 2000.

Conversion of the trichloroacetyl to the methyl ester **97** was smooth and undemanding. Reduction of the nitro group by hydrogenation furnished the imidazole amine in 83% yield. Interestingly, the amine **98**, thus obtained, crystallized upon solvent evaporation, and was stable enough to be stored in the freezer. This was in marked contrast to the behaviour of its pyrrole amine counterpart. Once again, this imidazole amine is a valuable building block in its own right as it can be coupled directly, without a deprotection step.

If the imidazole amine is stable, it is also a poor nucleophile. So poor in fact, that Dervan and co-workers presynthetised dimers in solution, to remove any coupling involving this amine on solid phase. The same conclusion was reached by the Krutzik and Chamberlin (2002), when working on solid phase. It was therefore decided to couple the imidazole amine at the beginning, to afford dimers or trimers, so that it would not be involved in any of the later couplings steps when it could prove problematic. As a result, it was not necessary to pursue the normal synthetic route, which would have entailed BOC protection followed by ester saponification.

Finally, a N-methyl-2-imidazole acid **100** is almost always included at the N-end of Dervan's hairpin design. (see chapter 3). Unfortunately, it did not find its place in any of the targets presented in this thesis, but its preparation is worth mentioning. It is achieved *via* a single step lithiation of N-methyl-imidazole followed by carbon dioxide quenching. Carbon dioxide can be introduced rapidly as chunks of dry ice. The resulting product is then neutralized, decanted and dried.
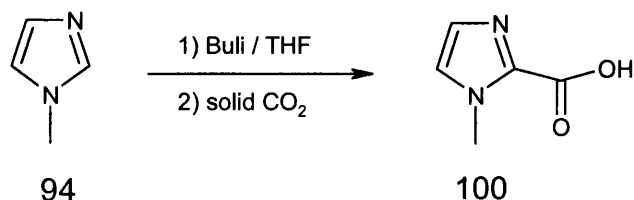
Scheme 4.3f: Synthesis of 1-Methyl-1H-imidazole-2-carboxylic acid

5 Pyrrole-Imidazole linked PBD dimer conjugates synthesis

5.1 Introduction

As already mentioned in previous chapters, the PBD dimer SJG-136 was found to have extremely interesting biological properties and has therefore entered phase I clinical trials. It is, however, a relatively short molecule, which spans only 6 base pairs; statistically SJG-136 can crosslink DNA selectively every 136 base pairs. (see **Table 5.1a** below, taking into account only the core sequence GATC). Although this figure is significantly lower than for other crosslinking molecules such as cis-platin and nitrogen mustards, it still suggests that undesired alkylation of healthy genes may occur too frequently.

Number of base pairs	Given sequence found every X bp
1	2
2	10
3	32
4	136
5	512
6	2080
7	8192
8	32896
9	131072
10	524800
11	2097152
12	8390656
13	33554432
14	134225920
15	536870912
16	2147516416

Table 5.1a: Occuring frequency of any given DNA sequences of a certain length, taking into account symmetry. (for n even: $(4^n + 4^{(n/2)})/2$ and for n odd: $(4^n)/2$). (Dr David Evans, Spirogen).

SJG-136
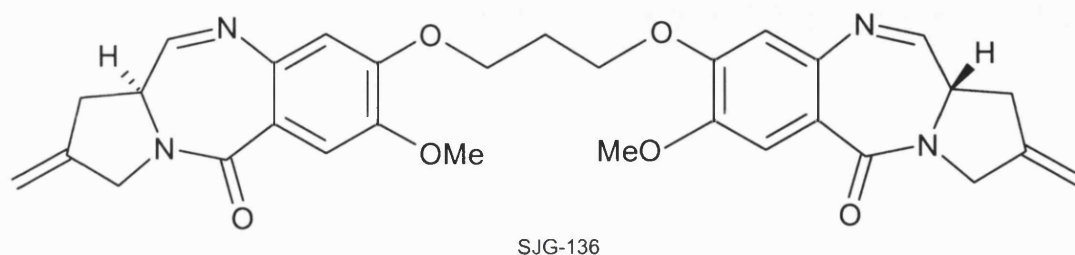
Extending the length of these molecules and hence increasing the selectivity should significantly reduce the number of undesired alkylations, and consequently the toxicity of the molecules. Ultimately, molecules could be envisaged that cross-link at a specific oncogenic sequence. This concept is illustrated in **Figure 5.1a**.

= NON-COVALENT DNA BINDING MOLECULES
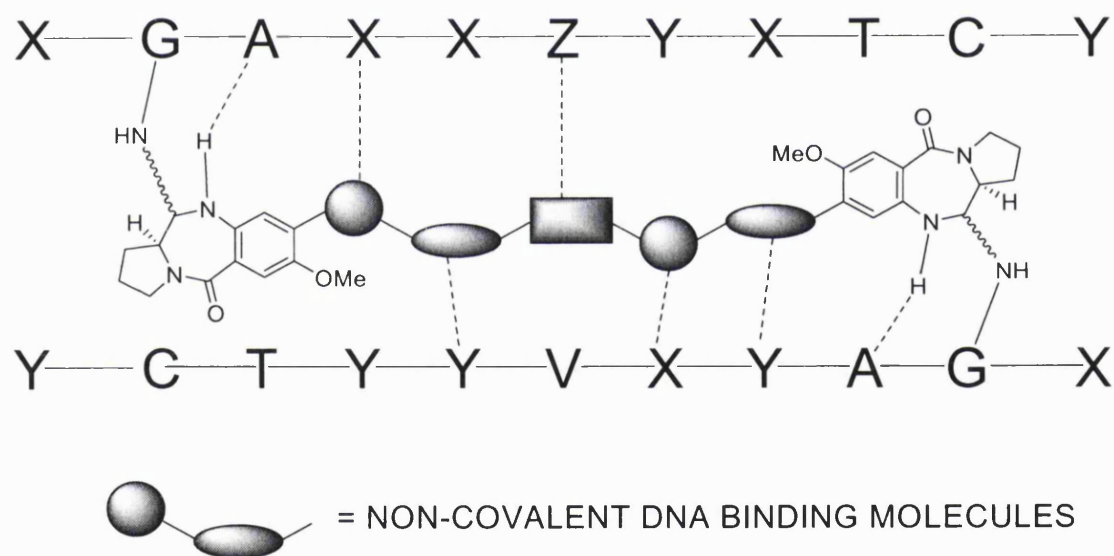
Figure 5.1a: How a PBD dimer featuring a DNA recognizing core could target a specific sequence.

The building blocks described in the previous chapter, lend themselves to the modular assembly of the molecules required to realise this concept. On paper, at least, synthesis of these dimers is relatively straightforward as the heterocyclic building blocks can be readily incorporated in the central core of the molecule through modified amide coupling chemistry.

A set of seven pyrrole-imidazole linked PBD dimers was synthesized using solution phase chemistry. Their biological properties including cytotoxicity, cross-linking ability and DNA selectivity will be described in chapter 7. They can be grouped into three families, based on their design and synthesis. (See **Table 5.1b**).

- Symmetrical; including a central N-methylpyrrole diacid.
- Symetrical; including a diaminopropane central linker.
- Unsymmetrical; based on a distamycin core.

Schematic representation	Family
AT217 AT234	Symmetrical including a central N-methylpyrrole diacid.
AT235	Unsymmetrical and based on distamycin core.

AT281
  AT242
  AT338
  AT288
	Symmetrical including a diaminopropane central linker.
	
	 (*white circles symbolize N-methylpyrroles, whereas black disks indicate N-methylimidazole*)

Table 5.1b: Schematic representation and classification of Pyrrole-Imidazole linked PBD dimers. Arrows point to N-terminus of heterocyclic core.

5.2 Symmetrical dimers, including a central N-methylpyrrole diacid.

This type of dimer was built around a central N-methylpyrrole 2,5-diacid **101**. The unusual geometry resulting from the 2,5 substitution (instead of the 2,4 substitution found in distamycin) could significantly alter the DNA binding properties of this type of conjugate by conferring a different radius of curvature on the molecules. (see chapter 3).

A batch of diacid **101** was synthesized via a Vilsmeier reaction (Barker *et al.*, 1978) by Dr Stephen J Gregson. It was readily activated to its corresponding *bis*-acid chloride **102** with oxalyl chloride and DMF. This *bis*-acid chloride was in turn coupled either to an amino pyrrole building block, or to the amino PBD capping unit **66**.

In the latter case, palladium (0) catalysed Alloc deprotection furnished the desired monopyrrole PBD dimer AT-217 (**104**) in excellent yield (80% for the two steps). (**Scheme 5.2a**).
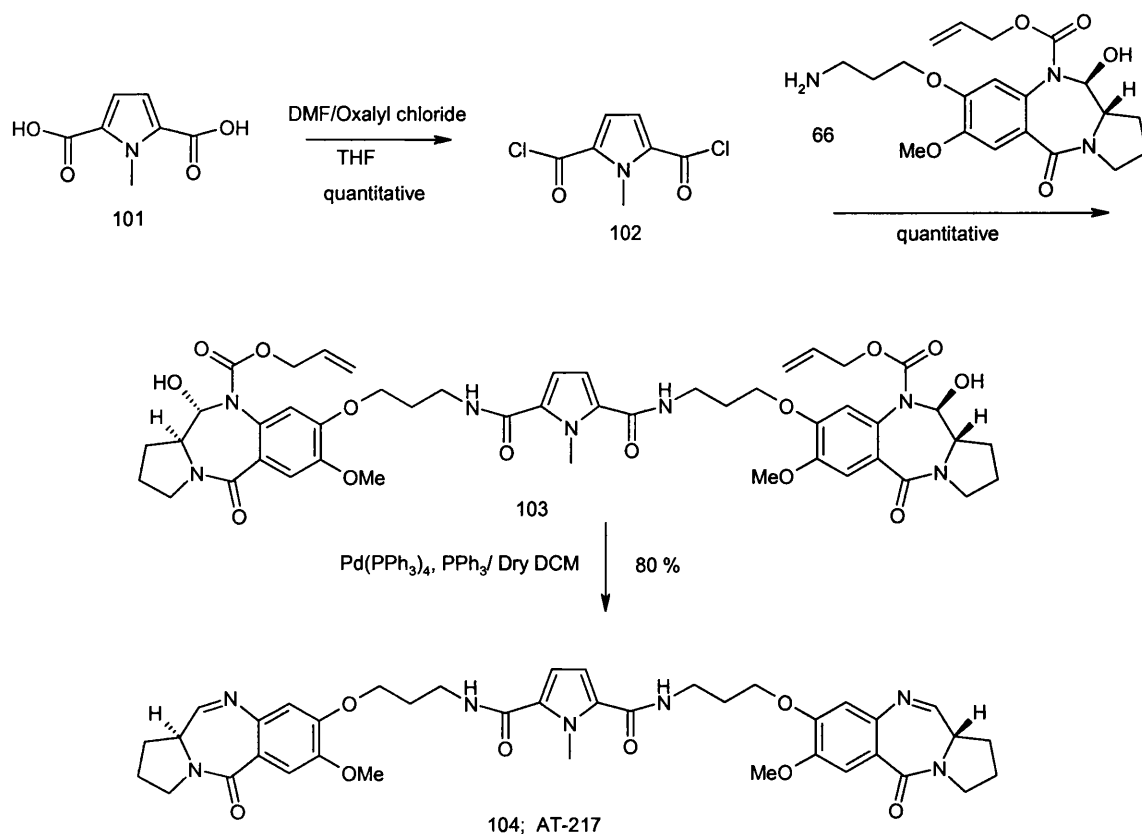
Scheme 5.2a: Synthesis of symmetrical dimer including a 2,5-pyrrole diacid core.

However, the symmetrical tripyrrole diacid required for the synthesis of **109** (**Scheme 5.2b**) could not be obtained by methyl ester saponification. The product appeared to decompose under the relatively harsh alkaline conditions. The problem was avoided by synthesizing the *bis*-benzyl ester, followed by hydrogenolysis. (The mono pyrrole benzyl ester was readily synthesized from BOC-protected benzotriazole ester **87** and benzyl alcohol in DMF, and obtained by filtration in 66% yield). The unstable tripyrrole diacid thus obtained was directly activated (EDCI/HOBt) overnight and coupled to the amino PBD capping unit. Alloc deprotection furnished the novel symmetrical tri-N-methylpyrrole PBD dimer AT-234 (**109**) in 88% yield.
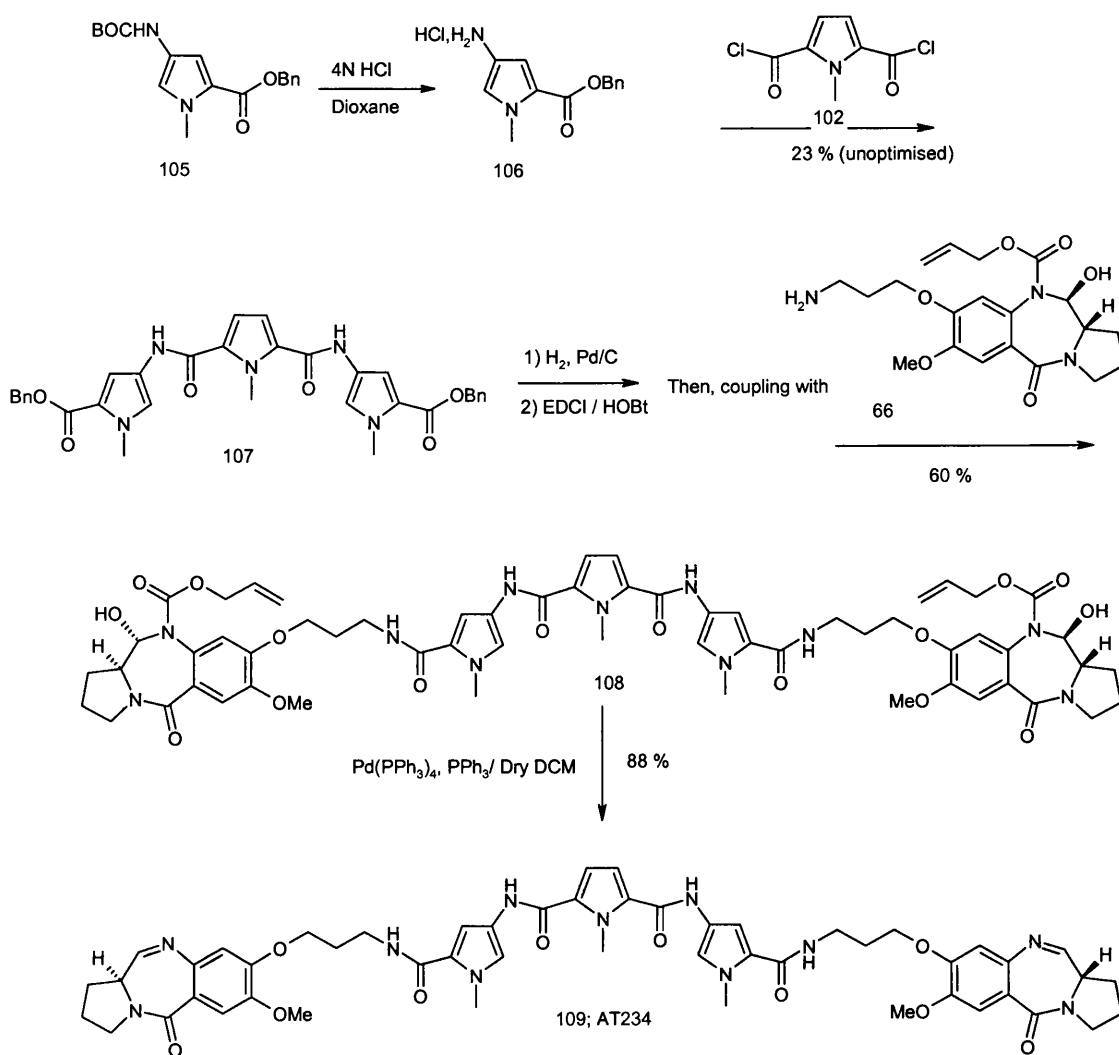
Scheme 5.2b: Synthesis of a symmetrical dimer including a tripyrrole core.

Sample Ref at234

Current Data Parameters
NAME   11-May16-2003-at1
EXPNO   10
PROCNO   1

F2 - Acquisition Parameters
Date_   20030516
Time   16.19
INSTRUM   spect
PROBHD   5 mm BBO BB-1H
PULPROG   zg30
TD   65536
SOLVENT   DMSO
NS   64
DS   0
SWH   8278.146 Hz
FIDRES   0.126314 Hz
AQ   3.9584243 sec
RG   362
DW   60.400 usec
DE   6.00 usec
TE   298.2 K
D1   2.00000000 sec

======== CHANNEL f1 ========
NUC1   1H
P1   7.50 usec
PL1   0.00 dB
SFO1   400.1324710 MHz

F2 - Processing parameters
SI   32768
SF   400.1299778 MHz
WDW   EM
SSB   0
LB   0.30 Hz
GB   0
PC   1.00

108

5.3 Unsymmetrical Dimers Based on Distamycin Core.

This type of dimer was designed to conserve the core structure of the natural product distamycin. Of course, this template would also lend itself to the inclusion of a diverse set of heterocyclic building blocks. (see **Figure 5.1a**, on possible substitutions). However, a substantial synthetic drawback arises from the unsymmetrical design, which requires two different PBD capping units which have to be sequentially coupled to the heterocyclic core. It was decided to couple the amino PBD first, as this would avoid exposure of the vulnerable PBD system to harsh saponification conditions (NaOH, 60°C, 4 hours). Although not mild (4N HCl in dioxane), the conditions required to deprotect the BOC group were well tolerated by the Alloc-protected PBD ring system.

The tripyrrole unit **112** found in distamycin is well known in the literature (Boger, Fink and Hedrick, 2000) and was required for the synthesis of a number of target compounds. Indeed, the tripyrrole unit could be considered as a key building block for the entire synthetic program. The tripyrrole could be synthesized by many methods, but the route shown in **Scheme 5.3a** was thought to be the most rapid and convenient. Interestingly, it includes both the haloform coupling reaction, and the more common EDCI/HOBt-driven coupling.

Nitropyrrole ester **84** was rapidly hydrogenated in DMF and the resulting amine solution was filtered to remove the catalyst and allowed to react with the nitrotrichloroketone pyrrole **83** in the buchner receiver flask. The resulting pyrrole dimer **110** was isolated by filtration, washed, and dried. Yields from this reaction were found to be only consistently moderate (50% to 60%) but the starting materials are considerably cheaper and easier to obtain than the more synthetically advanced BOC pyrrole acid. (see BOC pyrrole synthesis, chapter 4). The nitro dimer **110** (Kumar and Lown, 2003a) was cleanly converted to an amine by hydrogenation and allowed to react with BOC pyrrole OBt ester **87** in DMF. This coupling was remarkably efficient, providing the desired trimer in excellent yield and purity (94%) after precipitation from water and filtration. The BOC tripyrrole acid equivalent could then be obtained quantitatively by standard saponification.
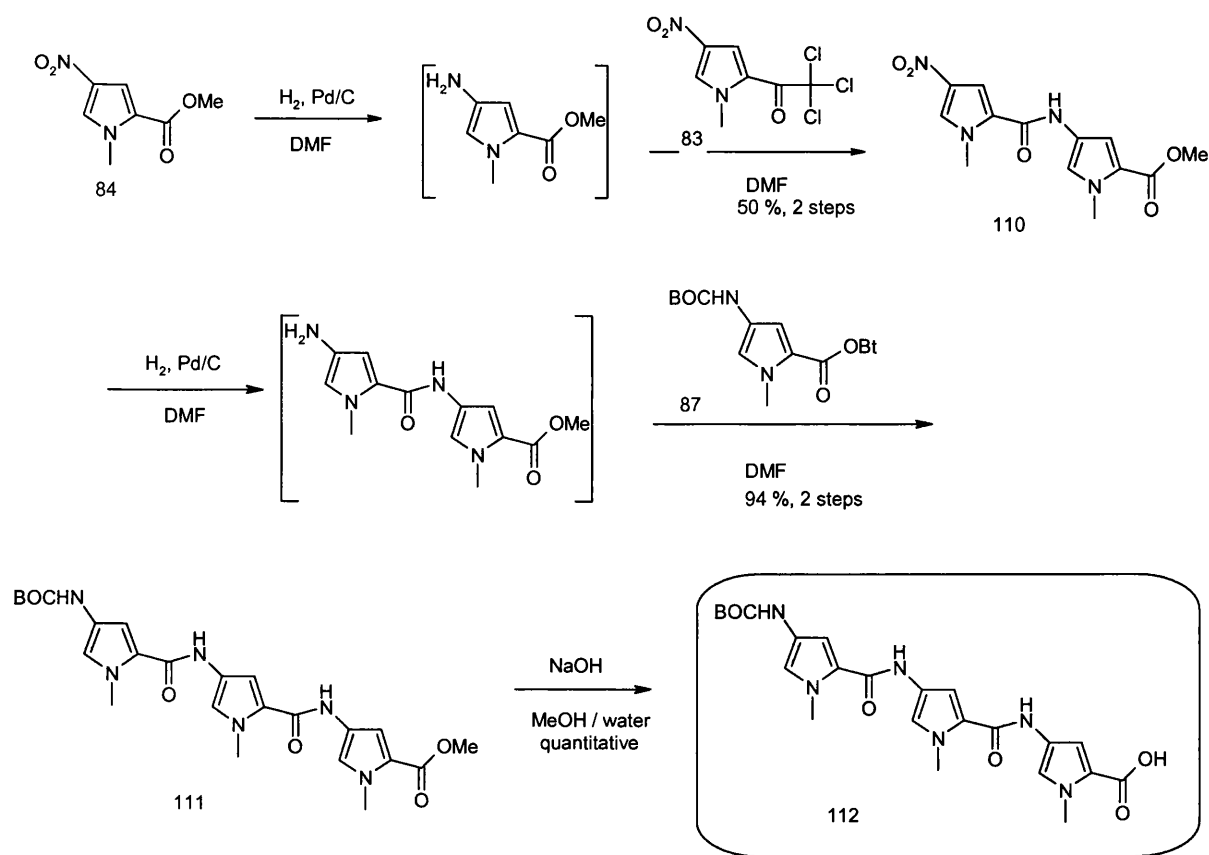
Scheme 5.3a: Convenient synthesis of the tripyrrole moiety.

The tripyrrole acid, thus obtained, was coupled to the amino PBD capping unit **66**, after EDCI/HOBt activation **(Scheme 5.3b)**. Hydrochloric acid mediated (4N in dioxane) BOC deprotection was followed by coupling with 4-C PBD acid capping unit. As the latter was introduced as its hydroxy 11 methyl ether **56**, an oxalyl chloride activation was possible. However this capping unit also contained approximately 10% of the undesired 11-R diastereoisomer, which was carried through to the final dimer AT-235 **(115)**.

EDCI / HOBt

then, coupling with
amino PBD 66

57 %

4N HCl in dioxane

then, coupling with
4C Methoxy 11 PBD acid chloride

44%

Pd(PPh₃)₄, PPh₃/ Dry DCM   85 %

112

113

114

115; AT-235
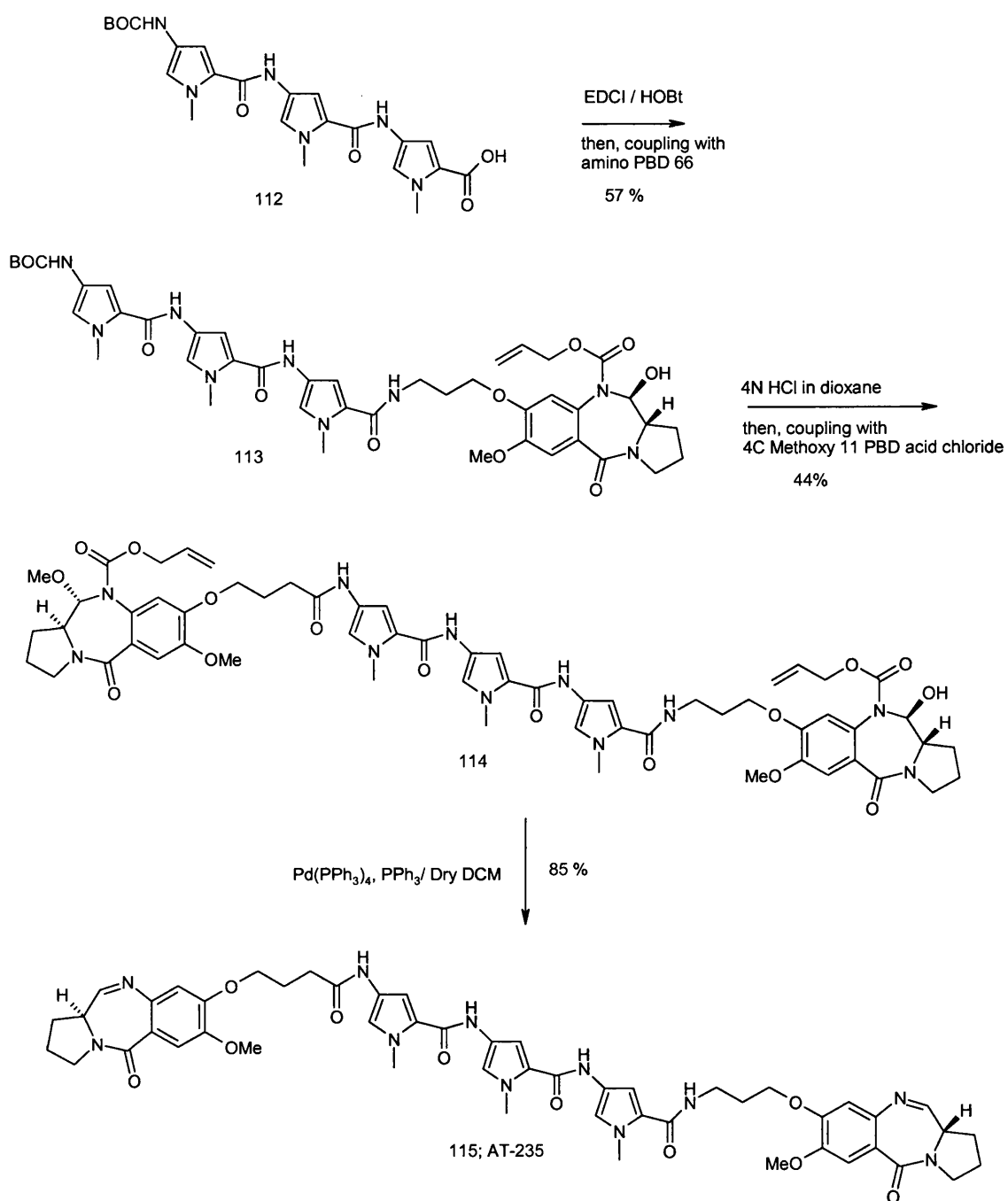
Scheme 5.3b: Synthesis of a PBD dimer including a distamycin core.

111

Sample Ref at235
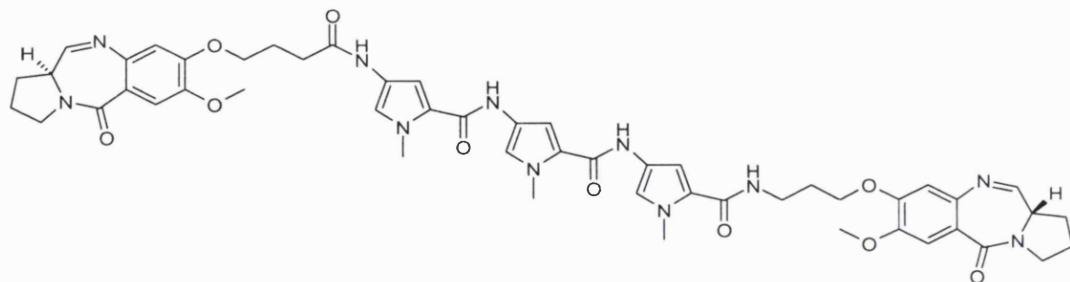
Current Data Parameters
NAME   12-May16-2003 at1
EXPNO   10
PROCNO

F2 - Acquisition Parameters
Date_   20030516
Time   16.26
INSTRUM   spect
PROBHD   5 mm BBO BB-1H
PULPROG   zg30
TD   65536
SOLVENT   DMSO
NS   16
DS   2
SWH   8278.146 Hz
FIDRES   0.126314 Hz
AQ   3.9584243 sec
RG   456.1
DW   60.430 usec
DE   6.00 usec
TE   298.2 K
D1   1.00000000 sec

======== CHANNEL f1 ========
NUC1   1H
P1   7.30 usec
PL1   0.00 dB
SFO1   400.1324710 MHz

F2 - Processing parameters
SI   32768
SF   400.1299966 MHz
WDW   EM
SSB   0
LB   0.30 Hz
GB   0
PC   1.00

10.0   9.5   9.0   8.5   8.0   7.5   7.0   6.5   6.0   5.5   5.0   4.5   4.0   3.5   3.0   2.5   2.0   1.5   ppm

3.00

0.97 1.70 1.69 0.19 1.11 1.99 0.12 0.97 2.00 1.69 0.19

0.18

5.20 14.33 2.95 2.10 4.51 0.61 3.81

2.03 3.75 8.36
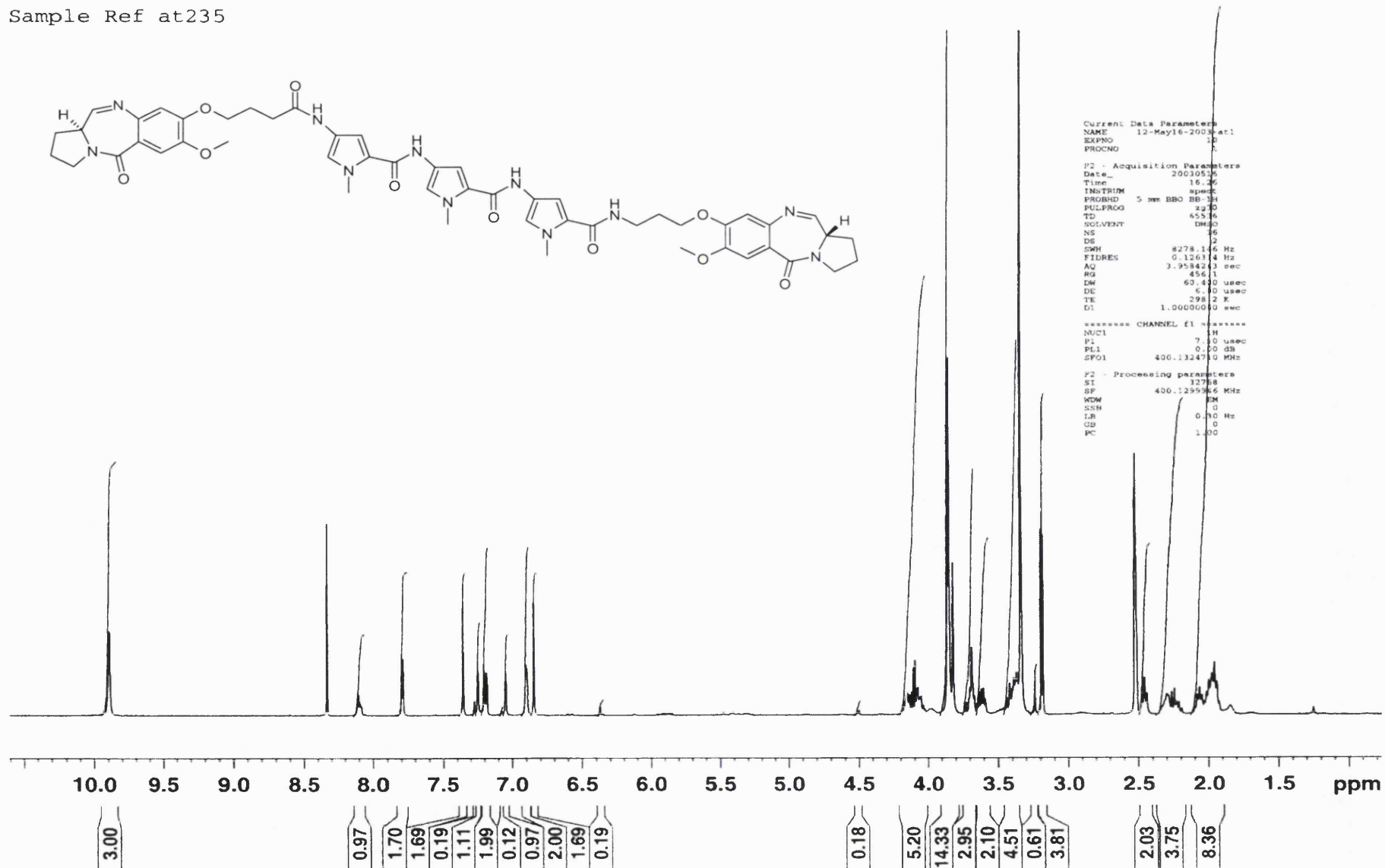
5.4 Symetrical Dimers; Including a Diaminopropane Central Linker.

Building the polyamide symmetrically from a diaminopropane core allows rapid and convenient synthesis of long pyrrole/imidazole linked PBD dimers. The polyamide DNA recognition unit would be expected to work in a 1:1 binding mode, and therefore have modest selectivity potential. However, the addition of another lexitropsin could actually lead to a 2:1 binding mode with enhanced recognition potential. (Bando *et al.*, 2002)

5.4.1 Synthesis

The synthesis of this type of compound is relatively straightforward. It can be initiated, either from the diaminopropane core with sequential addition of heterocyclic building blocks, or from a preformed polyamide chain coupled in one step to 1,3-diaminopropane. The flexibility of the synthetic approach allowed optimal use of diverse building blocks throughout the project. For example, coupling of diaminopropane with the nitrotrichloroacetylpyrrole **83** smoothly provided the *bis* nitropyrrole core in good yield. After hydrogenation, the *bis* amine could then be coupled, either to the PBD acid capping unit and give rise to AT-281 (**118**), or to another pyrrole to provide the *bis* BOC protected amino bipyrrole **119**. This, in turn, can be converted to its PBD dimer homologue AT-242 (**121**). (**Scheme 5.4a** and **Scheme 5.4b**). (NB: the tetrapyrrole PBD dimer AT-242 was initially synthesized with the partially racemized 11-methoxy PBD acid capping unit, but was later resynthesized enantioselectively as AT-360)
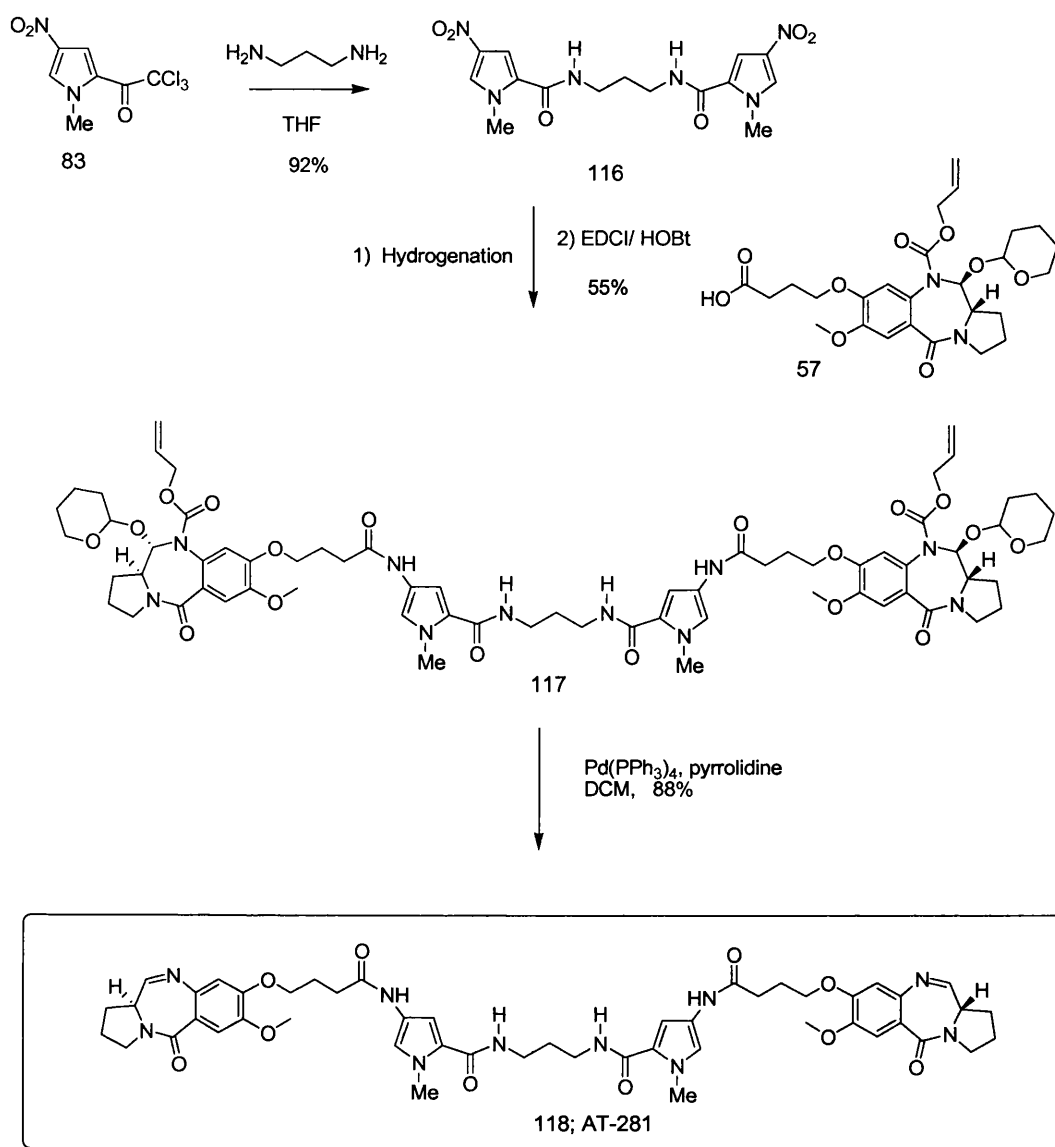
Scheme 5.4a: Synthesis of dipyrrole symetrical dimer AT281.
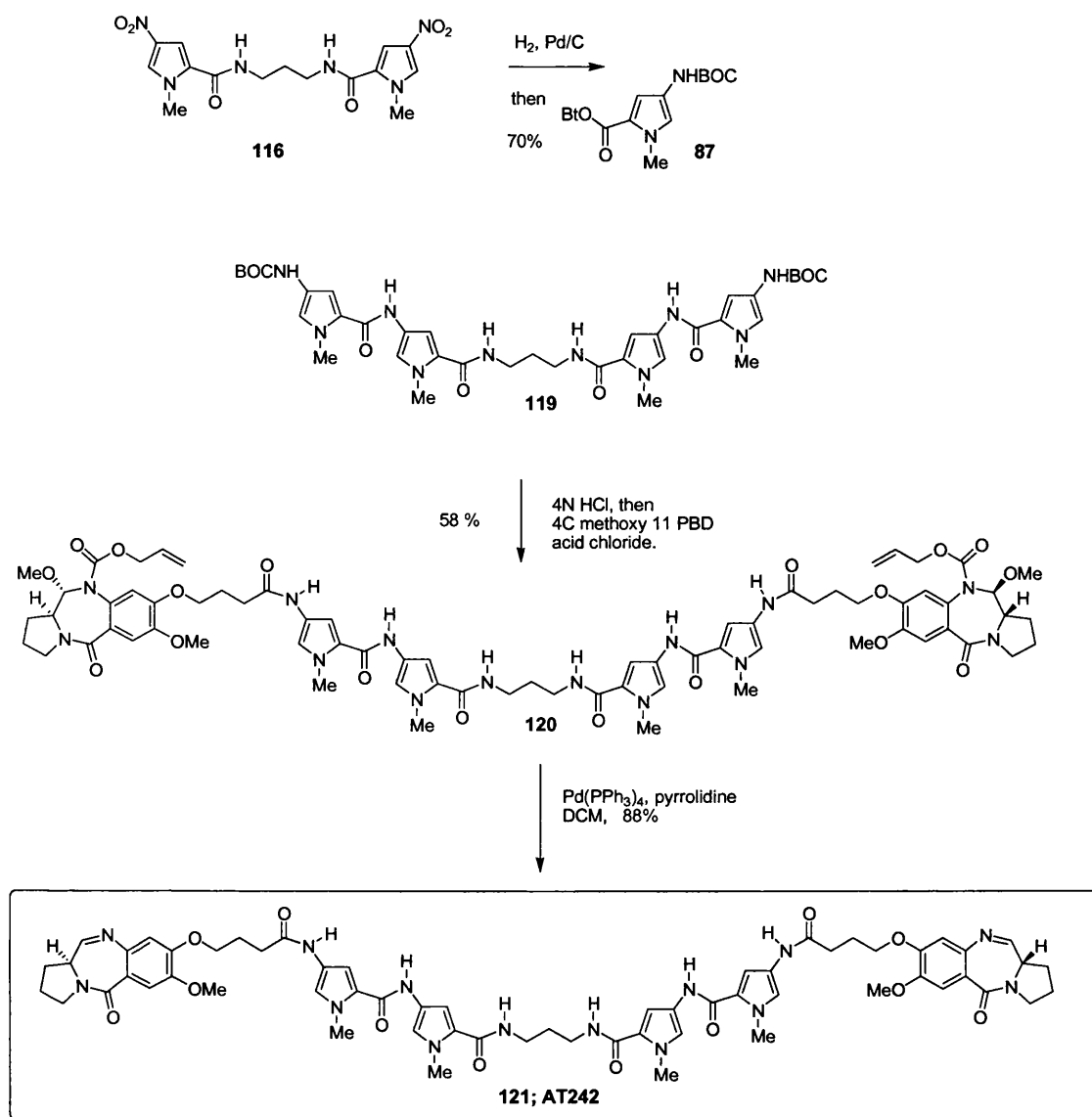
Scheme 5.4b: Synthesis of tetrapyrrole symetrical dimer AT242.

Sample Ref AT360
after 4 days
PROTON DMSO {D:\u} atl 45

Current Data Parameters
NAME   atl-18-06-2006-45
EXPNO   10
PROCNO   1

F2 - Acquisition Parameters
Date_   20060618
Time   17.06
INSTRUM   spect
PROBHD   5 mm BBO BB-1H
PULPROG   zg30
TD   65536
SOLVENT   DMSO
NS   64
DS   0
SWH   8278.146 Hz
FIDRES   0.126314 Hz
AQ   3.9584243 sec
RG   162
DW   60.400 usec
DE   6.00 usec
TE   298.0 K
D1   1.00000000 sec
MCREST   0.00000000 sec
MCWRK   0.01500000 sec

======== CHANNEL f1 ========
NUC1   1H
P1   7.60 usec
PL1   0.00 dB
SFO1   400.1324710 MHz

F2 - Processing parameters
SI   32768
SF   400.1300025 MHz
WDW   no
SSB   0
LB   0.00 Hz
GB   0
PC   1.00

10.0   9.5   9.0   8.5   8.0   7.5   7.0   6.5   6.0   5.5   5.0   4.5   4.0   3.5   3.0   2.5   2.0   1.5   1.0   ppm

2.18   1.10 1.00   1.02 2.05   2.99   2.58 8.57 2.58 1.75 2.08   2.10 2.22 4.40 1.43

In contrast, the core of the hexapyrrole dimer AT-288 (**124**) (**Scheme 5.4c**) was made in one step by coupling the tripyrrole acid **112** (synthesized previously on a large scale) with the diaminopropane core. Again, it was coupled to the PBD acid capping unit and deprotected under standards conditions (Deziel, 1987), to obtain the dimer in 77% yield.

Similarly, AT338 (**Scheme 5.4d**), the bis-imidazole analogue of AT242, could have been synthesized from diaminopropane and nitrotrichloroacetylimidazole **96**, however the availability of the BOCPyImCOOH dimer **125** from another synthesic route (see chapter 6) suggested an alternative approach. The BOCPyImCOOH dimer was coupled to diaminopropane and provided rapid access to the pyrrole/imidazole PBD dimer AT-338 (**128**).
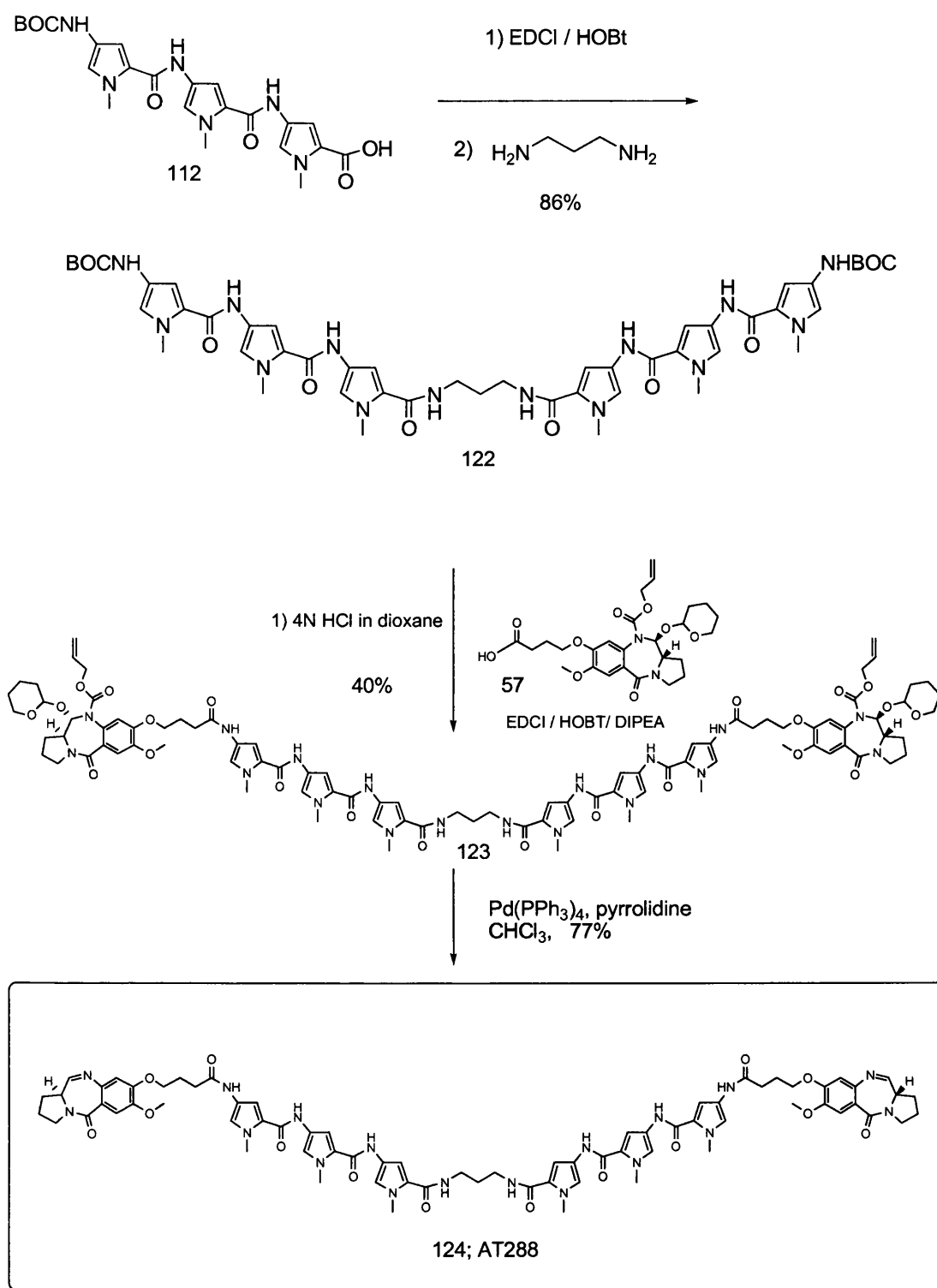
Scheme 5.4c: Synthesis of hexapyrrole symetrical dimer AT288.
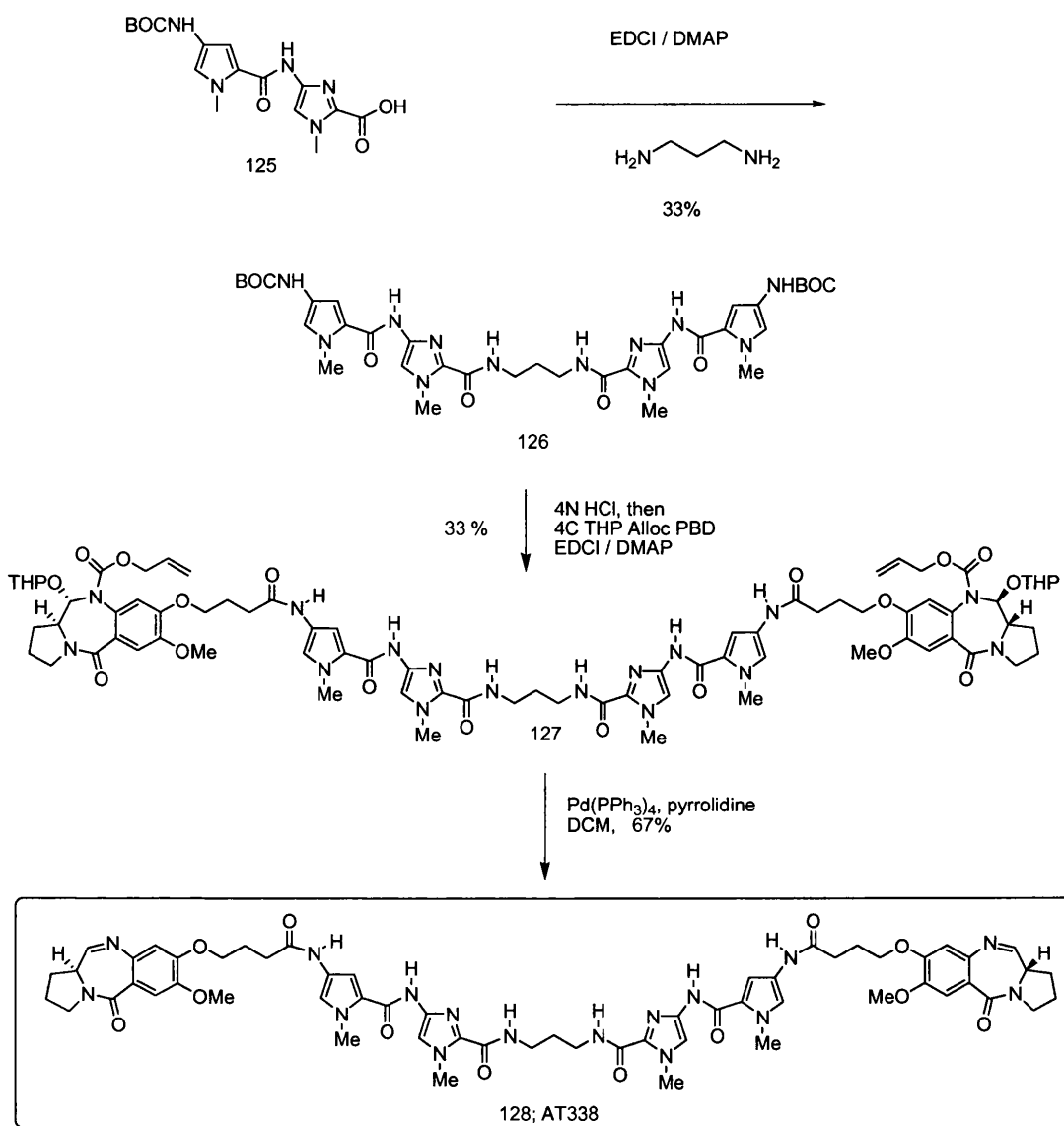
Scheme 5.4d: Synthesis of bis pyrrole-imidazole dimer AT338.

Sample Ref AT338b
after 5 days
PROTON DMSO {D:\u} atl 18
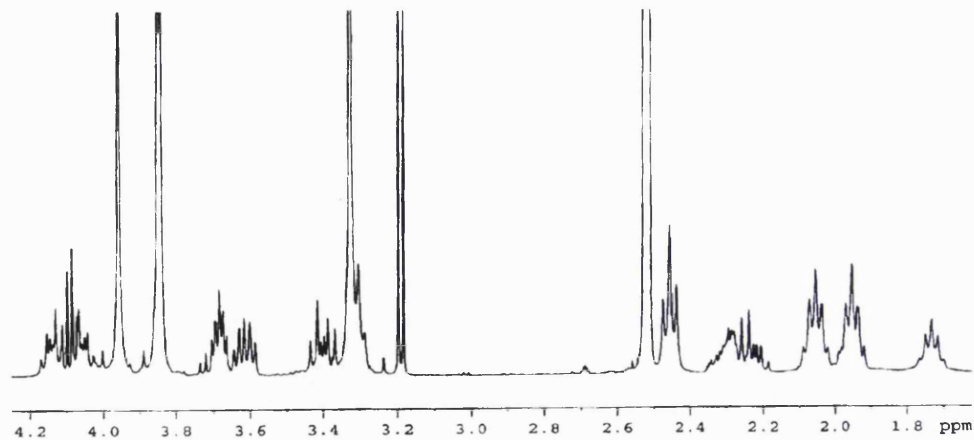
Current Data Parameters
NAME   at1-26-04-2004-18
EXPNO   10
PROCNO   1

F2 - Acquisition Parameters
Date_   20040426
Time   15:20
INSTRUM   spect
PROBHD   5 mm BBO BB-1H
PULPROG   zg30
TD   65536
SOLVENT   DMSO
NS   64
DS   0
SWH   8278.146 Hz
FIDRES   0.126314 Hz
AQ   3.9584243 sec
RG   362
DW   60.400 usec
DE   6.00 usec
TE   300.1 K
D1   2.00000000 sec
MCREST   0.00000000 sec
MCWRK   0.01500000 sec

-------- CHANNEL f1 --------
NUC1   1H
P1   7.60 usec
PL1   0.00 dB
SFO1   400.1324710 MHz

F2 - Processing parameters
SI   32768
SF   400.1299949 MHz
WDW   EM
SSB   0
LB   0.30 Hz
GB   0
PC   1.00
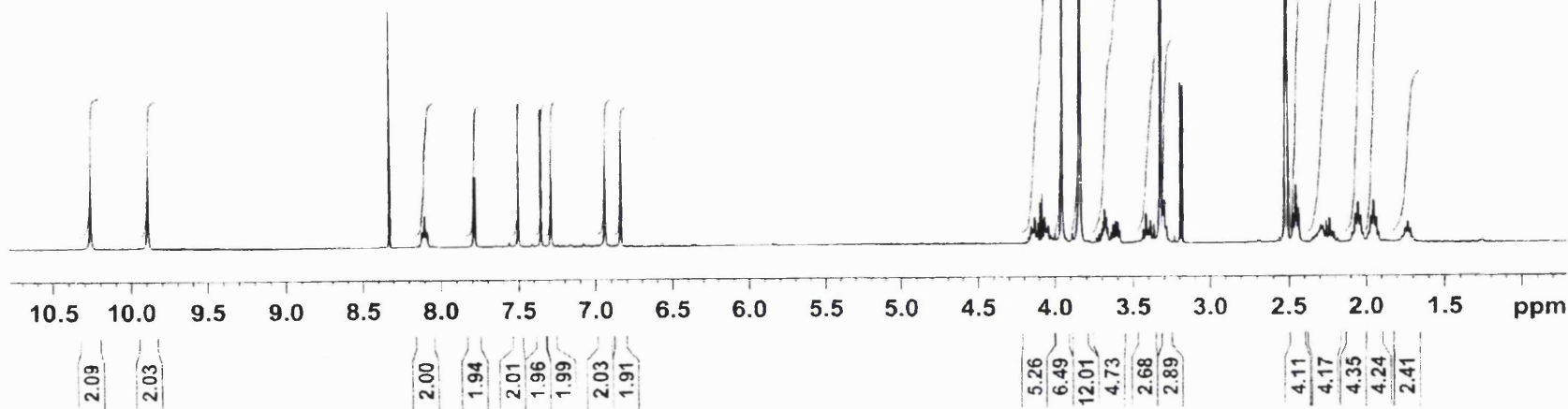
6 Hairpin polyamide conjugates

6.1 Introduction

Whereas the previous chapter focused on pyrrole/imidazole PBD dimers, designed to recognise DNA in a 1:1 fashion and form crosslinked adducts, this chapter will describe the synthesis of pyrrole/imidazole PBD hybrids designed to recognise and monoalkylate DNA in a 2:1 fashion. Hopefully, this would allow rational, predetermined, DNA targeting according to Dervan's rules.

Instead of focusing on one particular design, a variety of molecules were synthesised in order to explore the role of the linker, the loop, the direction of the polyamide chain, and the degree of freedom of the polyamides chains. After biological evaluation, the most efficient design could then be used as a template for the future synthesis of small libraries.

The different types of these pyrrole/imidazole PBD hybrids are classified in **Table 6.2a.**

6.2 Hairpins Based on an Iminodiacetic acid loop

6.2.1 Introduction

This template was exemplified by the molecule AT-293 shown below.
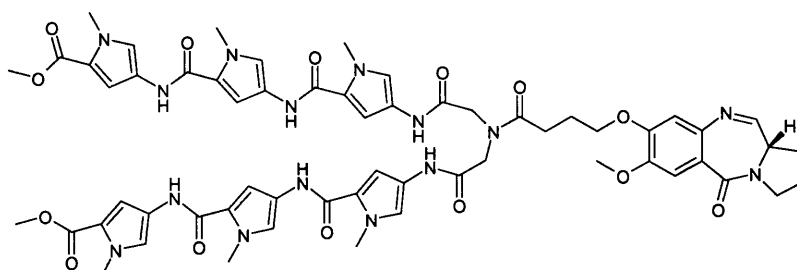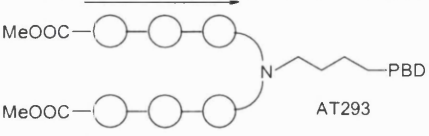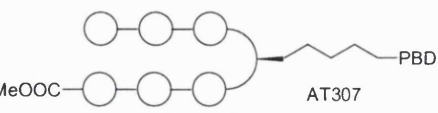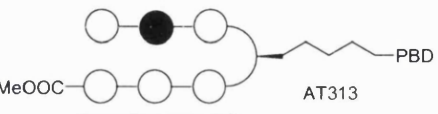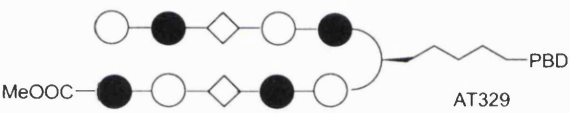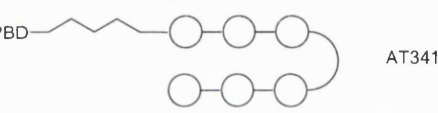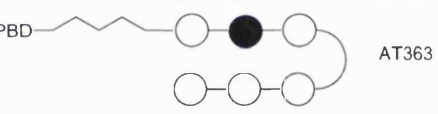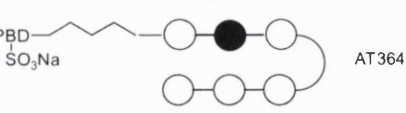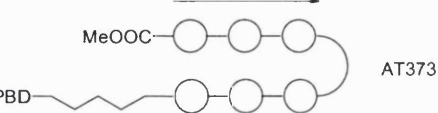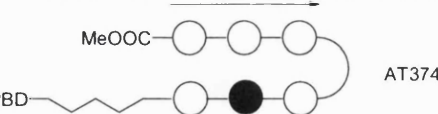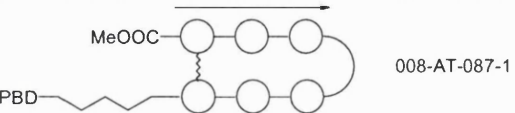
Schematic representation	Family (Branches direction, characteristic feature and PBD linkage point)
MeOOC—◯◯◯ / MeOOC—◯◯◯ —N—PBD AT293	- Parallel - Aminodiacetate loop - Branched at the loop
◯◯◯ / MeOOC—◯◯◯ —PBD AT307	
◯●◯ / MeOOC—◯◯◯ —PBD AT313	- Antiparallel - R 2,4-diaminobutyric acid - Branched at the loop
◯●◇◯● / MeOOC—●◯◇●◯ —PBD AT329	
PBD—◯◯◯ / ◯◯◯ AT341	
PBD—◯●◯ / ◯◯◯ AT363	- Parallel - Diaminopropane loop - Linked at the N-end
PBD—SO₃Na —◯●◯ / ◯◯◯ AT364	
MeOOC—◯◯◯ / PBD—◯◯◯ AT373	- Antiparallel - Aminobutyric acid loop - Linked at the N end
MeOOC—◯◯◯ / PBD—◯●◯ AT374	
MeOOC—◯◯◯ / PBD—◯◯◯ 008-AT-087-1	- Antiparallel - Cyclised - Aminobutyric acid loop - Linked at the N-end

Table 6.2a: PBD-polyamide conjugates that should form hairpins and recognise DNA in a 2:1 fashion. White circles represent N-methylpyrrole amino acid, whereas black circles are for N-methylimidazole. Arrows point to N-terminus of heterocyclic chains.

122

The key structural feature of AT-293 is the presence of an iminodiacetic loop and branching element. The central nitrogen avoids the creation of a chiral center when joining the PBD to the loop. The symmetry of this loop element forces the short polyamides chain to run parallel to each other, from their methyl ester C-terminus. Polyamides running parallel to each other are relatively unknown and their DNA binding properties would have to be thoroughly investigated and compared with the more common antiparallel binding mode.

6.2.2 Synthesis

Paradoxally, despite its relatively simple structure, AT-293 has been the most difficult compound to synthesise during the course of this project. As the first hairpin target, the synthesis suffered several setbacks. However, these difficulties gave valuable insights to the choice of coupling conditions, protecting groups, reaction solvents, PBD capping units, NMR solvents and chromatographic systems. The knowledge accumulated during the synthesis of AT-293 (**131**) paved the way for the success of the following syntheses.

The problems encountered can be summarized below:

<u>Problems and solutions:</u>

- Problems during the coupling the PBD capping unit to the amine of iminodiacetic acid:

A) <u>Using the amine salt</u>. Problems were encountered when attempting to couple the PBD capping unit to the protonated form of "iminodiacetic ester". These problems occurred whether using the commercially available starting material or late stage intermediates obtained through acid-mediated Boc deprotection. Simply, using additional equivalents of base (e.g. DIPEA), *in situ,* to generate the free base, were consistently unsuccessful. However, isolating the free base prior to coupling solved this problem.

B) <u>The 4C BOC PBD acid capping unit</u>. The unprotected 11 hydroxy capping unit **46** led to formation of impurities when the EDCI/DMAP coupling system was employed.

This could be avoided by the use of the less reactive EDCI/HOBt system, but subsequent deprotection of the BOC group generated additional impurities. This problem was ultimately resolved by synthesizing, and utilizing, the 4C Alloc THP PBD capping unit **57**.

C) Cbz protection for the secondary amine of the loop

The problems encountered with acid-mediated BOC deprotection prompted the use of the Cbz group. The Cbz protected hairpin could be readily synthesized, but hydrogenolysis was slow and produced significant amount of impurities. This may have been due to the presence of small quantities of halogenated solvents poisoning the catalyst. Eventually, protecting group issues at the loop nitrogen were simply resolved by coupling to the PBD capping unit first. The successful synthesis of AT-293 is depicted in **Scheme 6.2a**.

After successful coupling of the iminodiacetate to the PBD capping unit (EDCI/HOBT, 94%), a swift saponification provided the PBD diacid intermediate **129** in good yield. BOC tripyrrole methyl ester **78** was deprotected using 4N HCl in dioxane and immediately treated with the PBD diacid in the presence of EDCI and DMAP. Although the reaction was successful, the yield was poor (20%). This could be alleviated in the future, by using a different solvent than DMF.

Indeed, use of DMF proved to be a recurrent problem in the synthesis of complex polyamides, as an aqueous work-up was always required. The use of DMF as a solvent triggers the need for an aqueous work-up. Under these conditions, intractable and viscous emulsions were often formed. As a result, some DMF remained in the organic phase and causing problems during chromatographic purification. The problem could be avoided by employing lower boiling point solvents that could be removed by rotary evaporation under reduced pressure. AT-293 (**131**) was finally obtained in good yield (88%) after standard PBD deprotection.
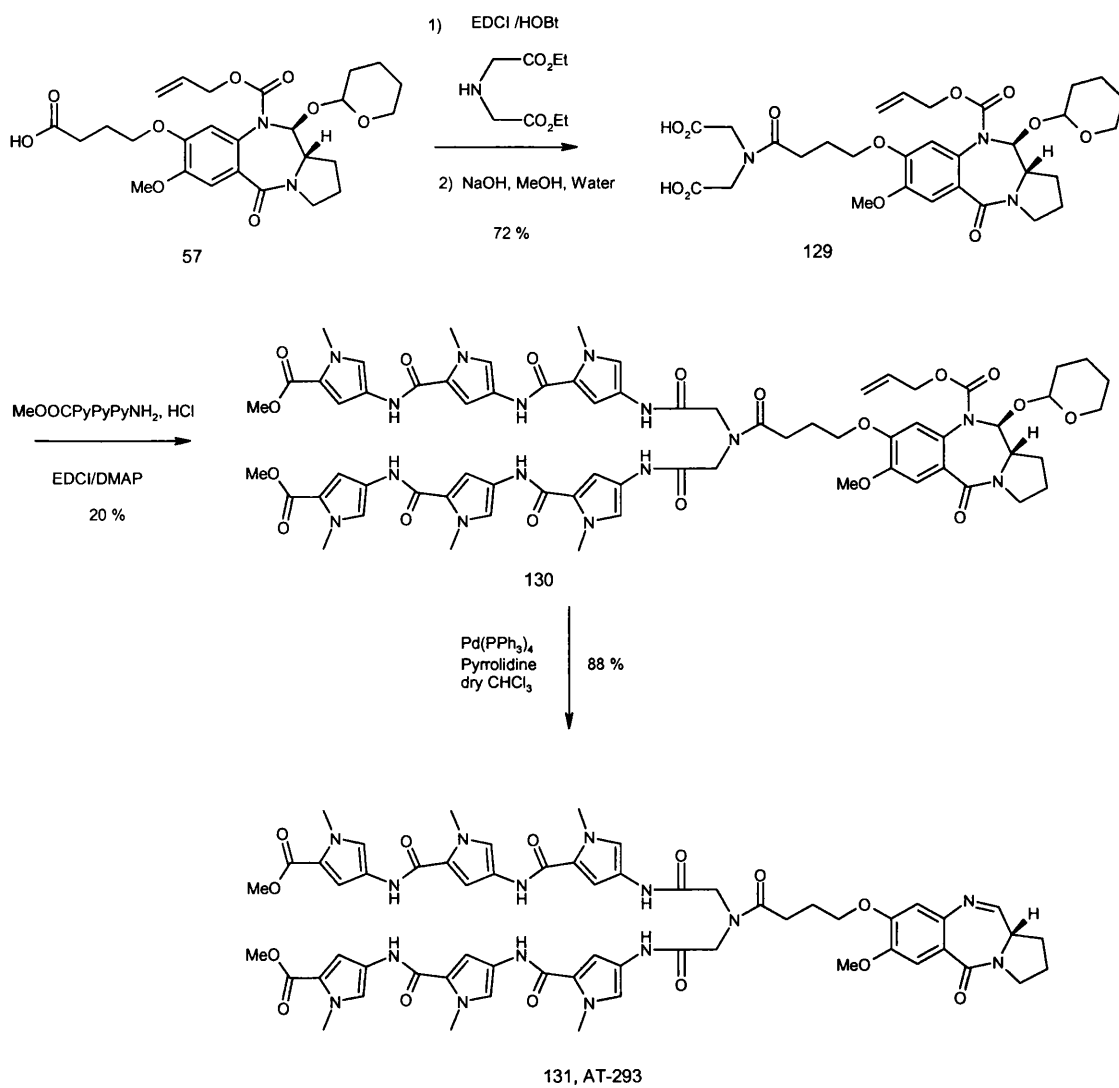
Scheme 6.2a: Synthesis of hexapyrrole conjugate AT-293

Sample Ref AT293 after 2 days
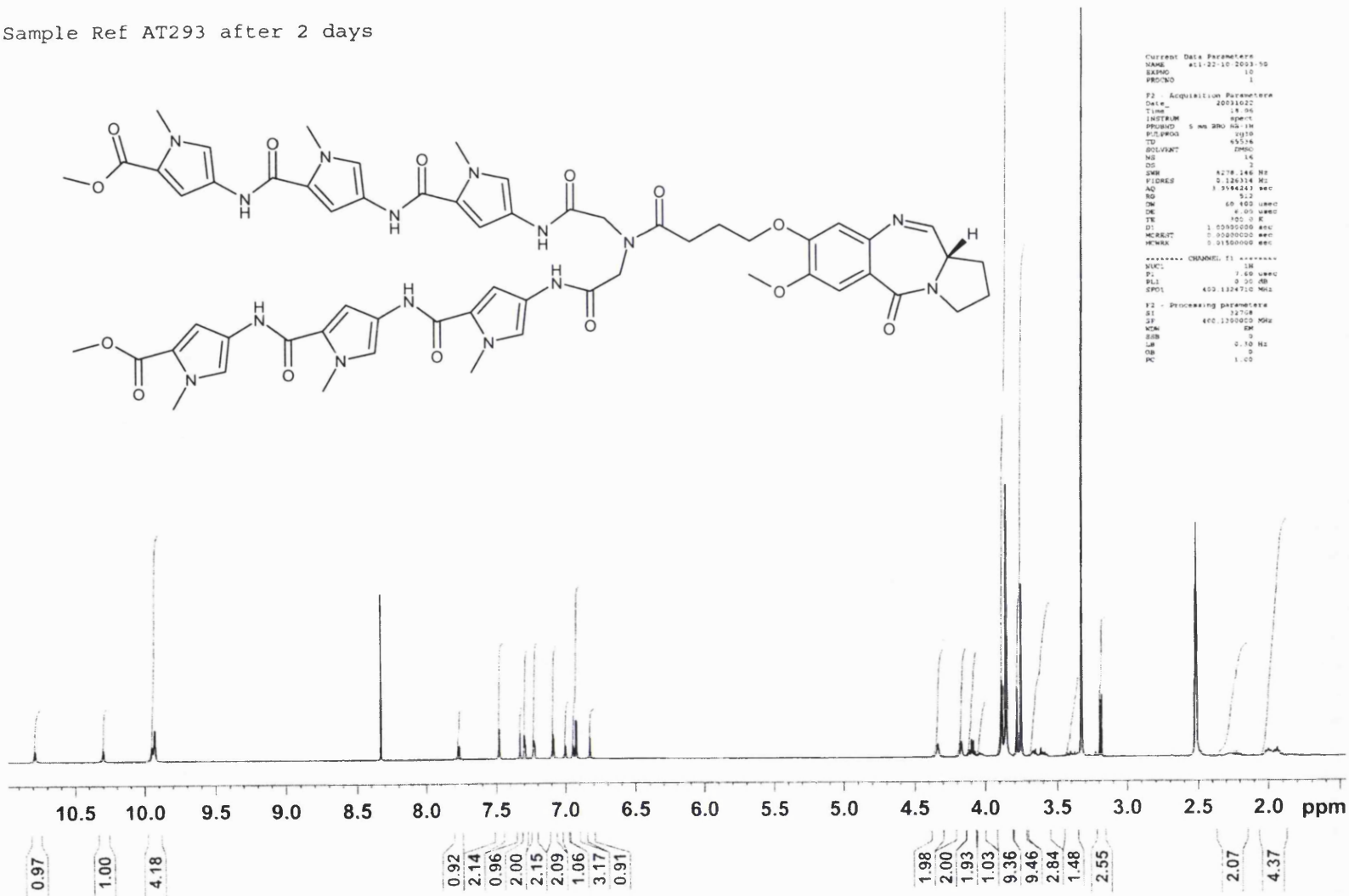
10.5 10.0 9.5 9.0 8.5 8.0 7.5 7.0 6.5 6.0 5.5 5.0 4.5 4.0 3.5 3.0 2.5 2.0 ppm

0.97   1.00   4.18   0.92 2.14 0.96 2.00 2.15 2.09 1.06 3.17 0.91   1.98 2.00 1.93 1.03 9.36 9.46 2.84 1.48 2.55   2.07 4.37

One potential drawback to the use of iminodiacetic acid template is the difficulty of introducing the two different polyamides chains required to exploit the 2:1 recognition mode. However, this problem could be overcome by using the six-membered ring anhydride shown below (**Scheme 6.2b**) (Cheng *et al.*, 1996).
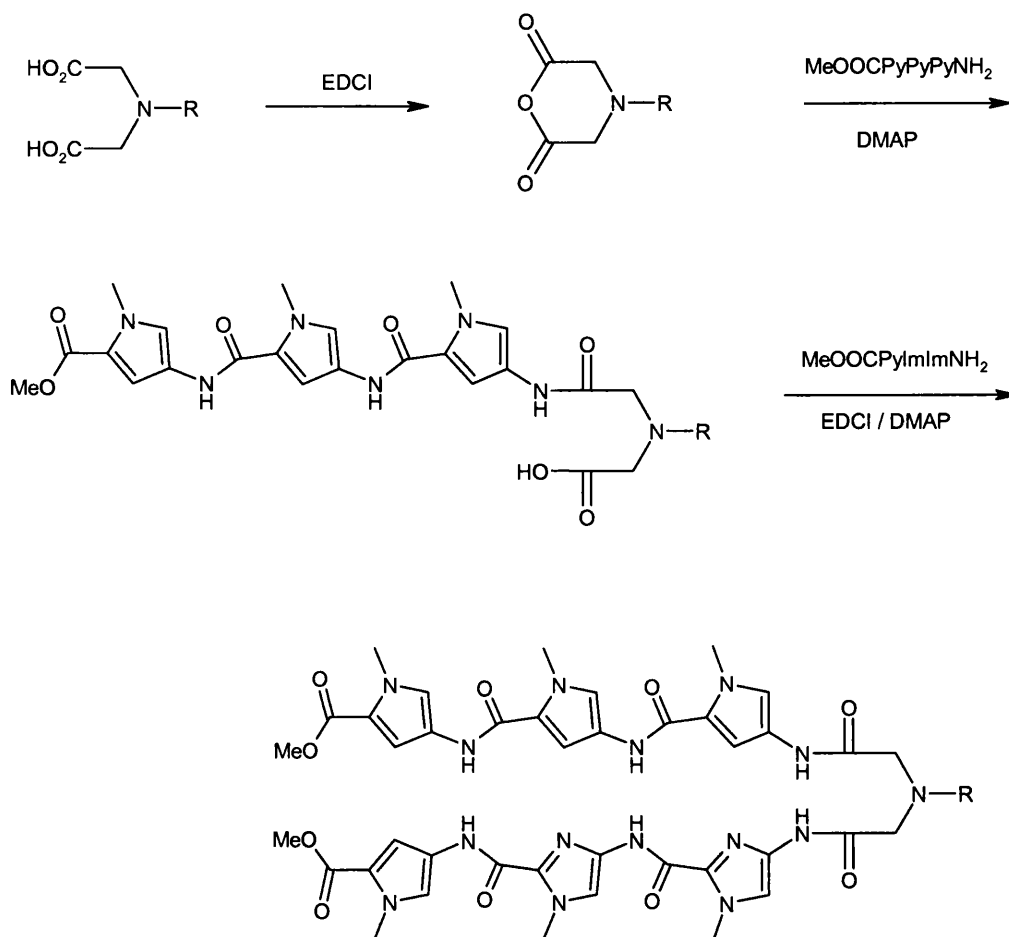
Scheme 6.2b: Possible synthesis of an asymmetrical diaminoacetamide hairpin

6.2.3 Conclusion

Despite its relatively simple design, the aminodiacetate hairpin remains synthetically challenging and will require further development. Biological evaluation of AT-293 may help to decide whether the activity justifies the synthetic effort.

6.3 Hairpins Based on the R-2,4-Diaminobutyric acid

6.3.1 Introduction

Peter Dervan and his team have synthetised pyrrole/imidazole polyamide conjugates with alkylating agents (Mustard, CPI) based on a R-2,4-diaminobutyric acid. One of these conjugates was found to selectively inhibit the expression of histone H4c gene (see chapter 3, Dickinson *et al.*, 2004). This template could clearly be adopted to the design and synthesis of PBD-Hairpin conjugates.

It was decided to synthesise three PBD-hairpins based on this design and study their biological activity. They would in turn become a reference to compare future PBD conjugates.

6.3.2 Synthesis

In order to gain rapid entry to R-2,4 diaminobutyric acid motif, the usual Dervan polyamide tail was substituted with the more convenient methyl ester. This substitution was not expected to dramatically affect base pair recognition but might have an effect on overall solubility in aqueous biological systems and DNA binding affinity.

The synthesis of these conjugates from the building blocks presented in the previous chapter is not, in itself, complex. In fact, The synthesis largely revolves around protecting group removal and amide coupling reactions. The real problems lay in the logistical arena. Possible causes of failure include:

- Launching the synthesis with insufficient quantities of material.
- Choice of protecting group strategy.
- Poor retrosynthetic strategy (i.e. coupling an amino imidazole to an imidazole carboxylate should be avoided, especially towards the end of the synthesis).
- Harsh protecting group removals conditions (*e.g.* ester saponification conditions can damage fragile parts of the molecule).

6.3.2.1 AT-307, hexapyrrole conjugate

After addressing the problems raised above, a successful synthesis of hairpin polyamide-PBD conjugate, AT-307 was successfully achieved in 10 steps. (**Scheme 6.3a**).

Although not as easily automated and, therefore, not as rapid as solid phase chemistry, solution phase approach allowed the synthesis to be performed in a highly convergent fashion. This, in turn, allowed the preparation of larger quantities of final compounds.

This type of hairpin polyamide can be disconnected at the amide bonds of the 2,4-diaminobutyric acid central element, revealing two heterocyclic polyamide branches and the PBD capping unit.

The first branch was made by coupling the protected (*R*)-2-Boc-4-Cbz-diaminobutyric acid unit to tripyrrole **78**. The second pyrrole chain could be installed following hydrogenolysis of the Cbz group. Unfortunately, the hydrogenolysis was slow and the resulting amine required purification by chromatography. The reaction conditions were revisited, and replacing ethanol by methanol significantly improved the purity of the resulting amine so that it could be used in the next step without further purification.

The second branch readily synthesised made from nitro pyrrole dimer **110** and commercially available 1-Methyl-1H-pyrrole-2-carboxylic acid. After reduction of the nitro group hydrogenation in DMF, the resulting amine was added to the activated OBt ester. The resulting trimer was immediately saponified and neutralized to yield the second branch **134** (91%).
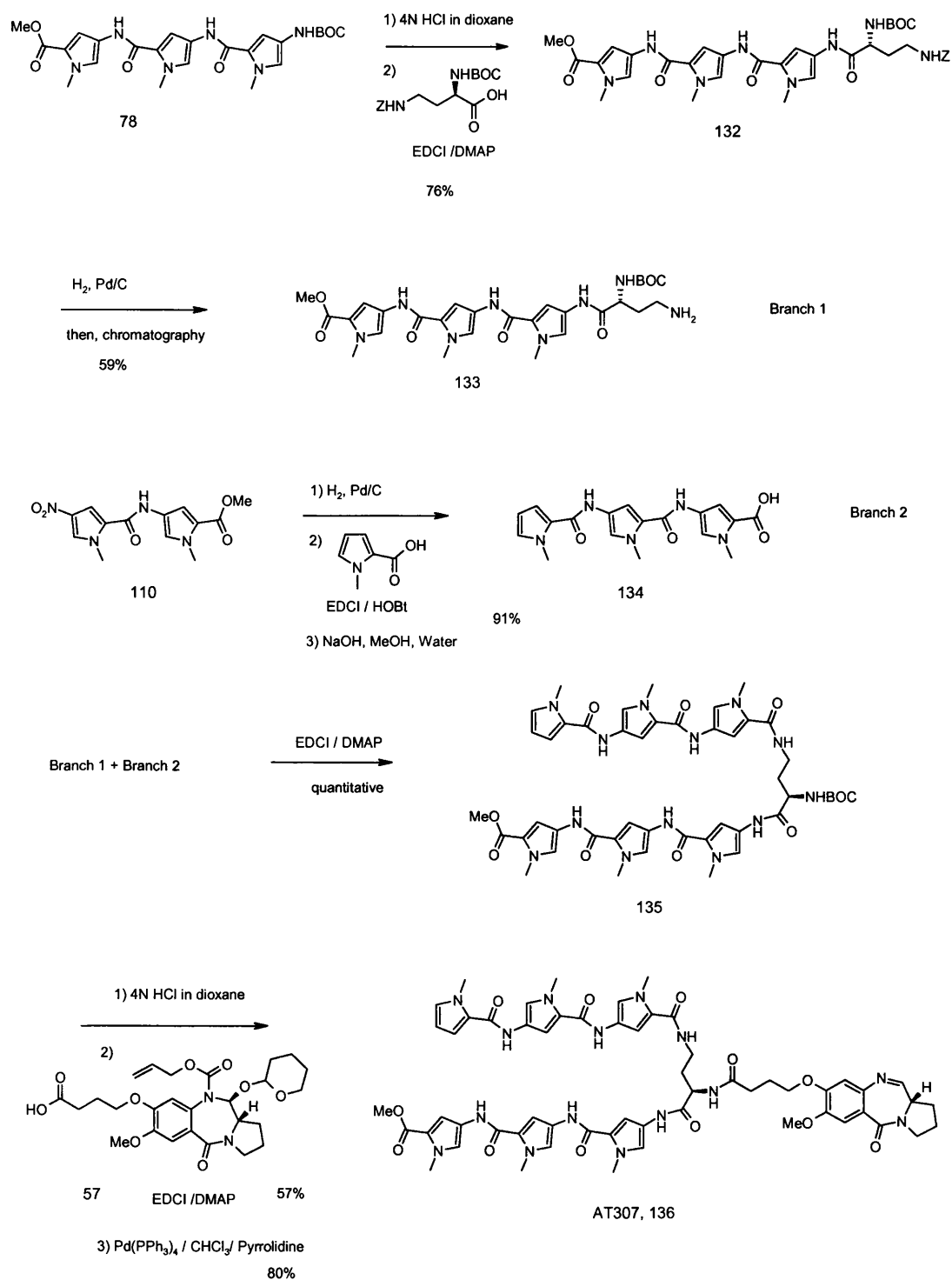
Scheme 6.3a: Synthesis of diaminobutyric acid hexapyrrole conjugate AT-307

The two branches of the hairpin were joined through an EDCI/DMAP mediated coupling in quantitative yield. The resulting BOC protected hairpin **135** was deprotected with 4N HCl in dioxane, followed by EDCI/DMAP mediated coupling to the PBD

capping unit, to furnish the protected PBD hairpin conjugate in 57% yield. Alloc and THP removal under classical Pd(0)/pyrrolidine conditions yielded the target conjugate AT-307 (**136**) in 80% yield.

6.3.2.2 AT-313, five pyrroles and one imidazole conjugate

The imidazole analogue AT313 was synthesized in the same fashion (**Scheme 6.3c**). On this occasion, one branch (Branch 2, **138**) included a central imidazole unit. As mentioned previously, the imidazole amine **98** was coupled first to remove any possibility of poor coupling at later stages of the synthesis (72%). The dimer **137**, thus obtained, was saponified and coupled again to a pyrrole amine under EDCI/DMAP activation conditions (61%). A final saponification yielded the second branch **138** in 80 % yield.

It should be noted that polyamide acids containing one or many imidazoles are difficult to retrieve by filtration as they crystallize in a spongy network upon neutralization. They are also particularly insoluble in common solvents. The latter stages of the synthesis were identical to the previously described AT-307.
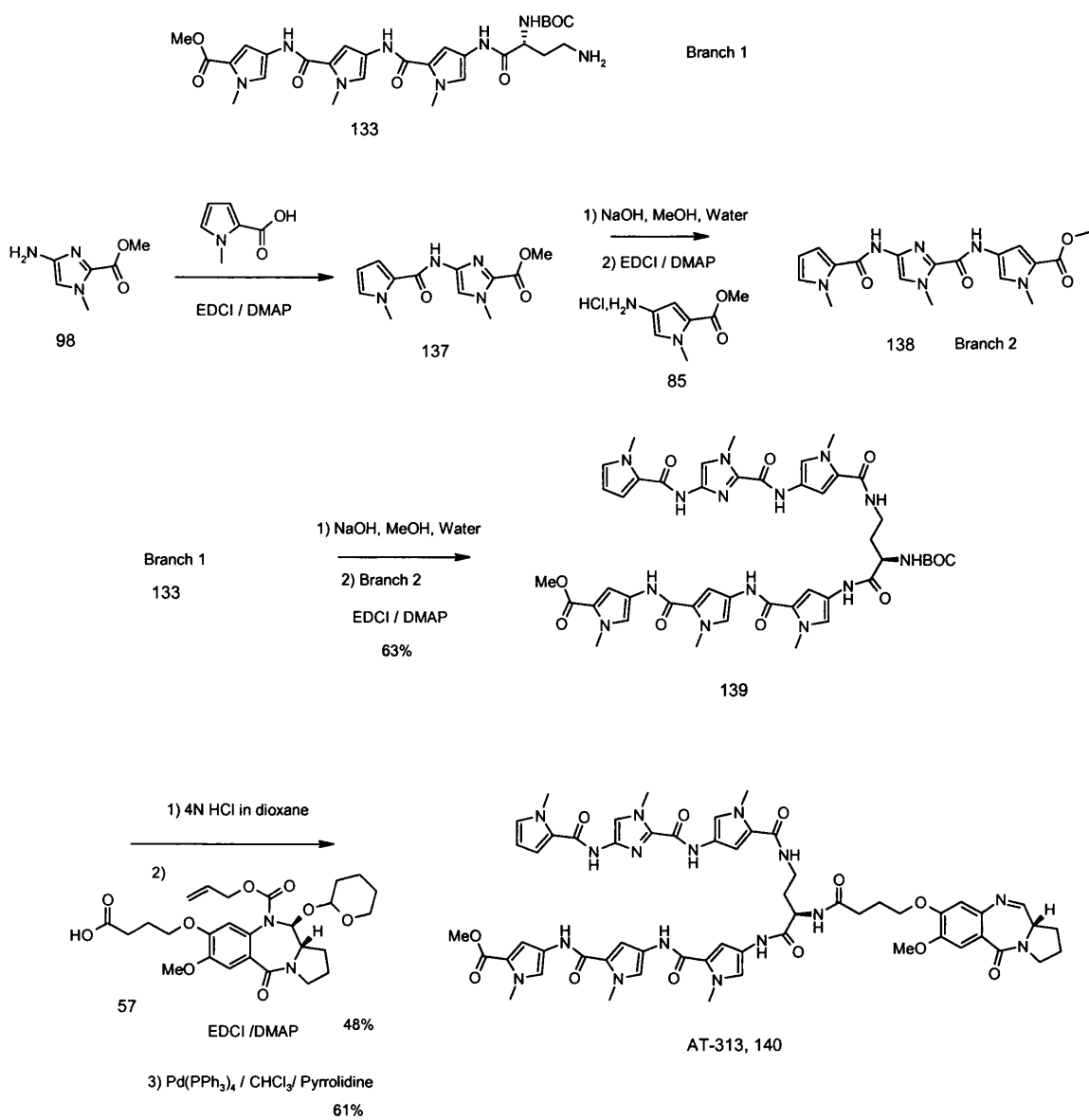
Scheme 6.3b: Synthesis of diaminobutyric acid pyrrole-imidazole conjugate AT-313

6.3.2.3 AT-329, tetra-pyrrole/tetra-imidazole/βalanine conjugate

The synthesis of the more complex hairpin –PBD conjugate AT-329 followed the same pattern (**Scheme 6.3c**). The first steps of the synthesis involved making relatively large quantities of BocPyImCO$_2$Me and its Boc derivative (BocβalaPyImCO$_2$Me, **142**). This was achieved relatively easily in two high yielding EDCI/DMAP couplings (80 and 83%). Quantitative BOC deprotection was acheived with 4N HCl in dioxane. Coupling the β-ala trimer with its precursor dimer **145** provided branch 1 (**146**, excluding the loop) in 60% yield. The same operation was carried out to form branch 2 (**144**).

As previously, the diaminobutyric acid loop was added to **146** and the Cbz was removed by hydrogenation in methanol. Again, the hydrogenolysis proceeded slowly and generated significant amount of impurities, which had to be removed by chromatography. The free amine **147** was therefore obtained in disappointing yield (32%).

The subsequent steps were identical to the previously described synthesis. Yields were somewhat lower (66% for branch 1 to branch 2 coupling, 33% for the PBD coupling and 60% for the final deprotection) as work-up procedures were made difficult by the large size and physicochemical properties of the molecule. It should be possible to avoid aqueous work-up and the resulting emulsions by removing the solvent and performing chromatography immediately.
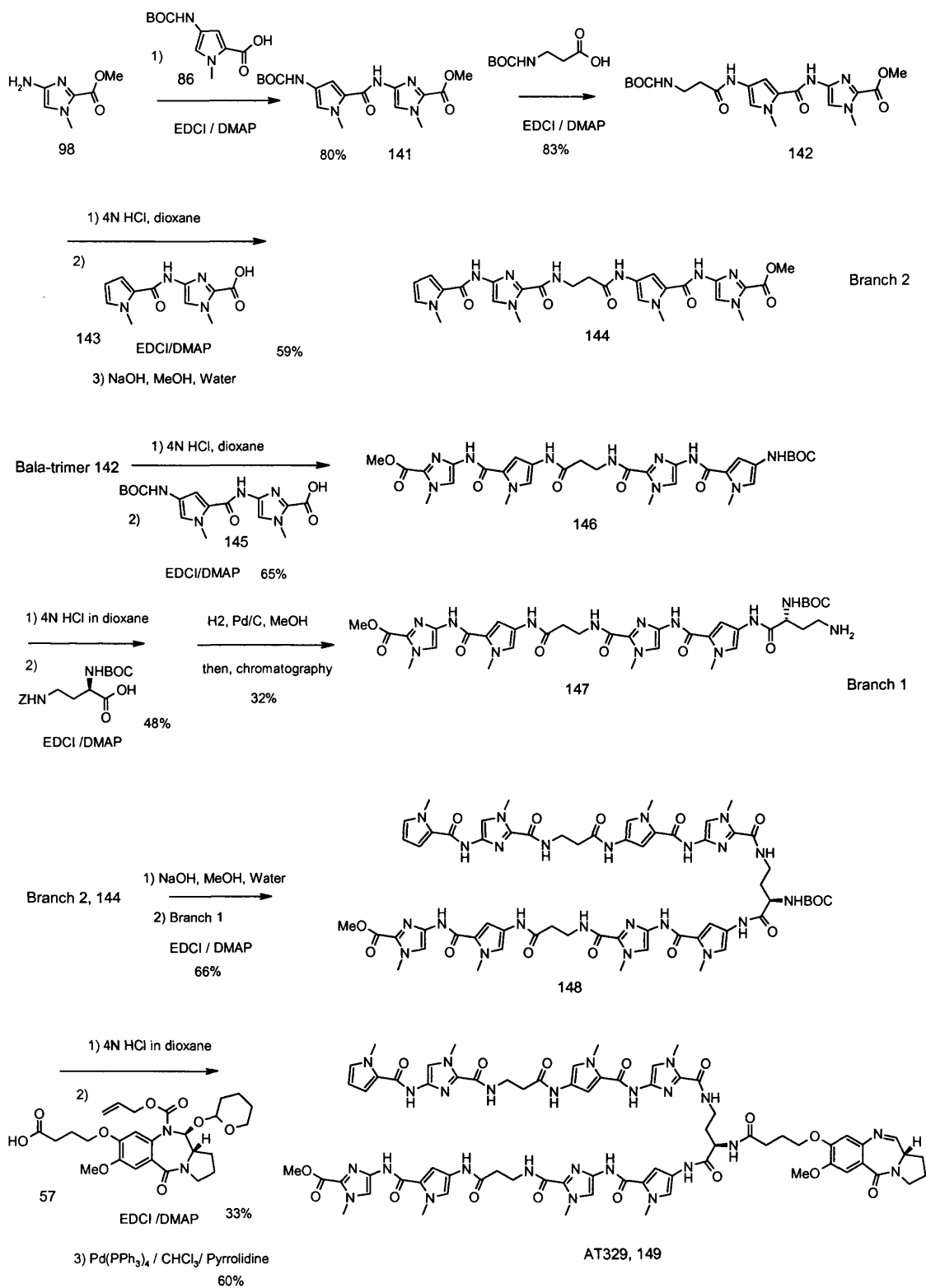
Scheme 6.3c: Synthesis of diaminobutyric acid mixed pyrrole-imidazole conjugate AT-329

6.4 Hairpins Based on a diaminopropane loop

6.4.1 Introduction

In the designs described previously, the PBD capping unit was linked to the polyamide through a iminodiacetate or diaminobutyric acid loop. However, the 4C (four carbons linker) PBD capping unit was designed to be directly attached to the polyamide, and as a result, linkage via the loop might not be structurally optimized.

Therefore, three PBD-polyheterocyclic templates were designed where the PBD would be directly attached to the heterocyclic polyamide **(Figure 6.4b)**.

The first template design was based on the PBD-heterocycle dimers; it was hoped that removal of one of the terminal PBD moieties would allow the molecule to fold back on itself and adopt the hairpin conformation.

6.4.2 Synthesis

Although very similar to the symetrical dimers based on 1,3-diaminopropane described in the previous chapter, the synthesis of these monoalkylating agents is slightly longer due to the loss of the symmetry. One branch of the molecule being different from the other, the synthesis requires additional protection and deprotection steps. **(Scheme 6.4a)**.

6.4.2.1 AT-341 hexapyrrole conjugate

Branch 1 was made by coupling a polypyrrole trimer **134** (Chapter 5) to Boc mono protected 1,3-diaminopropane. Surprisingly, although the first coupling occurred in high yield (88%), a subsequent coupling involving the same amino group following Boc deprotection was very disappointing (20%). This could be attributed to at least two reasons. The use of DMF as a solvent at this stage of the synthesis causes loss of yield by introduction of moisture to the reaction mixture, and complications during the work-

up. This can be alleviated by substitution of DMF by DCM. The second problem arose from the amino group being present as the hydrochloride salt after Boc deprotection.
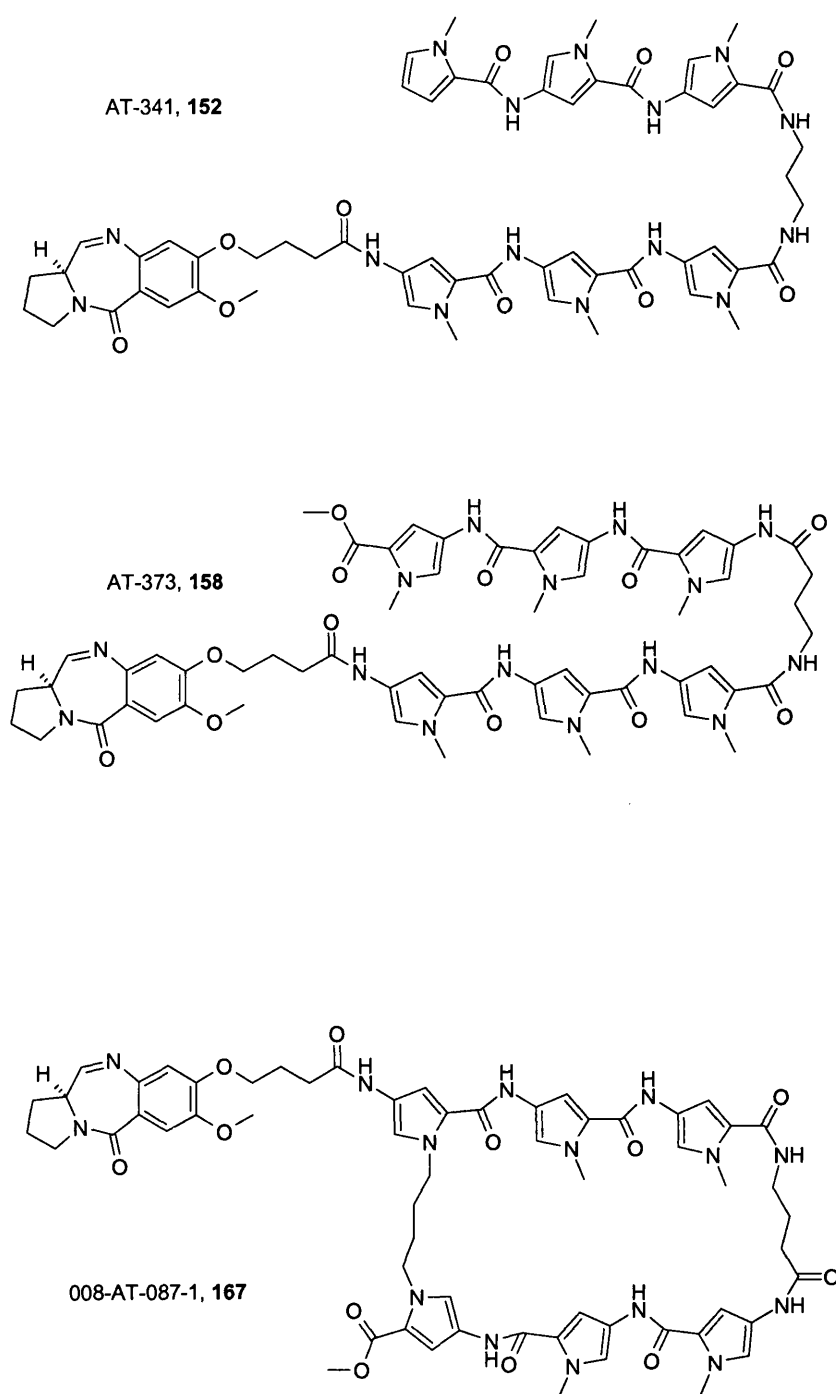
Figure 6.4a: Three designs where the PBD is directly attached to the heterocyclic chains.

Attempting to obtain the free-base *in-situ* with DMAP was found to be less efficient than converting to the free base prior to reaction. The problem may be addressable by using an ion exchange column to generate the free base.

Once again, coupling efficiency, when attaching the polyamide chain to the PBD acid capping unit, was disappointing (20%), probably because of the presence of moisture in the DMF. The route nonetheless provided access to the first hairpin of this type AT-341 (**152**) in 64% yield after final deprotection.
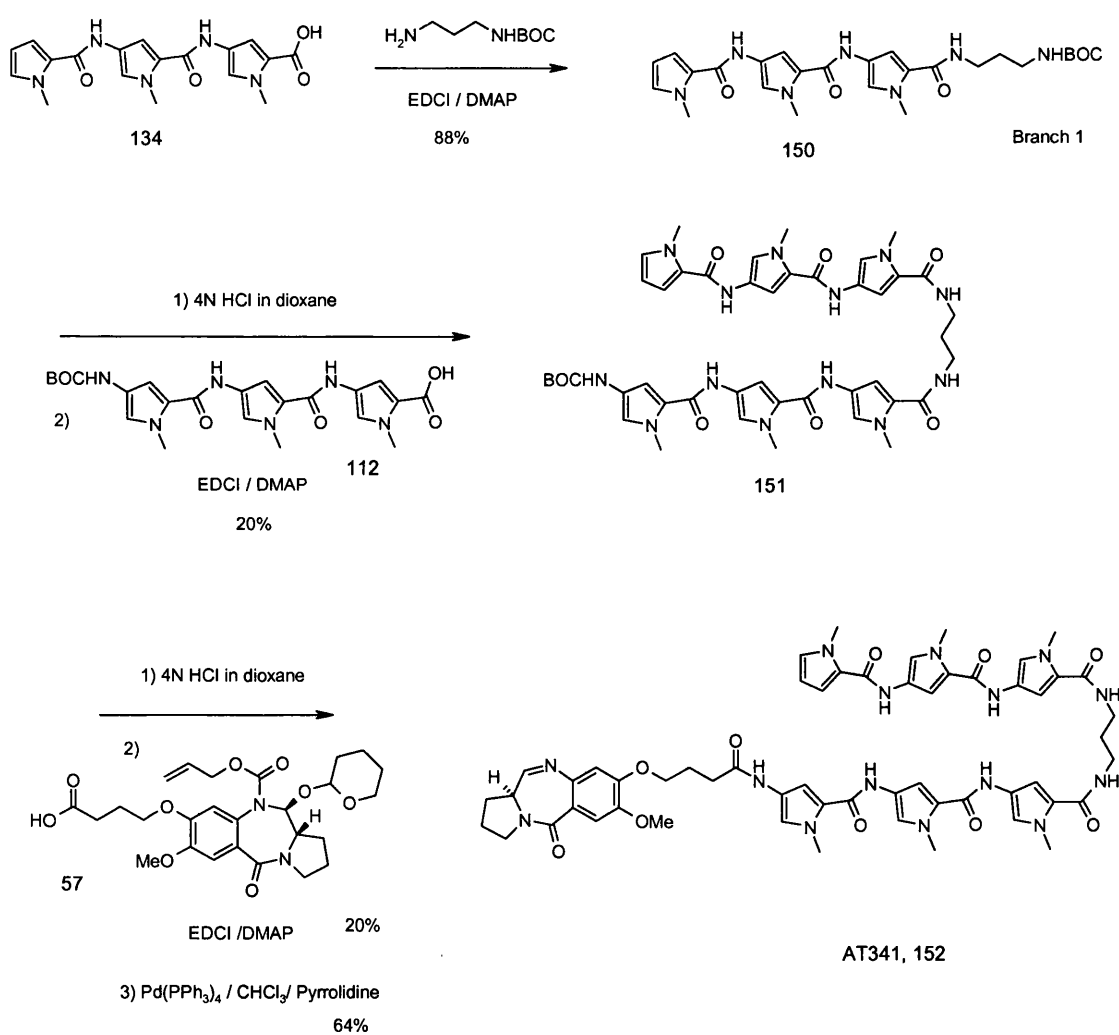
Scheme 6.4a: Synthesis of diaminopropane-based PBD hairpin conjugates. (Pyrroles only, AT-341).

6.4.2.2 AT-363, five pyrroles, one imidazole conjugate

The same route was used again to synthesise an analogue including a single imidazole heterocycle in the central position. Happily replacing DMF with DCM increased the coupling yields two-fold (42% and 52% instead of 20%).
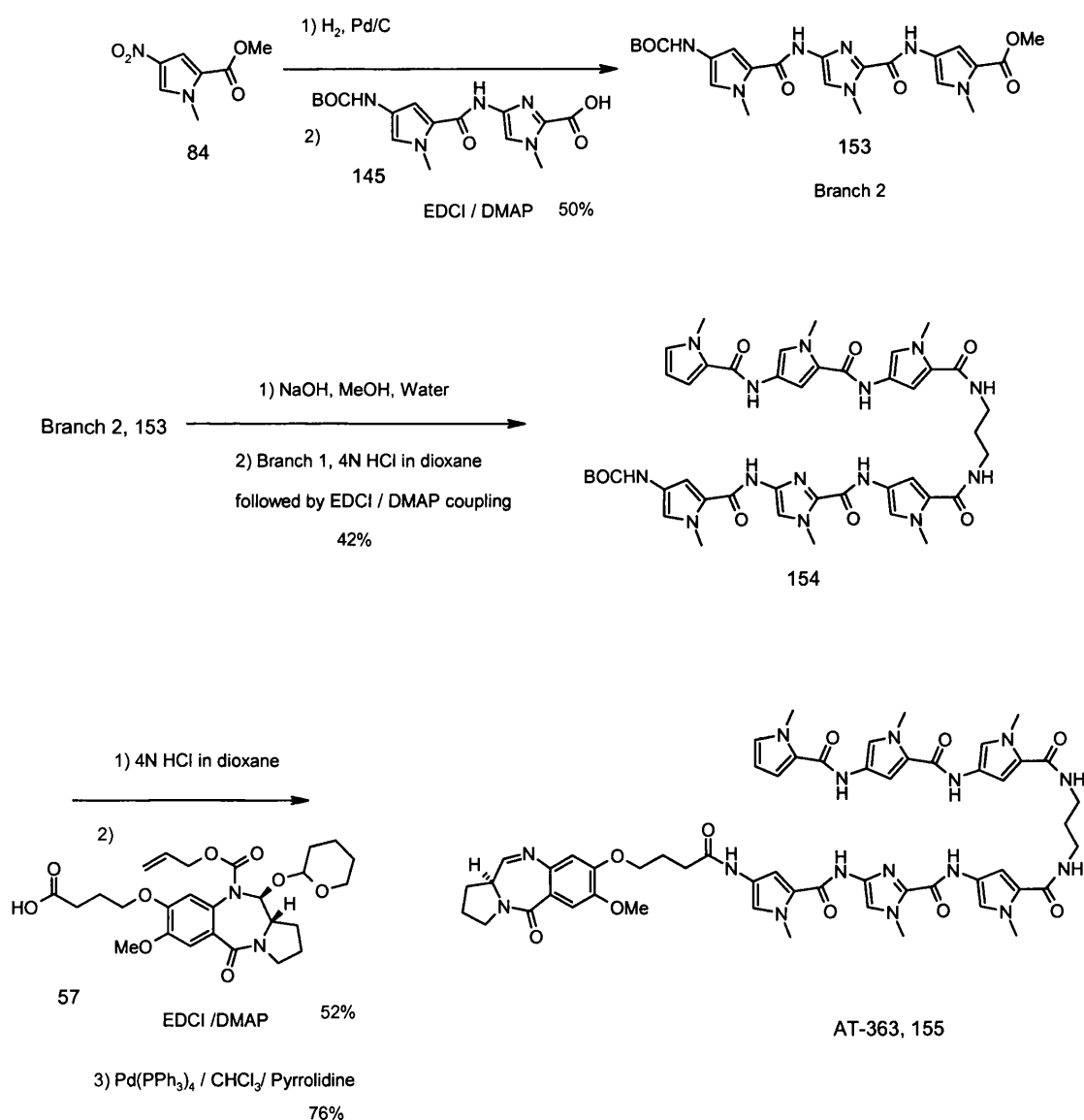
Scheme 6.4b: Synthesis of diaminopropane-based PBD hairpin conjugates. (five pyrroles, one imidazole, AT-363).

Sample Ref AT363
after 2 nights
PROTON DMSO {D:\u} at1 40
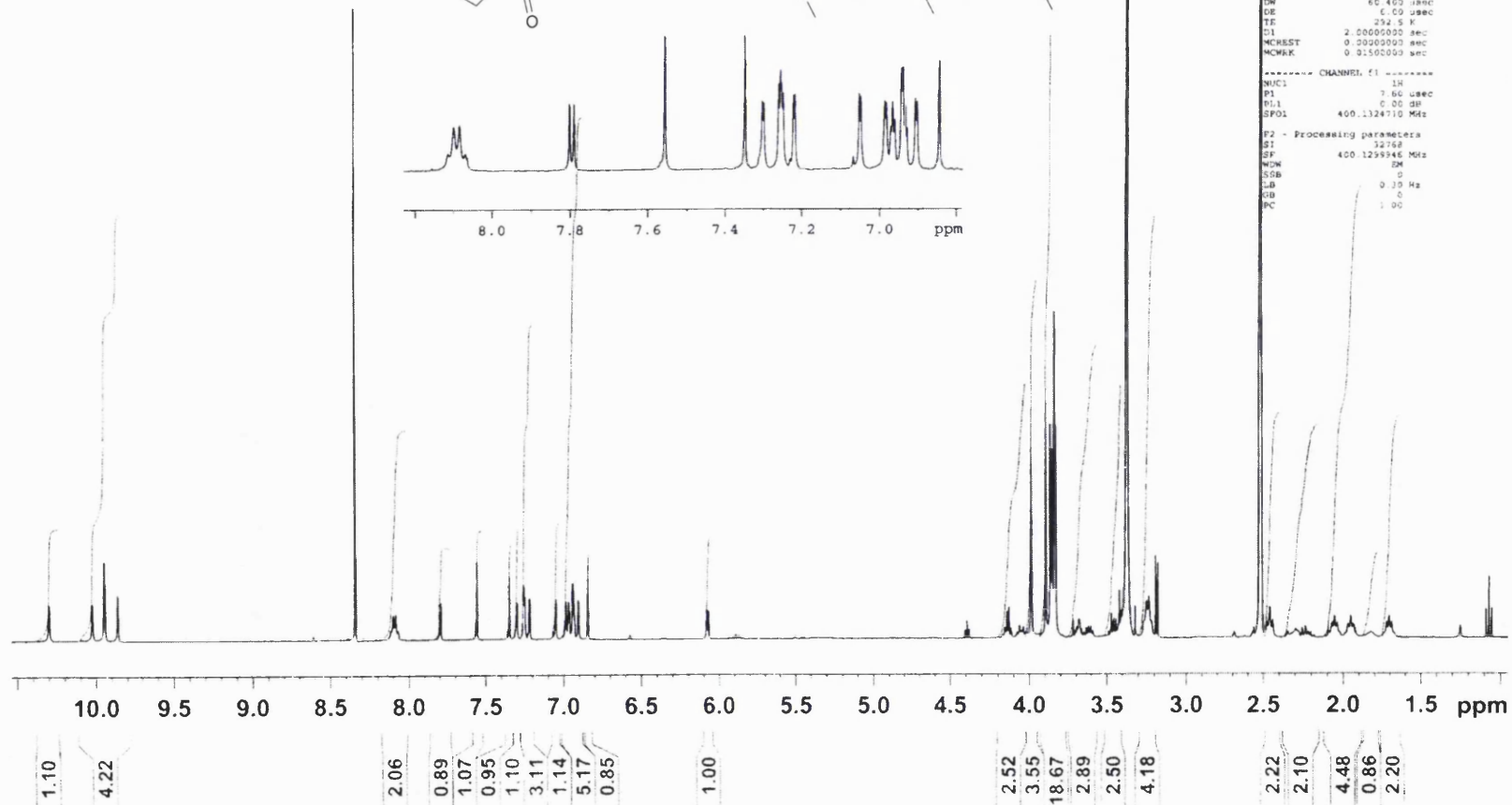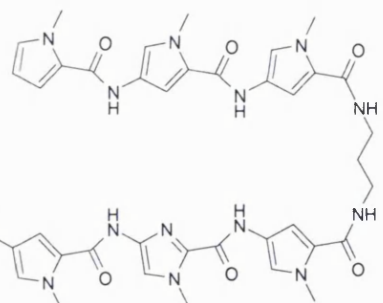
Current Data Parameters
NAME   at1-24-06-2004 40
EXPNO   10
PROCNO   1

F2 - Acquisition Parameters
Date_   20040624
Time   10.50
INSTRUM   spect
PROBHD   5 mm BBO BB-1H
PULPROG   zg30
TD   65536
SOLVENT   DMSO
NS   64
DS   0
SWH   8278.146 Hz
FIDRES   0.126314 Hz
AQ   3.9584243 sec
RG   362
DW   60.400 usec
DE   6.00 usec
TE   292.5 K
D1   2.00000000 sec
MCREST   0.00000000 sec
MCWRK   0.01500000 sec

------- CHANNEL f1 -------
NUC1   1H
P1   7.60 usec
PL1   0.00 dB
SFO1   400.1324710 MHz

F2 - Processing parameters
SI   32768
SF   400.1299946 MHz
WDW   EM
SSB   0
LB   0.30 Hz
GB   0
PC   1.00

6.5 Hairpins Based on an aminobutyric loop

The first generation of hairpin polyamides designed by Peter Dervan were based on a simple aminobutyric acid loop. Even though they have now been superseded by the more complex diaminobutyric acid template, they have been extensively studied and represent a benchmark for the field. It was therefore considered important to synthesise some PBD conjugates based on this design, for comparison purposes.

Their syntheses are very similar to the previously employed route for the diaminopropane-based hairpins and do not require detailed comment (**Scheme 6.5a and 6.5b**). It should be noted, however, that the coupling involving the hydrochloride salt of the aliphatic amino group (synthesis of **157**), was once again disappointing (even in dichloromethane) suggesting that neutralization and isolation prior to reaction is required.
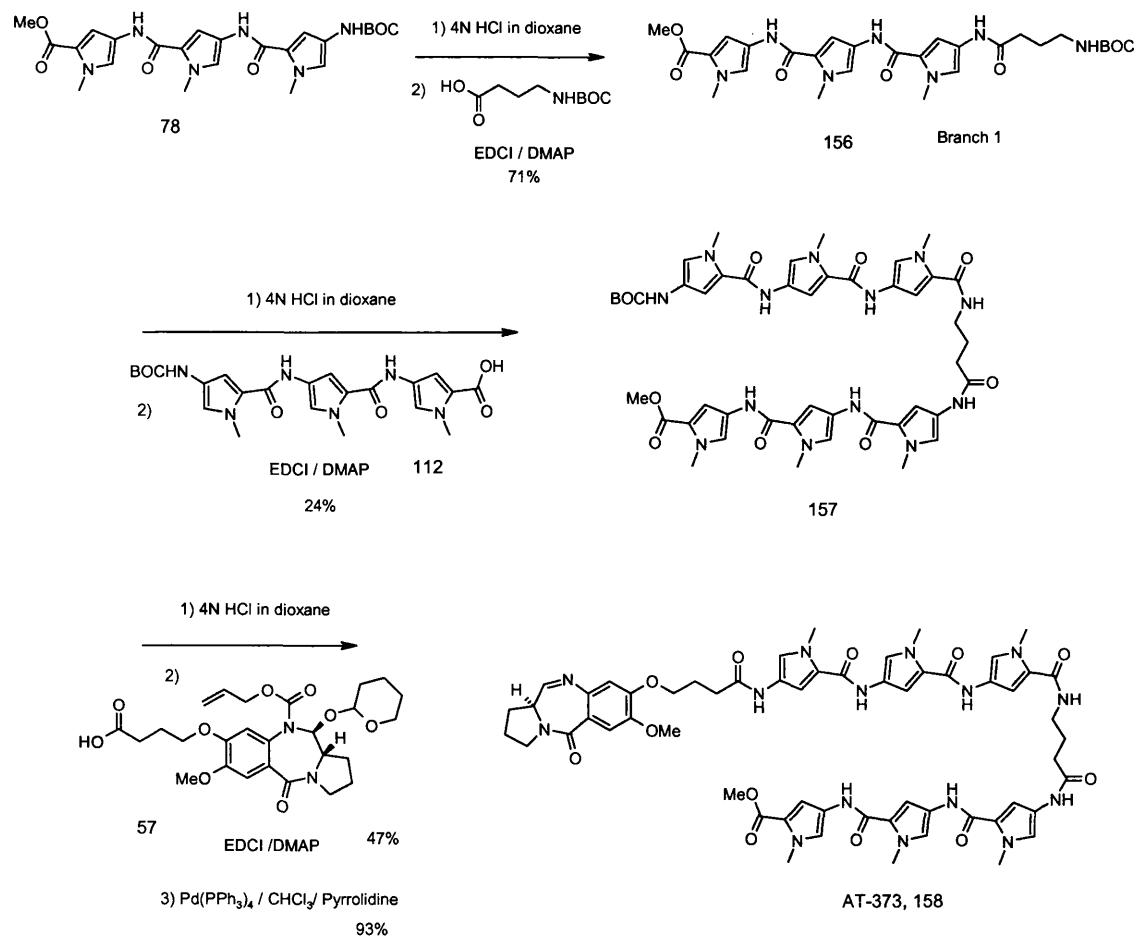
Scheme 6.5a: Synthesis of aminobutyric acid-based PBD hairpin conjugate AT-373 (pyrroles only).

141

153

1) NaOH / MeOH / water

2)

156   4N HCl in dioxane

followed by EDCI / DMAP coupling
24%

159

1) 4N HCl in dioxane

2)

57

EDCI /DMAP   36%

3) Pd(PPh₃)₄ / CHCl₃/ Pyrrolidine
80%

AT-374, 160
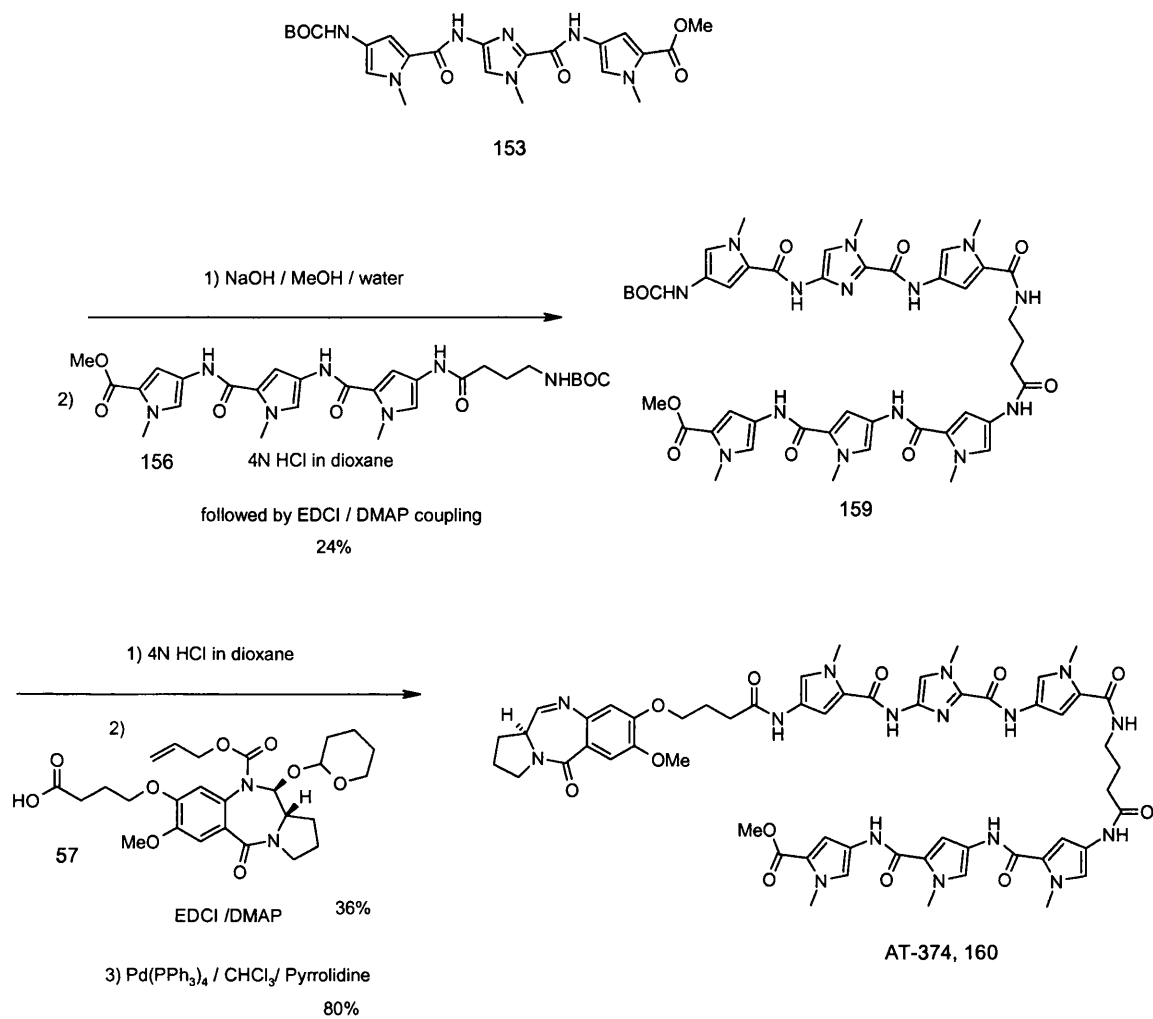
Scheme 6.5b: synthesis of aminobutyric acid-based PBD hairpin conjugate AT-374 (Five pyrroles, including one imidazole).

Sample Ref AT374
after 72 hours
PROTON DMSO {D:\u} at
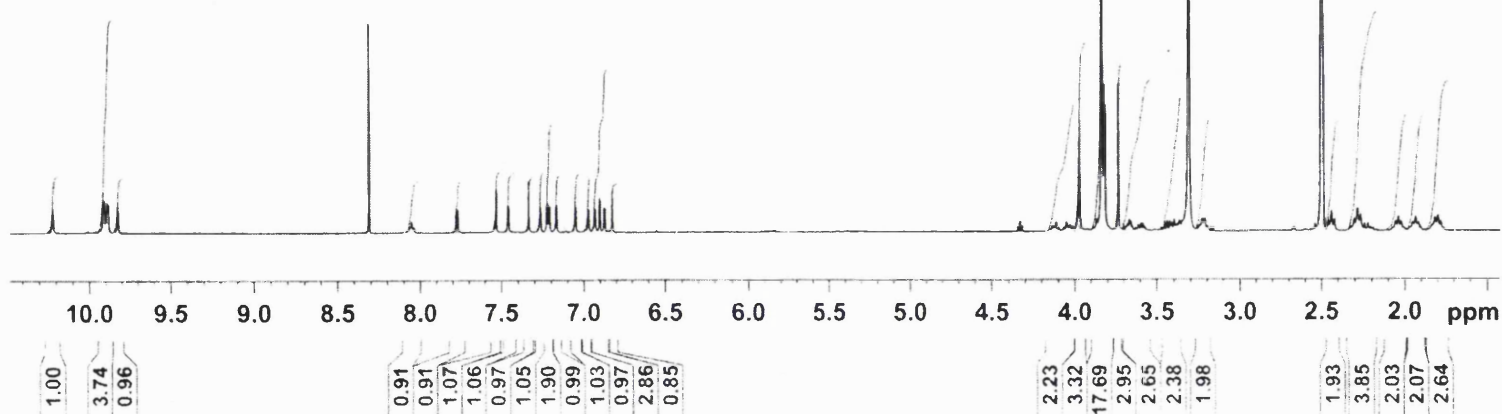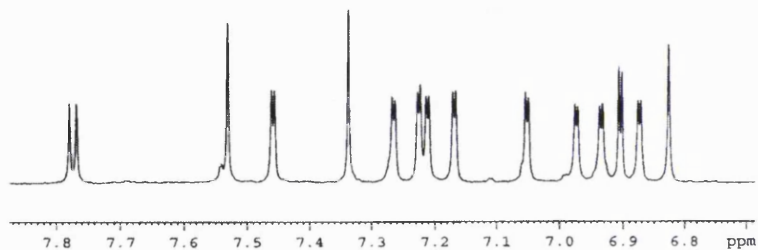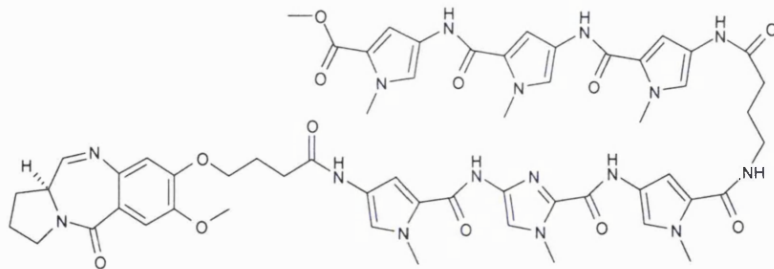
Current Data Parameters
NAME   at1-26-07-2004-20
EXPNO   10
PROCNO   1

F2 - Acquisition Parameters
Date_   20040726
Time   12 23
INSTRUM   spect
PROBHD   5 mm BBO BB-1H
PULPROG   zg30
TD   65536
SOLVENT   DMSO
NS   64
DS   0
SWH   8278.146 Hz
FIDRES   0.126314 Hz
AQ   3.9584243 sec
RG   362
DW   60.400 usec
DE   6.00 usec
TE   300.0 K
D1   2.00000000 sec
MCREST   0.00000000 sec
MCWRK   0.01500000 sec

======= CHANNEL f1 ========
NUC1   1H
P1   7.60 usec
PL1   0.00 dB
SFO1   400.1324710 MHz

F2 - Processing parameters
SI   32768
SF   400.1300029 MHz
WDW   EM
SSB   0
LB   0.30 Hz
GB   0
PC   1.00

7.8 7.7 7.6 7.5 7.4 7.3 7.2 7.1 7.0 6.9 6.8 ppm

10.0 9.5 9.0 8.5 8.0 7.5 7.0 6.5 6.0 5.5 5.0 4.5 4.0 3.5 3.0 2.5 2.0 ppm

1.00 3.74 0.96 0.91 0.91 1.07 1.06 0.97 1.05 1.90 0.99 1.03 0.97 2.86 0.85 2.23 3.32 17.69 2.95 2.65 2.38 1.98 1.93 3.85 2.03 2.07 2.64

6.6 Cyclic Polyamide PBD conjugates (Cyclin)

6.6.1 Introduction

The first hairpin templates described in this chapter had the PBD capping unit attached to the loop. This design type is expected to encourage the polyamide chain to curl back on itself, and adopt the desired hairpin conformation necessary for 2:1 DNA recognition. Interestingly the introduction of a single amino group under the shape of a 2,4-diaminobutyric acid loop increased DNA binding affinity and selectivity by a factor of 10 (Herman *et al.*, 1998*)*. This demonstrates that restricting the degree of freedom of the molecule is a beneficial factor for DNA targeting.

The two later designs discussed in the previous (hairpins based on aminobutyric acid or diaminopropane loop) lack this restriction of movement and could still be able to follow the 1:1 DNA binding mode, or overlap, as well as adopting the desired hairpin shape. Macrocyclisation of the polyamide would ensure that the, desired 2:1 conformation is achieved. This strategy has already been successfully demonstrated by Herman *et al.* in 1999. It was therefore highly desirable to synthesise a macrocyclic analogue of the templates described in the previous sections.

6.6.2 Retrosynthesis

Although it might have been possible to achieve macrocyclisation by a direct approach involving *bis*-alkylation of opposing heterocyclic nitrogens (this reaction is unlikely to proceed smoothly, as the ring nitrogen is a poor nucleophile), the modern ring closing metathesis (RCM) reaction provided the most attractive alternative. It is recognized as a very efficient and general reaction, taking place under mild conditions. It is, however, an indirect method, which lengthens the synthesis by several steps (initial installation of olefin, and reductive hydrogenation). (**Scheme 6.6a**).

144

Scheme 6.6a: Retrosynthetic analysis of macrocyclisation strategies.
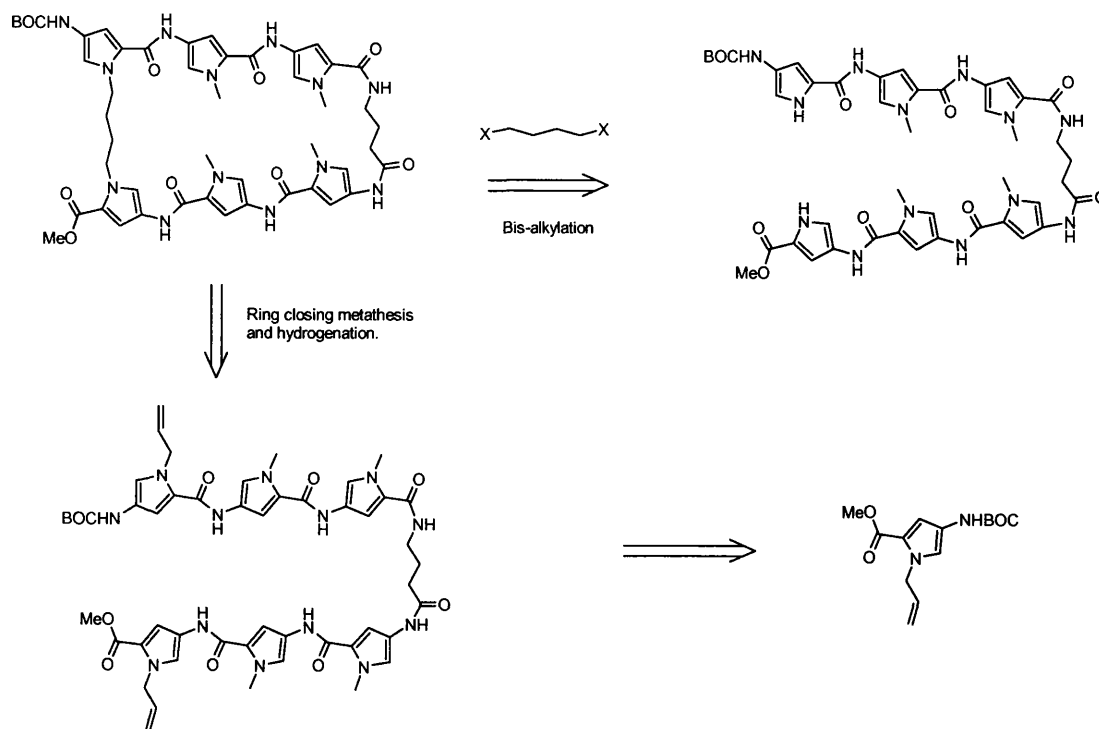
6.6.3 Synthesis of 008-AT-087-1 (hexapyrrole conjugate)

Once again, the polyamide coupling strategy was influenced by the availability of starting materials and building blocks. As the nitropyrrole dimer **110** was available in sufficient quantitity, it formed the basis of the polyamide, being coupled, both to Boc protected aminobutyric acid and the allyl pyrrole acid **93**, after reductive hydrogenation. Polyamide synthesis was completed through a series of EDCI/DMAP or EDCI/HOBt couplings, Boc deprotection and alkali mediated saponification. No major problems were encountered, and the yields were satisfactory (65% per average coupling cycle). Gratifyingly, the allyl group was found to be resistant both to the relatively harsh acidic and basic deprotection conditions. It also improved the solubility profile of the polyamide in organic solvents.
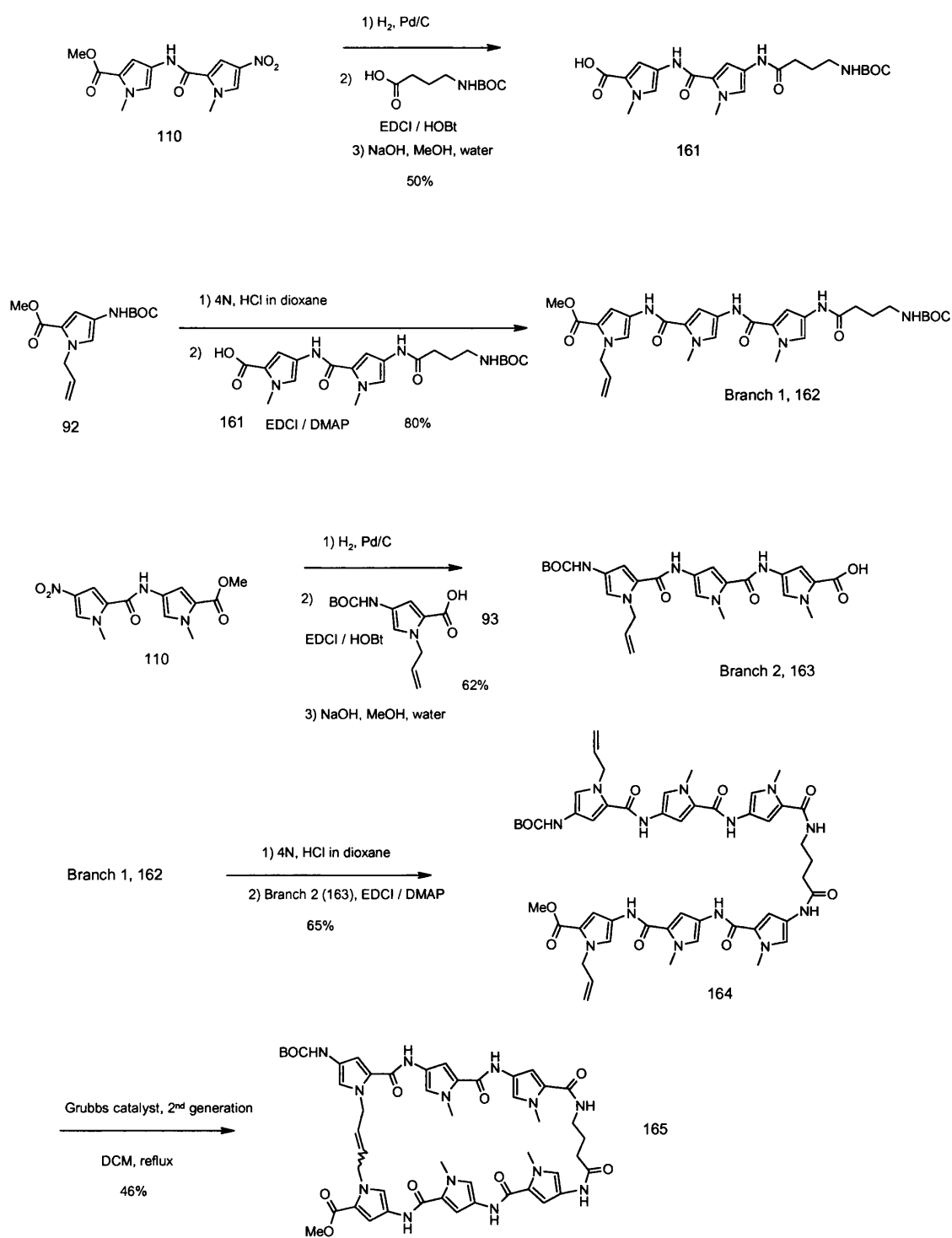
Scheme 6.6b: Synthesis of PBD-cyclin conjugates 008-AT-087-1 (early stages).

146

A trial ring closing metathesis was attempted on a small quantity of material but generated large quantities of impurities, mainly through catalyst stoichiometry problems. It appeared that the Grubbs catalyst (second generation) could remain bound to the polyamide, and consequently, be detrimental if present in high concentration. The ratio of catalyst/polyamide was therefore lowered to 1% (molar). Careful monitoring revealed that the reaction appeared to stop at 20% away from completion, probably as the catalyst was consumed through non-catalytic reaction cycles. Addition of fresh catalyst allowed the reaction to reach completion and provided the cyclic polyamide **165** in 47% yield after purification. (**Scheme 6.6b**).

Reductive hydrogenation of the remaining olefin was slow and the substrate prone to crystallization in acetone. Heating and addition of dimethylformamide were necessary to drive the reaction to completion (73 % after chromatography).The PBD acid capping unit could then be coupled and deprotected under classical conditions to yield the final PBD cyclic polyamide conjugate 008-AT-087-1, **167**.(**Scheme 6.6c**).
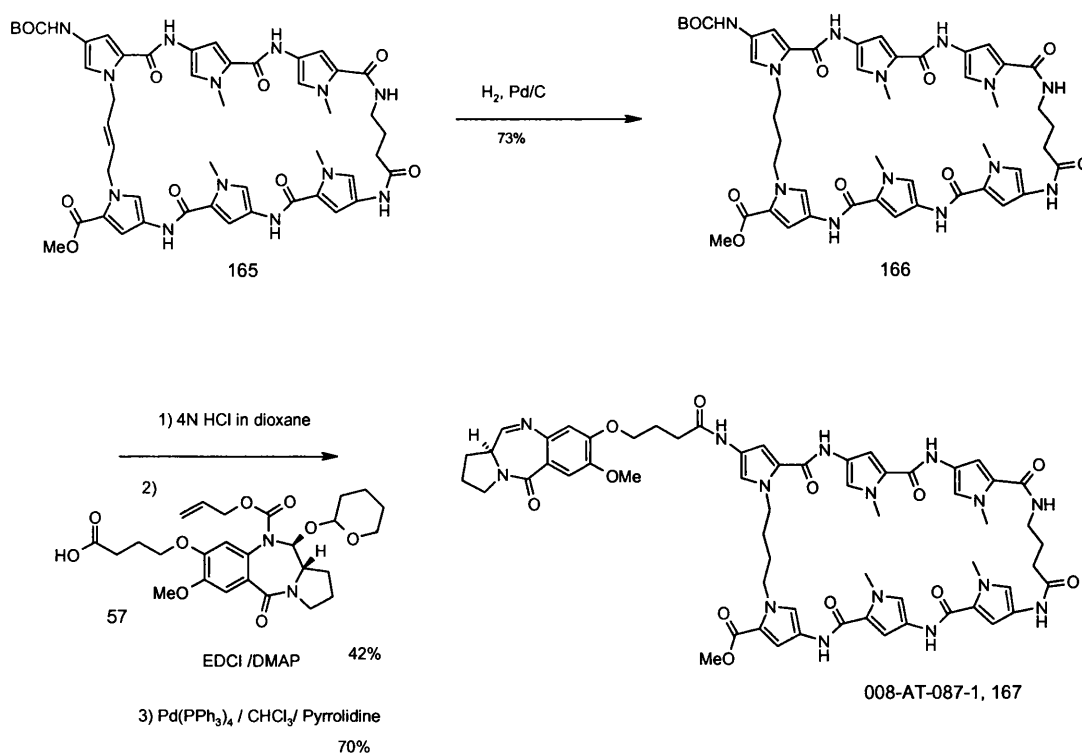
Scheme 6.6c: Synthesis of PBD-cyclin conjugate 008-AT-087-1 (final stages).

147

008-AT-087-1

5.98

0.80
0.81
0.88
0.86
5.17
2.20
3.85
1.00

4.16
1.98
14.99
3.46
3.93
2.54
2.75

2.54
4.51
8.76

4.80

10.0 9.5 9.0 8.5 8.0 7.5 7.0 6.5 6.0 5.5 5.0 4.5 4.0 3.5 3.0 2.5 2.0 1.5 1.0 ppm

7.9 7.8 7.7 7.6 7.5 7.4 7.3 7.2 7.1 7.0 6.9 6.8 6.7 ppm

7 Biological evaluation of heterocycle-linked PBD dimers.

7.1 Introduction

The PBD dimers synthesised over the course of the project were subjected to a series of biological assays including *in vitro* cytotoxicity, crosslinking in naked DNA and in cells, DNase I footprinting, and murine *in vivo* xenograft. These assays yielded preliminary information, which helped to decide what would be the best course of action for the future.

7.2 In vitro cytotoxicity

7.2.1 Introduction

All the compounds were tested in the standard NCI (United States National Cancer Institute) 60 cell-lines assay. The NCI assay consists of a 48h incubation of fast growing cancer cells in the presence of the drug, followed by an estimation of cell growth or death. The assay delivers data points at three threshold levels: GI50 (the concentration of drug necessary to inhibit growth by half), TGI (the concentration of drug necessary to completely inhibit cell growth), and LC50 (the concentration of drug required to kill 50 % of the cells). The shape of the resulting graph is important too, as it can yield further information about the drug mode of action.

7.2.2 Cytotoxic and Cytostatic agents

A cytotoxic agent is a molecule which kills cells at a given concentration. A cytostatic agent is a molecule which prevents cell growth without disturbing its vital functions. Cytostatic activity manifests itself as a flat curve on NCI graphs, above the 0 % cell growth threshold.

There is a continuing debate as to whether cytotoxic drugs should continue to be developed in this modern era of cancer chemotherapy. Many oncologists tend to favour the cytostatic approach as this type of compound should warrant lower toxicity and fewer side effects. Disabling a key oncogenic pathway (i.e. growth or survival signalling) can be sufficient to weaken the cancer cells enough for removal by the body immune. If this does not happen, the drug has to be administered continuously and the cancer may become manageable as a chronic condition. This does not represent an ideal situation for the patient, as a mutation in the remaining cancer cells can lead them to escape the drug and multiply again. (e.g. Glivec, also called imatinib, "Resistance develops frequently and rapidly in the more advanced tumors such as CML in blast crisis. Resistance is less of a problem in chronic leukemias, but resistance could become more important for these patients too as they are followed over longer time periods, especially since imatinib is unable to eradicate all BCR-ABL1 positive cells in most patients" (Cools *et al.*, 2005)). It would therefore be unwise to dismiss cytotoxic drugs as a class. Both approaches should be considered, and cytotoxic drugs can be accepted depending on their therapeutic windows.

7.2.3 Results for the dimer set

The NCI data is summarized in bar charts and dose response curves. In the bar chart, the activity of the agent in each individual cell line is compared with the average across all 60 cell lines. The bar chart focuses on the three threshold values described previously: GI50, TGI and LC50. A table including these average data points can be found below (**Table 7.2a**). The K562 column corresponds to data points measured in an independent assay (Spirogen Biology, Alamar blue, 96h continuous exposure), for further correlation with the NCI data.
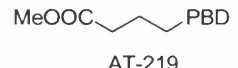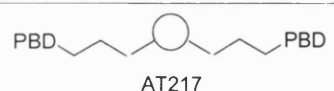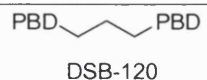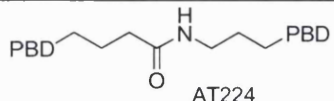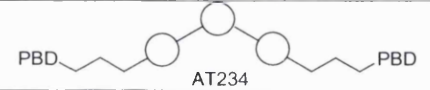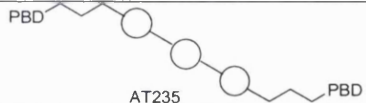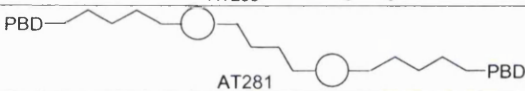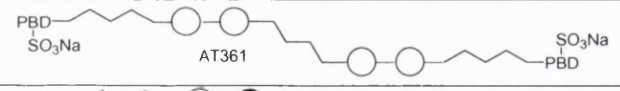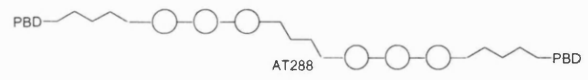
Molecules	NCI data (first assay only)			K562
	GI50	TGI	IC50	96h exp
MeOOC PBD AT-219	1.7 μM	11.7 μM	47 μM	---
PBD PBD AT217	19 μM	69 μM	95 μM	> 3 μM
PBD PBD DSB-120	3.2 μM	43.6 μM	85 μM	---
PBD H N O PBD AT224	2.1 μM	22.4 μM	76 μM	---
PBD PBD AT234	13 nM	234 nM	8.91 μM	---
PBD PBD AT235	14 nM	490 nM	23 μM	37 nM
PBD PBD AT281	13 nM	588 nM	35.4 μM	12 nM
PBD PBD Chirally pure AT360	42 nM	812 nM	28.8 μM	182 nM
PBD SO₃Na SO₃Na PBD AT361	22 nM	389 nM	33.8 μM	18.2 nM
PBD PBD AT338	29 nM	831 μM	34.6 μM	40.4 nM
PBD PBD AT288	20 nM	794 μM	30.2 μM	32.5 nM
AcHN NHAc AT336				Non active

Table 7.2a: Average data points from the standard NCI assay and comparison with Spirogen K562 measurement. Pyrrole units are represented by a white circle and imidazoles by a black disk.

151

Unexpectedly, many agents produced flat dose-response curves (see discussion on curves shape, further on), missing a number of threshold values and leading to indeterminate GI50, TGI and LC50 values. This weakened the significance of the average values stated in the table. However, a visual analysis of the curves showed that the TGI values were still representative of the general potency of the compounds.

In addition, the K562 figures listed in **Table 7.2a** are perfectly valid.

7.2.4 Discussion

The following conclusions can be drawn from the figures in **Table 7.2a**.

- The PBD capping unit is necessary for activity. The heterocyclic chain alone is poorly active, or inactive.

- Heterocycles in the core of the molecule increase the activity compared with DSB-120 which only has a short aliphatic core linker.

- The activity quite clearly increases from one heterocycle to three heterocycles. No further potentiation of activity can be observed when increasing the number of heterocycles to four or six. Most heterocycle-linked PBD dimers show low nanomolar growth inhibition, which is 3 order of magnitude better than DSB-120.

- The water-soluble bisulphite adduct AT-361 is slightly more active than its parent compound, demonstrating the potential usefulness of this prodrug approach.

- Substitution of two pyrroles with two imidazoles in AT-338 did not significantly affect the activity.

Although activity levels are quite comparable for most heterocycle-linked PBD dimers, individual compounds show significant differential activity in their NCI profile (see bar charts and dose response curves for AT-234 and AT-360). For example, AT-234 seems to be particularly efficient at blocking growth in renal cancer and melanoma cell lines. AT-360 is complementary by inhibiting growth in SK-MEL-5, a cell line that seems to initiate a resistance mechanism with increasing concentration of AT-234. Both molecules show multilog difference between various cell lines. The roots of this selectivity are probably

152

multifactorial; a balance between active transport mechanisms (uptake or excretion by P-glycoprotein (Guichard *et al.*, 2005), scavenging by protein nucleophiles, and potential differential inhibition of gene expression.

Another intriguing feature of these compounds is the shape of the dose response curve they produce. Typically, an anticancer compound features a dose response curve starting from 0 % inhibition at very low concentration and going down to a high percentage of inhibition or cell kill at high concentration (as in the leukaemia group in the upper left corner of the curves for AT-360). This is the expected and logical shape for a dose response curve produced by a cytotoxic compound.

However, several heterocyles-PBD hybrids often reveal a "flat" growth inhibition profile. A typical example can be found the leukaemia group for AT-234. These intriguing profiles may be the combination of two factors:

First, a response at very low concentration (10 nanomolar). If these compounds were tested from 10 picomolar onwards, it would be possible to observe a dose response originating from very low growth inhibition.

Second, a saturation occurring from very low concentrations onwards. In other words, these compounds did <u>not</u> have a greater effect when the cells were incubated at higher concentration.

The saturation is unlikely to be linked to solubility since the water-soluble bisulphite adduct AT-361 reveals a set of dose-response curves identical to those of its parents compound AT-360. The saturation may therefore be linked to biological factors that remain to be investigated. Is the transport system saturated, or are the DNA binding sites saturated? An investigation with radiolabelled dimer could shed light on this interesting observation.

In conclusion, most heterocycles-linked PBD dimers have shown activity at low concentration in the NCI-60 cell line screen and feature interesting dose-response curve and selectivity profiles.

Panel/Cell Line	Log₁₀GI50	GI50	Log₁₀TGI	TGI	Log₁₀LC50	LC50
Leukemia						
CCRF-CEM	-5.86		-5.23		> -4.00	
K-562	-5.69		> -4.00		> -4.00	
MOLT-4	-5.46		-5.05		> -4.00	
RPMI-8226	-5.77		-5.39		-5.01	
SR	-5.58		> -4.00		> -4.00	
Non-Small Cell Lung Cancer						
A549/ATCC	< -8.00		-6.41		> -4.00	
EKVX	-7.38		-7.66		> -4.00	
HOP-82	< -8.00		< -8.00		> -4.00	
NCI-H226	< -8.00		< -8.00		< -8.00	
NCI-H23	< -8.00		> -4.00		> -4.00	
NCI-H322M	< -8.00				> -4.00	
NCI-H460	-6.88		> -4.00		> -4.00	
NCI-H522	< -8.00		< -8.00		> -4.00	
Colon Cancer						
COLO 205	-5.62				> -4.00	
HCT-116	< -8.00		> -4.00		> -4.00	
HT29	-6.92					
KM12	< -8.00		-7.45			
SW-620	< -8.00					
CNS Cancer						
SF-268	-6.65		> -4.00		> -4.00	
SF-295	< -8.00		> -4.00		> -4.00	
SNB-19	-5.82		> -4.00		> -4.00	
SNB-75	< -8.00		> -4.00		> -4.00	
U251	< -8.00					
Melanoma						
LOX IMVI	< -8.00		-7.10			
MALME-3M	< -8.00		< -8.00		-6.78	
M14	< -8.00		-6.75		> -4.00	
SK-MEL-2	-7.67		> -4.00		> -4.00	
SK-MEL-28	-7.46		-7.86		-7.30	
SK-MEL-5	< -8.00		-5.77			
UACC-257	-6.55		< -8.00		-7.40	
UACC-62	< -8.00					
Ovarian Cancer						
OVCAR-3	-7.74		-4.22		> -4.00	
OVCAR-5	< -8.00		> -4.00			
OVCAR-8	-5.83		> -4.00		> -4.00	
SK-OV-3	-5.26		> -4.00		> -4.00	
Renal Cancer						
786-0	< -8.00		< -8.00			
A498	< -8.00		< -8.00		-7.53	
CAKI-1	< -8.00		-6.49		> -4.00	
RXF 393	< -8.00		-6.61		> -4.00	
SN12C	< -8.00				> -4.00	
TK-10	-7.62		-6.63		> -4.00	
UO-31	< -8.00		< -8.00			
Prostate Cancer						
PC-3	< -8.00		-5.54		-4.16	
Breast Cancer						
MCF7	-7.18		> -4.00		> -4.00	
NCI/ADR-RES	< -8.00		-7.54		-6.38	
MDA-MB-231/ATCC	< -8.00		< -8.00			
HS 578T	< -8.00		> -4.00		> -4.00	
MDA-MB-435	< -8.00		< -8.00			
BT-549	< -8.00		< -8.00			
T-47D	-5.79		> -4.00		> -4.00	
MG_MID	-7.37		-6.09		-4.54	
Delta	0.63		1.91		3.46	
Range	2.74		4.0		4.0	

AT360 NCI 60 cell-lines bar chart.

154

National Cancer Institute Developmental Therapeutics Program	NSC : D729102 / 1	Units : Molar	SSPL : 0CCJ	EXP. ID : 0309NS50
Mean Graphs	Report Date : April 27, 2005		Test Date : September 02, 2003	

Panel/Cell Line	Log$_{10}$GI50	Log$_{10}$TGI	Log$_{10}$LC50
Leukemia			
CCRF-CEM	< -8.00	< -8.00	-4.75
K-562	-8.00	-4.80	> -4.00
MOLT-4	< -8.00	-4.81	> -4.00
RPMI-8226	< -8.00	< -8.00	< -8.00
Non-Small Cell Lung Cancer			
A549/ATCC	< -8.00		> -4.00
EKVX	< -8.00	-5.45	> -4.00
HOP-62	< -8.00	< -8.00	-4.06
NCI-H226	< -8.00	< -8.00	
NCI-H23	< -8.00	< -8.00	-7.63
NCI-H322M	-6.63	-6.21	> -4.00
NCI-H460	< -8.00	> -4.00	> -4.00
NCI-H522	< -8.00	> -4.00	> -4.00
Colon Cancer			
COLO 205	< -8.00	> -4.00	> -4.00
HCC-2998	< -8.00	< -8.00	< -8.00
HCT-116	< -8.00	< -8.00	
HCT-15	< -8.00	< -8.00	
HT29	< -8.00	> -4.00	
KM12	-6.75	-6.40	> -4.00
SW-620	< -8.00		> -4.00
CNS Cancer			
SF-268	< -8.00	> -4.00	> -4.00
SF-295	< -8.00	< -8.00	-6.18
SF-539	< -8.00	< -8.00	-4.91
SNB-19	< -8.00	> -4.00	> -4.00
SNB-75	< -8.00	-4.94	-4.20
U251	< -8.00	< -8.00	-4.73
Melanoma			
LOX IMVI	< -8.00	< -8.00	< -8.00
M14	< -8.00	< -8.00	< -8.00
SK-MEL-2			-4.00
SK-MEL-28	< -8.00	< -8.00	> -4.00
SK-MEL-5	< -8.00	< -8.00	> -4.00
UACC-257	< -8.00	< -8.00	
UACC-62	< -8.00	< -8.00	< -8.00
Ovarian Cancer			
IGROV1	< -8.00	> -4.00	> -4.00
OVCAR-3	-6.87	-6.52	-6.16
OVCAR-4	< -8.00	> -4.00	> -4.00
OVCAR-5	< -8.00		
OVCAR-8	< -8.00	< -8.00	> -4.00
SK-OV-3		> -4.00	> -4.00
Renal Cancer			
786-0	< -8.00	< -8.00	-4.30
ACHN	< -8.00	< -8.00	< -8.00
CAKI-1	< -8.00	< -8.00	-7.48
RXF 393	< -8.00	< -8.00	-4.51
SN12C	< -8.00	< -8.00	< -8.00
TK-10	-6.69	-6.31	> -4.00
UO-31			> -4.00
Prostate Cancer			
PC-3	< -8.00	-5.41	> -4.00
DU-145	< -8.00	-7.55	> -4.00
Breast Cancer			
MCF7	< -8.00	< -8.00	> -4.00
NCI/ADR-RES	< -8.00	< -8.00	< -8.00
MDA-MB-231/ATCC	< -8.00	< -8.00	-4.36
HS 578T	< -8.00	-4.92	> -4.00
MDA-MB-435	-6.89	-6.53	-6.16
BT-549	< -8.00	-6.92	> -4.00
T-47D	< -8.00	> -4.00	> -4.00
MG_MID	-7.88	-6.63	-5.05
Delta	0.12	1.37	2.95
Range	1.37	4.0	4.0

AT234 NCI 60 cell-lines bar chart.

National Cancer Institute Developmental Therapeutics Program
Dose Response Curves

| NSC : D733783 / 1 | SSPL : 0CCJ | EXP. ID : 0408NS67 |
| Report Date : April 27, 2005 | Test Date : August 23, 2004 | |

AT360 NCI 60 dose-response curves.

National Cancer Institute Developmental Therapeutics Program
Dose Response Curves

NSC : D729102 / 1

SSPL : 0CCJ   EXP. ID : 0309NS50

Report Date : April 27, 2005

Test Date : September 02, 2003

AT234 NCI 60 dose-response curves.

7.3 Crosslinking activity

7.3.1 Introduction

The compounds discussed in this chapter are bifunctional alkylating agents. They therefore have the potential to form DNA adducts such as interstrand and intrastrand crosslinks. It is thought that the interstrand crosslink is the critical cytotoxic lesion produced by most bifunctional drugs (McHugh *et al.*, 2001). This hypothesis is supported by the conceptual difficulty of repairing such a lesion. Both strand of the DNA being involved in the lesion, the repair mechanism has to recruit the correct genetic information from an external source (sister chromosome, or multiple copies), and insert it through relatively complex recombination maneuvers. (Homologous recombinant repair), (McHugh *et al.*, 2001). It is therefore essential to quantitatively measure the interstrand crosslinking activity, and evaluate whether it correlates with cytotoxicity levels. If a correlation is established, there will be a strong link between this mode of action and the biological outcome.

7.3.2 Plasmid assay

Interstrand crosslinks can be detected by chromatographic or eletrophoretic techniques, on isolated DNA. This allows relatively high-throughput testing at increasing concentration of drugs. Dr Kostas Kiakos, from the CRUK drug-DNA interaction research group, has investigated six heterocycle-linked dimers for their crosslinking activity following the method of Hartley and Souhami (Hartley *et al.*, 1993). The results are summarized in **Table 7.3a** and express the concentration of drug necessary to achieve interstrand crosslinking in half the DNA double strands. The figures differ depending on the method of DNA denaturation (heat or alkaline) by an order of magnitude, but are consistent with each other.
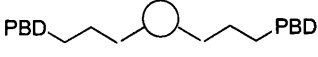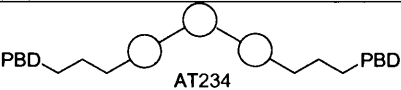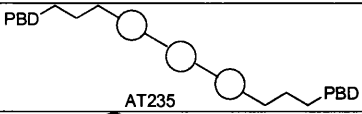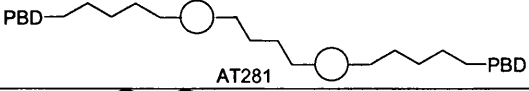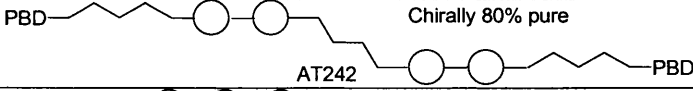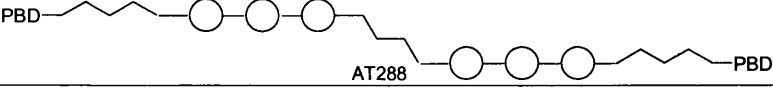
Compounds	Crosslinking (XL50; μM)
PBD~~~◯~~~PBD AT217	Base : 0.35 Heat : 3.8
PBD~~~◯~◯~◯~~PBD AT234	Base : 0.1 Heat : 0.4
PBD~~◯~◯~◯~~PBD AT235	Base : 0.1 Heat : 0.23
PBD~~~◯~~◯~~~PBD AT281	Base : 0.03 Heat : 0.1
PBD~~~◯─◯~~ Chirally 80% pure ~◯─◯~~~PBD AT242	Heat : 0.18
PBD~~~◯─◯─◯~~ ~◯─◯─◯~~~PBD AT288	Base : 0.02 Heat : 0.1

Table 7.3a: DNA crosslinking values for six dimers of the series. (Dr Kostas Kiakos UCL).

Some representative exemples of crosslinking gels obtained for AT-234, AT-235 and AT-242 are shown in **Figure 7.3a**. In the case of AT-235, it is clear that 100% interstrand crosslinking occurred at 1 μM concentration. However, further testing (Hartley and Klee, unpublished results) revealed that long heterocycle-linked PBD dimers such as AT-242 have a tendency to aggregate the DNA before eletrophoresis, impairing migration through the gel. Although some DNA moved down the gel, most of the material remained trapped in the wells, making it impossible to use the electrophoresis in a quantitative fashion. An alternative approach to assaying crosslinkers was therefore required.

AT234   XL$_{50}$= 0.4µM

AT235   XL$_{50}$= 0.23 µM

AT242   XL$_{50}$= 0.18 µM
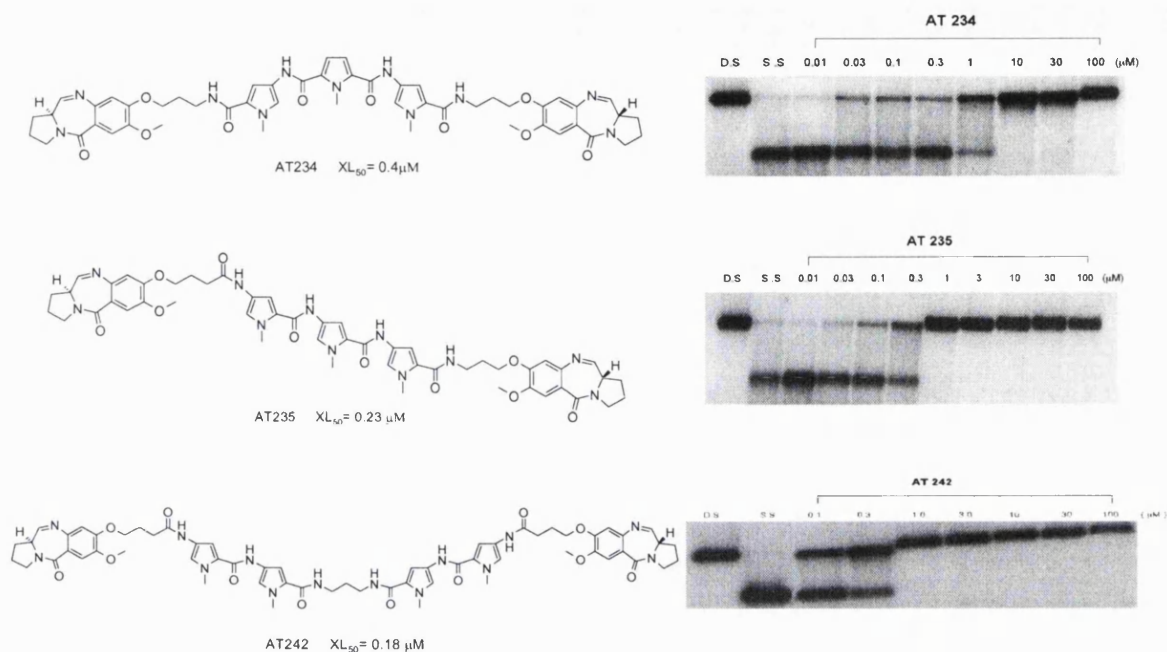
Figure 7.3a: Pictures of gels obtained when assaying the crosslinking abilities of compounds AT-234, AT-235 and AT-242 on small oligonucleotides.

7.3.3 Single cell "comet" assays

In 1999, the Hartley's group published a new method of evaluating DNA crosslinking in cells based on the "comet" assay. (Hartley *et al.* 1999). When cellular DNA is exposed to ionizing radiation, damage in the form of strand breaks occurs, producing randomly sized fragments. Gel eletrophoresis elutes these fragments away from the heavier undamaged DNA, thus forming a comet shaped distribution of DNA. The smaller fragments forming the far end of the tail, and the longer ones staying close from the head.

When the cells are treated with a DNA interstrand crosslinker prior to ionization, the resulting fragments are much heavier (the broken DNA being linked together by the crosslinker) and do not elute as far during the electrophoresis. The comet tail is reduced. (see pictures in **Figure 7.3b**). In fact, the tail length (or more precisely, the product of the tail length by the percentage of DNA in the tail, referred to as tail moment) correlates linearly with the concentration of the interstrand crosslinker.

160
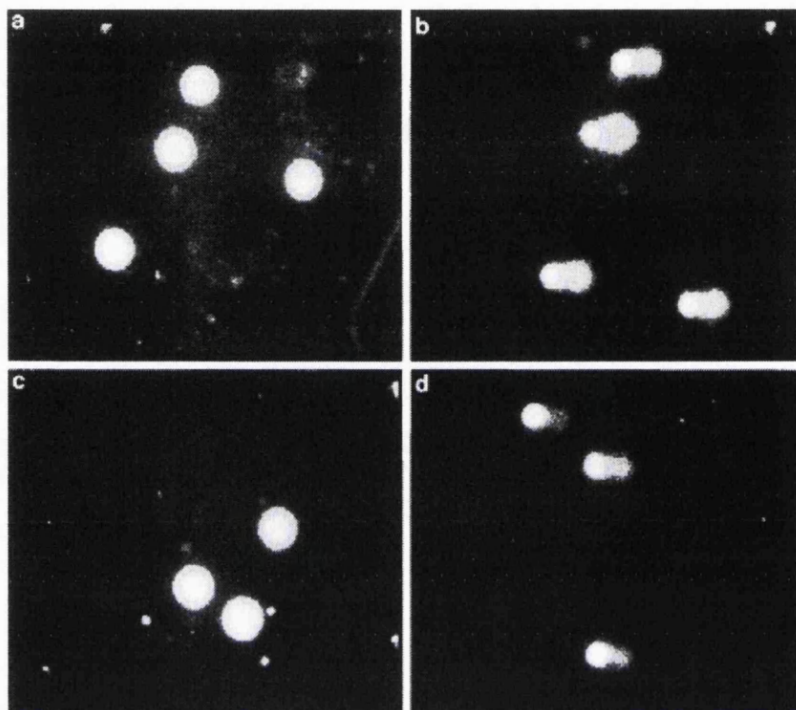
Figure 7.3b: Typical Comet Images. A) no drug, no irradiation. B) no drug, irradiation. C) drug, no irradiation. D) irradiation and drug. (Hartley *et al.* 1999), (*drug = interstrand crosslinker.*).

The water soluble bisulphite adduct AT-361 was investigated in a comet assay by Janet Hartley (CRUK Drug-DNA Interaction Research Group, UCL, London). Reduction in tail moment (and therefore, crosslinking) was proportional to the drug concentration (see **Figure 7.3c**). It is noteworthy that this assay gave an XL_{50} value of 0.1 μM which is in the same range as the XL_{50} values from plasmid DNA.
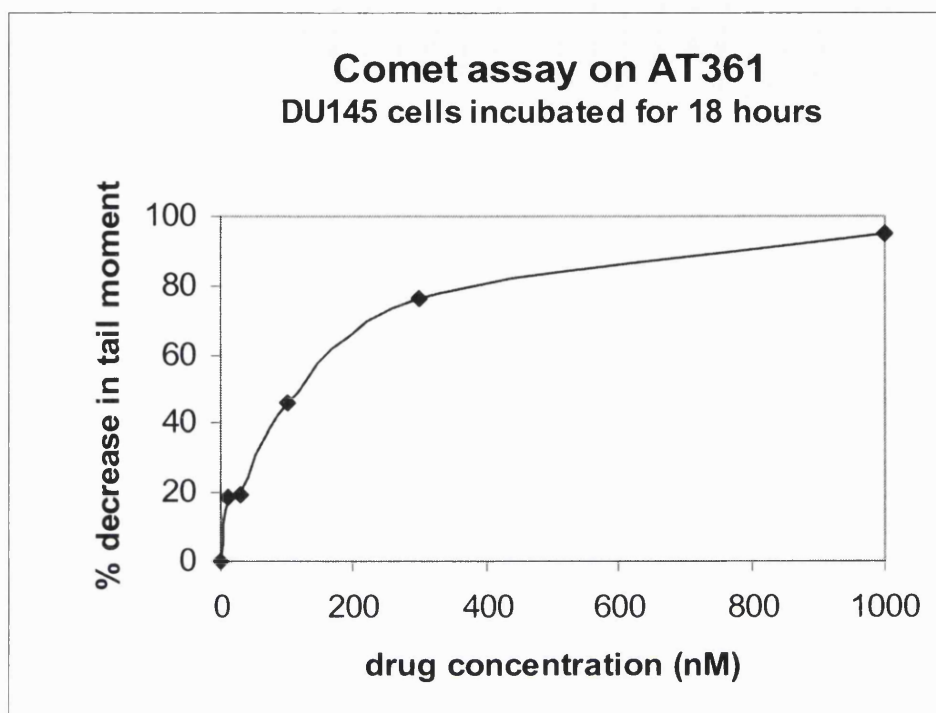
Figure 7.3c: Comet assay on AT-361. The XL_{50} in DU145 cells was 0.1 µM.

The results presented in **Figure 7.3c** demonstrate that a high molecular weight polyamide such as AT-361 (Mw = 1400 g.mol^{-1}) can penetrate the cellular and the nuclear membranes, and crosslink DNA with surprising efficiency. These properties were an essential requirement of the drug development research program. In conclusion, the "comet" assay seems perfectly adapted to measure the crosslinking ability of heterocycle-linked PBD dimers reported in this thesis. At the time of writing, more compounds are being submitted to such an evaluation.

7.4 Footprinting experiments

7.4.1 Discussion

In one attempt to assess the sequence selectivity of heterocycle-linked PBD dimers, the prototype compound AT-242 was subjected to a footprinting experiment on a 230 bp long MS2 DNA sequence (Lavesa and Fox, 2001). This sequence was originally designed to include all possible combinations of 4 bp long sequences and is best suited for short molecules spanning circa 4 bp; however, the diversity of this DNA sequence makes it a good indicator of DNA binding affinity and sequence selectivity.

The footprinting assay was performed by Dr. C. Martin (Cambridge University). The raw gel data (**Figure 7.4a**) was plotted against drug concentration, with footprints appearing as troughs.

Clear footprints were observed at a concentration of 10 nM. Additional footprints appear at 100 nM. The deepest troughs (between nucleotide 50 and 60, as well as between 110 and 120) are in close proximity to binding sequences approximating the predicted interstrand crosslinking binding site PuGPuWWWWWWPyCPy (see boxes). For instance the site 5'-51-TCCATATGCGGC-62-3' possesses canonical flanking PBD binding sites (TCC on this strand would translate as AGG on the other strand), and an A/T rich sequence at its core. Unfortunately, due to its construction, there is no sequence with six A/T in a row separated by two PBD binding sites in the MS2 DNA sequence. Similarly, the trough at position 110 matches with 5'-107-AGGTTAAGCTCC-120-3', with again only a GC mismatch in the core of the sequence. A weaker footprint (red box starting at 60; 59-GGCAATACACA-70) also corresponds to the predicted requirement for two guanines on opposite strands separated by an A/T rich core sequence, but bear a non-favourable PBD binding site (ACA, corresponding to TGT on the other strand). Less favourable binding sites (monoalkylation and unfavourable sequences) can also be seen further along the fragment.

163
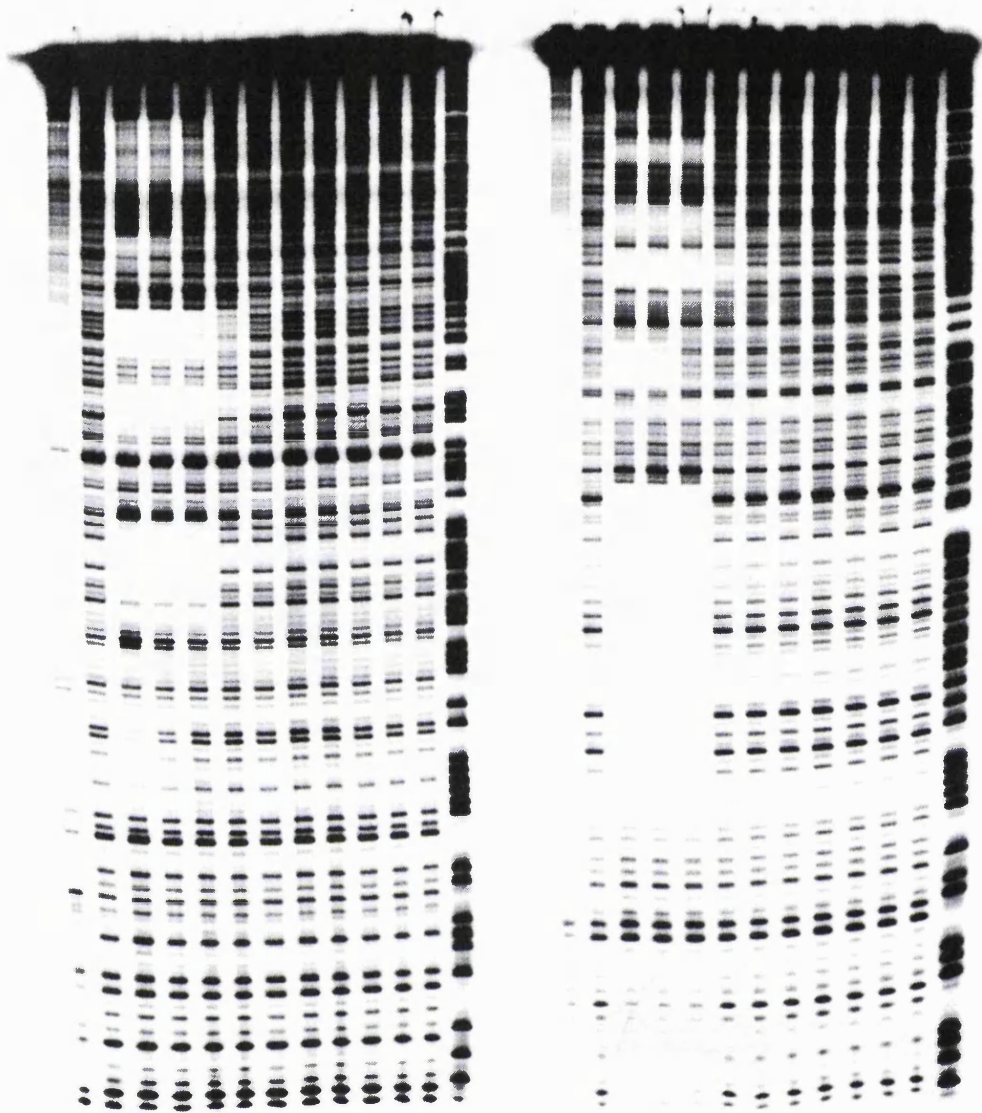
Figure 7.4a: Raw footprinting gel of AT-242 on the MS2 sequence. Control lanes on the far right; increasing concentration of drug from right to left

AT242

Differential Cleavage vs Nucleotide Sequence

1 nM
10 nM
100 nM

t a c g a a t t c g a g c t c g g t a c c c g g g g a t c c a t a t g c g g c a a t a c a c a t g g c c g a t t t c c a a c t g c a c t a g t c g t a g c g c g a t c a a g g t t a a g c t c c c g t t

AT242

Differential Cleavage vs Nucleotide Sequence

1 nM
10 nM
100 nM

a t c c t g g t a t g c a a t t a g g g c g t g a a g a g t t a t g t a a a g t a c g t c c g g t g g g g t c t g t t t t g t c a t c t c a g c c t c g a a t g c g g a t c c t c t a g a g t c g a c c t g c a g g c a t g c a a

Some footprints arising from potential intrastrand crosslinks were observed, but the footprints were of weaker intensity and slightly shifted compared to the expected binding site.

7.4.2 Conclusion and future work

Overall, the observed footprints appear to conform to the predicted PuGPuWWWWWWPyCPy. As this binding site was not present in the MS2 sequence, a small oligonucleotide comparative study (As in Smellie *et al.*, 2003) has been suggested. The selection of oligonucleotides shown in **Figure 7.4b** below should probe the selectivity of the dimer AT-242 in a rigorous fashion. (Note: all terminal G bases have been replaced with inosines to avoid the possibility of PBD units binding to terminal GC base pairs.)

Oligonucleotide Structure	Comments
5'-CGCAGAAAATTTTCTGCG-3' 3'-GCGTCTTTTAAAAGACGC-5'	Control oligonucleotide with GC on ends
5'-CICAGAAAATTTTCTICI-3' 3'-ICITCTTTTAAAAIACIC-5'	Terminal GCs replaced with ICs
5'-CICAGAAAAATTTTCTICI-3' 3'-ICITCTTTTTAAAAIACIC-5'	Addition of one AT in the centre
5'-CICAGAAAAATTTTTCTICI-3' 3'-ICITCTTTTTAAAAAIACIC-5'	Addition of one AT & one TA in centre
5'-CICAGAAAATTTCTICI-3' 3'-ICITCTTTTAAAIACIC-5'	Reduction of one TA in centre
5'-CICAGAAATTTCTICI-3' 3'-ICITCTTTAAAIACIC-5'	Reduction of one TA & one AT in centre

5'-CICAGIIIICCCCCTICI-3'   Centre changed to

3'-ICITCCCCCIIIIGACIC-5'   all IC base pairs

5'-CICAGATGTTGTTCTICI-3'   Centre changed to mix

3'-ICITCTACAACAAIACIC-5'   of ATGTTGTT

Figure 7.4b: Suitable oligonucleotides for a sequence selective crosslinking studies

7.5 Preliminary evaluation in an solid tumour in vivo model

In-vivo studies on AT-360 were performed by Dr.M. Suggitt at the Institute of Cancer Therapeutics (Bradford University). Mice bearing a solid tumour implant (LOX IMVI) were injected with AT-360 at the MTD. A control group bearing the same implant was not injected and simply observed. The mice were observed for 8 days and relative tumours volumes (treated/control) were measured. Unfortunately, it was observed that tumours in the treated group did not show any signs of regression. In fact, the treated mice showed obvious signs of toxicity when examined post-mortem. (Damaged gastro intestinal tract and liver).

LOX IMVI AT360 0.05mg/kg
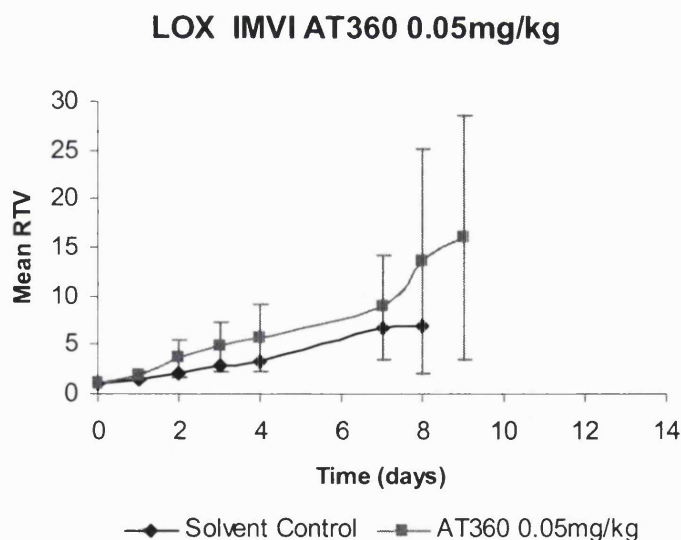
Figure 7.5a: *In vivo* studies of AT-360 in LOX IMVI at the MTD.

The observed toxicity could be due to non-selective protein alkylation. The fully unsaturated PBD C-ring has already been held responsible for this kind of toxicity

(Gregson *et al.,* 2001). In addition, a contribution from the pyrrole unit to the toxicity cannot be discounted either.

In conclusion, it would be particularly interesting to test analogues of AT-360 bearing the C2-exo unsaturated PBD capping unit or different core heterocycles.

7.6 Conclusion and future work

Novel heterocycled-linked PBD dimers have been evaluated through a series of biological assays. They revealed a series of interesting properties such as significant cytotoxicity profiles, strong and selective DNA binding and efficient cellular interstrand crosslinking of the DNA. More work remains to be done to demonstrate whether their DNA binding preferences can be understood and ultimately predicted. Analogues will also have to be developed in order to improve the therapeutic window of this type of molecule.

8 Biological evaluation of hairpin polyamides-PBD conjugates.

8.1 In vitro cytotoxicity

8.1.1 Introduction

As with the previously described monomer and dimer PBD-heterocycle polyamide conjugates, the full set of PBD-hairpins conjugates was submitted to the NCI 60 cell-lines assay and the results are summarized in **Table 8.1a**.
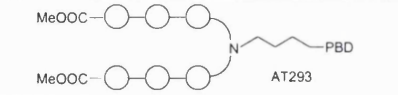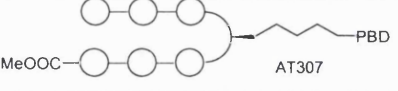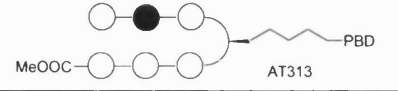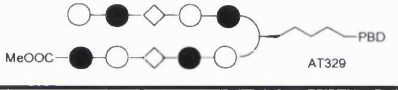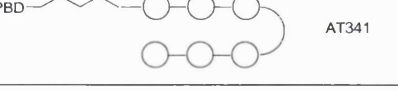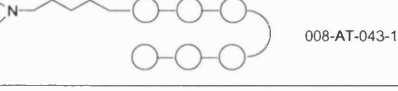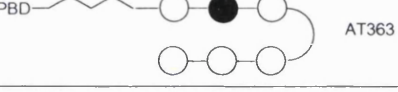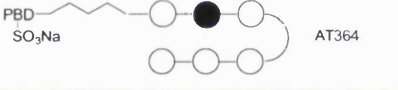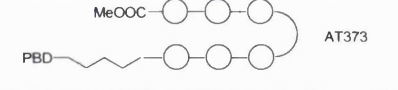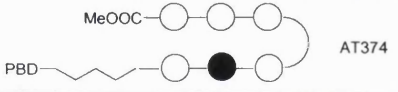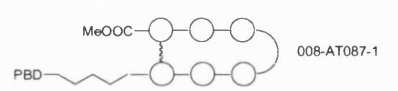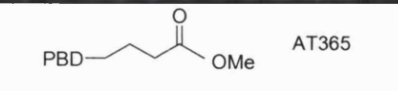
8.1.2 Effect of the design on cytotoxicity

Over the course of the project, four different designs have been assayed. (imino diacetic acid AT-293; (*R*)-diamino butyric acid AT-307, AT-313 and AT-329; diaminopropane AT-341, AT-363 and AT-364; and amino butyric acid AT-373 and AT-374). The molecules differ in the precise nature of their central linker (or loop), which can allow them to adopt the hairpin conformation. This, in turn, should allow them to bind in the 2:1 mode and obey the Dervan's rules of recognition.

Table 8.1a clearly shows that there are significant differences in activity between each design. The diaminopropane design represented by AT-341 and AT-363 is the most active with average TGIs of 105 and 158 nM respectively. It is noteworthy that the results obtained in K562 cells (Spirogen biology) correlate well with the NCI results for these sets of compounds. Indeed, the diaminopropane design was also found to be the most active in the K562 assay, and the general order of potency was found to be the same. Significantly, the control molecule 008-AT-043-1 with the PBD substituted by a dimethylamino tail, was found to be completely inactive. This result reinforces the idea that the PBD is necessary for cytotoxic activitity.

The imino diacetic acid design seems to be the second most active, although only represented by AT-293. The amino butyric acid design ranked third in activity. Perhaps more surprisingly, the compounds based on (*R*)-diamino butyric acid seemed to have consistently moderate to low activity in both assays.

Table 8.1a: cytotoxicity data for the set of hairpin polyamide-PBD conjugates

PBD-hairpin conjugates		NCI data (first assay only)			K562
		GI50	TGI	IC50	96h exp
R-2,4-diaminobutyric acid	AT293	17 nM	3.2 µM	49 µM	50.3 nM
	AT307	870 nM	16 µM	72 µM	980 nM
	AT313	158 nM	16 µM	> 50 µM	473 nM
	AT329	77 µM	> 100 µM	>100 µM	>3 µM
Diaminopropane loop/ spacer	AT341	10 nM	105 nM	14 µM	28.5 nM
	008-AT-043-1	83 µM	> 100 µM	>100 µM	>3 µM
	AT363	13 nM	158 nM	25 µM	36.4 nM
	AT364	13 nM	302 nM	20 µM	11.9 nM
Amino butyric acid loop	AT373	389 nM	10 µM	> 50 µM	91.0 nM
	AT374	123 nM	1.7 µM	15 µM	82.7 nM
	008-AT087-1	140 nM	2.7 µM	19 µM	614 nM
Controls	AT365	1.7 µM	12 µM	47 µM	0.52 µM
	GWL-82	10 nM	54 nM	1.90 µM	32 nM

Two controls molecules were also investigated. The PBD methyl ester, AT365, gives an indication of the activity arising from the PBD alone. The cytotoxic activity of this molecule is low, with an average TGI around 10 µM. The second control molecule: GWL-82 (Wells *et al.,* 2006) is interesting because it is identical to AT-373, but lacks a

loop element. The heterocyclic chain in GWL-82 is therefore rigid and cannot adopt a hairpin conformation. Interestingly, GWL-82 is also the most cytotoxic molecule appearing in the table, with an average TGI of 54 nM.

8.1.3 Discussion

A number of issues arise from these experimental results. In particular, it would be interesting to know the extent of the influence of the molecular conformation on the activity. Indeed, if the K562 results are plotted on a line (see **Figure 8.1a**), it can be seen quite clearly that the compounds which are held in hairpin or cyclic conformation (AT-307 and 008-AT-087-1) are much less active than the compounds which can adopt a linear conformation (GWL-82, and possibly the diamino propane-looped compound AT-341). A notable exception is AT-293 which should be forced to adopt a hairpin conformation by its diaminoacetic acid linker, but is still potent (50 nM). Compound AT-373 is flexible, and therefore can adopt both conformations.

It could be argued that the compounds held in a hairpin conformation should be more selective and inflict fewer DNA lesions than other compounds bearing more flexible loops, therefore explaining a lower activity. However, the footprinting data discussed in the next section tends to contradict this hypothesis.

A more likely explanation could be linked to cellular penetration. It is possible that the compounds locked in a hairpin conformation have more difficulty crossing the nuclear membrane. The poor activity exhibited by AT-329 is also probably due to its larger size and poor nuclear penetration as it is known to recognize and bind to naked DNA effectively (see next section).
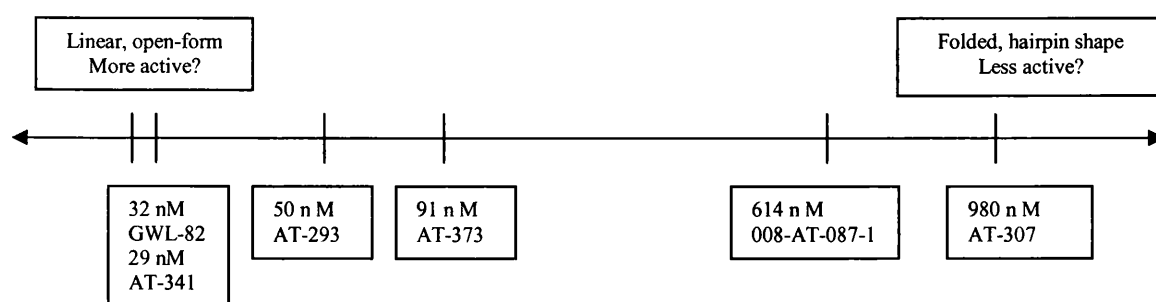
Figure 8.1a: Does activity depends on the molecule conformation?

Another factor that could explain the lower activity of the 2,4-diaminobutyric acid family is the lack of optimisation of the PBD linker. The four carbon PBD linker was designed for direct attachment to the polyheterocyclic chain, and not for attachement to an intermediate linker such as the loop.

8.1.4 Conclusions and future work

The different PBD-polyamide conjugates synthesised during the course of the project exhibit a wide range of activities. The most potent compounds were based on the diaminopropane loop. It would be of particular interest to synthesise an analogous compound locked in a cyclic conformation (such as 008-AT-087-1) to study the effect of conformation on cytotoxicity. Compounds based on the 2,4-diaminobutyric acid loop, as well as the iminodiacetic acid loop, should be modelled and possibly redesigned if the linker is not optimal. Compounds including different imidazole/pyrrole sequences should be synthesised to study the effect of the sequence on cytotoxicity.

8.2 Footprinting experiments

8.2.1 Introduction

The set of ten hairpin polyamide-PBD conjugates was subjected to infrared (IR) DNAse footprinting. The DNA sequences examined were 500 bp long and belonged to two human genes involved in cancer: The BCL-2a gene and the androgen receptor (AR) gene. The experiments were performed by Dr Thomas Ellis, (Spirogen biology), with the exception of compound 008-AT-087-1 which was footprinted by Dr Christopher Martin, (Spirogen biology).

The lowest footprinting concentration was determined first. The lane corresponding to this concentration was then scanned visually. The footprints were noted and the corresponding DNA sequence was deduced by reference to the control lanes. (See example on the next page).

In order to facilitate discussion, the footprint sequences are compiled the Table 8.2a and Table 8.2c (further below) and compared with the theoretical binding sites of the compounds. A score was then attributed (1 for a match, and 0 for a mismatch). A high score (i.e. 7/8 or 8/8) indicates a satisfactory level of DNA targeting. When the score was lower, the relatives contributions of the PBD and hairpin components were determined within the footprint sequence. The results were summarized in the "cooperation PBD/Hairpin?" column.

Finally, the DNA fragments were searched for the compounds match sites. The results are summarized in **Table 8.2b** and **Table 8.2d**.

Example: AT-373 footprinted on BCL-2a

1. Gel image is displayed - roughly 500 bp are shown.
2. Footprinting is observed in the 4th lane (40 nM).
3. Two sites of footprinting are highlighted in the 40 nM lane.
4. Using the marker lane as a guide, the sites are revealed.

40 nM: 5'-GATTGAAGACAC-3'
                              92   103

40 nM: 5'-TTCTTTCTCT-3'
                              160   169

061 GGGGGAAACA CCAGAATCAA GTGTTCCGCG

091 TGATTGAAGA CACCCCCTCG TCCAAGAATG

121 CAAAGCACAT CCAATAAAAT AGCTGGATTA

151 TAACTCCTCT TCTTTCTCTG GGGGCCGTGG

174

Compound Structure	Lowest Footprinting Conc. (nM)	Footprint sequences	Score	Theoretical binding sites	Cooperation PBD/Hairpin ?
AT293	1000	5'-TATAACTC-3' (149-156)	8/8	WWWW(X)PuGPu	Yes
		5'-TATAAGCTG-3' (297-305)	7/8	WWWW(X)PyCPy	Yes
		5'-CGGGCACAC-3' (397-405)	6/8	PuGPu(X)WWWW	PBD only
				PyCPy(X)WWWW	
AT307	5000	5'-AGATCCGAAAG-3' (15-25)	5/8		PBD only
		5'-TGATCTCATGCC-3' (46-58)	6/8		PBD only
		5'-CTGTTCCGCG-3' (81-90)	5/8	WWWWXPuGPu	PBD only
		5'-CAGGGTACGATAAC-3' (256-269)	6/8	WWWWXPyGPy	Poor
		5'-ATTATAAGCTGC-3' (295-307)	7/8	PuGPuXWWWW	Yes
		5'-GGGATGCGGGAGA-3' (325-337)	5/8	PyCPyXWWWW	PBD only
		5'-CTTCTCCTCCC-3' (380-390)	5/8		PBD only
		5'-CGGGCACACG-3' (385-394)	6/8		PBD only
AT313	1000	5'-GGAAACACCAG-3' (64-74)	7/7	WG/CWWXPuGPu	Yes
		5'-AGAACAGGGTACG-3' (252-264)	5/8	WG/CWWXPyCPy	PBD only
		5'-CGGGCACACGC-3' (385-394)	6/8	PyCPyXWWG/CW	Possible
				PuGPuXWWG/CW	
AT329	1000	5'-AAATAGCTGGA-3' (127-137)	7/10	CGWCGW(X)PuGPu	Possible if compressed (9 bp binding site)
		5'-CGGGCACACGC-3' (385-394)	7/10	CGWCGW(X)PyGPy	
		5'-GGGGCCGTGG-3' (171-180)	8/9	PuGPu(X)WGCWGC	
				PyCPy(X)WGCWGC	
AT341	5000	5'-CTGCATC-3' (45-51)	5/8	PuGPuXWWWW	PBD only
		5'-CCGGGCA-3' (396-402)	4/8	WWWWXPyCPy	PBD only
		5'-ATTATAAGCT-3' (295-304)	7/8	(PyCPyXWWWW)	Yes
				(WWWWXPuGPu)	

Table 8.2a part 1: BCL2 footprinting results for the set of hairpin polyamide-PBD conjugates
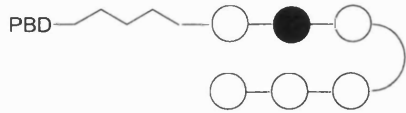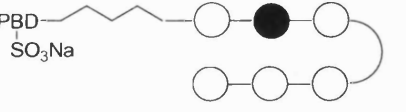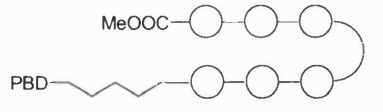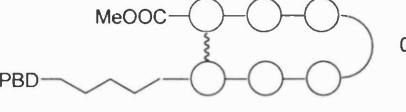
Structure	Name	Conc.	Sequence	Ratio	Motif	Result
PBD — (diagram)	AT363	200	5'-ATTGAAGACA-3' (93-101) 5'-TCTTTCTCTG-3' (161-170)	7/8 7/8	PuGPuXWGWW WWCWXPyCPy (PyCPyXWGWW) (WWCWXPuGPu)	Yes Yes
PBD — SO$_3$Na (diagram)	AT364	1000	5'-CTGCATC-3' (45-51)	6/8	PuGPuXWGWW WWCWXPyCPy (PyCPyXWGWW) (WWCWXPuGPu)	Hint
			5'-ACACCAGA-3' (68-75)	4/8		No
			5'-ATTGAAGACA-3' (93-101)	6/8		Hint
			5'-AATAGCTGGA-3' (138-147)	6/8		Weak
			5'-TTTCTCTG-3' (163-170)	Short		PBD only
			5'-GATAGTGATG-3' (275-284)	6/8		Weak
MeOOC — (diagram) PBD —	AT373	200	5'-GATTGAAGACA-3' (92-101) 5'-TTCTTTCTCT-3' (160-169)	7/8 6/8	PuGPuXWGWW WWCWXPyCPy (PyCPyXWGWW) (WWCWXPuGPu)	Yes Weak
MeOOC — (diagram) PBD —	AT374	1000	5'-GATTGAAGACA-3' (92-101) 5'-GGATGCGGGAG-3' (336-346) 5'-TCTTCTTTCTCTG-3' (158-170)	6/8 5/8 6/8	PuGPuXWGWW WWCWXPyCPy (PyCPyXWGWW) (WWCWXPuGPu)	PBD only PBD only PBD only
MeOOC — (diagram) PBD —	008-AT087-1	40	5'-AACCTT	Short	PuGPuXWGWW WWCWXPyCPy (PyCPyXWGWW) (WWCWXPuGPu)	PBD only
			5'-TCACAGA	Short		PBD only
			5'-TAGACTGATATTA	6/8		Poor
			5'-TGTTCCGC	No		PBD only
			5'-ACATCCAATAAAATAGCTG	8/8		Yes
			GATTATAACTCCTCTTCTTT	multiple		PBD only
			5'-TCTGGG	multiple short		PBD only

Table 8.2a part 2: BCL2 footprinting results for the set of hairpin polyamide-PBD conjugates (continued)

Theoretical binding sites	Match sites	Theoretical binding sites	Match sites
WWWWXPuGPu	10-AATAAAGA	PuGPuXWGWW	657-GGGGTGAA
WWWWXPyGPy	38-AAATTCC 39-AATTCCT 150-ATAACTCC	WWCWXPyCPy	160-TTCTTTCT NO HITS
PuGPuXWWWW	31-GGAATAAA 145-GGATTATA	(PyCPyXWCWW)	NO HITS
PyCPyXWWWW	130-TCCAATAA 292-TCCATTAT	(WWGWXPuGPu)	
WWWXPuGPu	27-AATTGGA 11-ATAAAGA	CGWCGW(X)PuGPu	NO HITS
WWWXPyGPy	163-TTTCTCT 40-ATTTCCT 151-TAACTCC 221-TTTTCCT 39-AATTTCC	CGWCGW(X)PyGPy	NO HITS NO HITS
PuGPuXWWW	145-GGATTAT 31-GGAATAA 62-GGGGAAA 24-AGGAATT 272-GGAGATA	PuGPu(X)WGCWGC	NO HITS
PyCPyXWWW	130-TCCAATA 292-TCCATTA	PyCPy(X)WGCWGC	

Table 8.2b: BCL2 possible match sites for the set of hairpin polyamide-PBD conjugates
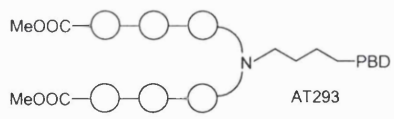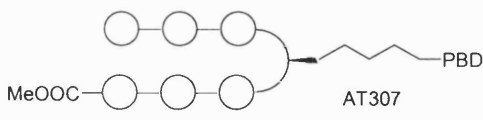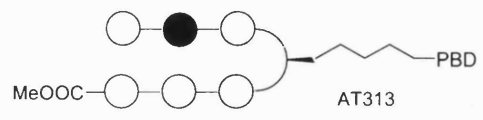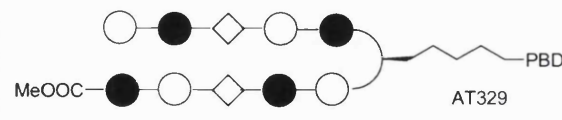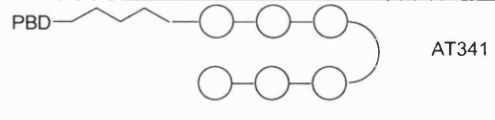
Compound Structure	Lowest Footprinting Conc. (nM)	Footprint sequences	Score	Theoretical binding site	Cooperation PBD/Hairpin ?
AT293	1000	5'-CGCGGTGAG-3' (113-121) 5'-GGGAAAAAGGG-3' (323-333) 5'-AAAAGGAGG-3' (154-162)	3/8 8/8 7/8	WWWW(X)PuGPu WWWW(X)PyCPy PuGPu(X)WWWW PyCPy(X)WWWW	PBD only Yes Yes
AT307	5000	5'-AGGGCTAGAG-3' (32-41) 5'-AAACTGTTGCA-3' (209-219) 5'-GAAGGCAAGG-3' (166-175)	4/8 5/8 5/8	WWWWXPuGPu WWWWXPyGPy PuGPuXWWWW PyCPyXWWWW	PBD only No PBD only
AT313	1000	5'-CCAAAAGCCAC-3' (87-96) 5'-AAACTGTTGCA-3' (209-219) 5'-GAAGGCAAGG-3' (166-175)	5/8 4/8 6/8	WG/CWWXPuGPu WG/CWWXPyCPy PyCPyXWWG/CW PuGPuXWWG/CW	Poor No Poor
AT329	1000	5'-CGCAAACTGTT-3' (206-216))	3/10	CGWCGW(X)PuGPu CGWCGW(X)PyGPy PuGPu(X)WGCWGC PyCPy(X)WGCWGC	Poor
AT341	5000	5'-CGCAAACTGTT-3' (206-216) 5'-AAAAGCTGCTAAAG-3' (483-496)	5/8 5/8	PuGPuXWWWW WWWWXPyCPy (PyCPyXWWWW) (WWWWXPuGPu)	Poor Cyclin only ?

Table 8.2c: AR footprinting results for the set of hairpin polyamide-PBD conjugates

178
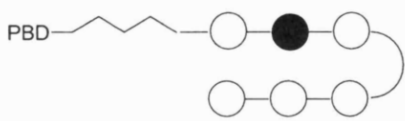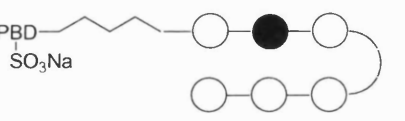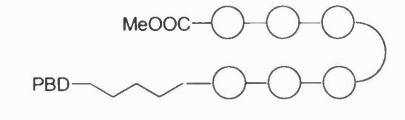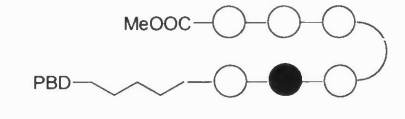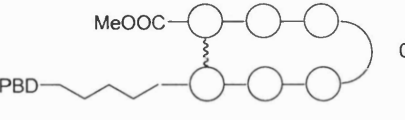
PBD—[chain]—○●○ ... ○○○ AT363	200	5'-CCAAAAGCCAC-3' (87-96) 5'-AAACTGTTGCA-3' (209-219) 5'-AGAGGGAAAAA-3' (320-330)	6/8 5/8 7/8	PuGPuXWGWW WWCWXPyCPy (PyCPyXWGWW) (WWCWXPuGPu)	Yes Poor Yes
PBD—SO₃Na—[chain]—○●○ ... ○○○ AT364	1000	5'-CCAAAAGCCAC-3' (87-96) 5'-AAAAAGCTGCTAAAG-3' (483-496) 5'-AAACTGTTGCA-3' (209-219)	5/8 7/8 4/8	PuGPuXWGWW WWCWXPyCPy (PyCPyXWGWW) (WWCWXPuGPu)	Poor Yes Poor
MeOOC—○○○ ... PBD—[chain]—○○○ AT373	200	5'-CTCCAAAGCC-3' (85-94)	6/8	PuGPuXWGWW WWCWXPyCPy (PyCPyXWGWW) (WWCWXPuGPu)	Yes
MeOOC—○○○ ... PBD—[chain]—○●○ AT374	1000	5'-AAACTGTTGCA-3' (209-219)	poor	PuGPuXWGWW WWCWXPyCPy (PyCPyXWGWW) (WWCWXPuGPu)	Poor
MeOOC—○○○ ... PBD—[chain]—○○○ 008-AT087-1	200	5'-TCTCGTTTACGTTG 5'-GGAGGA 5'-CCGATCGAGATC 5'-GGGA	7/8 Short 6/8 short	PuGPuXWGWW WWCWXPyCPy (PyCPyXWGWW) (WWCWXPuGPu)	Yes PBD only Poor PBD only

Table 8.2c part2: AR footprinting results for the set of hairpin polyamide-PBD conjugates (continued)

Theoretical binding sites	Match sites	Theoretical binding sites	Match sites
WWWWXPuGPu	NO HITS	PuGPuXWGWW	126-GGGGAGAA
WWWWXPyGPy	NO HITS		601-TTCTCTCC
		WWCWXPyCPy	656-TTCTCCCC
	128-GGAGAAAA		595-CCCGTCTT
PuGPuXWWWW	323-GGGAAAAA	(PyCPyXWCWW)	NO HITS
	150,322-AGGGAAAA		
		(WWGWXPuGPu)	
PyCPyXWWWW	NO HITS		
WWWXPuGPu	138-AAAGGGG	CGWCGW(X)PuGPu	NO HITS
	326-AAAAAGG		
	10-ATTCAGG		
	327-AAAAGGG	CGWCGW(X)PyGPy	NO HITS
	132,154-AAAAGGA		
			NO HITS
	107-TTAGCGC		
WWWXPyGPy	514-AAAGTGC	PuGPu(X)WGCWGC	
	209-AAACTGT		
			NO HITS
	150,322-AGGGAAA	PyCPyXWGCWGC	
	151,323-GGGAAAA		
PuGPuXWWW	128-GGAGAAA		418-TCTTGCAGC
	324-GGAAAAA		
PyCPyXWWW		PyCPyXWGCWGC	
	NO HITS		

Table 8.2d: AR possible match sites for the set of hairpin polyamide-PBD conjugates.

8.2.2 Discussion

8.2.2.1 DNA binding affinity; influence of the local nuclear structure.

Overall, the conjugates produced visible footprints at various concentrations, ranging from 5000 nM down to 200 nM. In contrast, the control molecule AT-219 (PBD methyl ester) did not produce any footprints at these concentrations (Wells *et al.*, 2006). The footprints produced by the individual conjugates showed some degree of differentiation indicating a degree of selectivity. However, one particular site in the AR gene: 5'-AAACTGTTGCA-3' (209-219) appeared to be alkylated by every conjugate. It is possible that the local DNA structure is particularly open at this sequence.

Quite strikingly, many of the possible target sites (**Table 8.2b** and **Table 8.2d**) were <u>not</u> footprinted indicating a failure of the conjugates to bind to these sites. Clearly, some sequences are much more accessible than some others, due to the local structure of the DNA. A similar situation was already noted by Gottesfeld and Dervan when investigating DNA binding properties of a polyamide-chlorambucil conjugate (Dickinson *et al.*, 2004). This paper specifies that two match sites out of four were not bound by the polyamide, probably because they were purine tracts. Unfortunately, it is not yet possible to predict precisely which sequences are accessible before performing the experiment. The likeliest option to ensure binding is to have many possible target sites in the footprinting fragment or to start with a gene, which is particularly down-regulated by the conjugates in microarray experiments, or to work with libraries of polyamide-PBD conjugates.

Interestingly, the lowest footprinting concentration and the overall footprinting profile does not correlate well with the IC_{50} values reported in the cytotoxicity section. The low cytotoxicity shown by the larger, hairpin-like conjugates could be explained by a number of reasons:
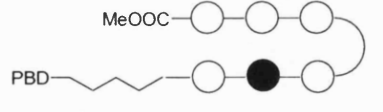
First, it can be reasonably expected that the larger size and bulky shape of the hairpin polyamide can impede crossing of the cellular membranes, ultimately resulting in lower cytotoxicity. In addition, Best *et al.* (2003) demonstrated that hairpin polyamide nuclear

penetration was dependent on the heterocyclic sequence. Another possibility is that, although the molecules entered the nucleus, the number of available target sites suitable for the larger, hairpin-like polyamide hybrids, may be smaller than anticipated.

Finally, the PBD-hairpin polyamide targeted at more specific sequence (i.e. AT-329 targets a GCWGC sequence when other hairpin such as AT-307 targets a WWWWW sequence) should bind to fewer sequences, doing less DNA damage. This could result in less cytotoxicity, although it is not antithetical with gene silencing. (Binding to a few key oncogenic regions can result in cytostatic dose/response curve).

8.2.2.2 Sequence selectivity

Overall, the selectivity demonstrated by the hairpin-polyamides conjugates was disappointing (see the score columns in **Table 8.2a** and **Table 8.2c**). The covalent and non-covalent components of the molecules rarely seemed to cooperate fully, and no single design appeared to be significantly more efficient than another. However, a degree of cooperation was often observed as illustrated by the high number of 6/8 scores.

It is unfortunate than no match sites for the highly selective AT-329 was present in the DNA fragments (**Table 8.2b**, last row). A potential strategy to analyse this molecule would be to tailor-make a plasmid DNA fragment including a variety of match and mismatch sites (Foister *et al.*, 2003). In many cases however, the PBD moiety seemed to alkylate one of its cognate binding sites with little regard for its polyamide partner. (scores from 5/8 downwards). So it seems that the main way to improve the selectivity of these molecules would be to prevent the PBD from reacting rapidly with the DNA.

8.2.3 Approaches to increasing selectivity

8.2.3.1 Design optimisation

This step is traditionally accomplished by classical molecular modelling. The molecule is immobilised at the target site and the PBD is bonded to the guanine *exo*-amino group. The total energy of the system is then calculated and minimized for the optimum conformation. Different designs can be compared in this fashion. The method can help to discover the best linker length and points of attachments and check if the DNA structure is altered by the presence of the molecule. In the future, this approach can also be used to predict which molecules would have the highest affinity for a particular binding site.

Molecular modelling assessment of molecules prior to synthesis is therefore a useful step in development. Unfortunately, it was not possible to carry out modelling on AT-293, or the diaminobutyric acid family (AT-307, AT-313, AT-329). The other hairpins were attached to the PBD acid capping unit directly, without the intermediate of a loop. This design was already optimised by molecular modelling for attachment to polyamide amino groups (Wells *et al.*, 2006).

8.2.3.2 Thermodynamics, kinetics and dynamics aspects of binding

One of the main flaws of the computational assessment described above is a ligand starting point in a position close to assumed binding site. Computers are not yet powerful enough to carry out simulations of a binding event from a distant starting point. While advances in computer science may provide a solution to this problem, it is left to one's imagination to understand the dynamics of the conjugate formation. The manner in which the ligand approaches and binds to the DNA may hold a key selectivity improvement. (**Figure 8.2a**).

This section deals with the thermodynamics, kinetics and dynamics aspects of the PBD-polyamide hybrid binding to the DNA.

A) Thermodynamic aspects

First, it is important to acknowledge the consequences of the quasi-irreversible (at 37°C, at a favored DNA sequence such as AGA) covalent binding of the PBD, on the selectivity of an hybrid PBD-hairpin.

| DNA bound and recognised by the hairpin moiety, at a hairpin targeted sequence | ⟶ ⟵ | DNA covalently bound and recognised by the PBD moiety, at a PBD targeted sequence |
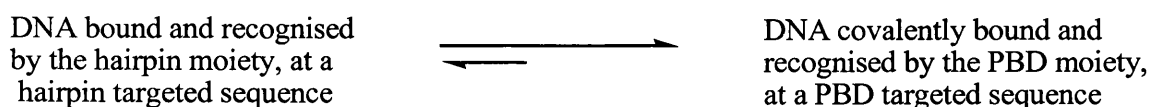
Figure 8.2a: The thermodynamic equilibrium favors the covalent binding moiety target sequence.

The heterocyclic polyamide binds the DNA through a series of non-covalent interactions. This binding is reversible and the molecule can leave a position and assess binding interactions further along the DNA groove. Even on a hairpin match sequence, the binding is reversible and the molecule could leave. On the other hand, when the PBD covalently bind to a favorable sequence such as AGA, the reaction is very difficult to reverse in physiological conditions. As illustrated on **Figure 8.2a**, this situation should bias the selectivity towards the target sequence of the covalently binding agent.

B) Kinetic aspects

Covalent binding of an agent proceeds in stages **Figure 8.2b**. First, the molecule enters the DNA groove, then it probes the DNA groove for favorable interaction (based on shape, hydrogen bonding and Van der Waals interactions). If the sequence is favorable, the molecule will stay a certain amount of time in this favorable binding region, held in place by non covalent interactions. This time was called "non-covalent residence time" on **Figure 8.2b**. During this time, the molecule has chance of breaking interactions, escaping binding, and probing another sequence further in the groove. If this period is of short duration as it is the case with a reactive, fast covalent binder, then it is likely that the whole sequence will happen only a few times. The total probing time for the covalent binder-heterocyclic polyamide hybrid will be short, and selectivity will be low.

If the covalent binder enjoys a relatively long period of reversible, non-covalent binding time, a high number a binding cycles will happen. Eventually, the heterocyclic polyamide will find a target site. The total number of non-covalent interaction will be high enough to prevent departure of the hybrid from the sequence and covalent binding will eventually occur with high selectivity.
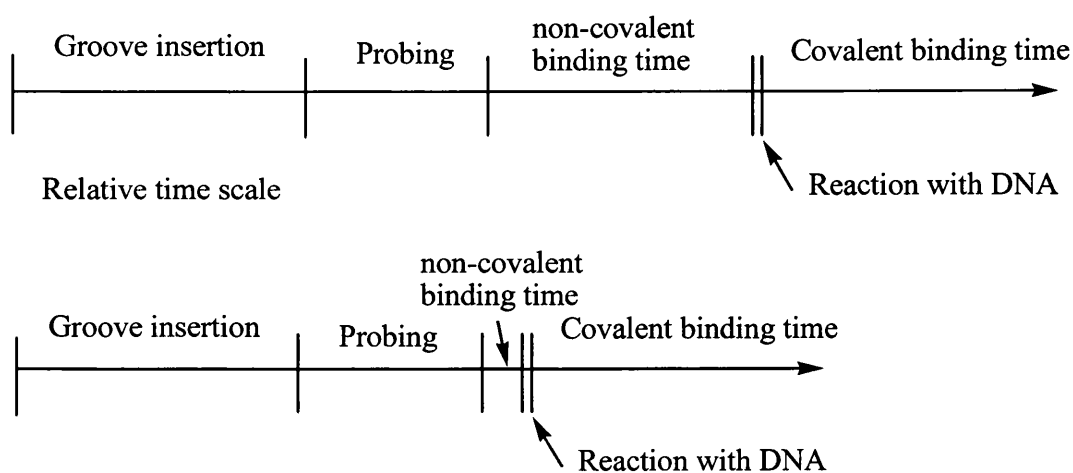
Figure 8.2b: Slow covalent binder (top) and fast covalent binder (bottom).

In agreement with this hypothesis, Dervan *et al.* wrote in 2005 "It is likely that the slower rate of alkylation for the chlorambucil moiety (versus *seco*-CBI alkylation) allows for an increased specificity of alkylation to polyamide match sites".

A possible experiment to study the importance of the non-covalent binding time would be to footprint the molecules versus the same DNA sequence as described in the previous section, but where the guanines would be substituted by inosines, therefore preventing covalent binding.

In conclusion, the study of slower (less reactive) PBDs, possibly by decreasing the electron density in the A-ring (removal of C7 methoxy, or substitution by an electrowithdrawing group), could be particularly beneficial to this project.

185

C) Dynamic aspects

The PBD-heterocyclic polyamide can enter the groove in three different ways (**Figure 8.2c**).

1) The PBD enters the groove first. This situation results in loss of selectivity as it gives the PBD some time to covalently bind the DNA without any interaction from the polyamide (a1 and a2).

2) The polyamide enters the groove first. As binding of the polyamide is reversible, this situation would not affect selectivity. If the probed sequence is not ideal for the whole hybrid molecule, it can breaks binding and probes another sequence

3) The polyamide and the PBD components of the molecule enter the groove simultaneously. This situation allows maximum groove-DNA binder interactions.
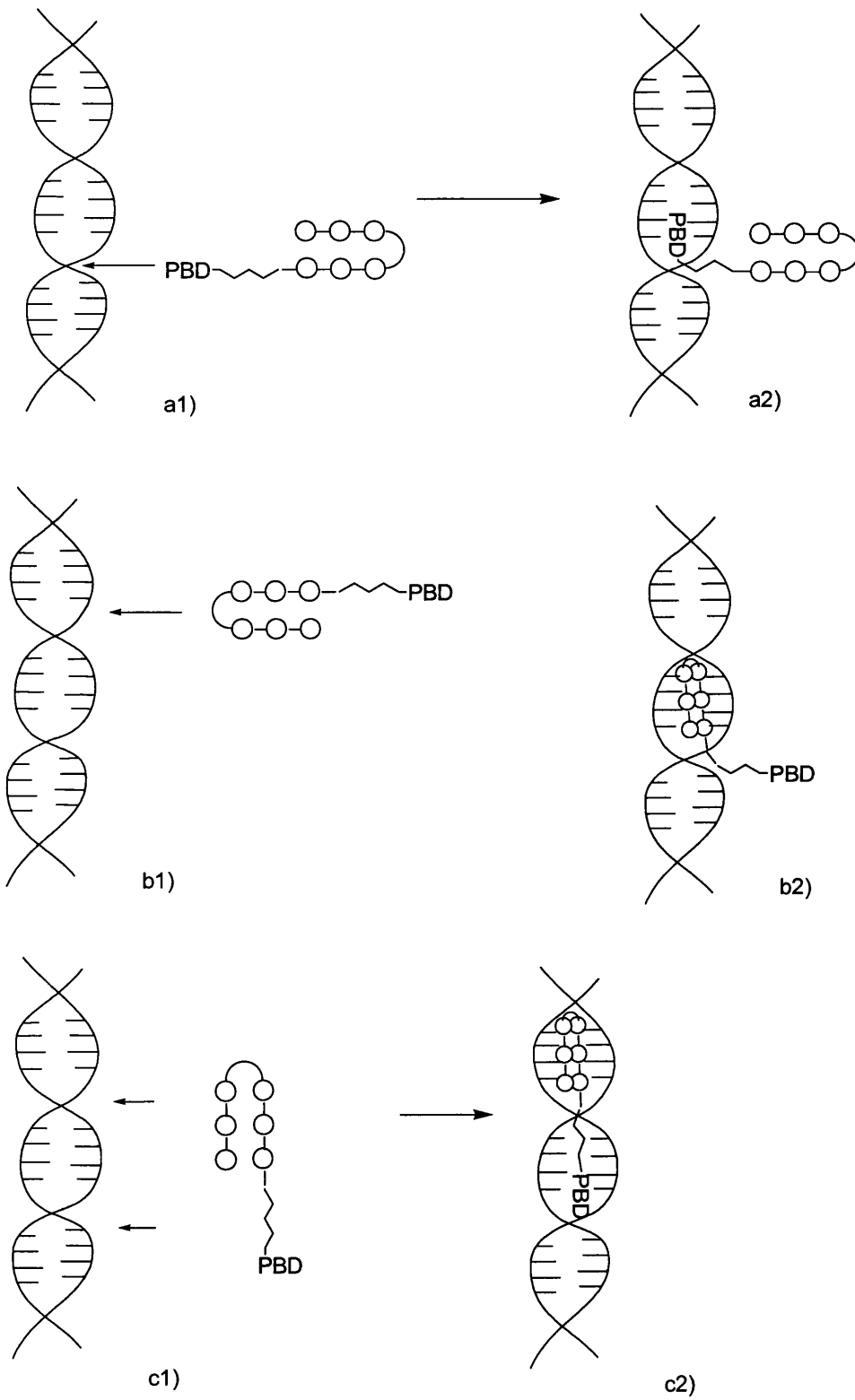
Figure 8.2c: Possible entry positions of the hybrid molecule.

It may be preferable, from a selectivity perspective, for the polyamide to enter the groove first to increase its chances of finding its optimum binding site before the PBD enters the groove and covalently bind.

The polyamide could be fitted with features acting at relatively long range (a cationic charge) in order to encourage the polyamide moiety to enter the groove first. A cationic charge should help to direct the polyamide towards the negatively charged sugar-phosphate skeleton. If this charge was placed at the end of the polyamide (Dervan *et al.*, 2005), it may also help the whole device to maintain contact with the groove while the molecule probes the DNA, searching for a matching site.

Following the same idea, a flexible linker may permit the PBD to alkylate the DNA with the polyamide moiety still incorrectly positioned. A rigid linker would force the two partners to interact fully with the groove before the alkylation event can take place. (methylene linker, Bando *et al.*, 2004a and b).
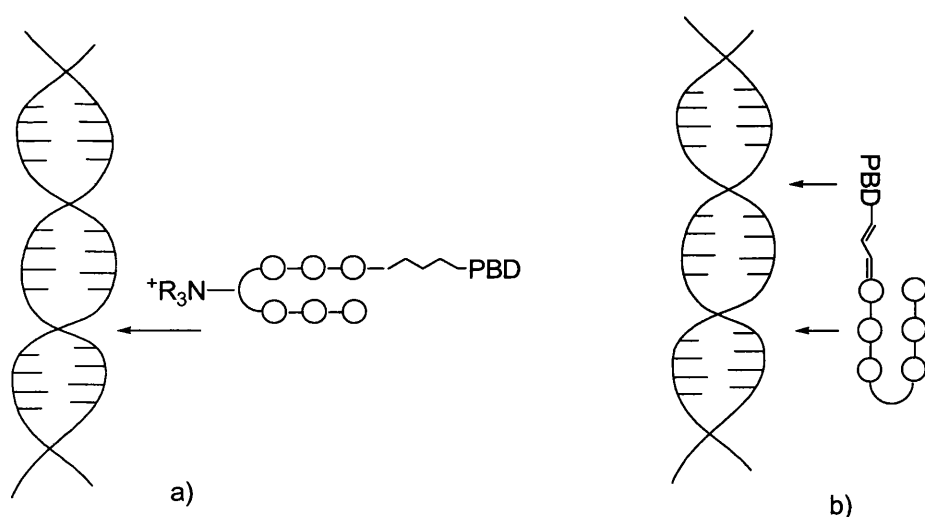
Figure 8.2d: a) A positive charge on the polyamide moiety can direct the entry position of the molecule. b) A rigid linker forces interaction of both moieties with the DNA.

188

8.2.4 Conclusions

The ten PBD-polyamide conjugates synthesised during the course of this project all bind DNA with a degree of selectivity and from concentrations as low as 200 nM. Loss of selectivity is thought to be due to irreversible alkylation by the PBD moiety prior to optimum positioning of the polyamide moiety. These problems should be improved by design alterations such as a rigid linker between the polyamide and the PBD, addition of a cationic tail, as well as reduced electron density in the PBD A-ring.

9 Biological evaluation of AT-355

9.1 Introduction

In a recent publication, Wells *et al.*, 2006, reported the synthesis and biological evaluation of a set of PBD-polypyrroles conjugates. The properties exhibited by these conjugates were extremely interesting, including a significant synergistic effect with regards to DNA-binding affinity and sequence selectivity. Two of these conjugates (GWL-78 and GWL-79) are now being evaluated *in vivo*, in a murine xenograft model.

As previously described in the introductory chapters, the presence of C2 *exo* unsaturation in SJG-136 dramatically improved the *in vivo* profile of the molecule as compared with its fully saturated analogue DSB-120. AT-355 was therefore synthesized to provide a direct analogue of GWL-79 and study the effect of C2 *exo* unsaturation on this template.
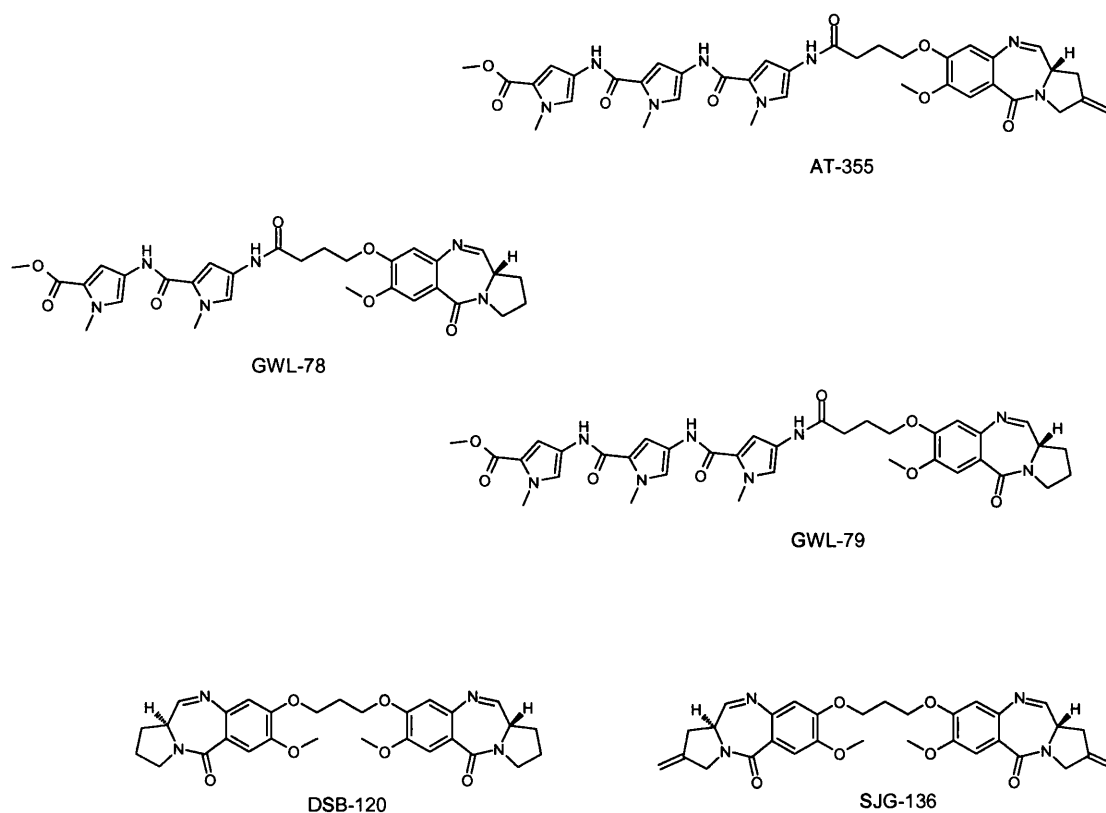
Figure 9.1a: Structures of AT-355, GWL-79 and GWL-78, DSB-120 and SJG-136.

9.2 Effect on *in vitro* cytotoxicity

GWL-79 and AT-355 were evaluated in the NCI 60 cell line panel. Both compounds revealed an interesting profile, with 100 % growth inhibition in a majority of cell lines, beginning at concentration below 10nM (see graph on the next pages). The assay should be repeated at lower concentration, as many GI50 and TGI values could not be obtained at these concentrations.

The compounds seem to be particularly active in clusters of cell lines such as the leukaemia panel, the renal cancer panel, and the melanoma panel. Although the melanoma panel sensitivity is a characteristic typical to the potent PBD drugs such as C2-aryls (e.g. Cooper *et al.*; 2001), the renal cancer and leukaemia panel sensitivity seems slightly enhanced by the tri-pyrrole moiety.

191

Again, the shape of the curve is of particular interest. Most dose-response curves are actually flat lines. This represents saturation of the drug receptor at very low concentration. In this particular case, the target receptors are the DNA binding sites. It is noteworthy that the binding of the drug does not determine the death of the cell. In fact, the responses are diverse ranging from "cytostaticity" in the whole of the cell population (flat line close from 0) to a mixture of "cytostaticity", cytotoxicity and growth depending on the initial cell population.

Altogether, these compounds possess potent anti-tumour activity *in vitro*. AT-355 appears to be active at lower concentration than GWL-79, but only retesting at concentration below 10nM can provide an accurate comparison.

Figure 9.2a: NCI Dose Response Curves for GWL-79

Figure 9.2b: NCI Dose Response Curves for AT-355

Panel/Cell Line	Log$_{10}$GI50	GI50	Log$_{10}$TGI	TGI	Log$_{10}$LC50	LC50
Leukemia						
CCRF-CEM	< -8.00		< -8.00		< -8.00	
HL-60(TB)	< -8.00		< -8.00		> -4.00	
K-562	< -8.00		< -8.00		> -4.00	
MOLT-4	< -8.00		< -8.00		< -8.00	
RPMI-8226	< -8.00		< -8.00		< -8.00	
SR	< -8.00		< -8.00		< -8.00	
Non-Small Cell Lung Cancer						
A549/ATCC	< -8.00		< -8.00			
EKVX	< -8.00		< -8.00			
HOP-62	< -8.00		< -8.00			
HOP-92	< -8.00		< -8.00		> -4.00	
NCI-H226	< -8.00		< -8.00			
NCI-H23	< -8.00		< -8.00		< -8.00	
NCI-H322M	< -8.00		< -8.00		> -4.00	
NCI-H460	< -8.00		-7.67			
NCI-H522	< -8.00		< -8.00		< -8.00	
Colon Cancer						
HCT-116	< -8.00		< -8.00			
HCT-15	< -8.00		< -8.00		> -4.00	
HT29	-5.56		-5.12		-4.07	
KM12	< -8.00		< -8.00		< -8.00	
SW-620	< -8.00		< -8.00			
CNS Cancer						
SF-268	-7.56		-5.26		> -4.00	
SF-295	< -8.00		< -8.00		> -4.00	
SF-539	< -8.00		< -8.00		-7.24	
SNB-19	< -8.00		> -8.00		> -4.00	
SNB-75	-5.25		> -8.00		> -4.00	
U251	< -8.00		< -8.00		> -4.00	
Melanoma						
LOX IMVI	< -8.00		< -8.00			
MALME-3M	< -8.00		< -8.00		< -8.00	
M14	< -8.00		< -8.00		< -8.00	
SK-MEL-2	< -8.00		< -8.00			
SK-MEL-28	-5.80		-5.20		-4.33	
SK-MEL-5	< -8.00		< -8.00		< -8.00	
UACC-257	< -8.00		< -8.00		< -8.00	
UACC-62	< -8.00		< -8.00		< -8.00	
Ovarian Cancer						
IGROV1	< -8.00		< -8.00			
OVCAR-3	< -8.00		< -8.00			
OVCAR-4	-5.46		-4.63		> -4.00	
OVCAR-5	< -8.00		< -8.00		> -4.00	
OVCAR-8	< -8.00		< -8.00		> -4.00	
SK-OV-3	< -8.00		> -8.00		> -4.00	
Renal Cancer						
786-0	< -8.00		-7.95		> -4.00	
A498	< -8.00		< -8.00		> -5.00	
ACHN	< -8.00		< -8.00			
CAKI-1	< -8.00		< -8.00		< -8.00	
RXF 393	< -8.00		< -8.00		< -8.00	
SN12C	< -8.00		< -8.00		-7.59	
TK-10	< -8.00		< -8.00		> -4.00	
UO-31	< -8.00		< -8.00			
Prostate Cancer						
PC-3	< -8.00		< -8.00		> -4.00	
Breast Cancer						
MCF7	< -8.00		< -8.00		> -4.00	
NCI/ADR-RES	< -8.00		-7.35		-5.64	
MDA-MB-231/ATCC	< -8.00		< -8.00		< -8.00	
HS 578T	< -8.00		< -8.00			
MDA-MB-435	< -8.00		< -8.00		< -8.00	
BT-549	< -8.00		< -8.00			
T-47D	-7.79		> -8.00		> -4.00	
MG_MID	-7.81		-7.49		-5.97	
Delta	0.19		0.51		2.03	
Range	2.75		4.0		4.0	

Figure 9.2c: NCI Mean Graphs for GWL-79

National Cancer Institute Developmental Therapeutics Program

Mean Graphs

	NSC : D733782 / 1	Units : Molar	SSPL : 0CCJ	EXP. ID : 0408NS67
	Report Date : April 28, 2005		Test Date : August 23, 2004	

Panel/Cell Line	Log₁₀ GI50	GI50	Log₁₀ TGI	TGI	Log₁₀ LC50	LC50
Leukemia						
CCRF-CEM	< -8.00		< -8.00		> -4.00	
K-562	< -8.00		-6.88		> -4.00	
MOLT-4	< -8.00		< -8.00		> -4.00	
RPMI-8226	< -8.00		< -8.00		> -4.00	
SR	< -8.00		< -8.00		> -4.00	
Non-Small Cell Lung Cancer						
A549/ATCC	< -8.00				> -4.00	
EKVX	< -8.00		> -4.00		> -4.00	
HOP-62	< -8.00		< -8.00			
NCI-H226	< -8.00		< -8.00			
NCI-H23	< -8.00		> -4.00		> -4.00	
NCI-H322M	< -8.00		< -8.00		> -4.00	
NCI-H460	< -8.00		< -8.00			
NCI-H522	< -8.00		< -8.00		> -4.00	
Colon Cancer						
COLO 205	< -8.00		-7.00		> -4.00	
HCC-2998	< -8.00				> -4.00	
HCT-116	< -8.00				> -4.00	
HT29	< -8.00		> -4.00		> -4.00	
KM12	< -8.00		< -8.00			
SW-620	< -8.00		< -8.00			
CNS Cancer						
SF-268	< -8.00		< -8.00		-6.19	
SF-295	< -8.00		< -8.00		> -4.00	
SF-539	< -8.00		< -8.00		-7.54	
SNB-19	< -8.00		> -4.00		> -4.00	
SNB-75	< -8.00		-7.92		> -4.00	
U251	< -8.00		< -8.00		-4.81	
Melanoma						
LOX IMVI	< -8.00		< -8.00		-7.66	
MALME-3M	< -8.00		< -8.00		< -8.00	
M14	< -8.00		< -8.00		< -8.00	
SK-MEL-2	< -8.00		< -8.00			
SK-MEL-28	< -8.00		> -4.00		> -4.00	
SK-MEL-5	< -8.00		< -8.00			
UACC-257	< -8.00		< -8.00		> -4.00	
UACC-62	< -8.00		< -8.00		< -8.00	
Ovarian Cancer						
OVCAR-3	< -8.00		< -8.00		> -4.00	
OVCAR-5	< -8.00		> -4.00		> -4.00	
OVCAR-8	< -8.00		-4.77		> -4.00	
SK-OV-3	< -8.00		> -4.00		> -4.00	
Renal Cancer						
786-0	< -8.00		< -8.00		-4.69	
A498	< -8.00		< -8.00			
CAKI-1	< -8.00		< -8.00		> -4.00	
RXF 393	< -8.00		< -8.00		> -4.00	
SN12C	< -8.00		< -8.00		> -4.00	
TK-10	< -8.00		< -8.00		> -4.00	
UO-31	< -8.00		< -8.00			
Prostate Cancer						
PC-3	< -8.00		-7.09		> -4.00	
Breast Cancer						
MCF7	< -8.00		< -8.00		< -8.00	
NCI/ADR-RES	< -8.00		> -4.00		> -4.00	
MDA-MB-231/ATCC	< -8.00		< -8.00		> -4.00	
HS 578T	< -8.00		> -4.00		> -4.00	
MDA-MB-435	< -8.00		< -8.00		< -8.00	
BT-549	< -8.00		< -8.00		> -4.00	
T-47D	< -8.00					
MG_MID	-8.0		-7.12		-4.72	
Delta	0		0.88		3.28	
Range	0.0		4.0		4.0	

+3 +2 +1 0 -1 -2 -3   +3 +2 +1 0 -1 -2 -3   +3 +2 +1 0 -1 -2 -3

Figure 9.2d: NCI Mean Graphs for AT-355

9.3 DNA binding and sequence-selectivity

Wells *et al.* (2006) have also revealed that GWL-79 increase CT-DNA melting by 21.2 °C (for 18 hours incubation at 37 °C). ΔT is more than 50-times greater than the equivalent PBD unit alone (0.4°C), and 5-times greater than the tripyrrole unit alone (ΔTm = 4.2°C) under identical conditions. Intriguingly, this ΔTm value is greater than that for the PBD-based interstrand cross-linking agent SJG-136 (ΔTm = 20.5 °C under identical conditions), which is known to establish formal covalent crosslinks between the complementary DNA strands. These significant values reflect the strength of the bonds and interactions between the molecule and the DNA.

The two molecules, GWL-79 and AT-355, were subjected to IR DNASE I footprinting on the two sequences previously discussed: BCL-2 and AR. The raw footprinting gels can be seen on the next page.

It was expected that the different PBD structures could alter the sequence selectivity by changing the alkylation kinetics. Interestingly, the two molecules revealed a set of footprints almost identical to each other. The C2 *exo* unsaturation appears to have a minimal effect on the sequence selectivity of this type of conjugate and this goes against the earlier argument that "potent" C2-exo unsaturated PBD would be less selective. It is possible that the speed of covalent binding of a C2-exo unsaturated PBD is not higher than for a saturated PBD, explaining the identical selectivity. More HPLC based experiments, (Morris *et al.* 1990), would be necessary to assess exactly the covalent binding kinetics of PBD analogues.

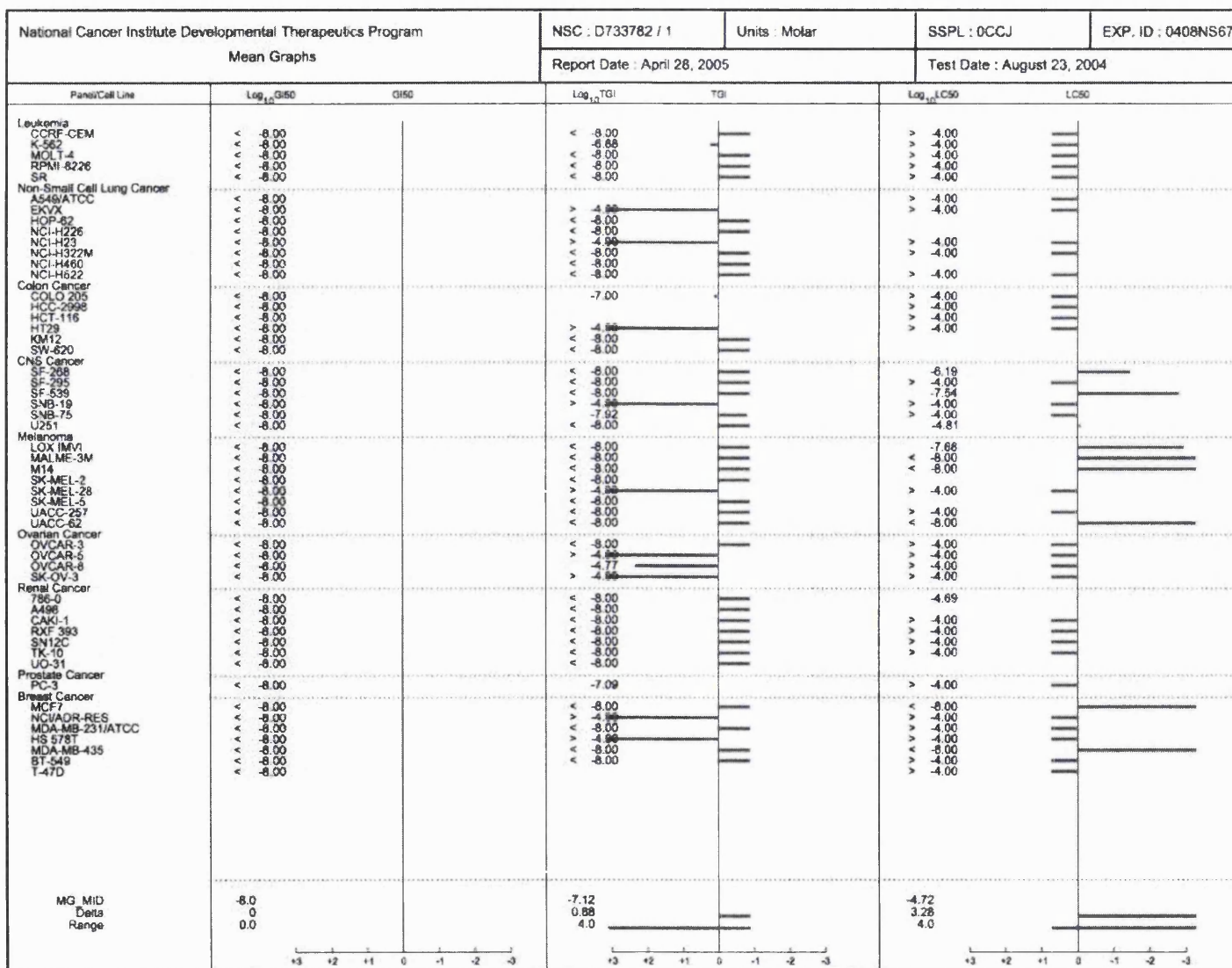Manual analysis of the footprints (Dr Thomas Ellis, Spirogen Biology) revealed two match sites for GWL-79 and AT-355, 39-A<u>ATTTCCT</u>GCA and 221-<u>TTTTCCT</u>CTG (BCL-2); at concentrations as low as 8 nM. In the AR fragment, three footprints corresponding to a match site: 150-A<u>GGGAAAA</u>GGAGGT and two single bp mismatch sites: 32-A<u>GGGCTA*GA*</u>G and 74-AGCACT<u>T*GT*TTCT</u> were observed from 8 nM.

These encouraging results contrast starkly from those obtained in the previous chapter on PBD-hairpin polyamide conjugates. It is possible that the smaller heterocyclic chain is able to make and maintain contact rapidly with the minor groove of the DNA, providing the necessary interaction before the alkylation reaction occurs at the PBD end.

Figure 9.3a: Raw footprinting gels for AT-355 and GWL-79 on the BCL2 sequence. The results are identical.

9.4 Conclusion

Both GWL-79 and AT-355 revealed exciting biological properties such as targeting of PuGPuXWWW DNA sequences and strong *in vitro* cytotoxic activity. At the time of writing, GWL-79 is being evaluated in murine xenographs. Considering the poor therapeutic window exhibited by the other PBD-polypyrrole conjugates evaluated during the course of this work (see previous chapters), AT-355 is also being submitted to *in vivo* evaluation. It is expected that the C2-unsaturated PBD of AT355 will widen the therapeutic window of this type of conjugates as it was the case for SJG-136.

10 Conclusion and future work

10.1 Chemistry

10.1.1 PBD capping units

Five PBD capping units were successfully synthesised over the course of the project. Amongst these capping units, three were found to be particularly useful and include an aliphatic acid PBD, an aliphatic amino PBD and an aliphatic acid PBD with *exo*-C2 unsaturation. The length of the linker (3 carbons, excluding the acid or amine) was optimised by molecular modelling for direct coupling with a pyrrole/imidazole polyamide. Particular emphasis was given to protecting group combinations, with N10 Alloc and C11-Hydroxy THP being the most efficient when used in solution phase chemistry. This combination, developed during the project, allows retention of stereochemistry and cleaner amide bond formation.

In the future, attention should be directed to altering the PBD alkylation kinetics (*e.g.* removal of C8 methoxy) and linker flexibility. These alterations should provide additional interaction between the PBD and the heterocycle polyamide.
Control molecules bearing different alkylation moieties (*i.e.* CPI or mustards) should also be synthesized to study the effect of alkylating kinetics on sequence selectivity.

10.1.2 PBD–pyrrole/imidazole polyamides

Three types of bis-alkylating and five types of mono-alkylating PBD-pyrrole/imidazole polyamide hybrid were developed. The chemistry used to synthesise the polyamides (solution phase amide bond formation) is effective and provides relatively large quantities of material. However, the synthesis time remains to be shortened. It is foreseeable that pyrrole/imidazole monomers and dimers will become cheaper and more readily available in the future. Modern chemical methods (i.e. solid supported reagents, solid phase chemistry, purification by ion-exchange resins...) and robotics can also help to shorten the synthetic cycles.

The design of the polyamides could also be further modified. For example, the core linker of dimer AT-360 could be stiffened to force an interstrand crosslink and prevent back-folding. Additionally, the ester tail could be replaced with a cationic tail with the idea of increasing DNA binding affinity. In general, more pyrroles could be substituted by beta-alanines. In the case of the cyclin 008-AT-087-1, the macrocyclic linker could be lengthened from four carbon to six carbons.

10.2 Biology

10.2.1 Heterocycles linked PBD dimers

The set of Pyrrole/Imidazole-linked PBD dimers was found to exhibit nanomolar antitumour activity in the NCI 60 cell lines panel. Some of these dimers (e.g.: AT-361) also exhibit nanomolar crosslinking activity in whole cell comet assay and with small oligonucleotides. Footprinting studies revealed that these dimers possess an innate selectivity for certain DNA sequences, at nanomolar concentrations, with an indication of cooperation between the PBD and the polypyrrole moieties.

However, these studies also revealed their limitations (*i.e.* the difficulty of studying a wide variety of predetermined sequences, as well as cost and time limitations). Future studies should rely on small oligonucleotides to assess sequence selectivity, intrastrand crosslinking over interstrand crosslinking, and binding site length determination. DNA melting studies could also yield useful information on DNA binding affinity and kinetics. Reaction of the conjugates with small oligonucleotides could also be followed by LC/MS, which would yield information on the stoeichiometry of the binding (2:1 or 1:1) and on the reaction kinetics.

NMR studies of the conjugates in the presence of an adequate oligonucleotide could deliver information on the PBD orientation and on cooperation with the polyheteroyclic moiety.

10.2.2 Hairpin/cyclin PBDs

The ten hairpin/cyclin PBD polyamide conjugates were observed to bind to DNA sequence selectively and exhibit nanomolar antitumour activity in cytotoxicity screening.

However, the actual bound sequences revealed by the footprinting assay could not be predicted in advance. In addition, the theoretical binding sequences, when they were present in the DNA used, were not always bound by the conjugates. It is likely that the PBD moiety is sometimes leading the hybrid to an undesired, unpredicted sequence.

To resolve these issues, structural modification can be tried as suggested above. However, it is of particular importance to model every type of conjugate prior to synthesis. Most of these conjugates still require molecular modelling studies at the time of writing. To render the footprinting assays more useful, a DNA sequence including the theoretical binding site and series of mismatch possible binding sites could be tailor-made. This procedure, however, is time-consuming.

As mentioned on the previous page, binding studies with small oligonucleotides could be particularly useful to quickly provide information on sequence selectivity (for example, by DNA-binding dyes displacement).

As it is likely that only a fraction of the cellular DNA is accessible for reading or binding at a given time, it is more logical to study the effect of a conjugate on whole cell. In this context, a Q-PCR assay could conclude if a gene is deactivated selectively by a particular conjugate and should be considered as part of the future studies.

10.2.3 In vivo biological activity

As was reported in chapter 7, the tetrapyrrole PBD dimer AT-360 failed to show any useful therapeutic window. Similar, excessive toxicity, was detected when assaying the pyrrole/imidazole PBD hairpin AT-363. (see **Figure 10.2a** below).
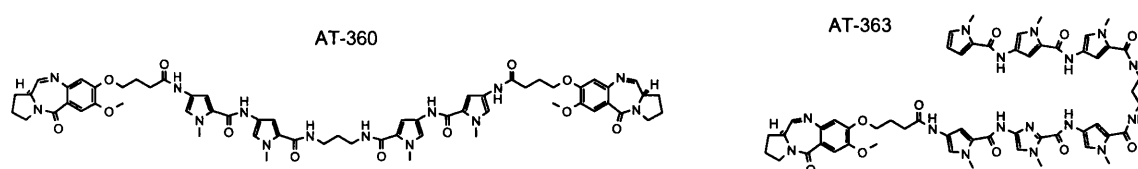
Figure 10.2a: Structures of AT-360 and AT-363

It was hypothesized that the saturated C-ring bearing PBD could be responsible for the lack of therapeutic window, by being excessively reactive with other bodily nucleophiles than DNA. Future studies will show if C-ring unsaturation can create a therapeutic window for these molecules.

More important would be to determine the cause of toxicity. For example, it would be particularly useful to know if the toxicity originates at a genetic or at the protein level, or both. In any cases, the binding event should be made more selective towards DNA, and then as targeted as possible.

11 Experimental section

11.1 General information and methods

11.1.1 Information

Reaction progress was monitored by thin-layer chromatography (TLC) using Merck Kieselgel 60 F254 silica gel, with fluorescent indicator on aluminium plates. Visualisation of TLC was achieved with UV light or iodine vapour unless otherwise stated. Flash chromatography was performed using Merck Kieselgel 60 F254 silica gel. Extraction and chromatography solvents were bought and used without further purification from Fisher Scientific, U.K. All chemicals were purchased from Aldrich, Lancaster or BDH.

^{1}H and ^{13}C NMR spectra were obtained on a Bruker Advance 400 spectrometer. All NMR experiments were recorded done in deuterated solvents $CDCl_3$ or DMSO-d_6. ^{13}C spectra were recorded at 100 MHz and ^{1}H at 400 MHz. Coupling constants are quoted in hertz (Hz). Chemical shifts are recorded in parts per million (ppm) downfield from tetramethylsilane. Spin multiplicities are described as s (singlet), bs (broad singlet), d (doublet), dd (doublet of doublets), t (triplet), q (quartet), p (pentuplet) and m (multiplet). IR spectra were recorded on a Perkin-Elmer FT/IR paragon 1000 spectrophotometer by application of the sample in a solution of chloroform, either on a KBr disk or using the ATR "golden gate" system as described. Mass spectrometry was performed on a ThermoQuest Navigator from Thermo Electron. Electrospray (ES) spectra were obtained at 20 to 30 V and fast atom bombardment (FAB) spectra were recorded using m-nitrobenzyl alcohol as matrix and xenon as reagent gas. Accurate mass measurements were done using Micromass Q-TOF global tandem or Micromass ZQ mass spectrometers. All samples were run under electrospray ionization mode using 50% acetonitrile in water and 0.1% formic acid as a solvent. Samples were run on W mode which gives a typical resolution of 19000 at FWHH. The instrument was calibrated with Glu-Fibrinopeptide B immediately prior to measurement.

Chiral HPLC analyses were done using a Daicel Chiracel column, OD 0.46 x 25 cm, 1:1 i-PrOH: hexane at 0.6 mL/min. (Tercel *et al.*, 2003).

Routine LC/MS was carried out using a Phenomenex 50 x 4.60 mm monolithic C18. The HPLC equipment consisted of the following: Waters 2695 separations module, Waters 2996 photodiode array detector and Waters micromass zq. The solvent was delivered at a flow rate of 3 mL.min^{-1} using gradient elution, Acetonitrile/Water + 0.1% formic acid.

HPLC analysis of compounds due for biological evaluation was carried out using both of the following: Phenomenex Luna 5μ C18(2) 250 x 4.6 mm or a Phenomenex Gemini 5μ C18(2) 100 x 4.6 mm. The solvent composition was the same for both columns: (A) Water + 0.1 % formic acid and (B) Acetonitrile + 0.1 % formic acid. The solvent was delivered at a flow rate of 1.5 ml/min using gradient elution:

Time	% A	% B
Initial	95	5
18.0	5	95
22.0	5	95
23.0	95	5
30	95	5

The HPLC equipment consisted of the following: A Waters 2767 sample manager fitted with a 20 μL loop, Waters 2525 pumps, Waters 2996 PDA and a Waters Micromass ZQ mass spectrometer. The ZQ was operated using electrospray ionization, scanning from 100 – 1500 Da in positive ion mode. All injections on columns were 20 μL with the flow being split 10 times ensuring that only 150 μL was entering the electrospray source.

Optical rotation values were recorded on a Bellingham and Stanley polarimeter at ambient temperature.

11.1.2 General methods

Method A: Peptide coupling between a Boc protected heterocyclic amino ester and a heterocyclic acid.

Finely powdered Boc protected amino ester was suspended in a solution of 4N HCl in dioxane (5 mL for 100 mg of starting material) and the reaction mixture was allowed to stir for 1h. The solvent was then removed by evaporation *in vacuo* to provide the amine HCl salt as a solid which was carried through to the next step without further purification. In a separate vessel, EDCI (1.2 eq) and DMAP (0.2 eq for catalysing the coupling + 1 eq for every equivalent of HCl to neutralise the acid) were added to a stirred solution of the acid (1 eq) in anhydrous DMF (1 mL per 100 mg of amino ester) at room temperature. The reaction mixture was added to the vessel containing the HCl salt and allowed to stir at room temperature over night. The reaction mixture was diluted with CHCl$_3$ (20 mL for every mL of DMF used during the reaction) and the organic phase was washed sequentially with water twice (10 mL per mL of DMF), saturated aqueous NaHCO$_3$ (10 mL per mL of DMF), brine (10 mL per mL of DMF) and dried over MgSO$_4$. Excess solvent was removed by rotary evaporation under reduced pressure to afford a yellow oil, which was purified by flash chromatography (gradient of MeOH in CHCl$_3$, starting from 0:100) to yield pure coupled product.

Method B: Peptide coupling between a heterocyclic amine and a heterocyclic acid using EDCI/HOBt.

The acid (1 eq) and HOBt (1.2 eq) were dissolved or suspended in DMF (5 mL for 100 mg of starting material). Solid EDCI (1.2 eq) was added and the reaction mixture was allowed to stir from 1 to 12 h depending on the reactivity of the acid. The amine (1 eq) was then added and the reaction mixture allowed to stir until the reaction was deemed complete by TLC or LC/MS. The reaction mixture was then diluted in cold water (50 times the volume of DMF). If the product precipitated as a solid, it was collected by filtration, washed with water and dried. In other cases, the mixture was extracted with DCM or CHCl$_3$ and washed sequentially with water twice (10 mL per mL of DMF), saturated aqueous NaHCO$_3$ (10 mL per mL of DMF), brine (10 mL per mL of DMF) and dried over MgSO$_4$. Excess solvent were removed by rotary evaporation under reduced pressure to afford a yellow oil, which was purified by flash chromatography (gradient of MeOH in CHCl$_3$, starting from 0:100) to yield pure coupled product.

Method C: saponification of an aromatic methyl ester.

The methyl ester (1 eq) was dissolved in MeOH (1 mL for 20 mg of ester) and treated with an aqueous solution of NaOH (3 eq, 1 mL of water per 50 mg of ester). The mixture was allowed to stir at 60 °C for 4 h, at which point TLC revealed complete reaction. The reaction mixture was diluted with water (1 mL per 50 mg of ester) and excess methanol removed by rotary evaporation under reduced pressure. The aqueous solution was then acidified to pH 3-4 with cold 1N HCl. The resulting precipitate was collected by vacuum filtration, washed with water and dried in a desiccator to provide the desired acid.

Method D: Standard Hydrogenation procedure.

The starting material (between 100 mg and 20 g) was dissolved in EtOH (maximum 120 mL) and a slurry of Pd/C (10% w/w compared with the starting material) in EtOH was added. The mixture was hydrogenated in a Parr apparatus at 45 psi until the H_2 uptake ceased. The reaction mixture was filtered through Celite and the residue washed with EtOH. The solvent was removed by rotary evaporation under reduced pressure to give the product (typically, quantitative yield).

## Method E: Alloc deprotection/ Activation of the PBD moiety.

A catalytic amount of *tetrakis*(triphenylphosphine)palladium (0.01 eq on large scale, up to 0.05 eq on small scale) was added to a stirred solution of the protected PBD-conjugate (1eq), and pyrrolidine (1.1 eq per PBD) in $CHCl_3$ (1 mL per 20 mg of conjugate). The reaction mixture was allowed to stir under a N_2 atmosphere at room temperature and the progress of reaction monitored by TLC. After 2 h stirring at room temperature, the reaction was deemed complete by TLC. The solvent was evaporated under reduced pressure and the resulting residue subjected to flash chromatography (gradient elution $CHCl_3$/MeOH) to yield the biologically active conjugate.

11.2 PBD building blocks: Synthesis

11.2.1 3C-Boc protected PBD acid: (Synthesis by the traditional route)

(as published by Masterson et al., 2004)

Synthesis of 4-(3-hydroxy-propoxy)-3-methoxy-benzoic acid 30
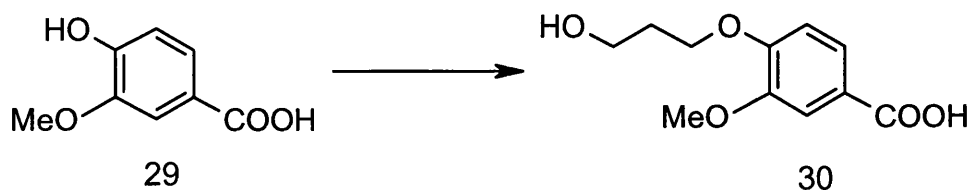
Neat 3-Bromopropan-1-ol (101.3 g, 0.73 mol, 1.07 eq) was added to a solution of vanillic acid (114.5 g, 0.68 mol) and sodium hydroxide (54.5 g, 1.36 mol) in water (400mL). The resulting mixture was heated under reflux for 5 hours, then cooled and acidified with 2.5 M HCl. The resulting precipitate was collected by filtration and dried *in vacuo*. Recrystallisation from butan-2-one gave the product **30** as an off white solid. (110 g, 71%). mp : 161-163°C; ^{1}H NMR (DMSO) δ 7.56 (dd, 1H, J = 1.98 Hz, J = 8.39 Hz), 7.44 (d, 1H, J = 1.96 Hz), 7.04 (d, 1H, J = 8.50 Hz), 4.55 (bs, 1H), 4.09 (t, 2H, J = 6.37 Hz), 3.80 (s, 3H, OMe), 3.57 (t, 2H, J = 6.20 Hz), 1.88 (p, 2H, J = 6.29 Hz); ^{13}C NMR (DMSO) δ 167.1, 152.0, 123.1, 122.7, 112.0, 111.7, 65.3, 57.2, 55.4, 31.9; IR (CHCl₃) v 1673, 1596, 1585, 1517, 1425, 1271, 1227, 1188, 1134, 1051, 1026, 951, 876, 814, 758 cm^{-1}; MS (ES⁻) m/z (relative intensity) 225.04 ([M - H]⁻, 100).

### Synthesis of 4-(2-Carboxy-ethoxy)-5-methoxy-2-nitro-benzoic acid 31
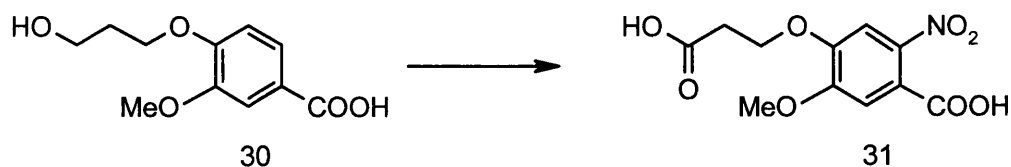
Fuming (70%) nitric acid (800 mL) was added to a 2L 3-necked round bottomed flask fitted with a powder funnel, overhead stirrer and thermometer, and cooled to 0°C (ice/acetone bath). The alcohol **30** (110 g, 0.486 mol) was added in portions over 1.5 hrs maintaining a temperature of 0°C. The mixture was allowed to stir at 0°C for 1 h, then

allowed to rise to room temperature. The precipitate was collected on a filter and washed with ice/water. The solids were dissolved in EtOAc, washed with brine (twice) and dried with magnesium sulphate. Excess solvents were removed by rotary evaporation under reduced pressuced to yield **31** as a yellow solid. (76 g, 55%)

^{1}H NMR (DMSO) δ 7.61 (s, 1H), 7.29 (s, 1H), 4.29 (t, 2H, J = 5.93 Hz), 3.90 (s, 3H), 2.74 (t, 2H, J = 5.98 Hz); ^{13}C NMR (DMSO) δ 171.9, 165.9, 151.6, 149.1, 141.3, 121.2, 111.3, 107.9, 65.1, 56.3, 33.7; IR (CHCl$_3$) v 1685, 1580, 1524, 1461, 1416, 1339, 1273, 1219, 1044, 1030, 866, 801 cm^{-1}; MS (ES$^-$) m/z (relative intensity) 284.0 ([M - H]$^-$, 60), 212.0 (100).

Synthesis of 4-(2-Benzyloxycarbonyl-ethoxy)-5-methoxy-2-nitro-benzoic acid 32.

31   32
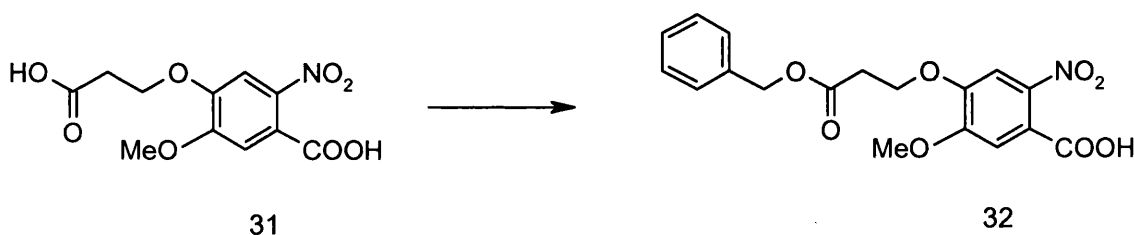
Benzyl alcohol (176.6 g, 169 mL, 6.14 eq) and para-toluenesulphonic acid (8.1 g, 0.16 eq) were added to a suspension of the diacid **31** (76 g, 0.266 mol) in toluene (760 mL). The mixture was allowed to stir under reflux for 3.5 h and then allowed to cool to room temperature. The reaction mixture was extracted with a saturated solution of aqueous sodium hydrogen carbonate and the combined aqueous extracts acidified to pH 2 with 1M HCl. The aqueous phase was extracted with ethyl acetate (3 X 300 mL). In parallel, the material precipitated during the acidification was dissolved in ethyl acetate (600 mL). The combined ethyl acetate solutions were dried (magnesium sulphate) and rotoevaporated *in vacuo* to give **32** as a yellow solid which was recrystallised from EtOAc/Hexane. (55.9 g, 56%).

^{1}H NMR (DMSO) δ 7.63 (s, 1H), 7.37-7.30 (m, 6H), 5.15 (s, 2H), 4.36 (t, 2H, J = 5.82 Hz), 3.90 (s, 3H), 2.91 (t, 2H, J = 5.88 Hz); ^{13}C NMR (DMSO) δ 170.4, 166.0, 151.7, 148.9, 141.3, 136.0, 128.3, 127.9, 127.7, 121.4, 111.4, 108.2, 65.6, 65.0, 56.4, 33.7; IR (CHCl$_3$) v 1704, 1603, 1537, 1424, 1395, 1349, 1278, 1213, 1181, 1050, 1022, 873, 753 cm^{-1}; MS (ES$^-$) m/z (relative intensity) 374.08 ([M - H]$^-$, 100).

Synthesis of 3-[4-(2-Hydroxymethyl-pyrrolidine-1-carbonyl)-2-methoxy-5-nitro-phenoxy]-propionic acid benzyl ester 33
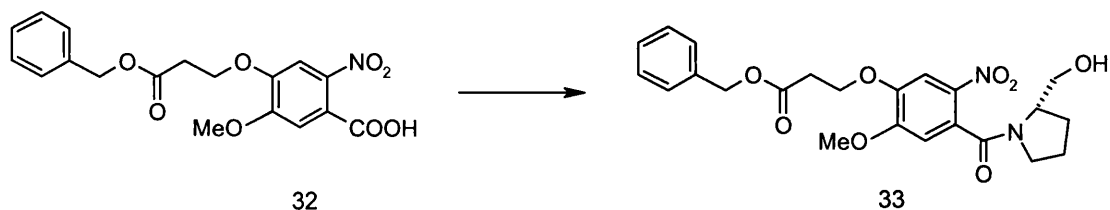
A few drops of DMF were added to a stirred mixture of benzyl ester **32** (30 g, 79.9 mmol) and oxalyl chloride (11.16 g, 7.66 mL, 1.1 eq) in dry DCM (300 mL) in a round-bottomed flask equipped with a drying tube. The mixture was allowed to stir overnight at room temperature. The resulting acid chloride solution was added dropwise over 6 h to a cold (–30°C) solution of triethylamine (17.75 g, 24.45 mL, 2.2 eq) and + (S)-pyrrolidine methanol (8.876 g, 8.66 mL, 1.1 eq) in dry DCM (150 mL) under nitrogen, maintaining the temperature below -30°C. The reaction mixture was allowed to stir overnight at room temperature. The resulting solution was extracted with 1N HCl (2 X 200 mL), twice with water, once with brine, then was dried with magnesium sulphate and concentrated by rotary evaporation to give a yellow, brown oil which solidifies. (quantitative yield). The resulting product was used in the next step without further purification.

^{1}H NMR (DMSO) Mixture of rotamers in a 35/65 ratio. δ 7.75 (m, 1H), 7.34 (m, 5H), 7.16 (s, 0.35H), 7.09 (s, 0.65H), 5.16 (s, 2H), 4.36 (m, 2H), 4.10 (m, 0.65H), 3.91 (s, 3H), 3.73-3.61 (m, 1H), 3.46-3.37 (m, 2.35H), 3.16-3.08 (m, 2H), 2.94-2.90 (m, 2H), 1.98-1.72 (m, 4H); ^{13}C NMR (DMSO) δ 170.4, 165.5, 154.0, 147.2, 136.9, 136.0, 128.6, 128.3, 128.2, 128.1, 127.9, 127.7, 109.9, 108.3, 79.1, 65.6, 64.8, 64.7, 61.7, 60.6, 59.9, 58.6, 56.6, 48.4, 45.7, 33.7, 27.4, 27.0, 23.4, 21.6; IR (CHCl₃) v 1735, 1618, 1577, 1519, 1453, 1427, 1383, 1332, 1275, 1218, 1171, 1058, 871, 750, 698, 649 cm^{-1}; MS (ES$^+$) m/z (relative intensity) 459.13 ([M + H]$^{+\cdot}$, 100); [α]^{25}$_D$ = -532° (c = 0.12, CHCl₃).

Synthesis of 3-[5-Amino-4-(2-hydroxymethyl-pyrrolidine-1-carbonyl)-2-methoxy-phenoxy]-propionic acid benzyl ester 34
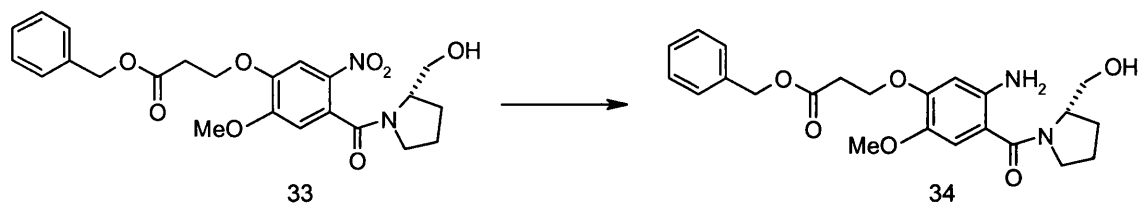
Tin chloride (130 g. 0.577 mol, 4.5 eq) was added to a solution of the nitro compound **33** (59 g, 0.128 mol) in methanol (650 mL). The reaction mixture was heated under reflux for 6 hours until completion of the reaction (TLC, 5% methanol in ethyl acetate). Excess methanol was removed by rotary evaporation *in vacuo* and the residue was dissolved in ethyl acetate (1 L) in a 5 L flask and 2 L of saturated sodium hydrogen carbonate aqueous solution was carefully added. [Effervescence !]. The mixture was mechanically stirred for 2 hours and the resulting emulsion (pH8) was allowed to settle overnight. It was filtered through celite. The solids were washed twice with ethyl acetate and the aqueous layer was extracted with ethyl acetate. The organic layers were combined, dried with magnesium sulphate, and concentrated *in vacuo* to yield the crude product **34** as a dark viscous oil (50 g). TLC analysis revealed presence of small quantities of impurities but the product was used in the next step with no further purification.

^{1}H NMR (CDCl$_3$) δ 7.36 (m, 5H), 6.74 (s, 1H), 6.28 (s, 1H), 5.19 (s, 2H), 4.28 (t, *J* = 6.2 Hz, 2H), 3.73 (s, 3H), 3.77-3.50 (m, 2H), 2.91(t, *J* = 6.2 Hz, 2H), 2.15 (m, 1H), 1.88-1.60 (m, 2H).

Synthesis of 3-[5-tert-Butoxycarbonylamino-4-(2-hydroxymethyl-pyrrolidine-1-carbonyl)-2-methoxy-phenoxy]-propionic acid benzyl ester 35.
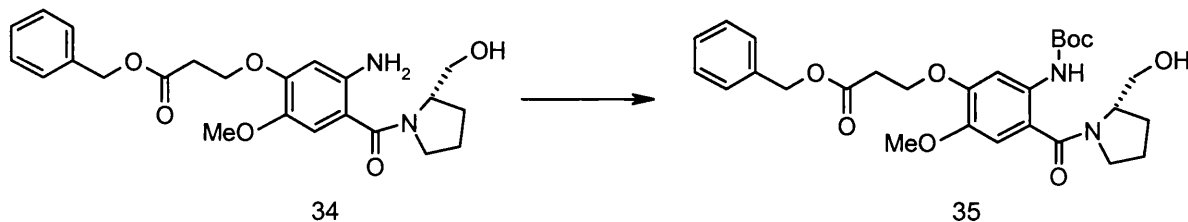
Boc anhydride (22.4 g, 0.103 mol) was added to a solution of crude amine **34** (39 g, 52.3 mmol) in THF (650 mL). The reaction mixture was heated under reflux overnight. TLC revealed complete reaction. (EtOAC). The THF was removed by rotary evaporation under reduced pressure and the residue dissolved in ethyl acetate (500 mL) and washed with water (2 X 200 mL), brine (200 mL), dried over magnesium sulphate and concentrated by rotary evaporation under reduced pressure to yield 53.2 g of a crude brown foam slightly contaminated with *tert*-butanol which was used in the next step with no further purification.

^{1}H NMR (CDCl$_3$) δ 8.41 (bs,1H), 7.82 (s, 1H), 7.34 (m, 5H), 6.81 (s, 1H), 5.18 (s, 2H), 4.39 (t, J = 6.2 Hz, 2H), 3.76 (s, 3H), 3.77-3.47 (m, 2H), 2.93 (t, J = 6.2 Hz, 2H), 2.05 (m, 1H), 1.88-1.60 (m, 2H), 1.50 (s, 9H).

Synthesis of the Boc protected 3C benzyl ester PBD capping unit 36
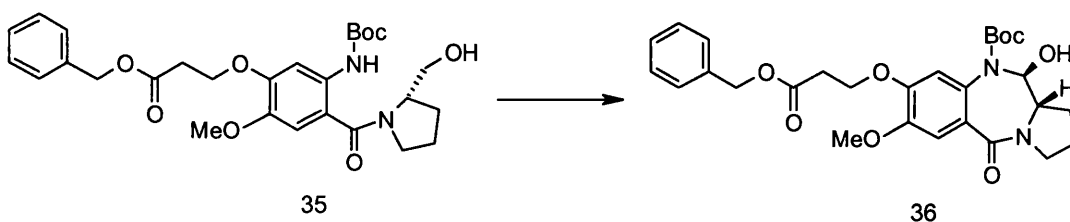
Pyridinium dichromate (43 g, 0.114 mol, 1.2 eq) was added to a solution of **35** (50 g, 0.094 mol) in dry DCM (500 mL) over molecular sieves (47 g) at room temperature under nitrogen. The reaction mixture was allowed to stir for 4h and was monitored by TLC. After completion of the reaction, the mixture was diluted with EtOAc (1L). The dark mixture was filtered through celite. The residue was mixed with warm EtOAc and removed by filtration. (3 X 200 mL). Rotoevaporation of the solvent yielded a dark foam which was subjected to column chromatography with 70/30 EtOAc/Pet Et as

eluant to give 16 g of pink coloured foam (32% yield). (further chromatography of mixed fractions furnished 2 g of additional product to give a final yield of **36** around 35%).

^{1}H NMR (CDCl$_3$) δ 7.34 (m, 5H), 7.22 (s, 1H), 6.66 (s, 1H), 5.55 (d, J = 6.37 Hz, 1H) 5.18 (s, 2H), 4.40-4.23 (m, 2H), 3.88 (s, 3H), 3.76-3.44 (m, 4H), 2.93 (t, J = 6.67 Hz, 2H), 2.14-1.98 (m, 4H), 1.36 (s, 9H); ^{13}C NMR (CDCl$_3$) δ 170.5, 167.0, 149.5, 148.5, 135.6, 129.2, 128.6, 128.5, 128.3, 128.2, 126.2, 114.8, 110.8, 85.7, 81.8, 66.6, 64.7, 59.7, 56.1, 34.4, 28.8, 28.4, 23.0; IR (CHCl$_3$) ν 2975, 2362, 1698, 1603, 1514, 1455, 1433, 1394, 1322, 1164, 1042, 852, 731 cm^{-1}; MS (ES$^+$) m/z (relative intensity) 527.12 ([M + H]$^+$, 30), 471.07 (50), 409.07 (100); [α]$^{25}_D$ = +335° (c = 0.212, CHCl$_3$).

Synthesis of the Boc protected 3C PBD acid capping unit 37
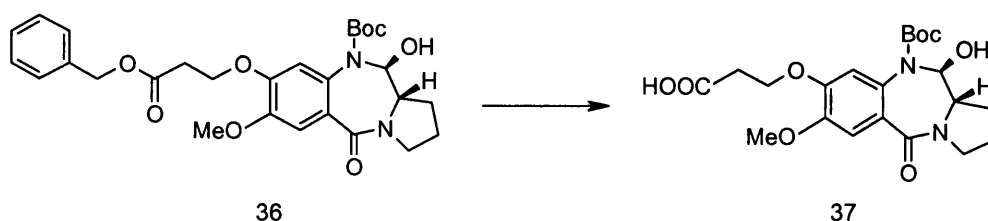
A slurry of Pd/C (0.5 g) in ethanol (caution! pyrophoric) was added to a solution of the benzyl ester **36** (9 g, 17.1 mmol) in ethanol (120 mL). The mixture was hydrogenated in a Parr hydrogenation apparatus at 16 psi until the hydrogen uptake ceased (2h). The reaction mixture was filtered through celite and the residue washed with ethanol. The solvent was removed by rotary evaporation under reduced pressure to give the 3C BOC protected PBD acid capping unit **37** as a white foam in quantitative yield.

^{1}H NMR (DMSO) δ 7.24 (s, 1H), 6.68 (s, 1H), 5.60 (d, J = 10 Hz, 1H) 5.18 (s, 2H), 4.31 (t, J = 7.5 Hz, 2H), 3.90 (s, 3H), 3.76-3.44 (m, 3H), 2.92 (t, J = 6.2 Hz, 2H), 2.14-1.98 (m, 4H), 1.38 (s, 9H).

Based on the ^{1}H NMR and the method employed, the product was found identical to the litterature description (Masterson *et.al.*, 2004)

11.2.2 4C-Boc protected PBD acid: (New route)

Synthesis of 4-(4-Formyl-2-methoxy-phenoxy)-butyric acid methyl ester 39
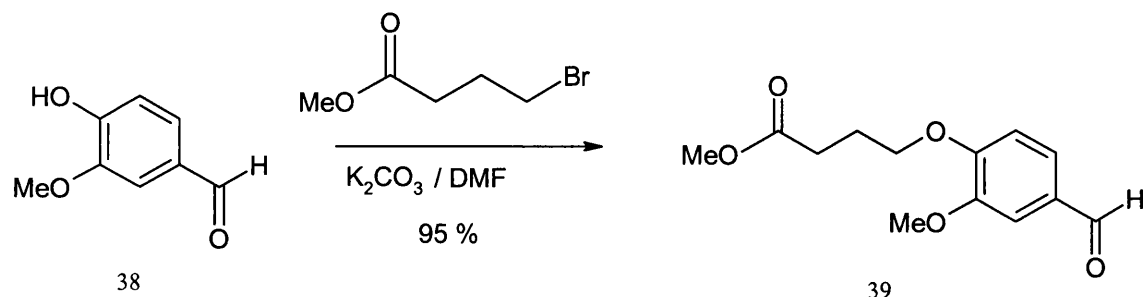
A slurry of vanillin (40 g, 0.262 mol), methyl-4-bromobutyrate (50 g, 34.2 mL, 1.05 eq) and potassium carbonate (54 g, 1.5 eq) in DMF (200 mL) was allowed to stir at room temperature overnight (16 h). The reaction mixture was diluted with water (1L). The resulting white precipitate was filtered, washed with water and dried on the filter then under vacuum to yield 60 g of product **39** (85%). mp 72-74°C

^{1}H NMR (CDCl$_3$) δ 9.80 (s, 1H, formyl) 7.43 (m, 2H, arom), 6.97 (d, J = 8.1 Hz, 1H, arom), 4.16 (t, J = 6.28 Hz, 2H), 3.92 (s, 3H), 3.70 (s, 3H), 2.57 (t, J = 7.15 Hz, 2H), 2.20 (p, J = 6.71 Hz); ^{13}C NMR (CDCl$_3$) δ 190.9, 173.4, 153.8, 149.9, 130.1, 126.8, 111.5, 109.2, 67.8, 56.0, 51.7, 30.3, 24.2; IR (golden gate) v 1728, 1678, 1582, 1508, 1469, 1426, 1398, 1262, 1174, 1133, 1015, 880, 809, 730 cm^{-1}; MS (ES$^+$) m/z (relative intensity) 253 ([M + H]$^+$, 100).

### Synthesis of 4-(4-Formyl-2-methoxy-5-nitro-phenoxy)-butyric acid methyl ester 40
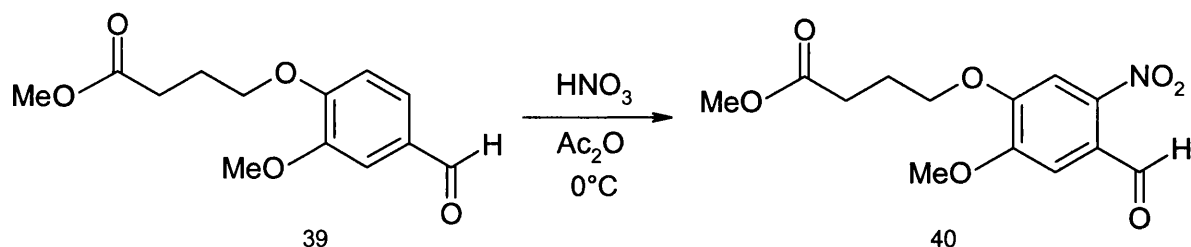
A solution of the aldehyde **39** (50 g, 0.197 mol) in acetic anhydride (150 mL) was slowly added to a mixture of 70% nitric acid (900 mL) and acetic anhydride (200 mL) at 0°C and the reaction mixture was allowed to stir for 2.5 h at 0°C. The solution was

poured onto ice in a large flask and the volume adjusted to 5 L with ice and water. The resulting light sensitive pale yellow precipitate was immediately collected by filtration in order to avoid hydrolysis of the ester, and washed with cold water. The product was sufficiently pure (TLC 50/50 EtOAc/Pet Et) to carry through directly to the next step.

^{1}H NMR (CDCl$_3$) δ 10.4 (s, 2H), 7.61 (s, 1H), 7.4 (s, 1H), 4.21 (t, J = 6.2 Hz, 2H), 4.00 (s, 3H), 3.71 (s, 2H), 2.58 (t, J = 7.1 Hz, 2H), 2.23 (p, J = 6.3 Hz, 2H); ^{13}C NMR (CDCl$_3$) δ 188.5, 172.8, 152.7, 151.0, 143.5, 124.7, 110.1, 108.2, 68.4, 56.4, 51.3, 29.7, 23.8; MS (ES$^+$) m/z (relative intensity) 298 ([M + H]$^+$, 100).

Synthesis of 5-Methoxy-4-(3-methoxycarbonyl-propoxy)-2-nitro-benzoic acid (41)
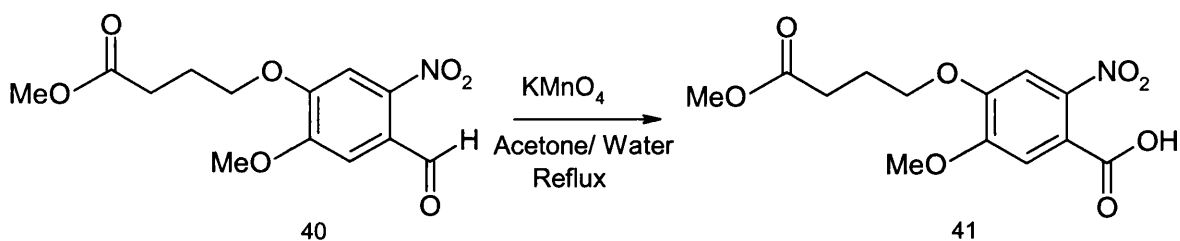
A hot solution of 10% potassium permanganate (50 g in 500 mL of water) was quickly added (in 5 to 10 minutes) to a solution of the nitroaldehyde **40** (80 g, slightly wet) in acetone (500 mL), in a 2L flask fitted with a condenser and a mechanical stirrer. Caution: halfway through the addition of KMnO$_4$ the reaction mixture began to reflux vigorously. This vigorous refluxing was maintained until the end of the reaction. The solution was allowed to cool for an hour, was then filtered through celite and the brown residue was washed with 1 L of hot water. The filtrate was transferred to a large flask and a solution of sodium bisulphite (80 g in 500 mL 1N HCl) was added. The final volume was adjusted to 3 L by addition of water, and the pH adjusted to 1 with conc. HCl. The product precipitated, was filtered, and dried. 31 g (50% yield over 2 steps). Product **41** was pure as proved by TLC (85/15/0.5 EtOAc/MeOH/Acetic acid).

^{1}H NMR (CDCl$_3$) δ 7.33 (s, 1H), 7.19 (s, 1H), 4.09 (t, J = 5.72 Hz, 2H), 3.91 (s, 3H), 3.64 (s, 3H), 2.50 (t, J = 6.98 Hz, 2H), 2.14 (p, J = 6.33 Hz, 2H); ^{13}C NMR (DMSO) δ 172.8, 166.0, 151.8, 149.1, 141.3, 121.2, 111.3, 107.8, 68.1, 56.4, 51.3, 29.7, 23.8; IR (golden gate) v 1736, 1701, 1602, 1535, 1415, 1275, 1220, 1054, 936, 879, 820, 655 cm^{-1}; MS (ES$^-$) m/z (relative intensity) 312.01 ([M - H]$^-$, 100).

Synthesis of 4-[4-(2-Hydroxymethyl-pyrrolidine-1-carbonyl)-2-methoxy-5-nitro-phenoxy]-butyric acid methyl ester 42.
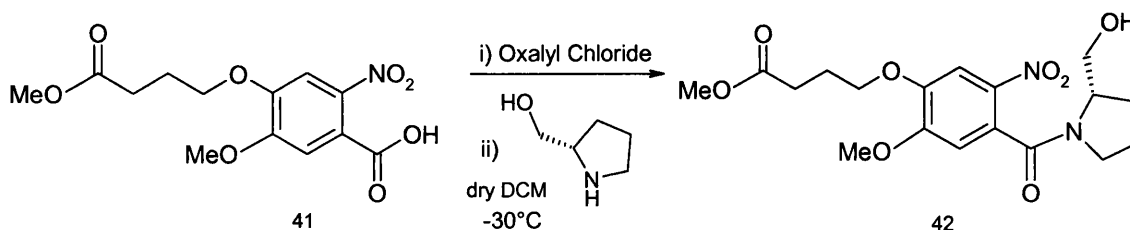
The reaction was performed according to the method described for the three carbon homologue **33** on a 30.4 g scale. Once again, the product **42** solidified to afford a clear, yellow glass. (38 g, 99%).

^{1}H NMR (CDCl$_3$) δ 7.70 (s, 1H, aro), 6.80 (s, 1H aro), 4.40 (br d, 1H), 4.16 (t, J = 6.2Hz, 2H, OCH$_2$), 3.97 (s, 3H, OMe), 3.97 to 3.70 (m, 2H, NCH$_2$), 3.71 (s, 3H, OMe), 3.17 (t, J = 6.7Hz, 2H, CH$_2$), 2.57 (t, J = 7.1Hz, 2H, CH$_2$), 2.20 (p, 2H, CH$_2$), 1.90 to 1.70 (m, 2H, CH$_2$); ^{13}C NMR (CDCl$_3$) δ 173.2, 154.8, 148.4, 109.2, 108.4, 68.4, 66.1, 61.5, 56.7, 51.7, 49.5, 30.3, 28.4, 24.4, 24.2; IR (golden gate) v 3400, 2953, 1734, 1618, 1517, 1432, 1327, 1271, 1219, 1170, 1051, 995, 647 cm^{-1}; MS (ES$^+$) m/z (relative intensity) 397.07 ([M + H]$^+$, 100); [α]^{24}$_D$ = -84° (c = 1, CHCl$_3$).
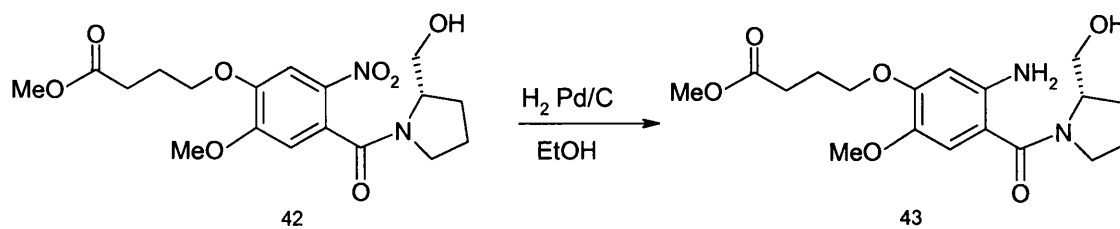
Synthesis of 4-[5-Amino-4-(2-hydroxymethyl-pyrrolidine-1-carbonyl)-2-methoxy-phenoxy]-butyric acid methyl ester 43

The reaction was performed according to the method described in standard hydrogenation procedure D on a 38 g scale. Complete reaction was confirmed by TLC

analysis (EtOAc). The resulting amine **43** was used directly in the next step. (35.5 g, quantitative yield).

Synthesis of 4-[5-tert-Butoxycarbonylamino-4-(2-hydroxymethyl-pyrrolidine-1-carbonyl)-2-methoxy-phenoxy]-butyric acid methyl ester 44
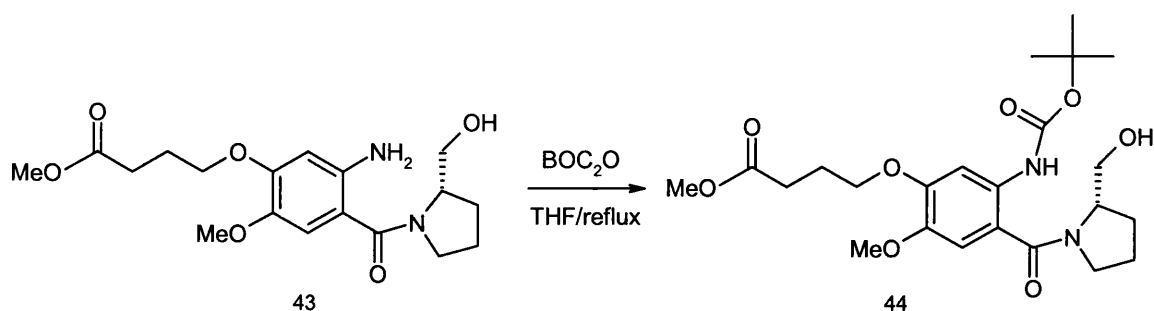
43   →   BOC₂O / THF/reflux   →   **44**

The reaction was performed according to the method described for the three carbon homologue **35** on a 35.5 g scale. Quantitative yield.

^{1}H NMR (CDCl₃) δ 8.38 (bs, 1H), 7.75 (s, 1H), 6.79 (s, 1H), 4.56-4.18 (m, 2H), 4.10 (t, J = 6.15 Hz, 2H), 3.80 (m, 4H), 3.68 (m, 4H), 3.62-3.37 (m, 2H), 2.53 (t, 2H, J = 7.37 Hz), 2.16 (p, 2H, J = 6.45 Hz), 1.97-1.59 (m, 4H), 1.51 (s, 9H); ^{13}C NMR (CDCl₃) δ 173.5, 171.1, 153.1, 150.6, 146.7, 143.8, 132.5, 111.9, 105.8, 85.1, 80.3, 67.7, 61.1, 60.4, 56.8, 51.6, 30.6, 28.4, 27.4, 24.4; IR (golden gate) ν 2974, 1721, 1596, 1521, 1406, 1240, 1158, 1116, 1013 cm^{-1}; MS (ES$^+$) m/z (relative intensity) 467.1 ([M + H]$^+$, 100); [α]^{23}_D = -65° (c = 0.17, CHCl₃).

Synthesis of the Boc protected 4C methyl ester PBD capping unit (45)

44   →   Swern Oxydation   →   **45**
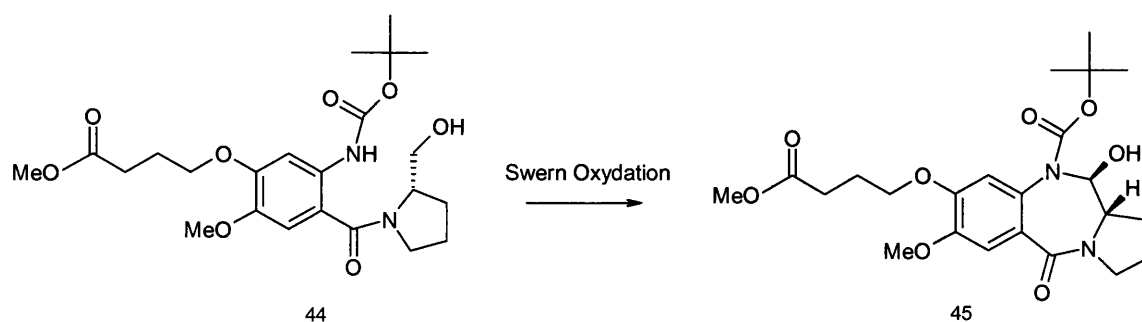
A solution of dry DMSO (24.1 g, 23.9 mL, 3.6 eq) in dry DCM (300 mL) was added dropwise to a solution of oxalyl chloride (26.57 g, 18.26 mL, 1.8 eq) in dry DCM (300

217

mL) at –40°C (Acetonitrile/ liquid nitrogen cooling bath). A white suspension was observed, which eventually redissolved. The crude Boc amine **44** (40 g, 85.8 mmol) in dry DCM (450 mL) was added dropwise over 3 h maintaining the temperature below – 37°C. The mixture was allowed to stir at -40°C for a further hour. A solution of DIPEA (64.2 mL, 4.3 eq) in dry DCM (150 mL) was added dropwise over 1 h and the reaction was allowed to warm to room temperature. The reaction mixture was extracted with a 10 % aqueous solution of citric acid. (pH of 2 to 3 after extraction). The organic phase was then washed with water (2 X 400 mL) and brine (300 mL), dried (magnesium sulphate) and the solvent removed by rotoevaporation under reduced pressure to yield a paste which was purified by column chromatography (70/30 EtOAc/Pet Ether), to yield 25 g of product **45**. (63%)

^{1}H NMR (CDCl$_3$) δ 7.21 (s, 1H), 6.63 (s, 1H), 5.55 (d, J = 6.3 Hz, 1H), 4.2 (m, 2H), 3.90 (s, 3H), 3.86 (bs, 1H), 3.69 (m, 1H), 3.68 (s, 3H), 3.50 (m, 2H), 2.55 (t, J = 7.2 Hz, 2H), 2.2-1.97 (m, 6H), 1.40 (s, 9H); ^{13}C NMR (CDCl$_3$) δ 173.43, 167.14, 149.82, 148.32, 129.27, 125.78, 114.16, 110.66, 85.68, 81.76, 67.99, 60.40, 59.79, 56.08, 51.66, 46.37, 30.37, 28.79, 28.27, 24.39, 23.07, 21.05, 14.20; IR (golden gate) v 2974, 1735, 1700, 1623, 1514, 1435, 1324, 1165, 1048, 756 cm^{-1}; MS (ES⁻) m/z (relative intensity) 463.15 ([M - H]⁻, 100); [α]^{24}$_D$ = +142° (c = 0.18, CHCl$_3$).

Synthesis of the Boc protected 4C PBD acid capping unit 46


45   NaOH / MeOH / water   46
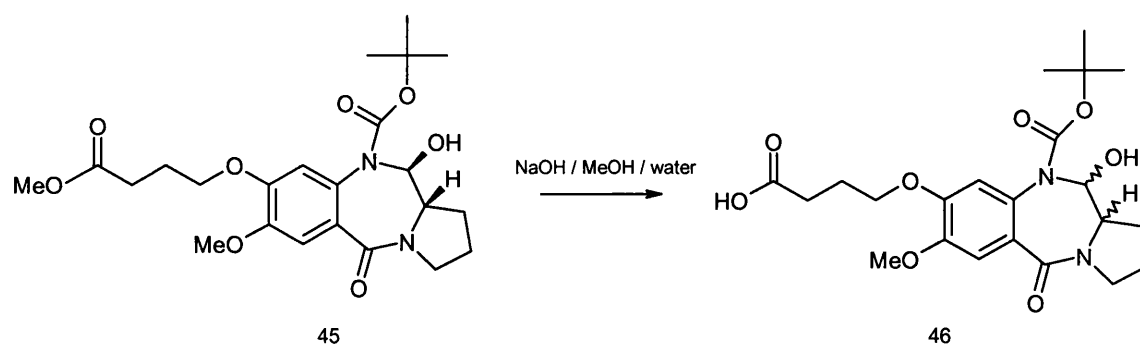
A solution of sodium hydroxide (4.31 g, 2 eq) in water (50 mL) was added to a solution of methyl ester **45** (25 g, 53.9 mmol) in methanol (250 mL) in a round bottomed flask. The flask was allowed to stir in the rotoevaporator bath at 60°C for 20 min until the hydrolysis was found complete as monitored by TLC and excess methanol was removed

under reduced pressure. Water (200 mL) was added, followed by a 10 % aqueous citric acid solution until no further precipitation occurs (pH 2 to 3). The resulting mixture was extracted with ethyl acetate (2 X 300 mL), dried (magnesium sulphate) and the solvent removed by rotary evaporation under reduced pressure. The product was dissolved in hot chloroform (500 mL), treated with activated charcoal and stirred for 10 minutes. The suspension was filtered through celite and the solvent removed by rotary evaporation under reduced pressure to yield **46** as a white solid (quantitative yield).

TLC system EtOAC/MeOH/AcOH 85/15/0.5; ^{1}H NMR (DMSO) δ 7.06 (s, 1H), 6.70 (s, 1H), 6.39 (bs, 1H), 5.44 (s, 1H), 4.0 (m, 2H), 3.82 (s, 3H), 3.54-3.20 (m, 3H), 2.42 (d, J = 7.2, 2H) 2.1-1.8 (m, 6H), 1.32 (s, 9H); ^{13}C NMR (DMSO) δ173.95, 166.09, 153.72, 149.13, 147.68, 129.39,114.58, 110.17, 80.11, 79.13, 67.54, 60.52, 55.61, 45.87, 29.89, 28.27, 27.88, 24.10, 22.70; High Res FABMS m/e 451.2063 (M+H calculated for $C_{22}H_{30}N_2O_8$: 451.2080); MS: 451 (M+H, 40%), 395 (35%), 350 (43%, M-Boc), 333 (100%, M-Boc-OH).

Removal of N-10 protecting group triggers 11-OR elimination to form an active PBD such as:

AT219
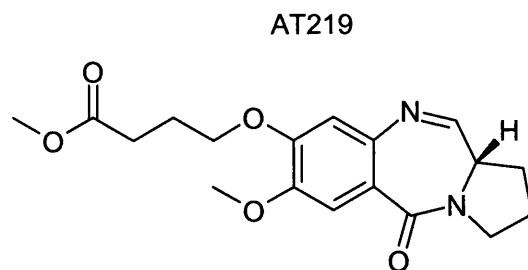
Compound 43.

Pd(PPh$_3$)$_4$ (2 mg, 1.7 µmol) was added to a stirred solution of AT218, **40** (75 mg,162 µmol) and pyrrolidine (14.7 µL,176 µmol) in anhydrous DCM (10 mL). The reaction mixture was allowed to stir for 1 h at which point TLC analysis revealed completion of the reaction. Excess solvent was removed by rotary evaporation under reduced pressure and the residue purified by flash chromatography (EtOAc, 100%). The pure fractions were combined to provide AT219, **43** (55 mg, 98%). ^{1}H NMR (CDCl$_3$) δ 7.66 (d, J = 4.4 Hz, 1H), 7.51 (s, 1H), 6.80 (s, 1H), 4.21-4.02 (m, 2H), 3.93 (s, 1H), 3.86-3.76 (m, 1H), 3.76-3.64 (m, 4H), 3.63-3.51 (m, 1H), 2.54 (t, J = 7.3 Hz, 2H), 2.39-2.34 (m, 2H), 2.24-2.13 (m, 2H), 2.12-1.95 (m, 2H). ^{13}C NMR (CDCl$_3$) δ 173.4, 164.5, 162.3, 150.5,

147.8, 140.6, 120.3, 111.6, 110.6, 67.7, 56.1, 53.6, 51.6, 46.6, 30.4, 29.6, 24.2, 24.1; MS (ES$^+$) m/z (relative intensity) 347.2 ([M + H]$^+$, 100); IR v 3323, 2952, 1734, 1625, 1601, 1506, 1433, 1372, 1262, 1217, 1173, 1127, 1092, 1021, 951, 875, 765, 729 cm^{-1}. [α]$^{25}_D$ = +20° made with the OMe protected capping unit, [α]$^{26}_D$ = +482° (chirally pure by chiral column; see general information); Acc. Mass $C_{18}H_{22}N_2O_5$ calc. 347.1602 found 347.1612. Purity by analytical HPLC : Luna : 92 %; Gemini : 78 %.

11.2.3 4C-Alloc THP PBD acid capping unit

Synthesis   of   4-[5-Allyloxycarbonylamino-4-(2-hydroxymethyl-pyrrolidine-1-carbonyl)-2-methoxy-phenoxy]-butyric acid methyl ester 54
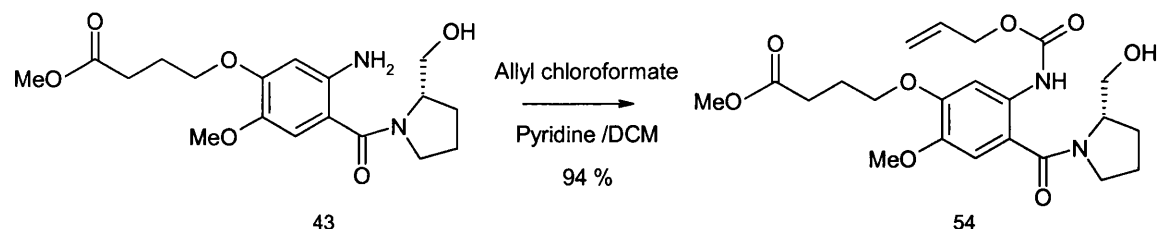
A solution of allyl chloroformate (7.17 mL, 67.5 mmol) in anhydrous DCM (200 mL) was added dropwise to a solution of amine **43** (22.5 g, 61.5 mmol) and anhydrous pyridine (10.9 mL, 134 mmol) in anhydrous DCM (300 mL) at 0°C. The resulting mixture was allowed to stir overnight at room temperature and then washed with cold 1N aqueous HCl (200 ml), water (200 mL), saturated aqueous NaHCO₃ (200 mL), and brine (200 mL). The solution was then dried over MgSO₄, and the solvent removed by rotary evaporation under reduced pressure to provide **54**, slightly contaminated by the product of diacylation (27 g, quantitative yield). The crude material was purified by flash chromatography (EtOAc/ Hexane) to provide an analytical sample.

^{1}H NMR (CDCl₃) δ 8.78 (bs, 1H), 7.75 (s, 1H), 6.82 (s, 1H), 5.97 (m, 1H), 5.38-5.24 (dd, 2H), 4.63 (m, 2H), 4.40 (bs, 2H), 4.11 (t, J = 6.3 Hz, 2H), 3.82 (s, 3H), 3.69 (m, 4H), 3.61-3.49 (m, 2H), 2.54 (t, J = 7.4 Hz, 2H), 2.18 (p, J = 6.7 Hz, 2H), 1.92-1.70 (m, 4H) ; ^{13}C NMR (CDCl₃) δ 173.4, 170.9, 153.6, 150.5, 144.0, 132.5, 132.0, 118.1, 115.4, 111.6, 105.6, 67.7, 66.6, 65.8, 61.1, 60.4, 56.6, 51.7, 30.5, 28.3, 25.1, 24.3; MS (FAB⁺) m/z 50 (451, M+H); IR (golden gate) v 2949, 2359, 1728, 1596, 1521, 1433, 1202, 1173, 1119, 998, 844, 652 cm⁻¹; $[\alpha]^{26}_D$ = -67 ° (c = 0.45, CHCl₃).

Synthesis of 11-Hydroxy-7-methoxy-8-(3-methoxycarbonyl-propoxy)-5-oxo-2,3,11,11a-tetrahydro-1H,5H-benzo[e]pyrrolo[1,2-a][1,4]diazepine-10-carboxylic acid allyl ester 55
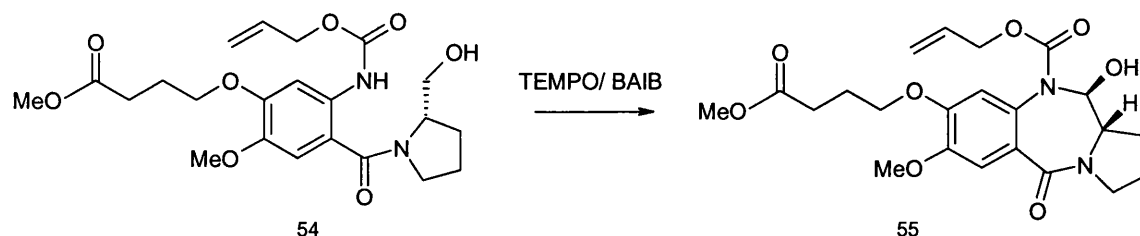
TEMPO (902 mg, 5.77 mmol) was added to a solution of crude **54** (26 g, 57.7 mmol) and diacetoxyiodobenzene (BAIB; 20.4 g, 63.5 mmol) in DCM (500 mL). The reaction mixture was allowed to stir overnight after which the reaction was found complete by TLC (EtOAc, with co-spot, very fine Rf difference). The solution was washed with saturated aqueous sodium metabisulphite (200 mL) followed by saturated aqueous NaHCO$_3$ (2 x 300 mL), brine (300 mL), and dried over MgSO$_4$. The solvent was removed by rotary evaporation under reduced pressure and the residue was purified by flash chromatography (EtOAc/Hexane, gradient from 60/40 to 90/10). Yield of **55**: (14.2 g, 55 %).

^{1}H NMR (CDCl$_3$) δ 7.23 (s, 1H), 6.69 (s, 1H), 5.80 (m, 1H), 5.63 (m, 1H), 5.15 (d, J = 12.9 Hz, 2H), 4.69-4.43 (m, 2H), 4.13 (m, 2H), 3.90 (m, 4H), 3.68 (m, 4H), 3.58-3.45 (m, 2H), 2.53 (t, J = 7.2 Hz, 2H), 2.18-1.94 (m, 6H); ^{13}C NMR (CDCl$_3$) δ 173.4, 167.0, 156.0, 149.9, 148.7, 131.8, 128.3, 125.9, 118.1, 113.9, 110.7, 86.0, 67.9, 66.8, 60.4, 59.9, 56.1, 51.7, 46.4, 30.3, 28.7, 24.2, 23.1, 21.1; MS (ES$^+$) m/z 100 (449.1, M+H); IR (golden gate) v 2951, 1704, 1604, 1516, 1458, 1434, 1313, 1272, 1202, 1134, 1103, 1041, 1013, 647 cm^{-1}; [α]^{26}$_D$ = +122 ° (c = 0.2, CHCl$_3$).

Synthesis of 7-Methoxy-8-(3-methoxycarbonyl-propoxy)-5-oxo-11S-(tetrahydro-pyran-2-yloxy)-2,3,11,11aS-tetrahydro-1*H***,5***H***-benzo[e]pyrrolo[1,2-a][1,4]diazepine-10-carboxylic acid allyl ester 52.**

55   52
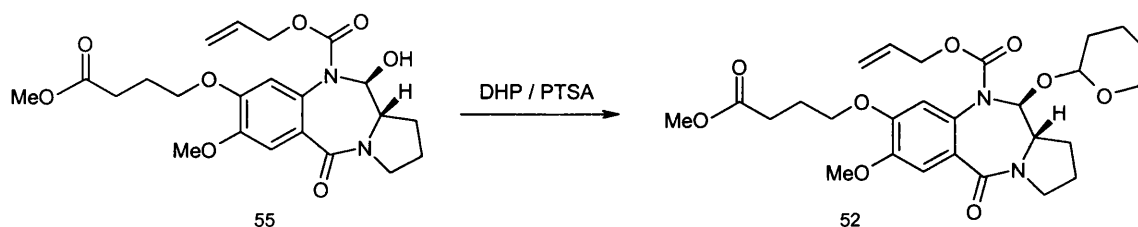
The protected carbinolamine **55** (2.0 g, 4.62 mmol) was added to a solution of DHP (4.22 mL, 46.2 mmol) and PTSA (catalytic quantity, 20 mg) in EtOAc (30 mL). The resulting reaction mixture was allowed to stir for 2 hours. At this time, TLC analysis (EtOAc) revealed completion and the solution was diluted with EtOAc (70 mL) and washed with saturated aqueous $NaHCO_3$ (50 mL), followed by brine (50 mL). The organic phase was then dried ($MgSO_4$), and the solvent was removed by rotary evaporation under reduced pressure. The oily residue was dried *in vacuo* to afford the product **52** in quantitative yield (2.38 g, 100%). The product was used directly in the next step. ^{1}H NMR ($CDCl_3$) as a mixture of 4/5 of epimers: δ 7.24-7.21 (2s, 2H), 6.88-6.60 (2s, 2H), 5.89-5.73 (m, 4H), 5.15-5.04 (m, 6H), 4.96-4.81 (m, 2H), 4.68-4.35 (m, 4H), 4.12-3.98 (m, 4H), 3.98-3.83 (m, 8H), 3.74-3.63 (m, 8H), 3.60-3.40 (m, 8H), 2.56-2.50 (m, 4H), 2.23-1.93 (m, 12H), 1.92-1.68 (m, 10H), 1.66-1.48 (m, 20H); ^{13}C NMR ($CDCl_3$) δ 173.4, 167.2, 149.1, 132.0, 114.5, 100.0, 98.4, 94.6, 91.7, 68.0, 67.7, 66.3, 63.9, 63.6, 63.3, 62.9, 56.1, 51.6, 51.5, 46.3, 46.3, 31.1, 30.9, 30.7, 30.4, 30.2, 29.0, 25.4, 25.3, 25.2, 24.2, 20.0, 19.8, 19.7; MS (ES$^+$) *m/z* (relative intensity) 533.2 ([*M* + H]$^+$, 100).

Synthesis of 8-(3-Carboxy-propoxy)-7-methoxy-5-oxo-11S-(tetrahydro-pyran-2-yloxy)-2,3,11,11aS-tetrahydro-1*H*,5*H*-benzo[e]pyrrolo[1,2-a][1,4]diazepine-10-carboxylic acid allyl ester 57.
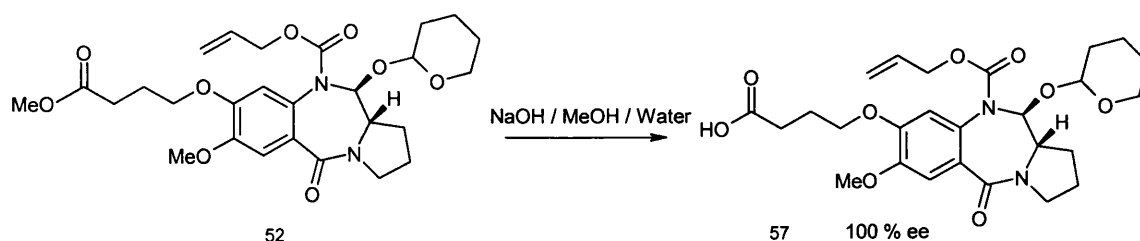

A solution of sodium hydroxide (340 mg, 8.5 mmol) in water (7 mL) was added to a solution of the methyl ester solution **52** (2.2 g, 4.26 mmol) in MeOH (30 mL). The reaction mixture was allowed to stir on a rotoevaporator at 70°C for 15 min under atmospheric pressure, at which point the reaction was found complete by TLC. Excess methanol was removed by rotary evaporation under reduced pressure and more water (20 mL) was added. The aqueous solution was allowed cool and a 5 % aqueous citric acid solution was added until the pH was < 4. The precipitate was then extracted with EtOAc (100 mL). The organic layer was washed with brine (30 mL) and dried over MgSO$_4$. Excess solvent was removed by rotary evaporation under reduced pressure. Diethylether (50 mL) was added to the residue and excess solvents further rotoevaporated under reduced pressure. The residue was dried *in vacuo* to yield the pure **57**, as white foam (2.10 g, 98 %). ^{1}H NMR (DMSO) as a mixture of 4/5 of epimers δ 7.10 (2s, 2H), 6.90-6.84 (2s, 2H), 5.84-5.68 (m, 4H), 5.45-4.91 (m, 6H), 4.72-4.30 (m, 4H), 4.09-3.93 (m, 4H), 3.91-3.75 (m, 8H), 3.60-3.44 (m, 4H), 3.44-3.22 (m, 8H), 2.46-2.33 (m, 4H), 2.20-1.76 (m, 14H), 1.76-1.31 (m, 12H). ^{13}C NMR (DMSO) δ 173.9, 173.9, 171.9, 166.1, 166.0, 149.6, 148.4, 148.3, 132.6, 116.5, 114.4, 110.5, 110.3, 99.2, 67.5, 67.4, 65.6, 65.5, 62.8, 59.4, 55.7, 45.9, 30.5, 30.2, 29.8, 29.7, 28.4, 28.3, 24.9, 24.8, 23.9, 23.8, 22.9, 22.7; MS (ES$^+$) *m/z* (relative intensity) 519.2 ([*M* + H]$^+$, 100). This compound was proved optically pure at C11a by reesterification (EDCI, HOBt, then MeOH), THP removal (AcOH/THF/H$_2$O) and chiral HPLC (see general information).

Synthesis of 4C N10-Alloc-O11-methyl-PBD acid capping unit: compound 11

(this methylation method produces 10 % of the wrong isomer, partial racemisation).

Synthesis of 7,11S-Dimethoxy-8-(3-methoxycarbonyl-propoxy)-5-oxo-2,3,11,11aS-tetrahydro-1*H*,5*H*-benzo[e]pyrrolo[1,2-a][1,4]diazepine-10-carboxylic acid allyl ester **49**.

55   49
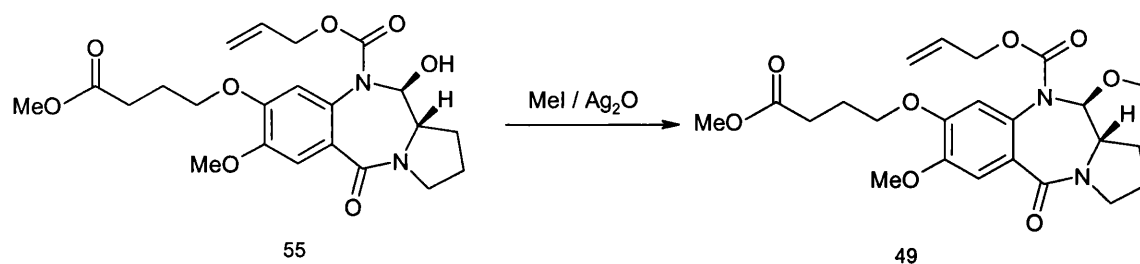
Silver (I) oxide (2.5 g, 10.8 mmol) was added to a solution of **55** (1.2 g, 2.77 mmol) and MeI (1.72 mL, 27.6 mmol) in anhydrous DCM. The resulting suspension was allowed to stir under reflux conditions for 24h. The reaction was then found complete by TLC (EtOAc). The suspension was filtered through celite and the volatiles were removed by rotoevaporation under reduced pressure (**Caution!**, MeI is carcinogenic, evaporate under a fumehood) to yield the pure **49**, (1.27 g, 99%). Chiral HPLC later revealed AT220 to be a mixture of two enantiomers in a 90/10 ratio. (90 % of the biologically active isomer, 10 % of the inactive isomer). ^{1}H NMR (CDCl$_3$) δ 7.22 (s, 1H), 6.65 (s, 1H), 5.86-5.65 (m, 1H), 5.43 (d, J = 9.09 Hz, 1H), 5.18-4.94 (m, 2H), 4.71-4.32 (m, 2H), 4.07 (t, J = 6.21 Hz, 2H), 3.89 (s, 3H), 3.66 (m, 4H), 3.47 (m, 4H), 3.40 (m, 1H), 2.54 (t, J = 7.19 Hz, 2H), 2.14 (p, J = 6.57 Hz, 2H), 2.09-1.91 (m, 4H). ^{13}C NMR (CDCl$_3$) δ 173.4, 167.2, 156.1, 150.1, 149.1, 131.9, 128.6, 126.8, 117.2, 114.3, 110.8, 93.3, 67.9, 66.4, 60.1, 56.5, 56.0, 51.6, 46.2, 30.2, 28.9, 24.2, 23.1; MS (ES$^+$) m/z (relative intensity) 463.3 ([M + H]$^+$, 100).

Synthesis of 8-(3-Carboxy-propoxy)-7,11S-dimethoxy-5-oxo-2,3,11,11aS-tetrahydro-1*H*,5*H*-benzo[e]pyrrolo[1,2-a][1,4]diazepine-10-carboxylic acid allyl ester 56.
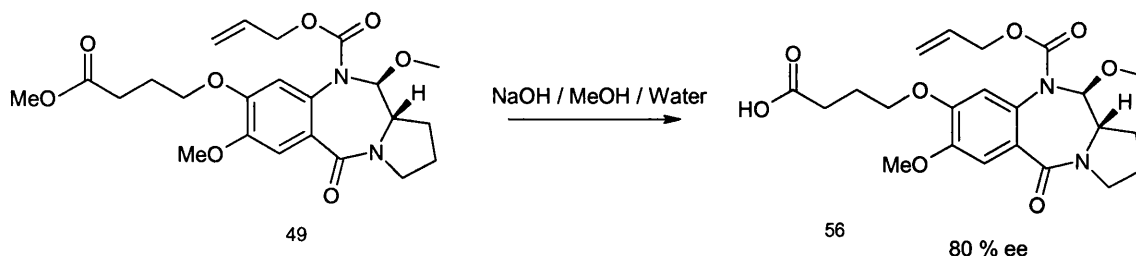
A solution of sodium hydroxide (207 mg, 5.19 mmol) in water (5 mL) was added to a solution of **49** (1.2 g, 2.59 mmol) in MeOH (20 mL). The reaction mixture was allowed to stir on a rotoevaporator at 70°C for 15 min under atmospheric pressure after which the reaction was deemed complete by TLC (EtOAc/ MeOH/ AcOH, 90/10/1). Excess methanol was removed under reduced pressure and more water (20 mL) was added. The aqueous solution was allowed to cool and a 1N aqueous HCl solution was added dropwise until pH < 3. The resulting precipitate was extracted with EtOAc (2 x 50 mL). The organic layers were combined, washed with brine (30 mL) and dried (MgSO$_4$). Excess solvent was removed by rotoevaporation under reduced pressure. Diethylether (50 mL) was added to the residue and removed by rotoevaporation under reduced pressure. The residue was dried further under hard vacuum to yield pure **56**, as white foam (1.15 g, 99 %). ^{1}H NMR (DMSO) δ 7.24 (s, 1H), 6.65 (s, 1H), 5.85-5.66 (m, 1H), 5.43 (d, J = 9.01 Hz, 1H), 5.17-4.95 (m, 2H), 4.68-4.34 (m, 2H), 4.09 (t, J = 6.95 Hz, 2H), 3.89 (s, 3H), 3.74-3.61 (m, 1H), 3.59-3.46 (m, 4H), 3.46-3.35 (m, 1H), 2.59 (t, J = 7.15 Hz, 2H), 2.16 (p, J = 6.58 Hz, 2H), 2.10-1.89 (m, 4H); ^{13}C NMR (DMSO) δ 177.8, 176.3, 167.3, 156.1, 150.1, 149.1, 131.9, 128.6, 126.7, 117.3, 114.4, 110.9, 93.3, 67.8, 66.5, 60.4, 60.1, 56.5, 56.1, 46.3, 30.2, 28.9, 24.0, 23.1, 21.0; MS (ES$^+$) m/z (relative intensity) 449 ([M + H]$^+$, 100); IR v 2942, 1712, 1603, 1516, 1467, 1436, 1408, 1314, 1275, 1205, 1111, 1087, 1040, 972, 918, 767, 731 cm^{-1}.

11.2.4 3-C N10 Alloc, amino PBD capping unit 66.

66
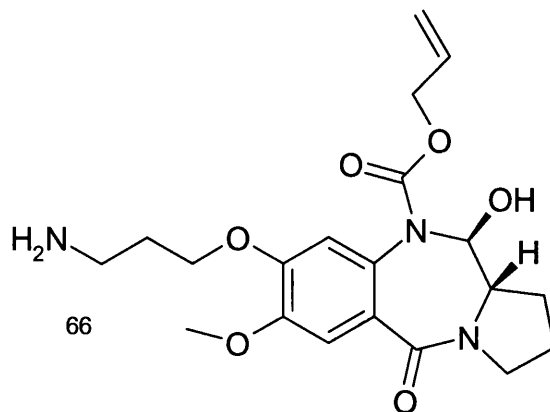
Synthesis of 4-(3-*tert*-Butoxycarbonylamino-propoxy)-5-methoxy-2-nitro-benzoic acid 61.

60   **61**
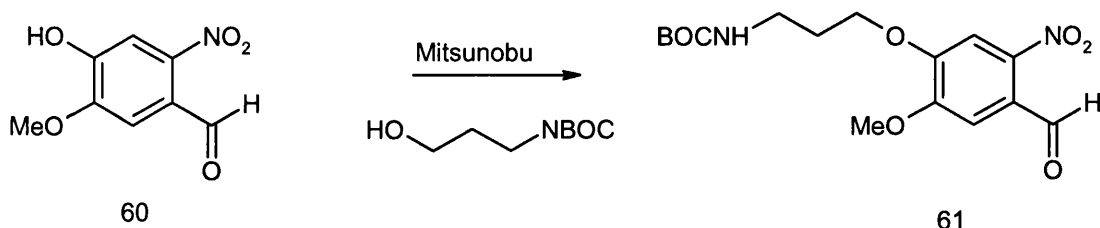
A solution of diethylazodicarboxylate (16 mL, 0.10 mol) in anhydrous THF (200 mL) was added dropwise to a solution of 4-hydroxy-5-methoxy-2-nitro-benzaldehyde **60** (Fukuyama *et al.,* 1990) (20 g, 0.10 mol), (3-hydroxy-propyl)-carbamic acid tert-butyl ester (17.35 mL, 0.10 mol), and triphenylphospine (26.63 g, 0.10 mol) in anhydrous THF (800 mL). The reaction mixture was allowed to stir overnight. Excess solvent was removed by rotoevaporation under reduced pressure. The residue was triturated with toluene (500 mL) and filtered. The filtrate was washed with 1N aqueous NaOH (300 mL), followed by brine (300 mL), and dried over MgSO₄. Excess toluene was removed by rotoevaporation under reduced pressure The residue was triturated with diethyl ether (400 mL). The resulting solid was collected by filtration and air dried to yield a pale yellow solid (20 g) of the desired phenol ether **61**, contaminated by small quantities of side-products. This batch was used directly in the next step without any further purification.

Synthesis of 4-(3-tert-Butoxycarbonylamino-propoxy)-5-methoxy-2-nitro-benzoic acid 62
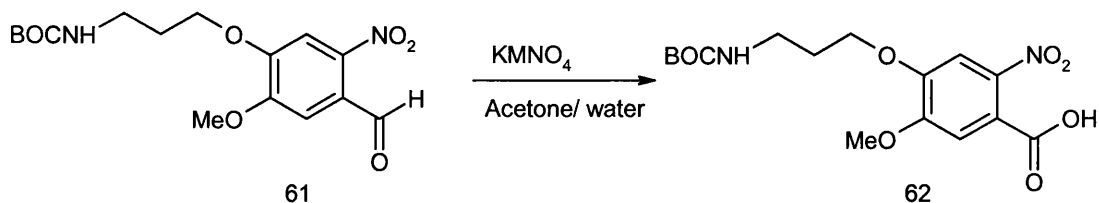
A hot solution (85°C) of KMnO₄ (20 g) in water (200 mL) was added portionwise to a mechanically stirred solution of **61** in acetone (200 mL). (**Caution!** vigorous reflux). The mixture was allowed to stir for one hour after which it was filtered through celite. Excess acetone was removed by rotary evaporation under reduced pressure. A solution of 1N aqueous sodium hydroxide was used to adjust the pH of the residue to 10. The solids were removed by filtration and the filtrate was washed with EtOAc (400 mL). The aqueous phase was acidified with 10% aqueous citric acid until the pH was adjusted to 2-3. The resulting suspension was extracted with EtOAc (400 mL), which was then washed with brine (100 mL) and dried over MgSO₄. Excess ethyl acetate was removed by rotary evaporation under reduced pressure to yield **62**, (12g, 32 % over two steps) as a dark oil which solidified in the freezer. A sample was recrystallised from EtOAc to yield a white solid, which provided analytical data. ^{1}H NMR (DMSO) δ 7.56 (s, 1H), 7.30 (s, 1H), 6.91 (t, J = 5.0 Hz, 1H), 4.11 (t, J = 6.0 Hz, 2H), 3.92 (s, 3H), 3.10 (q, J = 6.0 Hz, 2H), 1.86 (p, J = 6.3 Hz, 2H), 1.38 (s, 9H). ^{13}C NMR (DMSO) δ 166.0, 155.5, 151.7, 149.3, 141.2, 121.0, 111.2, 107.7, 77.5, 66.9, 56.3, 36.7, 28.8, 28.17. IR (CHCl₃) ν 3357, 1698, 1680, 1518, 1341, 1278, 1213, 1169, 1054, 812, 649 cm⁻¹; MS (ES⁻) m/z (relative intensity) 369.12 ([M - H]⁻, 100).

Synthesis of {3-[4-(2S-Hydroxymethyl-pyrrolidine-1-carbonyl)-2-methoxy-5-nitro-phenoxy]-propyl}-carbamic acid *tert*-butyl ester 63.
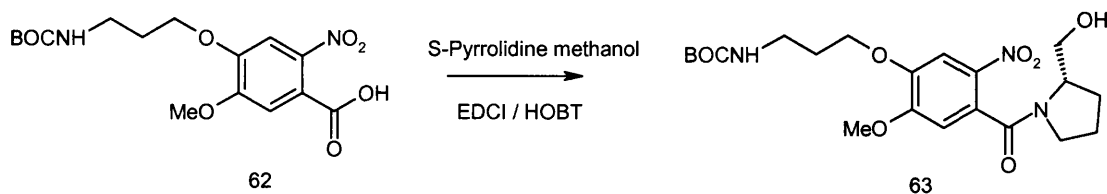
EDCI (4.16 g, 21.7 mmol) was added to a solution of acid **62** (5.36 g, 14.4 mmol) and HOBt (3.32 g, 21.7 mmol) in anhydrous DMF (80 mL). The resulting mixture was allowed to stir at 30°C for 3 hours. Pyrrolidine-methanol (1.57 mL, 15.9 mmol) was added slowly at room temperature and the reaction mixture allowed to stir overnight. It was then diluted with EtOAc (250 mL) and washed with 10% aqueous citric acid (100 mL), water (2 x 200 mL), saturated aqueous NaHCO$_3$ (200 mL), brine (200 mL) and dried over MgSO$_4$. Excess solvent was removed by rotary evaporation under reduced pressure to yield **63** (6.1 g, 93 %). TLC (EtOAc). ^{1}H NMR (CDCl$_3$) δ 7.68 (s, 1H), 6.81 (s, 1H), 5.24 (m, 1H), 4.38 (m, 2H), 4.18 (t, J = 5.7 Hz), 3.99 (s, 3H), 3.95-3.80 (m, 2H), 3.38 (m, 2H), 3.18 (t, J = 6.6 Hz, 2H), 2.19-1.74 (m, 6H), 1.45 (s, 9H). ^{13}C NMR (CDCl$_3$) δ 156.0, 154.7, 148.3, 137.1, 127.9, 109.0, 108.1, 79.1, 68.4, 66.1, 61.5, 56.6, 49.5, 38.4, 29.1, 28.4, 24.39 ; IR (golden gate) v 3427, 2968, 1684, 1616, 1574, 1520, 1434, 1327, 1272, 1223, 1164, 1059, 868, 647 cm^{-1}; MS (ES$^+$) *m/z* (relative intensity) 454.13 ([M + H]$^+$, 100); [α]$^{24}_D$ = -70° (c = 1, CHCl$_3$). Calculated for C$_{21}$H$_{31}$N$_3$O$_8$: C 55.6, H 6.89, N 9.27. Found : C 55.4, H 7.03, N 9.05

## Synthesis of [5-(3-*tert*-Butoxycarbonylamino-propoxy)-2-(2S-hydroxymethyl-pyrrolidine-1-carbonyl)-4-methoxy-phenyl]-carbamic acid allyl ester 64.
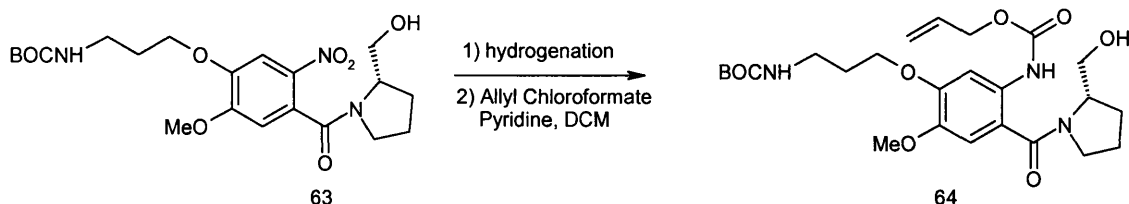
64 (6.1 g, 13.4 mmol) was hydrogenated with 10% Pd/C (600 mg) under 45 PSI in EtOAc (100 mL) using a Parr apparatus. When hydrogen uptake ceased, the reaction was stopped and TLC analysis revealed completion of the reaction. The Pd/C was

removed by filtration through celite. The filtrate was dried over MgSO₄ and excess solvent removed by rotary evaporation under reduced pressure to yield the crude amine. A solution of allyl chloroformate (1.28 mL, 12.1 mmol) in anhydrous DCM (60 mL) was added dropwise to a solution of the crude amine and anhydrous pyridine (2.34 mL, 28.9 mmol) in anhydrous DCM (200 mL) at 0°C (Acetone/ ice bath). The reaction mixture was allowed to stir at room temperature overnight. The reaction mixture was washed with 10% aqueous citric acid (100 mL), water (200 mL), saturated NaHCO₃, brine, and dried over MgSO₄. Excess solvent was removed by rotary evaporation under reduced pressure to yield **64** (5.85 g, 86 %) slightly contaminated by the bis alloc protected compound. TLC (EtOAc). ^{1}H NMR (CDCl₃) δ 8.76 (bs, 1H), 7.77 (s, 1H), 7.26 (s, 1H), 5.98 (m, 1H), 5.47 (m, 1H), 5.38-5.24 (dd, 2H), 4.63 (d, 2H), 4.45-4.20 (m, 2H), 4.15 (m, 2H), 3.85 (m, 4H), 3.80-3.45 (m, 3H), 3.35 (m, 2H), 2.18-1.60 (m, 6H), 1.46 (s, 9H); ^{13}C NMR (CDCl₃) δ 170.8, 156.0, 153.6, 150.2, 144.0, 132.4, 131.8, 118.1, 111.0, 105.4, 78.8, 68.6, 67.9, 65.7, 61.0, 56.3, 38.7, 31.5, 29.0, 28.4, 28.3, 22.62. IR ν 3398, 2973, 1711, 1597, 1523, 1457, 1407, 1328, 1228, 1204, 1172, 1117, 1052, 917, 730 cm^{-1}; $[\alpha]^{25}_D$ = -0.48° (c = 0.3, CHCl₃); MS (ES⁺) m/z (relative intensity) 508.20 ([M + H]$^+$·, 100.

Synthesis of 8-(3-*tert*-Butoxycarbonylamino-propoxy)-11S-hydroxy-7-methoxy-5-oxo 2,3,11,11aS-tetrahydro-1*H*,5*H*-benzo[e]pyrrolo[1,2-a][1,4]diazepine-10 carboxylic acid allyl ester 65.
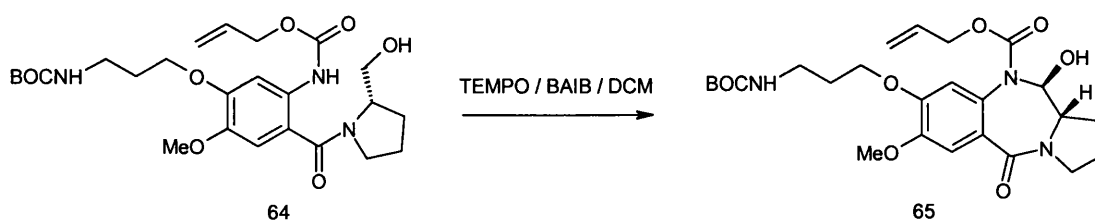
TEMPO (182 mg, 1.15 mmol) was added to a solution of **64** (5.85 g, 11.5 mmol) and diacetoxy-iodobenzene (4.1 g, 12.7 mmol) in DCM (100 mL). The reaction mixture was allowed to stir overnight. TLC (EtOAc) revealed completion of the reaction and the solvent was consecutively washed with saturated aqueous sodium metabisulphite, saturated aqueous NaHCO₃, brine and dried over MgSO₄. Excess ethyl acetate was removed by rotary evaporation under reduced pressure. The residue was purified further

by column chromatography (gradient from 60/40 EtOAc/ Hexane to 100% EtOAc). The pure fractions were combined and the solvent was removed by rotary evaporation under reduced pressure to yield the ring-closed product **65** as a white foam. (4.19 g, 72 %). ^{1}H NMR (CDCl₃) δ 7.24 (s, 1H), 6.67 (s, 1H), 5.80 (m, 1H), 5.64 (m, 1H), 5.47 (m, 1H), 5.13 (m, 2H), 4.68 (m, 1H), 4.45 (m, 1H), 4.15-3.98 (m, 2H), 3.92 (s, 3H), 3.78-3.67 (m, 1H), 3.60-3.42 (m, 2H), 3.34 (m, 2H), 2.18-1.95 (m, 6H); ^{13}C NMR (CDCl₃) δ 166.9, 156.1, 155.9, 149.7, 148.5, 131.8, 128.3, 126.0, 117.9, 113.6, 110.4, 85.9, 79.0, 68.2, 66.7, 60.4, 59.9, 56.0, 46.3, 38.8, 29.0, 28.6, 28.4, 23.0; MS (ES$^+$) *m/z* (relative intensity), 506.4 ([*M* + H]$^+$, 100).

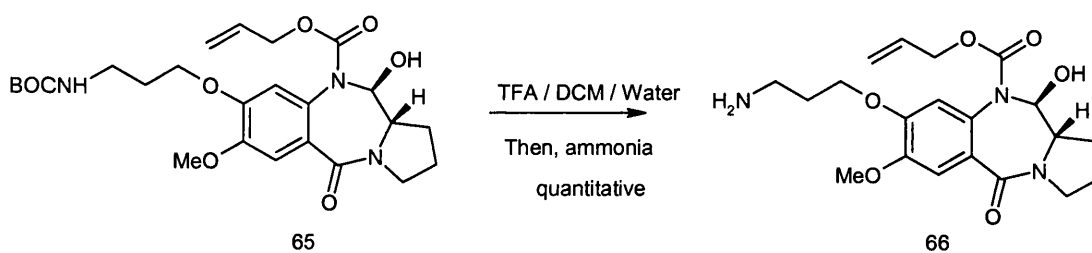**Synthesis of 8-(3-Amino-propoxy)-11S-hydroxy-7-methoxy-5-oxo-2,3,11,11aS-tetrahydro-1*H*,5*H*-benzo[e]pyrrolo[1,2-a][1,4]diazepine-10-carboxylic acid allyl ester 66.**

65 (1.1 g, 2.17 mmol) was allowed to stir 20 min in a mixture of TFA (4 mL), DCM (6 mL), and water (0.5 mL) at room temperature. TLC (CHCl₃) revealed completion of the reaction and the mixture was diluted with ice and concentrated aqueous ammonium hydroxide until the pH reached 10 or more. The diluted reaction mixture was then extracted with CHCl₃ (2 x 100 mL), which was then washed with brine and dried over MgSO₄. Excess CHCl₃ was removed by rotary evaporation. The residue was further dried under hard vacuum to yield a colourless powder which was proved pure by TLC (90:10:1 v/v/v CHCl₃/MeOH/NH₄OH). (880 mg, 100%). This fairly unstable **3C-amino PBD capping unit (compound 66)** was used directly in the next coupling step without further purification. The product was proved optically pure by chiral HPLC.

11.2.5 4-C Alloc THP C2 exo-unsaturated acid PBD capping unit and tripyrrole conjugate AT-355.

Synthesis of 4-{4-[2-(tert-Butyl-dimethyl-silanyloxymethyl)-4-hydroxy-pyrrolidine-1-carbonyl]-2-methoxy-5-nitro-phenoxy}-butyric acid methyl ester 69
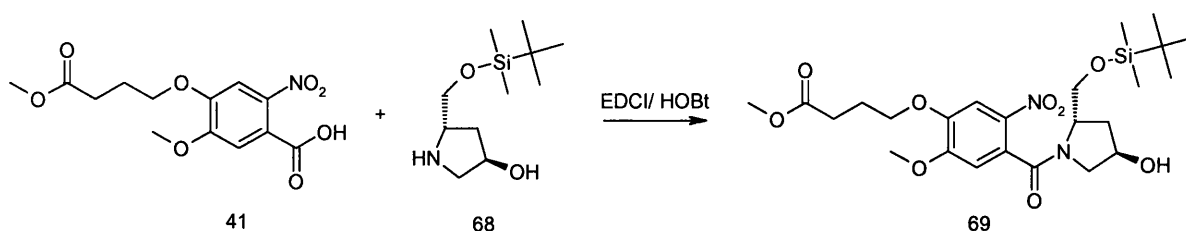
EDCI (1.83 g, 9.55 mmol) was added to a stirred solution of acid **41** (2 g, 6.39 mmol) and HOBt (1.47 g, 9.60 mmol) in dry DCM (100 mL). The mixture was allowed to stir for 5 hours. A solution of PBD C-ring **68** (1.63 g, 7.03 mmol) (prepared according to Gregson *et al.*, 2000) in dry DCM (50 mL) was then added. The resulting mixture allowed to stir overnight. The mixture was diluted with DCM (200 mL), washed with 10 % w/w aqueous citric acid (100 mL), water (100 mL), saturated aqueous NaHCO$_3$ (100 mL), brine (50 mL), and dried over MgSO$_4$. Excess solvent was removed by rotary evaporation under reduced pressure. The residue was subjected to flash chromatography (ethyl acetate / hexane). The pure fractions were combined to afford the desired coupled product **69** (1.2 g, 35 %).

^{1}H NMR (CDCl$_3$) Mixture of rotamers in a 100/20/5 ratio. Description of the main rotamer only δ 7.67 (s, 1H), 6.76 (s, 1H), 4.55 (m, 1H), 4.41 (m, 1H), 4.17-4.11 (m, 3H), 3.92 (s, 3H), 3.78 (d, 1H, J = 5.14 Hz), 3.71 (s, 3H), 3.38-3.34 (dd, 1H, J = 4.47 Hz, J = 11.2 Hz), 3.09 (d, 1H, J = 11.3 Hz), 2.56 (t, 2H, J = 7.14 Hz), 2.36-2.30 (m, 1H), 2.23-2.16 (p, 2H, J = 6.27 Hz), 2.10 (t, 1H, J = 10.3 Hz), 2.01 (d, 1H, J = 6.23 Hz), 0.91 (s, 9H), 0.10 (d, 6H, J = 3.88 Hz); ^{13}C NMR (CDCl$_3$) δ 173.2, 166.6, 154.6, 154.5, 148.3, 137.5, 128.2, 109.4, 108.5, 70.4, 64.9, 68.4, 62.7, 57.2, 56.6, 56.5, 51.7, 37.7, 36.5, 30.3, 25.9, 25.8, 24.2, 18.2 ; MS (ES$^+$) m/z 527.4 ([M+H]$^{+\bullet}$, 100); IR (Golden gate) v 2950, 1736, 1614, 1578, 1523, 1434, 1335, 1277, 1221, 1051, 836, 781 cm^{-1}; $[\alpha]^D_{24}$ -120° (c = 0.35, CHCl$_3$).
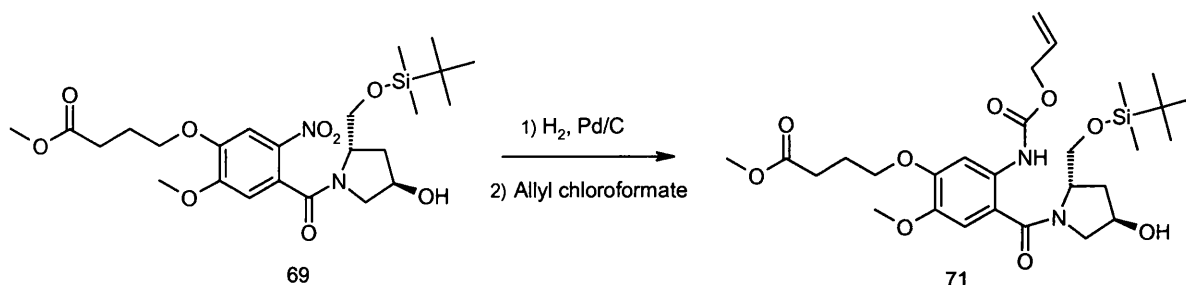
Synthesis of 4-{5-Allyloxycarbonylamino-4-[2-(tert-butyl-dimethyl-silanyloxymethyl)-4-hydroxy-pyrrolidine-1-carbonyl]-2-methoxy-phenoxy}-butyric acid methyl ester 71

Pd/C 10% (120 mg) was added to a solution **69** (1.2 g, 2.28 mmol) in EtOAc:EtOH (1:3 v/v, 100 mL). The suspension was hydrogenated in a Parr apparatus under 45 PSI. The reaction was deemed complete by TLC after 2 hours. Filtration and evaporation of the solvent afforded the amine **70** as a yellow oil (1g, 2.02 mmol) which was redissolved in anhydrous DCM (100 mL). Pyridine (0.326 mL, 4.03 mmol) was added, followed by dropwise addition of a solution of allyl chloroformate (0.200 mL, 1.88 mmol) in anhydrous DCM (20 mL) at 0°C. The reaction mixture was allowed to warm up to room temperature and stir overnight. The mixture was diluted with DCM (100 mL), washed with 10 % w/w aqueous citric acid (100 mL), water (100 mL), saturated aqueous NaHCO$_3$ (100 mL), brine (50 mL) and dried over MgSO$_4$. Excess solvent was removed by rotary evaporation under reduced pressure. The residue **71** was found sufficiently pure to be carried out through the next step without further purification (1.1 g, 94 %).

^{1}H NMR (CDCl$_3$) δ 8.86 (bs, 1H), 7.72 (s, 1H), 6.78 (s, 1H), 5.98-5.89 (m, 1H), 5.36-5.21 (m, 2H), 4.65-4.56 (m, 3H), 4.41 (s, 1H), 4.10 (bs + t, 3H, J = 6.15 Hz), 3.78 (s, 3H), 3.69 (s, 3H), 3.65-3.44 (m, 3H), 2.54 (t, 2H, J = 7.39 Hz), 2.32-2.26 (m, 1H), 2.17 (p, 2H, J = 7.09 Hz), 2.06-2.00 (m, 2H), 0.89 (s, 9H), 0.04 (d, 6H, J = 3.85 Hz); ^{13}C NMR (CDCl$_3$) δ 173.4, 169.4, 153.8, 150.4, 144.1, 132.5, 132.2, 118.0, 116.14, 111.8, 105.9, 70.55, 67.77, 65.74, 62.32, 57.17, 56.47, 51.63, 35.67, 30.56, 29.69, 25.84, 25.52, 24.41, 18.14; MS (ES$^+$) m/z 581.4 ([M+H]$^{+*}$, 100); IR (Golden gate) v 2951, 1731, 1598, 1524, 1467, 1408, 1324, 1258, 1203, 1173, 1121, 1001, 836, 777 cm^{-1}; $[\alpha]^D_{24}$ = -62° (c = 0.29, CHCl$_3$).
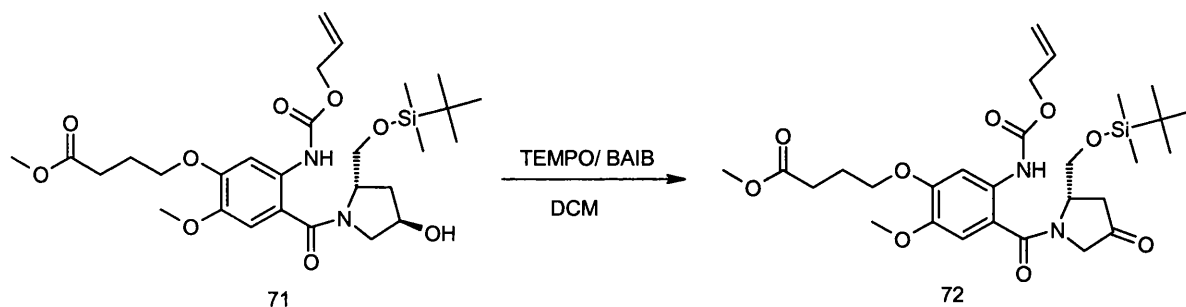
Synthesis of 4-{5-Allyloxycarbonylamino-4-[2-(tert-butyl-dimethyl-silanyloxymethyl)-4-oxo-pyrrolidine-1-carbonyl]-2-methoxy-phenoxy}-butyric acid methyl ester 72

TEMPO (28 mg, 0.18 mmol) was added to a solution of secondary alcohol **71** (1.05 g, 1.81 mmol) and BAIB (874 mg, 2.71 mmol) in DCM (50 mL). The solution was allowed to stir for 76 hours, at which point the reaction was deemed complete by TLC. The mixture was diluted with DCM (200 mL), washed with saturated aqueous $NaHSO_3$ (100 mL), water (100 mL), saturated aqueous $NaHCO_3$ (100 mL), brine (50 mL) and dried over $MgSO_4$. Excess solvent was removed by rotary evaporation under reduced pressure. The residue was subjected to flash chromatography (gradient elution from 10:90 to 40:60 v/v ethyl acetate/hexane). The pure fractions were combined to afford the desired coupled ketone **72** (400 mg, 38 %).

^1H NMR (CDCl$_3$) δ 8.32 (bs, 1H), 7.78 (s, 1H), 6.74 (s, 1H), 5.98-5.91 (m, 1H), 5.36-5.22 (m, 2H), 4.81 (bs, 1H), 4.61 (d, 2H, J = 5.51 Hz), 4.13-4.08 (m, 2H), 4.01 (m, 2H), 3.93-3.84 (m, 1H), 3.79 (s, 3H), 3.68 (s, 3H), 3.68-3.55 (m, 1H), 2.75-2.68 (dd, 1H, J = 9.57 Hz, J = 18.1 Hz), 2.59-2.45 (m, 3H), 2.17 (p, 2H, J = 6.93 Hz), 0.86 (s, 9H), 0.03 (d, 6H, J = 3.22 Hz); ^{13}C NMR (CDCl$_3$) δ 208.9, 173.4, 169.1, 153.5, 150.8, 144.2, 132.4, 118.2, 111.1, 106.0, 67.8, 65.8, 60.4, 56.5, 51.6, 30.5, 25.7, 24.4, 21.0, 18.0, 14.2 ; MS (ES$^+$) m/z 579.3 ([M+H]$^{+*}$, 100); IR (Golden gate) v 2953, 1764, 1730, 1601, 1524, 1468, 1408, 1259, 1202, 1167, 1108, 1014, 871, 837, 778 cm^{-1}; $[\alpha]^D_{24}$ = 0° (c = 0.2, CHCl$_3$).
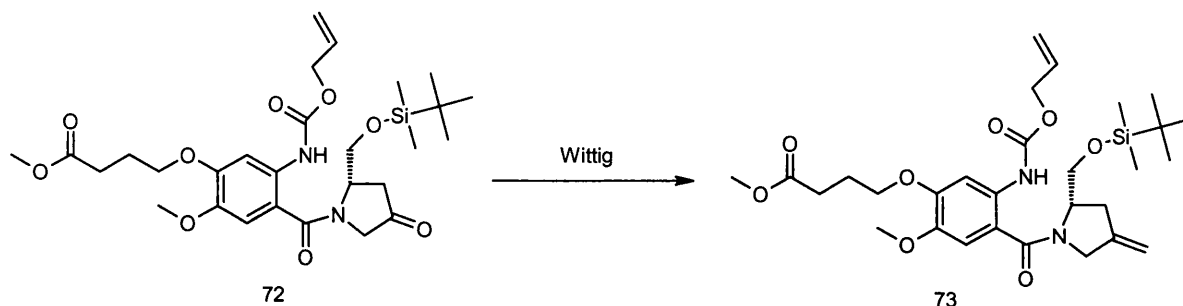
Synthesis of 4-{5-Allyloxycarbonylamino-4-[2-(tert-butyl-dimethyl-silanyloxymethyl)-4-methylene-pyrrolidine-1-carbonyl]-2-methoxy-phenoxy}-butyric acid methyl ester 73.

A 1 M solution of potassium tert-butoxide in THF (3.46 mL, 3.46 mmol) was added dropwise to a suspension of methyltriphenyl phosphonium bromide (1.23 g, 3.44 mmol) in anhydrous THF (3 mL) at 0°C under a nitrogen atmosphere. The mixture was allowed to stir for 2 h at 0°C. A solution of ketone 72 (350 mg, 0.605 mmol) in anhydrous THF (3 mL) was added dropwise and the reaction mixture was allowed to warm up to room temperature. After being stirred for 30 min, the reaction mixture was diluted with ethyl acetate (100 mL), washed with water (2 x 100 mL), brine (50 mL) and dried over MgSO4. Excess solvent was removed by rotary evaporation under reduced pressure. The residue was subjected to flash chromatography (gradient elution from 10:90 to 45:55 v/v ethyl acetate/hexane). The pure fractions were combined to afford the desired coupled olefin 73 (205 mg, 58 %).

^{1}H NMR (CDCl$_3$) δ 9.14-8.44 (bs, 1H), 7.82 (s, 1H), 6.81 (s, 1H), 6.00-5.90 (m, 1H), 5.37-5.22 (m, 2H), 4.98 (bs, 1H), 4.91 (bs, 1H), 4.65-4.58 (m, 3H), 4.20-4.09 (m, 4H), 3.81 (s, 3H), 3.69 (s, 3H), 3.66 (bs, 1H), 2.69 (m, 2H), 2.54 (t, 2H, J = 7.39 Hz), 2.17 (p, 2H, J = 7.20 Hz), 0.88 (s, 9H), 0.03 (bs, 6H); ^{13}C NMR (CDCl$_3$) δ 173.4, 171.1, 168.7, 153.5, 150.4, 144.0, 132.5, 118.0, 111.5, 107.1, 105.6, 67.8, 65.7, 63.7, 60.4, 56.6, 51.6, 30.6, 25.8, 24.4, 21.0, 18.1, 14.2; MS (ES$^+$) m/z 577.4 ([M+H]$^{+\bullet}$, 100); IR (Golden gate) v 2950, 2855, 1731, 1598, 1520, 1404, 1224, 1199, 1172, 1114, 1006, 836, 776 cm^{-1}; [α]$^D_{24}$ = -36.1° (c = 1.84, CHCl$_3$).

Synthesis of 11-Hydroxy-7-methoxy-8-(3-methoxycarbonyl-propoxy)-2-methylene-5-oxo-2,3,11,11a-tetrahydro-1H,5H-benzo[e]pyrrolo[1,2-a][1,4]diazepine-10-carboxylic acid allyl ester 76

74   1) TBAF
                                    ────────────→
   2) TEMPO/ BAIB   76
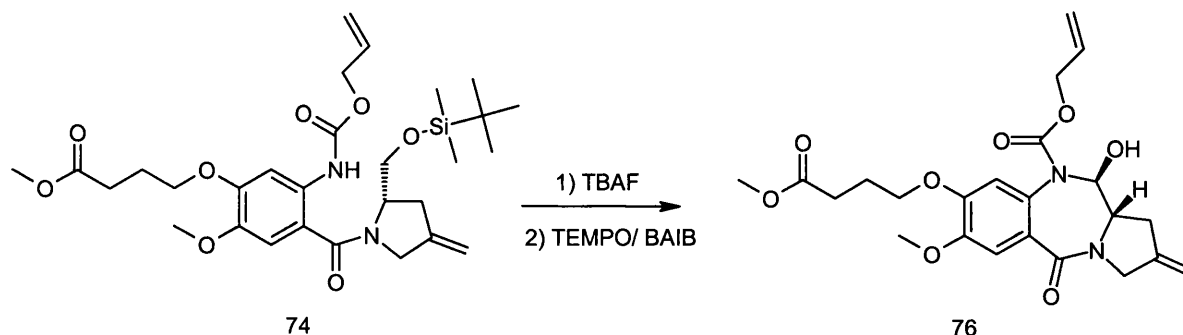
A 1N solution of TBAF in THF (2 mL, 2.0 mmol) at 0°C was added to TBDMS protected olefin **74**. The reaction mixture was allowed to stir at 0°C for 1h at which point the reaction was deemed complete by TLC. The reaction mixture was diluted with ethyl acetate (50 mL), washed with water (2 x 50 mL), brine (30 mL) and dried over MgSO$_4$. Excess solvent was removed by rotary evaporation under reduced pressure to afford the crude primary alcohol **75**, which was immediately redissolved in DCM (20 mL). BAIB (130 mg, 0.404 mmol) and TEMPO (6 mg, 0.038 mmol) were added and the reaction mixture allowed to stir overnight. Further amounts of BAIB (130 mg, 0.404 mmol) and TEMPO (3 mg, 0.019 mmol) were added and the mixture allowed to stir for a further 24 h at which point the reaction was deemed complete by TLC. The mixture was diluted with DCM (100 mL), washed with saturated aqueous NaHSO$_3$ (30 mL), water (100 mL), saturated aqueous NaHCO$_3$ (30 mL), brine (30 mL) and dried over MgSO$_4$. Excess solvent was removed by rotary evaporation under reduced pressure. The residue was subjected to flash chromatography (gradient elution from 50:50 to 80:20 v/v ethyl acetate/hexane). The pure fractions were combined and subjected to rotoevaporation under reduced pressure to afford the desired coupled cyclised compound **76** (120 mg, 74 %).

^{1}H NMR (CDCl$_3$) δ 7.21 (s, 1H), 6.68 (s, 1H), 5.80 (bs, 1H), 5.66-5.46 (d, 1H, J = 6.11 Hz), 5.29-5.11 (m, 4H), 4.65 (dd, 1H, J = 5.55 Hz, J = 13.3 Hz), 4.44 (d, 1H, J = 10.4 Hz), 4.29 (d, 1H, J = 16.0 Hz), 4.13 (d, 1H, J = 15.9 Hz), 4.08-3.99 (m, 2H), 3.89 (s, 3H), 3.68 (s, 3H), 3.62 (t, 1H, J = 8.62 Hz), 2.93-2.87 (m, 1H), 2.69 (d, 1H, J = 16.1 Hz), 2.53 (t, 2H, J = 7.22 Hz), 2.14 (p, 2H, J = 6.75 Hz); ^{13}C NMR (CDCl$_3$) δ 173.4, 166.7, 150.1, 148.8, 141.8, 131.8, 128.4, 125.3, 118.2, 113.9, 110.7, 109.7, 85.9, 68.0,

66.8, 59.6, 56.1, 51.6, 50.7, 35.0, 30.3, 24.3; MS (ES⁺) *m/z* 461.2 ([M+H]⁺˙, 100); IR (Golden gate) v 2948, 2357, 1710, 1623, 1603, 1514, 1467, 1437, 1407, 1300, 1279, 1208, 1123, 1046, 996, 768, 668 cm⁻¹; $[\alpha]^D_{27}$ = +135.2° (c = 1.05, CHCl₃).

Synthesis of 8-(3-Carboxy-propoxy)-7-methoxy-2-methylene-5-oxo-11-(tetrahydro-pyran-2-yloxy)-2,3,11,11a-tetrahydro-1H,5H-benzo[e]pyrrolo[1,2-a][1,4]diazepine-10-carboxylic acid allyl ester 77

1) DHP/ PTSA in EtOAc

2) NaOH in Water/ MeOH

76

77
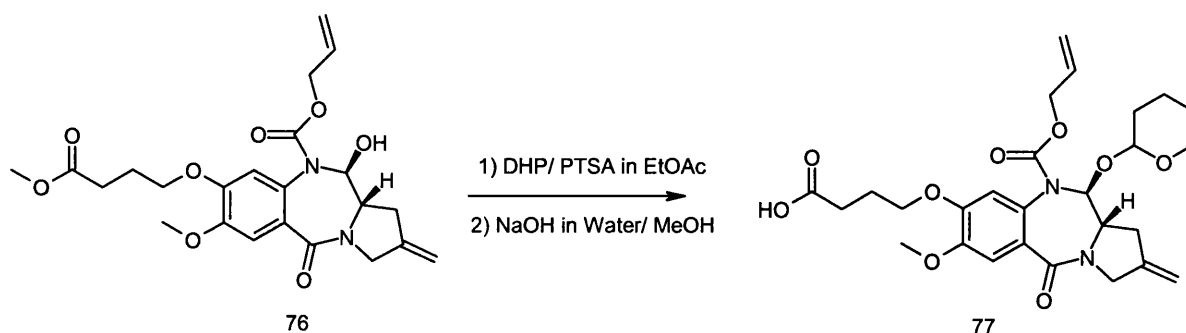
A few small crystals of PTSA were added to a stirred solution of DHP (0.25 mL, 2.74 mmol) in ethyl acetate (3 mL) at 0°C and the resulting reaction mixture allowed to stir for 10 min. A solution of the secondary alcohol **76** (120 mg, 0.261 mmol) in ethyl acetate (2 mL) was added and the resulting reaction mixture allowed to warm up to room temperature. After 1 h, the reaction was deemed complete by TLC analysis. The reaction mixture was washed with saturated aqueous NaHCO₃ (3 mL), brine (3 mL) and dried (MgSO₄). Filtration and removal of the solvent by rotary evaporation under reduced pressure yielded the crude protected ester, which was immediately redissolved in a mixture of THF (2 mL) and MeOH (1 mL). A solution of NaOH (50 mg, 1.25 mmol) in water (1 mL) was added and the resulting reaction mixture was allowed to stir at 60°C for 5 min. Water (2 mL) was added and excess organic solvents were removed by rotary evaporation under reduced pressure. The resulting aqueous solution was washed with ethyl acetate (5 mL) and then acidified with 10 % w/w aqueous citric acid (10 mL) and extracted with ethyl acetate (10 mL). The extract was washed with brine (10 mL) and dried over MgSO₄. Filtration and evaporation of the solvent by rotary evaporation under reduced pressure afforded the pure C2 exo unsaturated 4C PBD Alloc, THP acid capping unit **77** (120 mg, 87 %). Mixture of 2 epimers.

¹H NMR (CDCl₃) δ 7.23 (s, 1H), 7.20 (s, 1H), 6.89 (s, 1H), 6.59 (s, 1H), 5.87-5.68 (m, 4H), 5.23-4.96 (m, 10H), 4.67-4.57 (m, 2H), 4.39-4.27 (m, 4H), 4.14-4.03 (m, 8H),

4.00-3.89 (m, 8H), 3.67-3.56 (m, 4H), 2.95-2.75 (m, 4H), 2.62-2.50 (m, 4H), 2.18-2.11

(m, 4H), 1.77-1.72 (m, 4H), 1.55-1.47 (m, 8H); ^{13}C NMR (CDCl$_3$) δ 177.5, 177.1,

176.0, 171.2, 167.2, 167.1, 149.3, 149.1, 142.0, 141.9, 132.2, 132.0, 126.1, 117.1,

115.1, 114.6, 110.8, 110.5, 109.6, 100.3, 88.7, 67.9, 67.6, 66.6, 64.3, 63.8, 60.4, 59.9,

56.1, 50.8, 50.7, 35.4, 35.0, 31.1, 31.0, 30.2, 30.1, 25.2, 25.1, 24.1, 24.0, 21.0, 20.6,

20.2, 20.1; MS (ES$^+$) m/z 531.3 ([M+H]$^{+\bullet}$, 100); IR (Golden gate) v 2944, 1715, 1646,

1602, 1435, 1407, 1212, 1022 cm^{-1}; $[\alpha]^D_{28}$ + 66° (c = 1.1, CHCl$_3$).

Synthesis of AT-355, 80
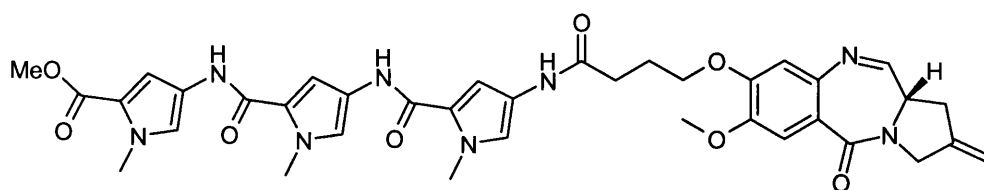
AT-355, 80

BocPyPyPyCO2Me **78** (125 mg, 0.249 mmol) was coupled to C2 exo unsaturated 4C-

Alloc-THP PBD acid **77** (120 mg, 0.226 mmol) according to method A. The crude

product was subjected to flash chromatography (gradient elution from 1:99 to 3:97

methanol:chloroform). Evaporation of the pure fractions yielded the desired coupled

product (114 mg, 0.125 mmol, 55 %), which was immediately deprotected following

method E. The crude product was subjected to flash chromatography (gradient elution

from 4:96 to 5:95 methanol:chloroform). Evaporation of the pure fractions yielded the

desired biologically active compound AT355, **80** (74 mg, 82 %).

^{1}H NMR (DMSO) δ 9.91 (s, 1H), 9.89 (s, 1H), 9.87 (s, 1H), 7.77 (d, 1H, J = 4.44 Hz),

7.46 (d, 1H, J = 1.89 Hz), 7.34 (s, 1H), 7.23 (d, 1H, J = 1.78 Hz), 7.16 (d, 1H, J = 1.78

Hz), 7.06 (d, 1H, J = 1.76 Hz), 6.91 (d, 1H, J = 1.94 Hz), 6.88 (d, 1H, J = 1.80 Hz),

6.84 (s, 1H), 5.14 (m, 2H), 4.18-3.91 (m, 4H), 3.90-3.80 (m, 13H), 3.74 (s, 3H), 3.04

(m, 2H), 2.44 (t, 2H, J = 7.32 Hz), 2.05 (p, 2H, J = 7.06 Hz); MS (ES$^+$) m/z 725.1

([M+H]$^{+\bullet}$, 100); HRMS (TOF MS ES$^+$) calcd for C$_{37}$H$_{40}$N$_8$O$_8$ (M+H): 725.3042. Found:

725.3002; Purity by analytical HPLC : Luna : 93.4 %; Gemini : 93.7 %.

11.3 Polyamide building blocks

11.3.1 Synthesis of the Pyrrole amino acid building block 86 and 87 (Baird and Dervan, 1996).

Synthesis of 2-(trichloroacetyl)-1-methylpyrrole 82
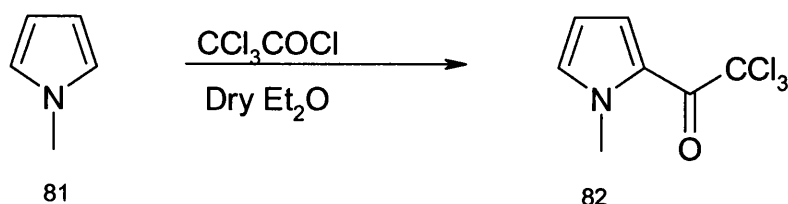
A solution of N-Methylpyrrole (90 g, 98.7 mL, 1.10 mol) in dry ether (300 mL) was added dropwise over 3 hours to a mechanicaly stirred solution of trichloroacetylchloride (200 g, 122.8 mL, 1.10 mol) in dry ether (300 mL) in a 2L flask. A substantial volume of HCl gas was produced during the course of the reaction, and was flushed out by a flow of nitrogen.

The reaction mixture was allowed to stir for an additional 3 hours then quenched by the dropwise addition of aqueous potassium carbonate. (80 g in 300 mL water). The layers were separated and the ether layer concentrated *in vacuo* to provide the 2-(trichloroacetyl)-1-methyl pyrrole 82 as a black crystalline solid. (236 g, 95%). The product was used in the next step without further purification.

Synthesis of 4-nitro-2-(trichloroacetyl)-1-methylpyrrole 83
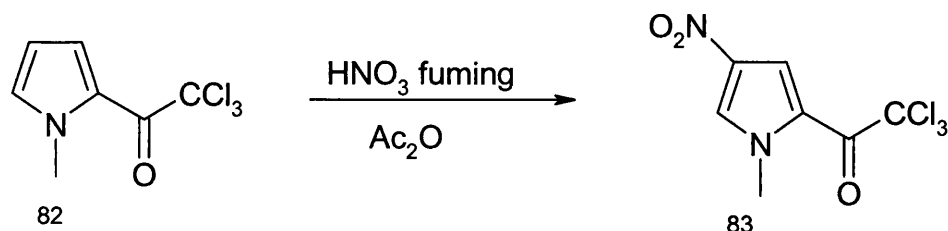
Fuming nitric acid (44 mL) was added dropwise over 1h to a mechanically stirred, cooled (-50°C, Chloroform/liquid Nitrogen) solution of 2-(trichloroacetyl)-1-methyl pyrrole (118 g, 0.51 mol) 82 in acetic anhydride (approximately 500 mL). (The temperature was kept close to –50°C during the course of the addition). The reaction mixture was then allowed to warm to 20°C at which point the reaction vessel was

placed in a water bath. The reaction mixture was allowed to stir for 4 hours at 20°C. (**Caution!** risk of sudden exotherm if the temperature rises above 25°C). The reaction mixture was then cooled to –30°C and diluted with isopropanol (600 mL). The mixture was allowed to stir at –20°C for 30 minutes and then allowed to stand for 15 min. The precipitate was collected by vacuum filtration to provide 2-(trichloroacetyl)-1-methyl-4-nitropyrrole **83** as a white solid (87 g, 63%). TLC system : 80/20 hexane/EtOAc.

^{1}H NMR (CDCl$_3$) 7.95 (s, 1H, arom), 7.77 (s, 1H, arom), 4.06 (s, 3H, Me).

Synthesis of Methyl-4-Nitropyrrole-2-carboxylate 84
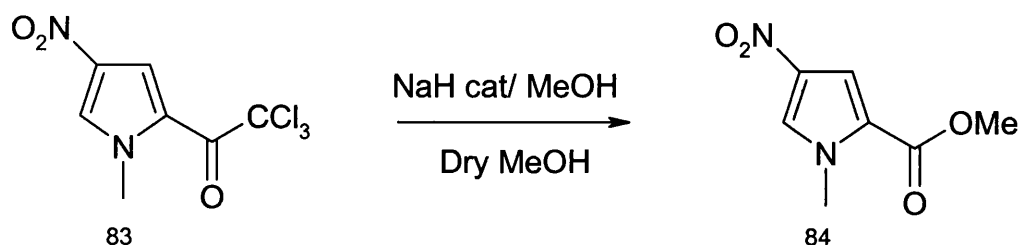
A solution of NaH (2.2 g, 60% dispersion in mineral oil) in dry MeOH (100 mL) was added dropwise to a stirred, cooled (5°C) solution of the trichloroacetate **83** (174 g, 0.64 mol) in dry methanol (500 mL) in a 2 L round-bottomed-flask. The suspension was allowed to stir at room temperature overnight and was then quenched by addition of concentrated sulphuric acid (5.4 mL). The reaction mixture was then heated to reflux and allowed to cool to room temperature.The crystalline ester **84** was then collected by filtration and dried under vacuum. (107 g, 91%).

TLC system: 70/30 hexane/EtOAc.

Synthesis of 4-amino-1-methylpyrrole-2-carboxylate hydrochloride 85

240
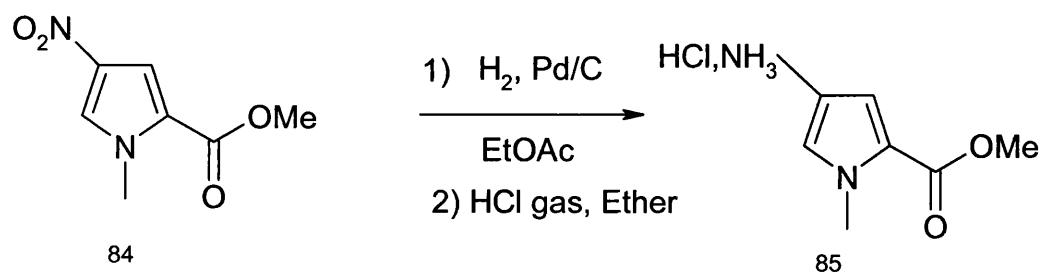
A solution of nitropyrrole ester **84** (20 g, 0.11 mol) in ethyl acetate (200 mL) was hydrogenated in a Parr apparatus at 15 psi in the presence of 10% Pd/C (1 g). When the hydrogen uptake had ceased, the Pd/C was allowed to settle for 15 min. The supernatant was transferred to a larger flask, taking care to keep the Pd/C in the original hydrogenation flask. The reaction was repeated five times until all the nitro ester **84** (106 g, 0.57 mol) was converted to the amine. The amine solutions were combined and any solids were removed by filtration through celite. The volume was reduced to under 500 mL by rotary evaporation under reduced pressure. The remaining liquor was diluted with diethylether (2 L), and HCl gas was bubbled through the solution accompanied by mechanical stirring. Acidification was complete when the colour of the reaction mixture changed from red to grey. The resulting salt was collected by filtration and dried. Total yield of **85**: 109 g (97%).

^{1}H NMR (DMSO) : 10.18 (bs, 3H, NH$_3^+$), 7.27 (s, 1H, aro), 6.84 (s, 1H, aro), 3.88 (s, 3H, Me), 3.78 (s, 3H, Me).

Synthesis of 4-[(*tert*-Butoxycarbonyl)amino]-1-methylpyrrole-2-carboxylic Acid 86.
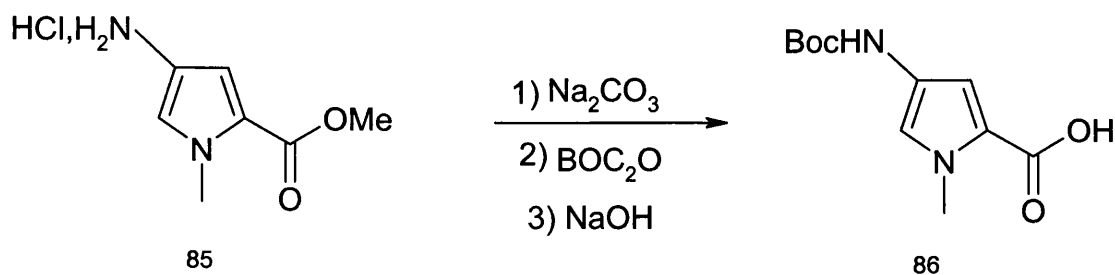

A solution of di-*tert*-butyl dicarbonate (128 g, 0.59 mol) in 160 mL of dioxane was added over a period of 30 min to a mechanically stirred suspension of **85** (109 g, 0.57 mol) in a 10% sodium carbonate aqueous solution (320 mL). The resulting mixture was allowed to stir for 4 hours at which point the reaction was deemed complete by TLC (EtOAc). The solids were collected by filtration and washed with water to yield the crude Boc-pyrrole ester. The crude Boc-pyrrole ester was partially dissolved in MeOH (225 mL) and 2M aqueous NaOH (285 mL, 1 eq, 0.57 mol) was added. The slurry was heated at reflux until complete hydrolysis of the ester. (TLC 50/50 hexane/ethyl acetate). Excess methanol was removed by rotary evaporation under reduced pressure. The remaining aqueous solution was washed with ether (4 X 300 mL). The aqueous layer was acidified to pH 2 or 3 and extracted with ethyl acetate (4 X 500 mL). The

combined ethyl acetate extracts were dried (magnesium sulphate) and concentrated *in vacuo* to provide a tan solid. The solid was suspended in dichloromethane (300 mL) and petroleum ether (1 L). The resulting slurry was concentrated by rotary evaporation under reduced pressure. Again, 300 mL of DCM and 1 L petroleum ether were sequentially added. The slurry was rotoevaporated to dryness to provide **86** as a fluffy, fine, off white powder. 125 g (91%).

^{1}H NMR (DMSO) δ 12.05 (very broad s, 1H, COOH), 9.03 (s, 1H, NHBoc), 7.04 (s, 1H, aro), 6.59 (s, 1H, aro), 3.78 (s, 3H, NMe), 1.47 (s, 9H, Boc).

Synthesis of 1,2,3-Benzotriazol-1-yl 4-[(*tert*-Butoxycarbonyl)amino]-1-methylpyrrole-2-carboxylic acid 87
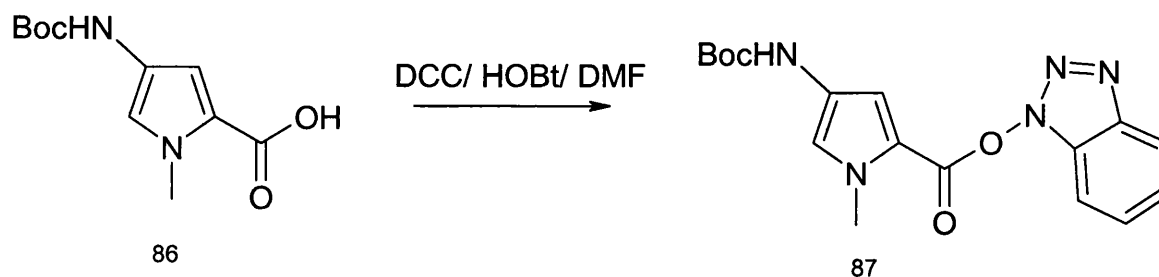
DCC (10.97 g, 53.2 mmol, 1.27 eq) was added to a solution of Boc pyrrole acid **86** (10 g, 41.6 mmol) and HOBt (5.61 g, 41.5 mmol) in DMF (160 mL). The reaction mixture was allowed to stir for 24 h. The solids were removed by filtration and the filtrate was added dropwise to a vigorously stirred mixture of ice/water (1.6 L). The precipitate was allowed to settle for 15 min at 0°C and then collected by filtration. The wet cake was dissolved in DCM (160 mL) and the resulting organic layer was added slowly to a stirred solution of cold petroleum ether. The mixture was allowed to stand at –20°C for 30 min. The solids were collected by vacuum filtration and dried *in vacuo* to yield **87** as a white powder (13.16 g, 89%).

^{1}H NMR (DMSO) δ 9.42 (s, 1H), 8.17 (d, 1H, *J* = 8.32 Hz), 7.83 (d, 1H, *J* = 8.33 Hz), 7.67 (t, 1H, *J* = 7.14 Hz), 7.51 (m, 2H), 7.21 (s, 1H), 3.86 (s, 3H), 1.49 (s, 9H). Identical to spectrum published by Baird and Dervan, 1996.

11.3.2 N-allyl, BOC pyrrole amino acid

Synthesis of 2,2,2-Trichloro-1-(4-nitro-1H-pyrrol-2-yl)-ethanone 89
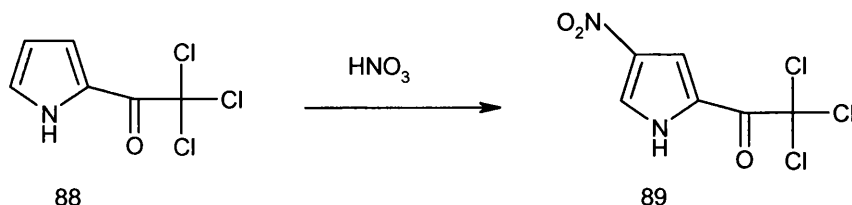
Fuming nitric acid (27 mL) was added dropwise over an hour to a solution of 2-trichloroacetylpyrrole **88** (50 g, 0.235 mol) in acetic anhydride (200 mL) at -15°C. The resulting reaction mixture was then allowed to warm to room temperature (22°C) and stirred for 5 hours. The mixture was then diluted with water (2 L) and the resulting precipitate was collected by filtration. The precipitate was dried by azeotropic removal of water with toluene (2 x 200 mL) by rotary evaporation under reduced pressure and recrystallised from a mixture of chloroform:ethanol (v/v 95:5, 150 mL) to yield **89** (25.5 g, 42 %).

^{1}H NMR (CDCl$_3$) δ 13.67 (s, 1H), 8.39 (d, 1H, J = 1.3 Hz), 7.71 (d, 1H, J = 1.3 Hz); ^{13}C NMR (CDCl$_3$) δ 173.0, 137.1, 127.9, 121.3, 114.3, 93.7; MS (ES$^-$) m/z 100 (256.78, M-H); IR v 3310, 3145, 1670, 1549, 1509, 1398, 1378, 1312, 1253, 1146, 1041, 974, 844, 812, 724, 688, 615 cm^{-1}.

Synthesis of 4-Nitro-1H-pyrrole-2-carboxylic acid methyl ester 90. (Rucker et al., 2003)
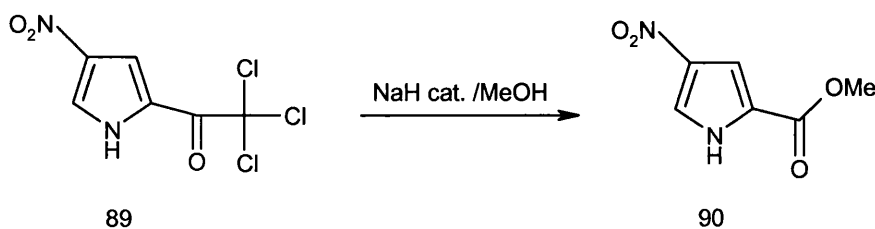
Freshly prepared sodium methoxide solution (NaH, 60% dispersion in mineral oil, 300 mg, 7.5 mmol in anhydrous methanol, 20 mL) was added to a stirred suspension of 4-nitro-2-trichloroacetylpyrrole **89** (25 g, 97 mmol) in anhydrous methanol (300 mL). The suspension thickened and an exotherm was observed. After 4 hours, the reaction was deemed complete by TLC. Concentrated sulphuric acid was added dropwise to neutralize the reaction mixture, at which point a change of colour from yellow to white was observed. The white precipitate was filtered and washed with methanol (50 mL) to provide pure methyl ester **90** (12.5 g, 76 %).

^{1}H NMR (CDCl$_3$) δ 13.18 (s, 1H), 8.06 (d, 1H, J = 1.7 Hz), 7.26 (d, 1H, J = 1.7 Hz), 3.82 (s, 3H); ^{13}C NMR (CDCl$_3$) δ 159.7, 136.6, 124.4, 122.7, 109.5, 51.9; MS (ES$^-$) m/z 100 (168.95, M-H); IR v 3261, 3145, 1686, 1500, 1452, 1382, 1320, 1264, 1209, 1089, 963, 822, 774, 752, 616 cm^{-1}.

Synthesis of 4-tert-Butoxycarbonylamino-1H-pyrrole-2-carboxylic acid methyl ester 91. (Bremer *et al.*, 2000).
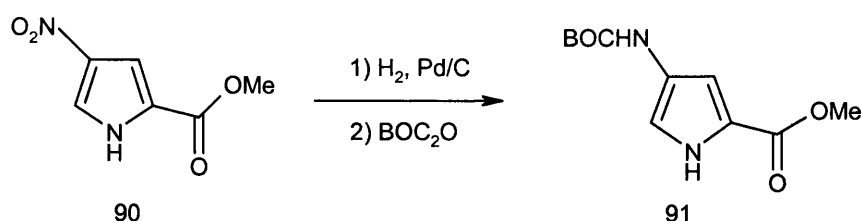
A suspension of nitro ester **90** (12.5 g, 74 mmol) in ethyl acetate (150 mL) over 10 % Pd/C (600 mg) was hydrogenated under 45 PSI for 30 min. Pd/C was removed by filtration and saturated aqueous NaHCO$_3$ (200 mL), followed by Boc anhydride (18 g, 82 mmol) were added to the filtrate. The reaction mixture was allowed to stir for 4 hours at room temperature. The layers were separated and the organic phase was washed with brine (100 mL) and dried over magnesium sulphate. Filtration and removal of the solvent by rotary evaporation under reduced pressure afforded the crude product which was resuspended in DCM (250 mL) and added to hexane (600 mL). The resulting mixture was allowed to stir vigorously and the white precipitate was collected by filtration and dried in a dessicator to afford pure **91** (16 g, 91 %).

^{1}H NMR (DMSO) δ 11.57 (s, 1H), 9.10 (s, 1H), 6.96 (s, 1H), 6.60 (s, 1H), 3.73 (s, 3H), 1.44 (s, 9H); ^{13}C NMR (DMSO) δ 160.7, 152.7, 125.0, 118.9, 112.6, 105.4, 78.4, 51.0, 28.1; MS (ES$^+$) m/z 100 (184.91), 15 (240.97, M+H); IR 3299, 1675, 1563, 1439, 1391, 1250, 1217, 1166, 1120, 1065, 971, 887, 832, 774, 669 cm^{-1}.

Synthesis of 1-Allyl-4-tert-butoxycarbonylamino-1H-pyrrole-2-carboxylic acid methyl ester 92
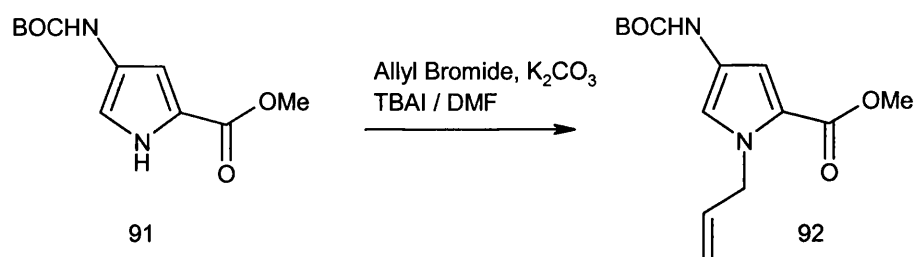
Allyl bromide (2.16 mL, 25 mmol) was added to a suspension of Boc protected pyrrole ester 91 (008-AT-037-1) (3 g, 12.5 mmol), TBAI (0.92 g, 2.5 mmol) and K$_2$CO$_3$ (2.6 g, 18.8 mmol) in anhydrous DMF (15 mL) and the reaction mixture was allowed to stir overnight. The reaction mixture was diluted with ethyl acetate (200 mL) and the organic phase was washed sequentially with water (2 x 200 mL), 10% w/w aqueous citric acid (100 mL), saturated aqueous NaHCO$_3$ (100 mL), brine (50 mL) and dried over MgSO$_4$. Excess solvent was removed by rotary evaporation under reduced pressure to afford a yellow oil, which was purified by flash chromatography (10:90 v/v ethyl acetate/hexane). Evaporation of the purest fractions provided the desired allyl pyrrole 92 (3 g, 86 %) slightly contaminated with a small amount of double allyl product.

^{1}H NMR (CDCl$_3$) δ 9.15 (s, 1H), 7.14 (s, 1H), 6.66 (s, 1H), 5.99-5.89 (m, 1H), 5.10-4.86 (m, 4H), 3.70 (s, 3H), 1.44 (s, 9H); ^{13}C NMR (CDCl$_3$) δ 160.4, 152.6, 135.3, 123.5, 118.1, 117.9, 116.1, 107.7, 78.5, 50.8, 50.1, 28.1; MS (ES$^+$) m/z 100 (225.0, M - butene + H); IR v 3305, 1704, 1684, 1558, 1446, 1397, 1366, 1284, 1248, 1219, 1159, 1093, 989, 929, 682 cm^{-1}.

Synthesis of 1-Allyl-4-tert-butoxycarbonylamino-1H-pyrrole-2-carboxylic acid 93
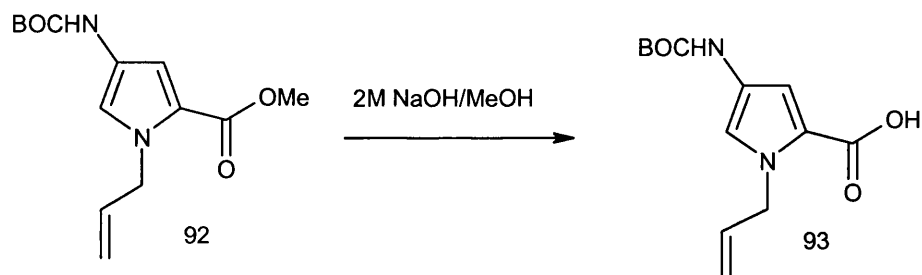
Boc methyl ester **92** (4 g, 14.2 mmol) was saponified according to method C (general methods) to provide Boc allyl pyrrole acid **93** (3.5 g, 92 %).

^{1}H NMR (DMSO) δ 9.12 (s, 1H), 7.08 (d, 1H, J = 1.34 Hz), 6.61 (d, 1H, J = 1.72 Hz), 5.99-5.89 (m, 1H), 5.07 (dd, 1H, J = 1.48 Hz, J = 10.2 Hz), 4.93-4.86 (m, 3H), 1.43 (s, 9H); ^{13}C NMR (DMSO) δ 161.6, 152.6, 135.5, 123.2, 119.1, 117.4, 115.9, 107.7, 78.4, 49.9, 28.1; MS (ES$^+$) m/z 30 (266.99, M+H), 100 (166.94); IR v 3324, 1674, 1589, 1560, 1460, 1389, 1268, 1171, 1087, 989, 788, 744 cm^{-1}.

11.3.3 BOC Imidazole amino ester 98.

Synthesis of 2,2,2-Trichloro-1-(1-methyl-1H-imidazol-2-yl)-ethanone 95

94 → 95
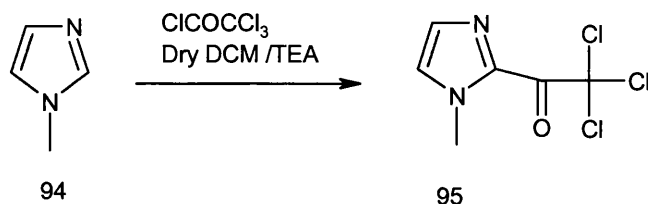
A solution of 1-Methylimidazole **94** (100 mL, 1.26 mol) in anhydrous DCM (400 mL) was added dropwise to a solution of trichloroacetyl chloride (140.7 mL, 1.26 mol) in anhydrous DCM (600 mL) over 1 hour at 5°C. The white slurry was allowed to stir for 3 hours at which point TEA (175 mL, 1.26 mol) was added dropwise at 5°C over 40 min. The resulting mixture was allowed to stir for 30 min. The reaction mixture was diluted with DCM (500 mL) and water (500 mL). The organic phase was washed sequentially with water (2 x 500 mL), brine (300 mL) and dried over MgSO$_4$. Filtration through a short pad of silica gel and removal of the solvent by rotary evaporation under reduced pressure, at room temperature, provided the product as white crystals, which were collected by suspension in hexane (300 mL) and filtration. **95** (227 g, 79 %). ^{1}H NMR (DMSO) δ 7.34 (s, 1H), 7.16 (s, 2H), 4.05 (s, 3H); ^{13}C NMR (DMSO) δ 172.2, 136.1, 130.6, 128.6, 94.8, 37.2; MS (ES$^+$) m/z 246.79 (100), 226.84 ([M+H]$^{+*}$, 30); IR (Golden gate) v 3140, 3114, 1678, 1382, 1293, 1222, 1167, 1013, 915, 848, 817, 788, 741, 695, 649, 607 cm^{-1}.

Synthesis of 2,2,2-Trichloro-1-(1-methyl-4-nitro-1H-imidazol-2-yl)-ethanone 96

95 → 96
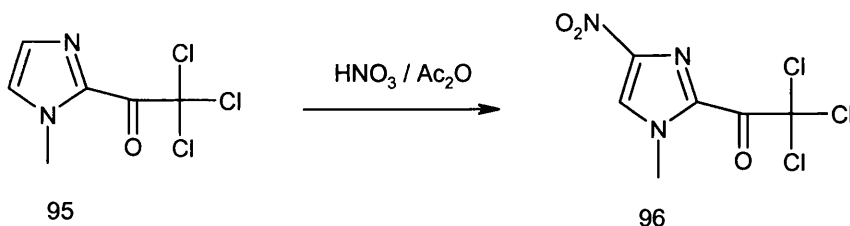
Fuming nitric acid (143 mL) was added dropwise over 40 min at –25°C to a solution of 2-trichloroacetyl-1-methylimidazole **95** (200 g, 0.88 mol) in acetic anhydride (1 L). Concentrated sulphuric acid (2 mL) was then added dropwise. (**Caution!** Reaction can be violently exothermic. The reaction mixture was split between two 5 L round bottomed flasks to minimise risks). The reaction mixture was then allowed to warm up to room temperature (23°C) and to stir overnight. The reaction mixture was poured to large evaporation trays and allowed to crystallise in a well ventilated fumehood (6 h). The solids were then rapidly washed and neutralized by saturated aqueous $NaHCO_3$ and collected by filtration. The product was washed with water, followed by a mixture of 3/1 v/v diethyl ether/acetone (2 x 300 mL) and dried in a dessicator to provide pure **96** (125 g, 52 %). ^{1}H NMR (DMSO) δ 7.97 (s, 1H), 4.17 (s, 3H); ^{13}C NMR (DMSO) δ 172.8, 145.8, 133.6, 126.1, 93.5, 38.3; MS (ES$^+$) m/z 291.83 (100), 271.83 ([M+H]$^{+\bullet}$, 30); IR (Golden gate) v 3156, 1704, 1535, 1487, 1336, 1313, 1226, 1133, 1022, 998, 815, 741, 712, 638 cm^{-1}.

Synthesis of 1-Methyl-4-nitro-1H-imidazole-2-carboxylic acid methyl ester 97
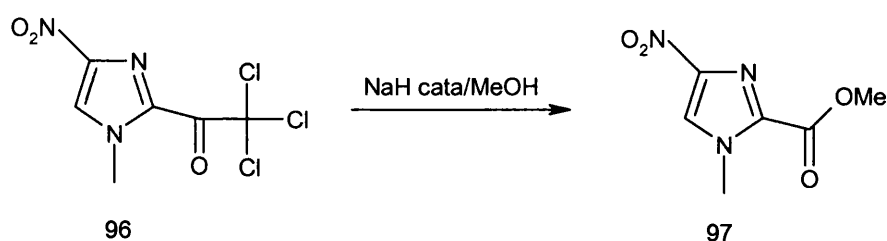
Freshly prepared sodium methoxide solution (NaH, 60% dispersion in mineral oil, 1 g, 25 mmol in anhydrous methanol, 60 mL) (*It should be possible to divide NaH quantities by 10)* was added to a stirred suspension 4-nitro-2-trichloroacetylimidazole **96** (100 g, 37 mmol) in anhydrous methanol (300 mL). After 3 hours, the reaction was deemed complete by TLC. Concentrated sulphuric acid was added dropwise to neutralize the reaction mixture, at which point a change of colour from yellow to white was observed. The white precipitate was filtered and washed with methanol (50 mL) to provide pure methyl ester **97** (50 g, 74 %). ^{1}H NMR (DMSO) δ 7.86 (s, 1H), 4.11 (s, 3H), 3.96 (s, 3H); ^{13}C NMR (DMSO) δ 158.6, 146.1, 134.7, 124.5, 53.0, 37.1; MS (ES$^+$) m/z 186.01 ([M+H]$^{+\bullet}$, 100); IR (Golden gate) v 3137, 1723, 1539, 1493, 1309, 1261, 1144, 1124, 995, 844, 651 cm^{-1}.

Synthesis of 2-Methoxycarbonyl-1-methyl-1H-imidazol-4-yl-ammonium 98
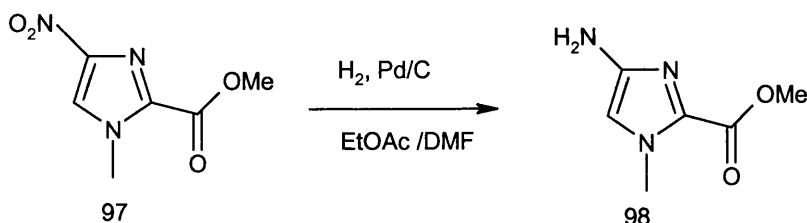
A suspension of nitro ester **97** (5 g, 27 mmol) in DMF (5 mL), over 10 % Pd/C (500 mg), was hydrogenated under 45 PSI for 1 hour. Pd/C was removed by filtration and solvents were removed by rotary evaporation under reduced pressure. The residue was triturated with diethyl ether (150 mL) and the resulting white precipitate was collected by filtration and dried in a dessicator to provide pure amino imidazole **98**. ^{1}H NMR (DMSO) δ 6.49 (s, 1H), 4.56 (s, 2H), 3.81 (s, 3H), 3.76 (s, 3H); ^{13}C NMR (DMSO) δ 158.9, 147.1, 129.9, 108.6, 51.2, 35.0; MS (ES$^+$) m/z 155.9 ([M+H]$^{+\bullet}$, 100); IR (Golden gate) ν 3419, 3340, 1690, 1619, 1566, 1489, 1458, 1411, 1382, 1335, 1257, 1207, 1192, 1131, 1052, 1026, 969 cm^{-1}.

11.4 Pyrrole-Imidazole linked PBD dimer conjugates synthesis

11.4.1 Symmetrical dimers, including a central N-methylpyrrole diacid.

11.4.1.1 Synthesis of monopyrrole dimer AT-217, **104**

Alloc protected monopyrrole dimer 103

103
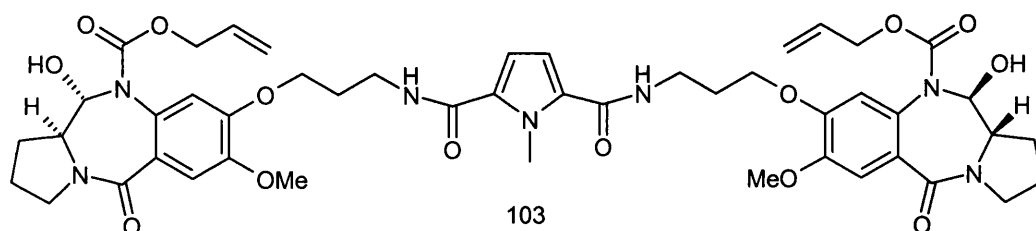
Oxalyl chloride (47 μL, 0.55 mmol) was added to a stirred solution of 1-methylpyrrole-2,5-dicarboxylic acid **101** (42 mg, 0.25 mmol) in anhydrous THF (5 mL) at room temperature. The mixture was then treated with a catalytic amount of DMF at which point vigorous effervescence occurred. The mixture was allowed to stir for 20 min after which time all effervescence ceased.

The resulting acid chloride solution was then added dropwise to a stirred solution of the 3C PBD amine capping unit **66** (200 mg, 0.49 mmol), TEA (151 μL, 1.08 mmol), in anhydrous THF (5 mL) at 0°C under nitrogen. A white precipitate was observed during the addition and the reaction mixture was allowed to rise to room temperature. After 4 hours, the solvent was removed by rotary evaporation under reduced pressure and the residue was partitioned between $CHCl_3$ (30 mL) and aqueous 1N HCl (20 mL). The organic phase was washed sequentially with saturated aqueous $NaHCO_3$, brine, dried over $MgSO_4$ and excess solvent removed by rotary evaporation under reduced pressure to yield **103** (230 mg, quantitative yield) as a white powder. The product was used in the next step without further purification. ^1H NMR (DMSO) δ 8.26 (t, J = 5.27 Hz, 2H), 7.10 (s, 2H), 6.79 (s, 2H), 6.68 (s, 2H), 6.51 (bs, 2H), 5.92-5-68 (m, 2H), 5.58-5.39 (m, 2H), 5.17-4.93 (m, 4H), 4.74-4.32 (m, 4H), 4.14-3.93 (m, 7H), 3.83 (s, 6H), 3.50 (m, 2H), 3.44-3.23 (m, 8H), 2.14-1.81 (m, 12H); ^{13}C NMR (DMSO) δ 165.9, 161.1, 154.3,

149.4, 147.9, 132.8, 129.9, 128.5, 116.8, 114.3, 110.6, 110.2, 85.3, 79.1, 66.6, 65.5, 64.8, 55.6, 45.8, 35.8, 33.9, 30.3, 28.8, 28.1, 25.0, 22.7, 15.1; MS (ES+) m/z (relative intensity) 944.5 ($[M + H]^{+\cdot}$, 35), 926.5 (40), 908.6 (100); IR v 3320, 2928, 2246, 1709, 1627, 1535, 1513, 1464, 1435, 1409, 1312, 1277, 1218, 1134, 1104, 1054, 1014, 913, 871, 770, 731, 646 cm^{-1}.

Monopyrrole dimer AT-217, 104

AT-217, 104
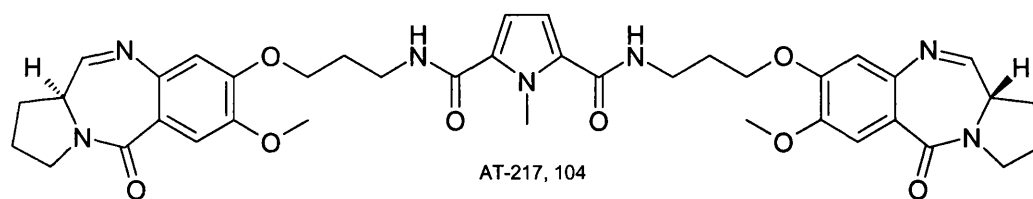
Tetrakis(triphenylphosphine)palladium (5 mg, 4 μmol) was added to a solution of protected carbinolamine **103** (190 mg, 0.2 mmol) and pyrrolidine (37 μL, 0.44 mmol) in dry DCM (5 mL) under nitrogen. After 30 secondes, a white precipitate was observed. TLC monitoring revealed complete reaction after 10 minutes. The solvent was removed by rotary evaporation under reduced pressure to yield a white residue which was purified by flash chromatography using a gradient (from 2:98 to 5:95 v/v MeOH/CHCl₃). Removal of the solvent from the pure fractions by rotary evaporation under reduced pressure yielded AT-217, **104** (120 mg, 81%) as a white solid. ^{1}H NMR (CDCl₃) δ 7.68 (d, J = 4.07 Hz, 2H), 7.51 (s, 2H), 6.96 (bs, 2H), 6.82 (s, 2H), 6.56 (s, 2H), 4.33-4.10 (m, 7H), 3.90-3.76 (m, 8H), 3.76-3.50 (m, 8H), 2.42-2.25 (m, 4H), 2.23-1.95 (m, 8H); ^{13}C NMR (CDCl₃) δ 164.4, 162.5, 161.8, 150.3, 147.5, 140.6, 130.7, 120.6, 111.5, 110.3, 68.8, 55.9, 53.7, 46.6, 38.1, 34.3, 29.6, 28.7, 24.1; MS (ES+) m/z (relative intensity) 740.5 ($[M + H]^{+\cdot}$, 100); IR v 3320, 2951, 2237, 1656, 1622, 1600, 1534, 1505, 1463, 1432, 1383, 1340, 1262, 1216, 1092, 1019, 914, 874 cm^{-1}. HRMS (TOF MS ES$^+$) calcd for C₃₉H₄₅N₇O₈ (M+H): 740.3402. Found: 740.3430; Purity by analytical HPLC : Luna : 93.7 %; Gemini : 84.1 %.

11.4.1.1 Synthesis of tripyrrole dimer AT-234, **109**

Bis-benzyl ester tripyrrole core 107
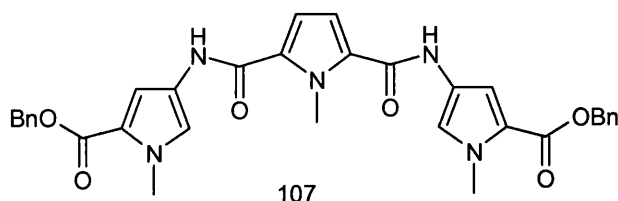
A catalytic amount of DMF was added to a stirred solution of 1-methylpyrrole-2,5-dicarboxylic acid **101** (200 mg, 1.18 mmol) and oxalyl chloride (227 µL, 2.6 mmol) in anhydrous THF (5 mL) at room temperature. (**Caution!** vigorous effervescence). The mixture was allowed to stir until all effervescence ceased. The resulting acid chloride solution was then added dropwise to a stirred suspension of the hydrochloride salt of 4-amino-1-methyl-1H-pyrrole-2-carboxylic acid benzyl ester **106** (631 mg, 2.36 mmol), TEA (1.6 mL, 11.5 mmol), in anhydrous THF (10 mL) at O°C under nitrogen. The resulting white slurry was allowed to rise to room temperature and stir for 4 hours. The solvent was then removed by rotary evaporation under reduced pressure and the residue was partitioned between $CHCl_3$ (100 mL) and aqueous 1N HCl (50 mL). The organic phase was washed sequentially with water, saturated aqueous $NaHCO_3$, brine, and dried over $MgSO_4$ and excess solvent was removed by rotary evaporation under reduced pressure to afford a white powder which was found to be a two component mixture by TLC (EtOAc/Hexane). The major, more polar component was isolated by recrystallisation in $CHCl_3$/ Diethyl ether and was found to be pure by proton NMR. Yield of **107**: 160 mg (23%). ^{1}H NMR (DMSO) δ 10.14 (s, 2H), 7.51 (d, J = 1.82 Hz, 2H), 7.47-7.30 (m, 10H), 6.97 (d, J = 1.90 Hz, 2H), 6.86 (s, 2H), 5.25 (s, 4H), 4.11 (s, 3H), 3.86 (s, 6H); ^{13}C NMR (DMSO) δ 160.0, 158.1, 136.5, 130.0, 128.4, 127.9, 127.7, 122.6, 121.1, 118.6, 111.4, 108.6, 79.1, 64.8, 54.8, 36.1, 34.0; MS (ES$^+$) m/z (relative intensity) 616.1 ($[M + Na]^+$, 60), 594.2 ($[M + H]^+$, 40), 353 (100); IR v 3266, 3121, 2953, 1710, 1638, 1585, 1545, 1438, 1390, 1333, 1258, 1194, 1150, 1109, 1109, 1086, 1029, 1005, 895, 873, 808, 781, 744, 694, 630, 609 cm^{-1}.

Synthesis of Alloc protected tripyrrole dimer 108

108

A solution of **107** (150 mg, 0.25 mmol) in DMF (5 mL), over 10 % Pd/C (30 mg), was hydrogenated under 45 PSI for 6 hours. The suspension was filtered through celite into a round-bottomed flask. The celite pad was quickly rinsed with anhydrous DMF (3 mL). EDCI (106 mg, 0.55 mmol) and HOBt (85 mg, 0.55 mmol) were added to the combined filtrate and the resulting clear yellow solution was allowed to stir overnight. The 3C amine PBD capping unit **66** (205 mg, 0.50 mmol) was then added and the solution allowed to stir for 24 hours. The solution was partitioned between $CHCl_3$ (100 mL) and 10% aqueous citric acid (100 mL). The organic phase was washed by saturated aqueous $NaHCO_3$ followed by brine and dried over $MgSO_4$. The solvent was removed by rotary evaporation under reduced pressure and the residue was purified by column chromatography (3:97 to 4:96 v/v $MeOH/CHCl_3$) to yield **108** (180 mg, 60%); ^1H NMR (DMSO) δ 10.10 (s, 2H), 8.13 (t, J = 4.94 Hz, 2H), 7.22 (d, J = 1.10Hz, 2H), 7.10 (s, 2H), 6.90 (d, J = 1.16 Hz, 2H), 6.84 (s, 2H), 6.79 (s, 2H), 6.53 (bs, 2H), 6.06-5.71 (m, 2H), 5.58-5.39 (m, 2H), 5.17-4.94 (m, 4H), 4.74-4.32 (m, 4H), 4.12 (s, 3H), 4.09-3.95 (m, 4H), 3.83 (m, 12H), 3.50 (m, 2H), 3.44-3.23 (m, 8H), 2.14-1.77 (m, 12H); ^{13}C NMR (DMSO) δ 165.9, 161.2, 158.1, 154.3, 149.4, 147.9, 132.8, 130.2, 123.0, 121.6, 118.0, 116.9, 114.2, 111.2, 110.2, 104.2, 85.3, 79.1, 66.6, 60.5, 55.6, 45.8, 35.9, 35.6, 33.9, 28.9, 28.1, 22.7; MS (ES$^+$) m/z (relative intensity) 1188.7 ([M + H]$^+$, 100); IR v 3320, 2928, 2246, 1709, 1627, 1535, 1513, 1464, 1435, 1409, 1312, 1277, 1218, 1134, 1104, 1054, 1014, 913, 871, 770, 731, 646 cm^{-1}.

Synthesis of tripyrrole dimer AT-234, 109

Tetrakis(triphenylphosphine)palladium (3 mg, 2.5 μmol) was added to a solution of protected carbinolamine **108** (150 mg, 0.126 mmol), triphenylphospine (3 mg, 0.01 mmol), and pyrrolidine (22 μL, 0.26 mmol) in anhydrous chloroform (10 mL) under nitrogen. TLC monitoring revealed complete reaction after 1 hour. The solvent was removed by rotary evaporation under reduced pressure to yield a white residue, which was subjected to column chromatography (gradient from 4:96 to 7:93 v/v MeOH/CHCl₃). Removal of the solvent from the pure fraction, by rotary evaporation under reduced pressure yielded AT-234, **109** (110 mg, 88%) as a white solid. ^{1}H NMR (DMSO) (diimine only) δ 10.1 (s, 2H), 8.12 (m, 2H), 7.78 (d, J = 4.4Hz, 2H), 7.35 (s, 2H), 7.23 (s, 2H), 6.89 (s, 2H), 6.84 (s, 4H), 4.12 (s, 3H), 4.22-3.92 (m, 4H), 3.84 (2s, 12H), 3.65-3.56 (m, 2H), 3.40-3.20 (m, 8H), 2.37-2.17 (m, 4H), 2.07-1.85 (m, 8H); ^{13}C NMR (DMSO) δ 164.2, 163.3, 161.2, 158.1, 150.2, 146.8, 140.5, 130.2, 123.0, 121.6, 119.7, 118.0, 111.2, 110.0, 104.2, 66.3, 55.5, 53.3, 48.5, 46.3, 35.9, 35.5, 34.0, 23.6; MS (ES$^+$) *m/z* (relative intensity) 984.5 ([M + H]$^+$, 100); IR ν 3316, 2952, 1632, 1602, 1530, 1436, 1387, 1264, 1217, 1199, 1090, 1066, 1010, 872, 664 cm^{-1}. HRMS (TOF MS ES$^+$) calcd for $C_{51}H_{57}N_{11}O_{10}$ (M+H): 984.4363. Found: 984.4414. Purity by analytical HPLC : Luna : 99.2 %; Gemini : 96.7 %.

11.4.2 Unsymmetrical and based on distamycin core.

11.4.2.1 Synthesis of tripyrrole dimer AT-235, **115**

Synthesis of tripyrrole PBD carbinolamine conjugate 113
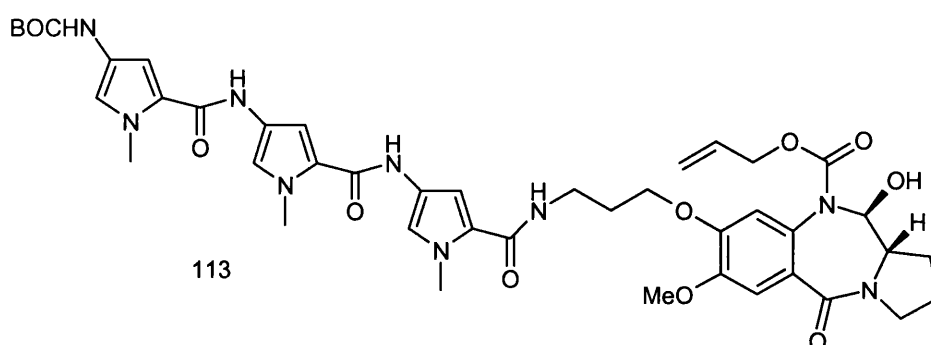

EDCI (81 mg, 0.422 mmol) was added to a solution of Boc-tripyrroleacid **112** (197 mg, 0.404 mmol) and HOBt (65 mg, 0.425 mmol) in anhydrous DMF (5 mL) and the reaction mixture was allowed to stir for 7 h.

A solution of the 3C amine PBD capping unit **66** (164 mg, 0.404 mmol) in anhydrous DMF (5 mL) was then added and the reaction mixture was allowed to stir overnight at RT. The reaction mixture was diluted with $CHCl_3$ (200 mL) and was washed sequentially with 5 % aqueous citric acid (100 mL), water (100 mL), saturated aqueous $NaHCO_3$ (100 mL), brine (100 mL) and dried over $MgSO_4$. The solvents were removed by rotary evaporation under reduced pressure to afford a yellow oil which was purified further by flash chromatography (1:99 v/v $MeOH/CHCl_3$) to yield **113**, (250 mg, 71%). ^1H NMR (DMSO) δ 9.88 (m, 2H), 9.09 (s, 1H), 8.09 (t, J = 5.24 Hz), 7.20 (m, 2H), 7.10 (s, 1H), 7.05 (d, J = 1.35 Hz, 1H), 6.90 (s, 1H), 6.85 (s, 1H), 6.79 (s, 1H), 6.53 (bs, 1H), 5.89-5.71 (m, 1H), 5.48 (m, 1H), 5.16-4.97 (m, 2H), 4.73-4.32 (m, 2H), 4.02 (m, 2H), 3.83 (m, 12H), 3.51 (m, 1H), 3.35 (m, 4H), 2.13-1.79 (m, 6H), 1.47 (s, 9H); ^{13}C NMR (DMSO) δ 165.9, 161.3, 158.4, 158.3, 154.3, 152.8, 149.4, 147.9, 132.7, 128.5, 122.7, 122.6, 122.2, 122.1, 122.1, 118.3, 117.8, 116.9, 114.1, 110.1, 104.6, 104.1, 103.7, 85.3, 79.1, 78.2, 66.6, 65.5, 60.5, 55.6, 45.9, 36.0, 35.9, 35.5, 28.9, 28.1, 22.6; IR

v 3315, 2976, 1698, 1633, 1587, 1515, 1465, 1435, 1405, 1314, 1269, 1206, 1163, 1105, 1061, 996, 754 cm^{-1}; MS (ES$^+$) m/z (relative intensity) 872.4 ([M + H]$^+$,100).

## Synthesis of Alloc protected tripyrrole PBD dimer 114

114
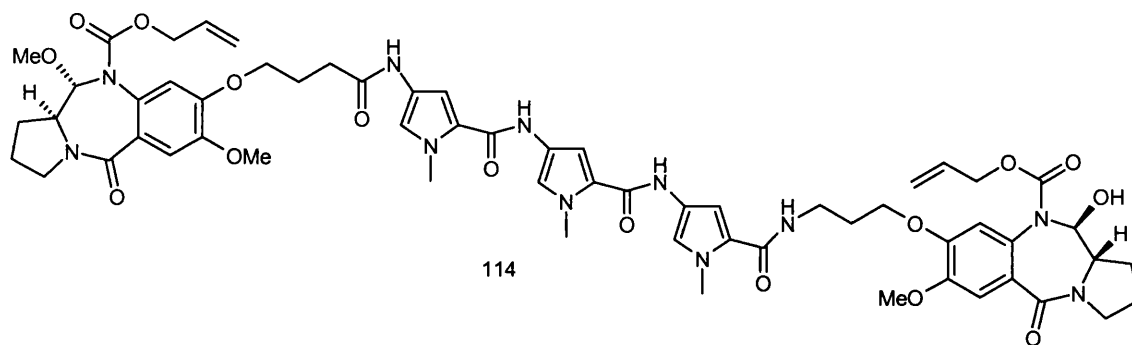
Boc protected tripyrrole conjugate **113** (180 mg, 0.206 mmol) was finely suspended in a solution of 4N HCl in dioxane (8 mL) and stirred for 1 h. Removal of excess dioxane by rotary evaporation under reduced pressure afforded the unprotected amine as its hydrochloride salt (**Caution!** corrosive vapours). The salt was redissolved in anhydrous THF (5 mL) in the presence of DIPEA (180 μL, 1.035 mmol) to convert it to the free base.

In parrallel, a catalytic amount of DMF was added to a solution of **56** (4C N10-Alloc-O11-methyl-PBD acid capping unit) (93 mg, 0.207 mmol) and oxalyl chloride (27 μL, 0.228 mmol) in anhydrous THF (5 mL) to provide the PBD acid chloride solution. The acid chloride solution was allowed to stir for 5 min, then added dropwise to the previously prepared free base solution at 0°C (ice/acetone bath). After 1h, the THF was removed by rotary evaporation under reduced pressure and the residue dissolved in CHCl$_3$ (100 mL). The organic layer was washed sequentially with 5 % aqueous citric acid (50 mL), water (50 mL), saturated aqueous NaHCO$_3$ (50 mL), brine (500 mL) and dried over MgSO$_4$. Excess solvent was removed by rotary evaporation under reduced pressure to afford a yellow oil which was purified further by flash chromatography (gradient from 3:97 to 4:96 v/v MeOH/CHCl$_3$) to yield **114** (110 mg, 44%); ^{1}H NMR (DMSO) δ 9.89 (s, 3H), 8.09 (m, 1H), 7.25 (d, J = 1.36 Hz, 1H), 7.19 (m, 2H), 7.11 (m, 2H), 7.05 (s, 1H), 6.92 (m, 3H), 6.79 (s, 1H), 6.53 (bs, 1H), 6.02-5.70 (m, 2H), 5.49 (m, 1H), 5.37 (d, J = 8.8 Hz, 1H), 5.14-4.95 (m, 4H), 4.72-4.32 (m, 4H), 4.04 (m, 4H), 3.85 (m, 15H), 3.47 (m, 5H), 3.40-3.20 (m, 6H), 2.45 (t, J = 7.04 Hz, 2H), 2.14-1.80 (m,

12H); ^{13}C NMR (DMSO) δ 168.7, 166.0, 161.3, 158.4, 154.3, 148.3, 122.8, 122.7, 122.6, 122.1, 121.9, 118.0, 114.2, 104.6, 104.2, 92.9, 79.1, 55.6, 45.8, 36.0, 35.9, 22.8; MS (ES$^+$) m/z (relative intensity) 1202.7 ([M + H]$^+$, 40), 292 (100).

## Synthesis of tripyrrole dimer AT-235, 115

115, AT-235
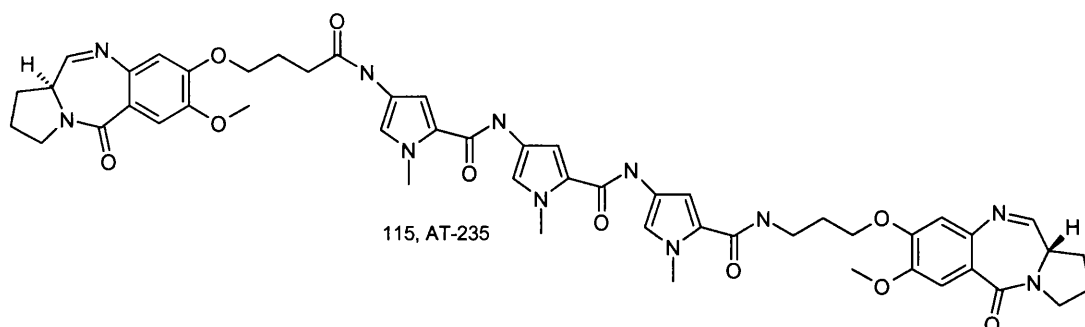
$Tetrakis$(triphenylphosphine)palladium (1.5 mg, 1 μmol) was added to a solution of protected carbinolamine **114** (80 mg, 0.067 mmol) and pyrrolidine (11.7 μL, 0.140 mmol) in anhydrous chloroform (5 mL) under nitrogen. Complete reaction was reached in 1h as monitored by TLC. The solvent was removed by rotary evaporation under reduced pressure and the residue purified by flash chromatography (gradient from 5:95 to 7:93 v/v MeOH/CHCl$_3$) to yield AT-235, **115**, as an off white solid (56 mg, 85 %). A sample was dissolved in deuterated DMSO and allowed to equilibrate to the diimine species over 48 hours. ^{1}H NMR (DMSO) (diimine only) δ 9.90 (s, 3H), 8.10 (m, 1H), 7.79 (d, 2H, J = 4.36 Hz), 7.35 (s, 2H), 7.25 (s,1H), 7.20 (2s, 2H), 7.05 (s, 1H), 6.90 (s, 2H), 6.84 (s, 2H), 4.21-4.01 (m, 4H), 3.85-3.81 (m, 15H), 3.61 (m, 2H), 3.46-3.35 (m, 6H), 2.45 (m, 2H), 2.38-2.17 (m, 4H), 2.13-1.89 (m, 8H); ^{13}C NMR (DMSO) δ 168.7, 164.2, 158.3, 150.2, 150.1, 146.8, 140.5, 122.7, 122.0, 121.9, 119.7, 118.4, 118.4, 117.8, 114.8, 111.2, 110.0, 104.6, 104.2, 103.9, 67.7, 66.4, 55.8, 55.5, 53.6, 53.3, 48.5, 46.3, 36.0, 35.8, 35.5, 30.2, 28.9, 28.9, 28.7, 24.7, 23.6, 22.3; MS (ES$^+$) m/z (relative intensity) 984.4 ([M + H]$^+$, 100); IR v 3306, 2949, 1638, 1597, 1555, 1508, 1465, 1435, 1405, 1262, 1216, 1090, 1064 cm^{-1}. HRMS (TOF MS ES$^+$) calcd for C$_{51}$H$_{57}$N$_{11}$O$_{10}$ (M+H): 984.4363. Found: 984.4359. Purity by analytical HPLC: Luna : 100 %; Gemini : 95.4 %.

11.4.3 Symetrical; including a diaminopropane central linker.

11.4.3.1 Synthesis of bipyrrole dimer AT-281, **118**

Synthesis of bis nitropyrrole core 116

116
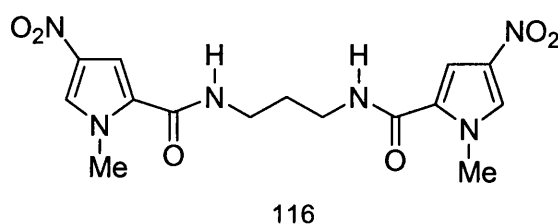
Neat 1,3-diaminopropane (307 μL, 3.67 mmol) was added to a solution of 1-methyl-2-trichloroacetyl-4-nitropyrrole, **83** (2 g, 7.36 mmol) in anhydrous THF (15 mL). A precipitate was observed after 5 min and the suspension was allowed to stir for 3 hours. The reaction mixture was then diluted with diethyl ether (60 mL), filtered and dried under vacuum to yield compound **116** as an off white fine powder. (1.28 g, 92 %); ^{1}H NMR (DMSO) δ 8.40 (t, J = 5.40 Hz, 2H), 8.12 (d, J = 1.51 Hz, 2H), 7.42 (d, J = 1.88 Hz, 2H), 3.92 (s, 6H), 3.26 (q, J = 6.49 Hz, 4H), 1.75 (p, J = 6.88 Hz, 2H); ^{13}C NMR (DMSO) δ 159.7, 133.7, 127.7, 126.4, 107.1, 37.2, 36.5, 28.8; MS (ES$^+$) m/z (relative intensity) 379.1 ([M + H]$^+$, 100); IR v 3414, 3364, 3116, 2950, 1654, 550, 1530, 1501, 1418, 1346, 1311, 1264, 1222, 1209, 1139, 1111, 1075, 984, 950, 827, 849, 811, 747, 707 cm^{-1}.

Synthesis of the bipyrrole Alloc protected carbinolamine conjugate 117

117
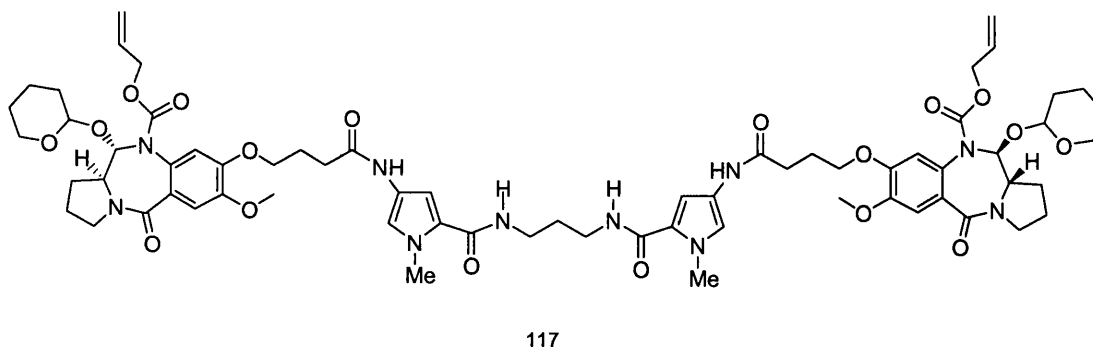
A solution of the bis nitro pyrrole **116** (100 mg, 0.264 mmol) in anhydrous DMF (5 mL) was hydrogenated over 10% Pd/C (40 mg) under 15 PSI for 5 hours.

In parrallel, a solution of 4C-N10Alloc-11OTHP-acid PBD capping unit, **57**, (265mg, 0.528 mmol), EDCI (152 mg, 0.792 mmol) and HOBt (121 mg, 0.790 mmol) in anhydrous DMF (4 mL) was allowed to stir for 3 hours to provide the activated acid solution.

The hydrogenation suspension was filtered through celite and the filtrate was added to the previously prepared activated acid solution. The reaction mixture was allowed to stir at 60°C for 3 hours and then overnight at room temperature. The mixture was diluted with CHCl₃ (200 mL) and washed sequentially with water (200 mL), 10% aqueous citric acid (100 mL), sat NaHCO₃ (100 mL), brine (100 mL) and dried over MgSO₄. The solvent was removed by rotary evaporation under reduced pressure and the residue purified further by flash chromatography (gradient from 1:99 to 3:97 v/v MeOH/CHCl₃) to yield the pure compound **117** as an off white solid (190 mg, 55 %); ^{1}H NMR (DMSO) δ 9.82 (s, 2H), 8.00 (t, J = 5.44 Hz, 2H), 7.12 (m, 4H), 6.93 (m, 1H), 6.83 (s, 1H), 6.67 (m, 2H), 5.79-5.68 (m, 4H), 5.88-5.58 (m, 6H), 4.70-4.31 (m, 4H), 4.06-3.96 (m, 4H), 3.79 (m, 14H), 3.58-3.46 (m, 4H), 3.35 (m, 4H), 3.20 (q, J = 6.41 Hz, 4H), 2.40 (t, J = 7 Hz, 4H), 2.19-1.77 (m, 12H), 1.65 (m, 6H), 1.55-1.28 (m, 8H); ^{13}C NMR (DMSO) δ 168.7, 168.5, 166.2, 166.0, 161.1, 148.3, 148.2, 132.6, 122.9, 121.9, 117.4, 116.5, 114.4, 110.2, 103.1, 79.1, 68.0, 67.8, 65.5, 64.8, 62.8, 59.4, 55.6, 45.9, 36.0, 35.8, 31.7, 31.6, 30.5, 30.2, 29.7, 28.4, 28.3, 24.9, 24.7, 24.6, 24.4; MS (ES⁺) m/z (relative intensity) 1320.1 ([M + H]⁺·, 100).

Synthesis of symmetrical diaminopropane bis pyrrole PBD 118.

118, AT-281

259
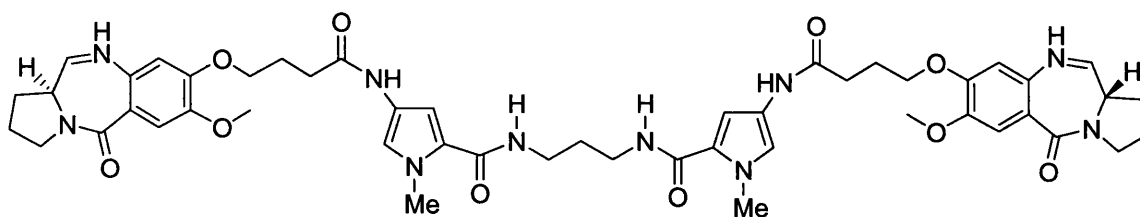
Pd(PPh₃)₄ (2.4 mg, 2.1 μmol) was added to a solution of **117** (138 mg, 0.104 mmol) and pyrrolidine (19.2 μL, 0.246 mmol) in anhydrous CHCl₃ (5 mL). Complete reaction was reached in an hour as observed by TLC. The solvent was removed by rotary evaporation under reduced pressure and the residue purified by flash chromatography (gradient from 3:97 to 7:93 v/v MeOH/CHCl₃) to yield AT-281, **118**, as an off white solid (99 mg, 90%). A sample was dissolved in deuterated DMSO and NMR data of the diimine form were recorded after 48h. ^{1}H NMR (DMSO) δ 9.83 (s, 2H), 8.01 (t, J = 5.73 Hz, 2H), 7.79 (d, J = 4.4Hz, 2H), 7.35 (s, 2H), 7.12 (s, 2H), 6.83 (s, 2H), 6.69 (s, 2H), 4.20-3.99 (m, 4H), 3.82 (m, 12H), 3.75-3.58 (m, 4H), 3.47-3.40 (m, 2H), 3.22 (m, 4H), 2.43 (t, J = 7.3 Hz, 4H), 2.33-2.15 (m, 4H), 2.12-1.94 (m, 8H), 1.67 (m, 2H); ^{13}C NMR (DMSO) δ 168.7, 164.2, 163.3, 161.1, 150.1, 146.9, 140.5, 122.9, 121.9, 119.7, 117.5, 111.2, 110.1, 103.3, 79.1, 67.8, 56.0, 55.5, 53.3, 46.3, 36.0, 35.8, 31.8, 29.7, 28.7, 24.7, 23.6, 18.5; MS (ES⁺) m/z (relative intensity) 947.6 ($[M + H]^{+}$, 100). HRMS (TOF MS ES⁺) calcd for C₄₉H₅₈N₁₀O₁₀ (M+H): 947.4410. Found: 947.4442; Purity by analytical HPLC : Luna : 100 %; Gemini : 89.4 %.

Synthesis of symmetrical Boc protected tetrapyrrole 119.
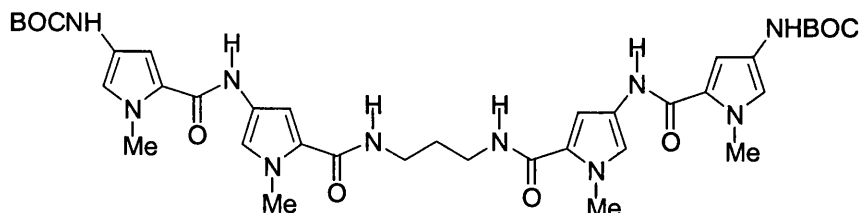
119

A solution of **116** (200 mg, 0.53 mmol) in anhydrous DMF (7 mL) was hydrogenated over 10% Pd/C (50 mg) under 15 PSI using a Parr apparatus over 6 hours. The supension was filtered through celite and into a round-bottomed flask containing 1-methyl-2-OBt-ester-4-NHBOC-pyrrole, **87**, (377 mg, 1.06 mmol). The reaction mixture was allowed to stir at 60°C for an hour and then overnight at room temperature. The mixture was then extracted with chloroform (200 mL) and washed with water (200 mL), 10% aqueous citric acid (100 mL), sat NaHCO₃ (100 mL), brine (100 mL) and dried over MgSO₄. The solvent was removed by rotary evaporation under reduced pressure and the residue purified further by flash chromatography (3.5:96.5 v/v MeOH/CHCl₃) to

yield the pure compound **119** as an off white solid (284 mg, 70 %); ^{1}H NMR (DMSO) δ 9.83 (s, 2H), 9.09 (s, 2H), 8.03 (t, J = 5.6 Hz, 2H), 7.19 (d, J = 1.37 Hz, 2H), 6.89 (s, 4H), 6.84 (s, 2H), 3.82 (s, 12H), 3.24 (q, J = 6.16 Hz, 4H), 1.71 (p, J = 6.70 Hz, 2H), 1.47 (s, 18H); ^{13}C NMR (DMSO) δ 161.2, 158.3, 152.8, 122.8, 122.8, 122.2, 122.1, 117.7, 116.9, 104.0, 103.7, 35.9, 35.8, 29.6, 28.1; MS (ES$^+$) m/z (relative intensity) 763.5 ([M + H]$^{+\cdot}$, 100); IR v 3311, 2977, 1697, 1643, 1586, 1529, 1434, 1402, 1364, 1248, 1206, 1161, 1098, 1063, 997, 895, 804, 757, 664 cm^{-1}.

Synthesis of the tetrapyrrole Alloc protected carbinolamine conjugate 120

120
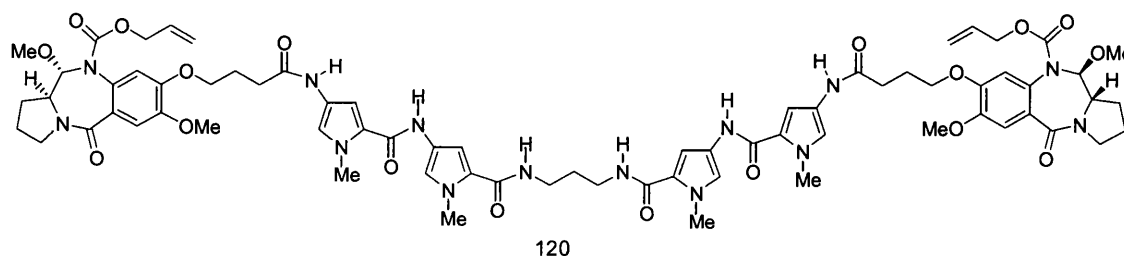
Finely powdered Boc protected **119** (200 mg, 0.262 mmol) was suspended in a solution of 4N HCl in dioxane (10 mL) and the reaction mixture was allowed to stir for 1h. The solvent was then removed by rotary evaporation under reduced pressure to provide the bis amine HCl salt as a solid which was carried through to the next step without further purification. In a separate vessel, a catalytic quantity of DMF was added to a solution of **56** (4C N10-Alloc-O11-methyl-PBD acid capping unit) (235 mg, 0.532 mmol) and oxalyl chloride (65 µL, 0.549 mmol) in anhydrous THF (8 mL). The reaction mixture was allowed to stir for 10 mins. The resulting acid chloride solution was added to a suspension of the afformentioned bis hydrochloride salt in anhydrous DMF (5 mL) and the reaction mixture was allowed to stir at room temperature. Completion of the reaction was observed after one hour by TLC and the solvent was removed by rotary evaporation under reduced pressure. The residue was dissolved in CHCl₃ washed with water (200 mL), 10% aqueous citric acid (100 mL), sat NaHCO₃ (100 mL), brine (100 mL) and dried over MgSO₄. The solvent was removed by rotary evaporation under reduced pressure and the residue purified further by flash chromatography (gradient up to 4:96 v/v MeOH/CHCl₃) to yield the pure compound **120** as an off white solid (217 mg, 58 %); ^{1}H NMR (DMSO) δ 9.88-9.86 (m, 4H), 8.04 (t, J = 5.6 Hz, 2H), 7.20-7.18 (m, 4H), 7.11 (s, 2H), 6.89 (m, 6H),5.79 (m, 2H), 5.36 (d, J = 9 Hz, 2H), 5.04 (m, 4H), 4.58-4.44

261

(m, 4H), 4.04 (m, 4H), 3.83 (s, 18H),3.47 (s, 8H), 3.33 (m, 4H), 3.24 (q, J = 6.10 Hz, 4H), 2.45 (t, J = 7.15 Hz, 4H), 2.06 (m, 6H), 1.97-1.85 (m, 6H), 1.71 (p, J = 6.56 Hz, 2H); ^{13}C NMR (DMSO) δ 168.7, 166.0, 161.2, 158.3, 149.7, 148.3, 132.069, 128.3, 122.9, 122.6, 122.0, 121.9, 118.0, 117.8, 114.3, 110.4, 104.0, 103.8, 92.8, 79.1, 68.0, 55.6, 45.8, 36.0, 35.9, 31.6, 28.3, 22.8; MS (ES$^+$) m/z (relative intensity) 1424.1 ([M + H]$^+$, 60), 680.6 (100); IR v 3311, 2977, 1697, 1643, 1586, 1529, 1434, 1402, 1364, 1248, 1206, 1161, 1098, 1063, 997, 895, 804, 757, 664 cm^{-1}.

Synthesis of symmetrical diaminopropane tetrapyrrole PBD 121.
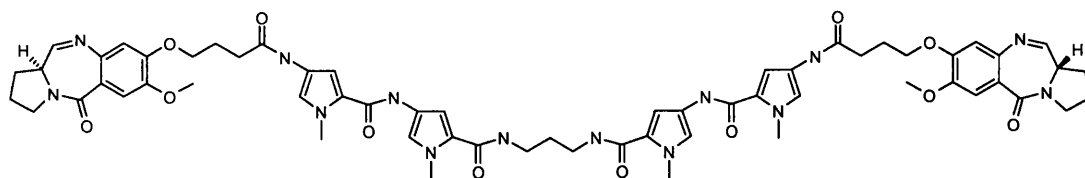
121, AT-242

Pd(PPh$_3$)$_4$ (2.7 mg, 2.3 μmol) was added to a solution of **120** (167 mg, 0.117 mmol) and pyrrolidine (20.6 μL, 0.246 mmol) in anhydrous CHCl$_3$ (5 mL). Complete reaction was reached in an hour as observed by TLC. The solvent was removed by rotary evaporation under reduced pressure and the residue purified by flash chromatography (gradient from 4:96 to 8:92 v/v MeOH/CHCl$_3$) to yield AT-242, **121** as an off white solid (123 mg, 88%). A sample was dissolved in deuterated DMSO and NMR data of the diimine form were recorded after 48h. ^{1}H NMR (DMSO) (diimine only) δ 9.88 (m, 4H), 8.04 (t, J = 5.4 Hz, 2H), 7.79 (d, J = 4.4 Hz, 2H), 7.35 (s, 2H), 7.20-7.18 (m, 4H), 6.88 (s, 4H), 6.84 (s, 2H), 4.15-4.04 (m, 4H), 3.84 (m, 18H), 3.70-3.58 (m, 4H), 3.43-3.36 (m, 2H), 3.24 (m, 4H), 2.45 (t, J = 7.3 Hz, 4H), 2.29-2.24 (m, 4H), 2.09-1.94 (m, 8H), 1.69 (m, 2H); ^{13}C NMR (DMSO) δ 168.7, 164.2, 163.3, 161.2, 158.3, 150.1, 146.8, 140.5, 122.9, 122.6, 122.0, 121.9, 119.7, 118.0, 117.8, 111.2, 110.1, 104.0, 103.8, 67.7, 55.5, 53.3, 46.3, 36.0, 35.8, 31.8, 29.6, 28.7, 24.7, 23.6; MS (ES$^+$) m/z (relative intensity) 1197.7 ([M + H]$^+$, 100). HRMS (TOF MS ES$^+$) calcd for C$_{58}$H$_{65}$N$_{15}$O$_{12}$ (M+H): 1191.5370. Found: 1191.5353. [α]^{25}$_D$ = +315° (c = 0.45, CHCl$_3$); IR v 3295.3, 2946.7, 1638.6, 1597.1, 1532.2, 1508.2, 1434.5, 1404.7, 1341.3, 1263.0, 1214.9, 1155.3, 1095.4, 1015.8, 752.1, 663.9 cm^{-1}. Purity by analytical HPLC: Luna : 100 %; Gemini : 98.0 %.

Synthesis of symmetrical tetrapyrrole PBD bisulphite adduct of 121. AT-361

AT361
Bisulphite adduct of 121
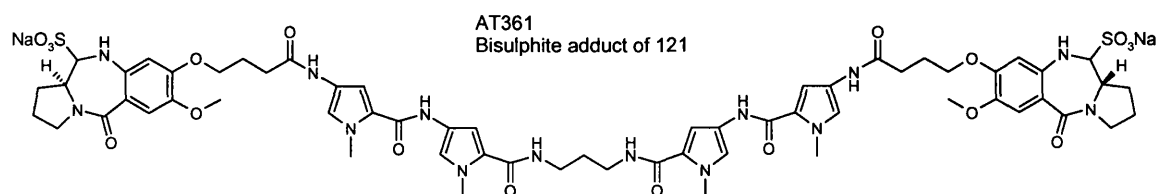
A solution of sodium bisulphite (12.6 mg, 0.12 mmol) in water (2 mL) was added to a stirred solution of enantiomerically pure **121**, (AT-360) (72.0 mg, 60.4 μmol) in dichloromethane (2.0 mL). The reaction mixture was allowed to stir vigorously for 5 h, after which time the organic and aqueous layers were separated. TLC analysis (eluent-90:10 v/v $CHCl_3$/MeOH) of the aqueous phase revealed absence of AT-360 and presence of baseline material with strong UV absorption. The aqueous layer was lyophilised to provide the bisulphite adduct AT-361 as a lightweight white solid (59.2 mg, 70%): ^{1}H NMR ($CDCl_3$) δ 9.89 (m, 4H), 8.03 (t, 2H, J = 5.61 Hz), 7.19 (dd, 4H, J = 10.4, 1.67 Hz), 7.02 (s, 2H), 6.90 (m, 4H), 6.40 (s, 2H), 5.04 (s, 2H), 3.98 (m, 4H), 3.84-3.77 (m, 14H), 3.70 (s, 6H), 3.51-3.43 (m, 4H), 3.26-3.21 (m, 4H), 2.56 (m, 2H), 2.44 (t, 4H, J = 7.27 Hz), 2.11-1.60 (m, 14H); ^{13}C NMR ($CDCl_3$) δ 168.8, 167.1, 161.3, 158.4, 150.8, 142.8, 140.1, 122.9, 122.7, 122.1, 122.0, 118.1, 117.8, 116.9, 112.6, 106.4, 104.1, 78.8, 67.6, 56.5, 55.8, 46.1, 36.0, 35.9, 31.9, 29.4, 22.6; HPLC/MS (ES^+) 2 peaks 1/1 ratio, both showing m/z 1191.97 ([M-2NaHSO$_3$+H]$^{+*}$, 40), 596.56 ([(M-2NaHSO$_3$+2H)/2]$^{+*}$, 100).

Synthesis of symmetrical Boc protected hexapyrrole 122.

122

263
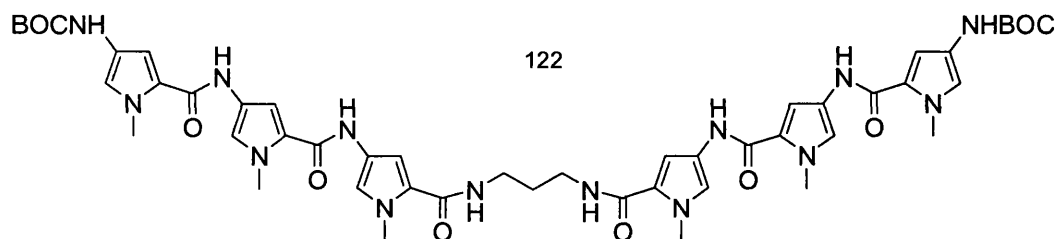
EDCI (195 mg, 1.02 mmol) was added to a solution of Boc-tripyrroleacid (**112**, 450 mg, 0.92 mmol) and HOBt (155.2 mg, 1.02 mmol) in anhydrous DMF (6 mL) and the reaction mixture was allowed to stir for 5 h. Neat 1,3-diaminopropane (42.2 µl, 0.50 mmol) was added and the resulting mixture was allowed to stir overnight. Complete reaction was observed by TLC and the reaction mixture was diluted with $CHCl_3$ (100 mL) and was washed sequentially with 5 % aqueous citric acid (50 mL), water (50 mL), saturated aqueous $NaHCO_3$ (50 mL), brine (50 mL) and dried over $MgSO_4$. The solvents were removed by rotary evaporation under reduced pressure to afford a yellow oil. The oil was triturated with diethylether to give a fine suspension which was allowed to decant over 30 min. The supernatant was removed and the residue was dried under vacuum to yield pure **122** as an off white powder (400 mg, 86%). ^1H NMR (DMSO) δ 9.86 (m, 4H), 9.08 (s, 2H), 8.05 (t, J = 5.61 Hz, 2H), 7.23 (m, 4H), 7.06 (s, 2H), 6.90 (m, 6H), 3.86 (m, 18H), 3.26 (q, J = 6.35 Hz, 4H), 1.71 (m, 2H), 1.47 (s, 18H); ^{13}C NMR (DMSO) δ 162.2, 161.3, 158.4, 158.4, 152.8, 122.9, 122.8, 122.7, 122.2, 122.1, 118.3, 117.8, 117.0, 104.7, 104.1, 103.8, 78.2, 64.8, 36.0, 35.9, 35.8, 35.7, 30.7, 29.7, 28.1, 15.1; MS (ES$^+$) m/z (relative intensity) 1007.6 ($[M + H]^+$, 7), 833.2 (100).

Synthesis of the hexapyrrole Alloc protected carbinolamine conjugate 123
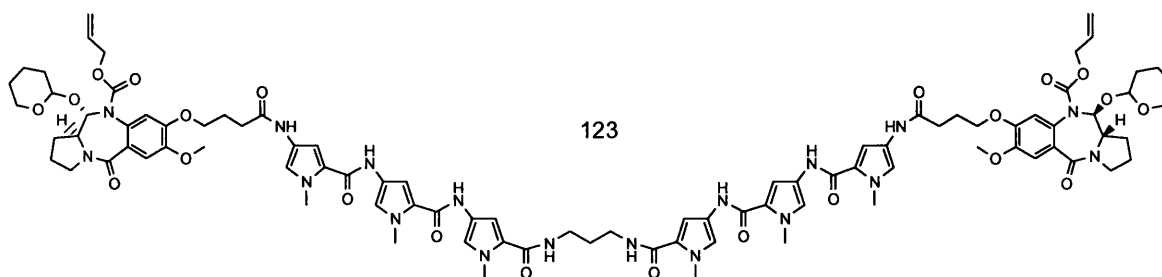
122 (300 mg, 0.298 mmol) was finely suspended in 4N HCl in dioxane (10 mL) and the reaction mixture was allowed to stir for 1 h, and exposed to ultrasound (3 min). The volatiles were removed by rotary evaporation under reduced pressure to afford a grey salt.

In parallel, EDCI (126 mg, 0.656 mmol) was added to a solution of the 4C-N10Alloc-11OTHP-acid PBD capping unit, **57**, (300 mg, 0.597 mmol) and HOBt (100 mg, 0.653

mmol) in anhydrous DMF (5 mL). The reaction mixture was allowed to stir for 3 hours to provide the activated acid solution.

The activated acid solution was then added to a solution of the aforementioned hydrochloride salt in anhydrous DMF (5 mL) and DIPEA (0.5 mL, 2.87 mmol) and the resulting mixture was allowed to stir at 60°C for 1h and then overnight at RT. Completion of the reaction was observed by TLC (interestingly, the product has the same Rf than the starting material **122**) and the mixture was diluted with CHCl$_3$ (100 mL) and washed sequentially with 5 % aqueous citric acid (50 mL), water (50 mL), saturated aqueous NaHCO$_3$ (50 mL), brine (50 mL) and dried over MgSO$_4$. The solvents were removed by rotary evaporation under reduced pressure to afford a yellow oil. The oil was triturated with diethylether and the resulting suspension was allowed to decant for 30 mins. The supernatant was removed and the residue was dried under vacuum to afford a tan solid. The solid was purified further by flash chromatography (gradient from 0:100 to 4:96 v/v MeOH/CHCl$_3$) to yield pure **123** (250 mg, 46%). ^{1}H NMR (DMSO) δ 9.89 (m, 6H), 8.06 (t, J = 5.55 Hz, 2H), 7.21 (m, 6H), 7.10 (m, 4H), 6.89 (m, 6H), 5.75 (m, 4H), 5.18-4.92 (m, 6H), 4.69-4.32 (m, 4H), 4.01 (m, 4H), 3.86 (m, 26H), 3.50 (m, 4H), 3.40 (m, 4H), 3.26 (q, J = 6.34 Hz, 4H), 2.44 (t, J = 7.04 Hz, 4H), 2.18-1.77 (m, 12H), 1.76-1.56 (m, 6H), 1.56-1.30 (m, 8H); ^{13}C NMR (DMSO) δ 168.7, 166.2, 161.3, 158.4, 158.4, 148.3, 148.2, 132.6, 122.9, 122.7, 122.7, 122.1, 122.0, 122.0, 118.4, 118.1, 117.8, 114.4, 104.6, 104.1, 103.8, 79.1, 68.0, 64.8, 55.6, 45.9, 40.1, 36.0, 35.9, 31.7, 30.3, 29.7, 28.4, 28.2, 24.9, 24.7, 24.4, 22.9, 19.2, 15.1; MS (Maldi) m/z (relative intensity) 1679.1 (100), 1663.0 (50). (calculated exact Mass = 1806).

Synthesis of symmetrical diaminopropane hexapyrrole PBD 124.

124, AT-288
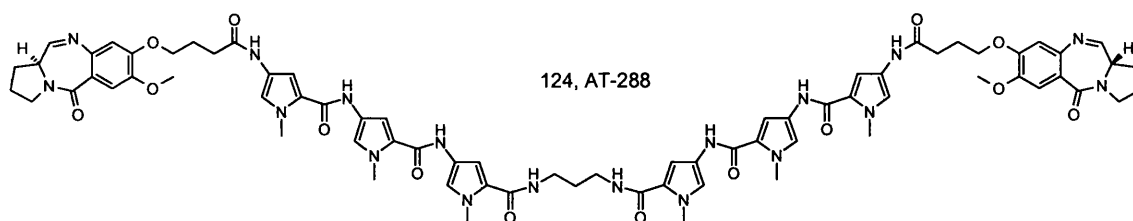
Pd(PPh₃)₄ (2.5 mg, 2.1 μmol) was added to a solution of **123** (200 mg, 0.111 mmol) and pyrrolidine (19.5 μL, 0.233 mmol) in anhydrous CHCl₃ (6 mL). Complete reaction was reached in 2h as observed by TLC. The solvent was removed by rotary evaporation under reduced pressure and the residue purified by flash chromatography (gradient from 4:96 to 9:91 v/v MeOH/CHCl₃) to yield AT-281, **124**, as an off white solid (123 mg, 77%). A sample was dissolved in deuterated DMSO and NMR data of the diimine form were recorded after 48h. ^{1}H NMR (DMSO) (diimine only) δ 9.89 (m, 6H), 8.04 (m, 2H), 7.79 (d, J = 4.4 Hz, 2H), 7.35 (s, 2H), 7.25 (s, 2H), 7.21 (s, 2H), 7.18 (s, 2H), 7.05 (s, 2H), 6.90 (s, 4H), 6.84 (s, 2H), 4.15-4.04 (m, 4H), 3.84 (m, 24H), 3.72-3.58 (m, 4H), 3.41-3.37 (m, 2H), 3.24 (m, 4H), 2.45 (t, J = 7.3 Hz, 4H), 2.30-2.24 (m, 4H, C1), 2.12-1.90 (m, 8H), 1.70 (m, 2H); ^{13}C NMR (DMSO) δ 168.8, 164.2, 163.3, 161.3, 158.4, 158.4, 151.1, 146.9, 140.5, 122.9, 122.7, 122.7, 122.1, 122.0, 121.9, 119.8, 118.4, 118.1, 117.8, 111.2, 110.1, 104.6, 104.1, 103.9, 79.1, 67.8, 55.6, 53.3, 48.5, 46.3, 36.0, 35.9, 31.8, 28.8, 24.7, 23.6, 22.6; MS (ES⁺) m/z (relative intensity) 1435.7 ([M + H]⁺, 35), 718.4 (100). HRMS (TOF MS ES⁺) calcd for C₇₃H₈₂N₁₈O₁₄ (M+H): 1435.6331. Found: 1435.6376; Purity by analytical HPLC: Luna : 100 %; Gemini : 98.6 %.

Synthesis of symmetrical Boc protected bis-imidazole-pyrrole 126.
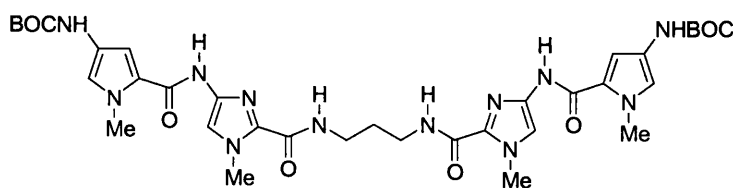
126

Boc-Pyrrole-Imidazole acid **125** (Baird *et al.*, 1996) (580 mg, 1.59 mmol) was coupled with diaminopropane (73 μL, 0.874 mmol) according to method A (omiting the initial Boc deprotection, and using 0.4 eq of DMAP) to yield 400 mg of title compound (33 % yield).

^{1}H NMR (DMSO) δ 10.18 (s, 2H), 9.07 (s, 2H), 8.11 (t, 2H, J = 6.05 Hz), 7.48 (s, 2H), 7.00 (s, 2H), 6.89 (s, 2H), 3.95 (s, 6H), 3.83 (s, 6H), 3.30 (q, 4H, J = 6.34 Hz), 1.60 (p, 2H, J = 6.53 Hz), 1.47 (s, 18H); ^{13}C NMR (DMSO) δ 158.9, 158.7, 152.8, 136.1, 133.9,

122.4, 121.9, 117.9, 114.3, 104.8, 78.2, 36.1, 35.9, 34.8, 30.7, 29.5, 28.2; MS (ES+) m / z 765.4 ([M+H]+•, 100).

Synthesis of bis-imidazole-pyrrole PBD 128, AT-338.
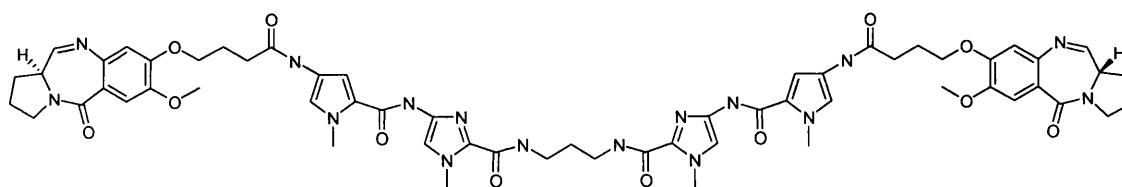
128, AT-338

The Boc protected bis-imidazole-pyrrole **126** (350 mg, 0.457 was deprotected and coupled with 4C-N10Alloc-11OTHP-acid PBD capping unit, **57**, (393 mg, 0.782 mmol) according to general method A to give the bis-imidazole-pyrrole N10Alloc-11OTHP PBD **127** (170 mg, 33 %). This compound was immediately deprotected following general method E to yield **128**, AT-338 (78 mg, 67 %). ^{1}H NMR (DMSO) (diimine only) δ 10.25 (s, 2H), 9.89 (s, 2H), 8.10 (t, 2H, J = 6.1 Hz), 7.79 (d, 2H, J = 4.4 Hz), 7.50 (s, 2H), 7.35 (s, 2H), 7.28 (d, 2H, J = 1.7 Hz), 6.94 (d, 2H, J = 1.8 Hz), 6.84 (s, 2H), 4.21-4.00 (m, 4H), 3.95 (s, 6H), 3.84 (s, 12H), 3.75-3.55 (m, 4H), 3.47-3.35 (m, 2H), 3.30 (m, 4H), 2.45 (t, 4H, J = 7.3 Hz), 2.32-2.20 (m, 4H), 2.05 (p, 4H, J = 6.5 Hz), 1.95 (m, 4H), 1.73 (m, 2H); MS (ES$^+$) m/z (relative intensity) 1193.6 ([M + H]$^+$,100); HRMS (TOF MS ES+) calcd for $C_{59}H_{68}N_{16}O_{12}$ (M+H): 1193.5276. Found: 1193.5259; Purity by analytical HPLC: Luna : 100 %; Gemini : 95.5 %.

11.5 Hairpins polyamide conjugates

11.5.1 Based on a iminodiacetic acid loop

11.5.1.1 Synthesis of hairpin PBD conjugate 131, AT-293

Synthesis of iminodiacetic acid PBD conjugate AT-290 and 129
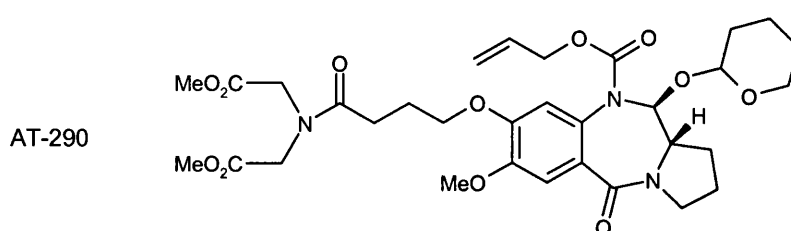
The 4C-N10Alloc-11OTHP-acid PBD capping unit **57** (567 mg, 1.13 mmol) was allowed to stir with EDCI (260 mg, 1.35 mmol) and HOBt (207 mg, 1.35 mmol) in anhydrous DMF (5 mL) for 2 hours under nitrogen. Iminodimethyldiacetate (273 mg, 1.69 mmol) was prepared from its hydrochloride salt by extraction with EtOAc from aqueous K_2CO_3. The free base of iminodimethyldiacetate was then added to the activated acid solution and the resulting mixture was allowed to stir for 48 h at RT. The reaction mixture was then diluted with $CHCl_3$ (100 mL) and was washed sequentially with 5 % aqueous citric acid (50 mL), water (50 mL), saturated aqueous $NaHCO_3$ (50 mL), brine (50 mL) and dried over $MgSO_4$. The solvents were removed by rotary evaporation under reduced pressure to afford the diester AT290 (700 mg, 94%) which was found pure by TLC (EtOAc) and NMR.

^{1}H NMR (CDCl$_3$) (mixture of the two epimers) δ 7.22 (m, 2H), 6.88-6.64 (2s, 2H), 5.80 (m, 4H), 5.10 (m, 6H), 4.66-4.35 (m, 4H), 4.20 (m, 8H), 4.04 (m, 4H), 3.91 (m, 8H), 3.70 (m, 14H), 3.67-3.44 (m, 8H), 2.55 (pseudo t, J = 6.6 Hz, 4H), 2.20-1.98 (m, 12H), 1.76 (m, 4H), 1.53 (m, 8H); ^{13}C NMR (CDCl$_3$)) (mixture of the two epimers) δ 172.90, 172.84, 169.70, 169.35, 167.40, 167.29, 162.49, 149.86, 149.05, 132.24, 132.07, 126.60, 117.18, 114.96, 114.56, 110.77, 110.41, 100.07, 91.78, 88.58, 67.89, 67.60, 66.55, 66.36, 64.03, 63.64, 60.11, 59.95, 56.04, 56.01, 52.47, 52.14, 49.97, 47.90, 46.37, 46.33, 36.44, 31.41, 31.12, 30.93, 29.07, 28.87, 28.69, 25.29, 25.22, 24.51, 24.34; MS (ES$^+$) m/z 100 (506.4, M+H).

129
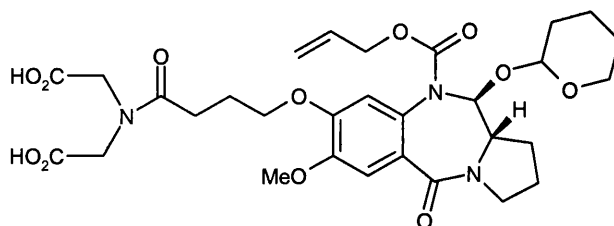
A solution of sodium hydroxyde (180 mg, 4.5 mmol) in water (6 mL) was added to a solution of diester AT-290 (680 mg, 1.03 mmol) in methanol (20 mL). The resulting solution was heated on a rotoevaporator at 70°C at atmospheric pressure for 5 min. More water (10 mL) was added and excess methanol was removed by rotary evaporation under reduced pressure. TLC analysis (EtOAc) revealed completion of the saponification. The aqueous solution was washed with EtOAc (50 mL), acidified with 10% aqueous citric acid to pH 4 and extracted with EtOAc (2 x 30 mL). The organic layers were combined, washed with brine (30 mL), and dried over MgSO₄. The solvent was removed by rotary evaporation under reduced pressure to afford **129** as white powder (500mg, 77 %). Pure by TLC (EtOAc/ MeOH/ Acetic acid: 80/20/0.5) and NMR.

^{1}H NMR (DMSO) (mixture of the two epimers) δ 7.10 (pseudo d, 2H), 6.93-6.83 (2s, 2H), 5.91-5.60 (m, 4H), 5.10 (m, 6H), 4.71-4.32 (m, 4H), 4.20 (m, 4H), 3.99 (m, 8H), 3.83 (m, 8H), 3.59-3.21 (m, 8H), 2.43 (pseudo t, J = 6.63 Hz, 4H), 2.20-1.76 (m, 12H), 1.76-1.59 (m, 4H), 1.58-1.32 (m, 8H); ^{13}C NMR (DMSO) (mixture of the two epimers) δ 174.48, 172.37, 171.22, 170.85, 170.59, 170.29, 166.21, 166.11, 148.43, 148.28, 132.68, 116.67, 114.53, 110.52, 110.32, 99.14, 94.85, 72.42, 67.69, 67.58, 65.70, 65.52, 62.83, 59.71, 59.48, 55.71, 59.48, 55.71, 48.06, 45.94, 42.63, 30.57, 30.29, 28.41, 28.31, 28.08, 27.95, 24.91, 24.80, 24.07, 23.88; MS (ES⁺) m/z 100 (560), 30 (679.1), M+H is not present.

Synthesis of Alloc protected hexa pyrrole diaminoacetate PBD conjugate 130
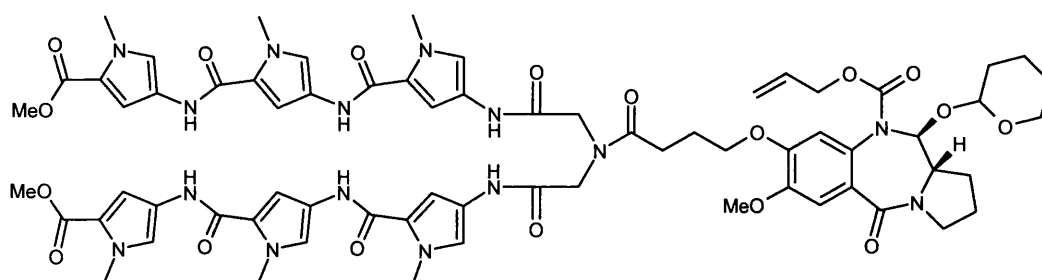
130

EDCI (146 mg, 0.760 mmol) was added to a solution of the diacid **129** (200 mg, 0.315 mmol) and HOBt (116 mg, 0.758 mmol) in anhydrous DMF (5 mL) for 2 hours. BOCNHPyPyPyCO$_2$Me **78** (318 mg, 0.633 mmol) was finely suspended in a 4N solution of HCl in dioxane (10 mL) and stirred for 1h, with occasional ultrasound baths. It was then dried under hard vac and redissolved in anhydrous DMF (5 mL), in the presence of DIPEA (1 mL, 5.75 mmol). The resulting solution was transferred into the previously prepared activated acid solution and stirred for 18 hours. The mixture was diluted with CHCl$_3$ (100 mL) and was washed sequentially with 5 % aqueous citric acid (50 mL), water (50 mL), saturated aqueous NaHCO$_3$ (50 mL). An emulsion was formed which was filtered trough celite and washed with brine (50 mL) and dried over MgSO$_4$. Excess solvent were removed by rotary evaporation under reduced pressure. The residue was purified by flash chromatography (gradient from 1% to 4% of MeOH in CHCl$_3$, with the product eluting from 3%) to yield **130** (90 mg, 20%).

^{1}H NMR (DMSO) (mixture of the two epimers) δ 10.77 (s, 2H), 10.28 (s, 2H), 9.95 (m, 8H), 7.48 (s, 4H), 7.30 (s, 4H), 7.22 (s, 4H), 7.08-6.82 (m, 16H), 6.04-5.57 (m, 4H), 5.40-4.88 (m, 6H), 4.72-4.25 (m, 8H), 4.16 (s, 4H), 3.98 (m, 4H), 3.92-3.62 (m, 56H), 3.58-3.34 (m, 8H), 2.43 (pseudo t, J = 6.63 Hz, 4H), 2.19-1.75 (m, 12H), 1.73-1.55 (m, 4H), 1.55-1.29 (m, 8H); MS (ES$^+$) m/z 60 (1394.4, M+H).

Synthesis of hexa pyrrole diaminoacetate PBD conjugate 131

131, AT-293
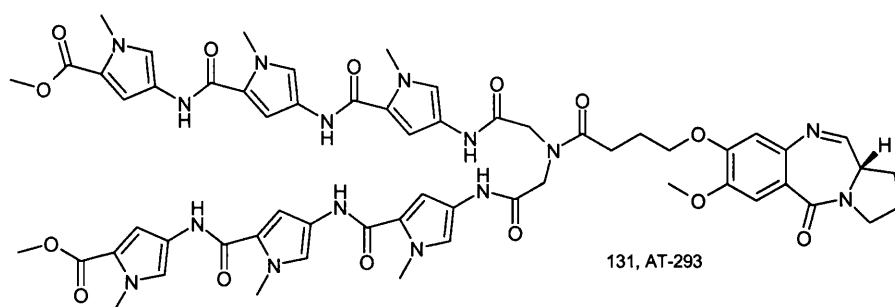
Pd(PPh₃)₄ (1.5 mg, 1 µmol) was added to a stirred solution of **130** (80 mg, 0.057 mmol) and pyrrolidine (5.3 µL, 0.063 mmol) in anhydrous CHCl₃ (4 mL). Complete reaction was reached in 1.5 hours as monitored by TLC. The solvent was removed by rotary evaporation under reduced pressure and the residue purified by flash chromatography (gradient of MeOH in CHCl₃ from to 3% to 7%) to yield AT-293, **131** as an off white solid (57 mg, 83 %). A sample was dissolved in deuterated DMSO and NMR data of the diimine form were recorded after 48h.

¹H NMR (DMSO) (imine only) δ 10.78 (s, 1H), 10.29 (s, 1H), 9.93 (m, 4H), 7.77 (d, *J* = 4.4Hz, 1H), 7.48 (s, 2H), 7.33 (s, 1H), 7.29 (s, 2H), 7.23 (s, 2H), 7.08 (s, 2H), 7.00 (s, 1H), 6.94 (m, 3H), 6.83 (s, 1H), 4.33 (s, 2H), 4.17 (s, 2H), 4.13-4.06 (m, 2H), 3.88 (2s, 18H), 3.78 (2s, 9H), 3.70-3.55 (m, 2H), 3.40-3.37 (m, 2H), 2.50 (m, 2H), 2.36-2.14 (m, 2H), 2.06-1.87 (m, 4H); MS (ES⁺) *m/z* 100 (1208.2, M+H). HRMS (TOF MS ES⁺) calcd for C₅₉H₆₅N₁₅O₁₄ (M+H): 1208.4908. Found: 1208.4856; Purity by analytical HPLC : Luna : 94.2 %; Gemini : 93.0 %.

11.5.2 Based on the R-2,4-diaminobutyric acid

11.5.2.1 Synthesis of hexa pyrrole conjugate **136**, AT-307.

Synthesis of 4-[(4-{[4-(4-Benzyloxycarbonylamino-2-tert-butoxycarbonylamino-butyrylamino)-1-methyl-1H-pyrrole-2-carbonyl]-amino}-1-methyl-1H-pyrrole-2-carbonyl)-amino]-1-methyl-1H-pyrrole-2-carboxylic acid methyl ester 132.
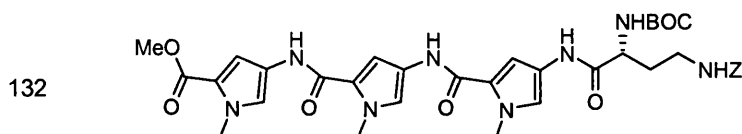
Boc-D-Dab(Z)-OH (720 mg, purchased from Bachem) and BocPyPyPyCOOMe **78** (818 mg) were coupled following method A. The product was purified using a gradient of MeOH in chloroform, from 0:100 up to 1:99. Pure product eluted from 0.6:99.4. Evaporation of the pure fractions provided the desired coupled product (615 mg, 51%). **(132)**.

^{1}H NMR (DMSO) δ 9.94-9.85 (m, 3H), 7.48 (d, 1H, J = 1.85 Hz), 7.38-7.32 (m, 5H), 7.25-7.19 (m, 3H), 7.08 (d, 1H, J = 1.68 Hz), 7.02 (d, 1H, J = 7.90 Hz), 6.93 (m, 2H), 5.03 (s, 2H), 4.08 (m, 1H), 3.87 (m, 9H), 3.76 (s, 3H), 3.07 (q, 2H, J = 5.91 Hz), 1.93-1.63 (m, 2H), 1.41 (s, 9H); ^{13}C NMR (DMSO) δ 169.1, 160.8, 158.5, 158.4, 156.0, 155.3, 137.1, 128.3, 127.8, 122.9, 122.8, 122.5, 122.2, 121.5, 120.7, 118.6, 118.5, 118.3, 108.4, 104.8, 104.2, 78.1, 65.2, 52.4, 50.9, 37.5, 36.1, 36.0, 32.1, 28.2; MS (ES$^+$) m/z 733.1 ([M+H]$^{+\cdot}$, 50), 633.1([M-BOC+H]$^{+\cdot}$, 70).

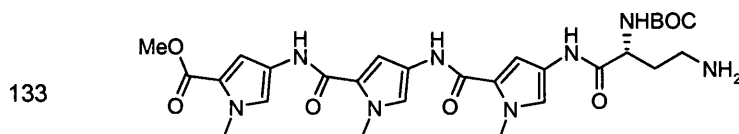**Synthesis of 4-[(4-{[4-(4-Amino-2-tert-butoxycarbonylamino-butyrylamino)-1-methyl-1H-pyrrole-2-carbonyl]-amino}-1-methyl-1H-pyrrole-2-carbonyl)-amino]-1-methyl-1H-pyrrole-2-carboxylic acid methyl ester 133.**


A solution of Cbz protected **132** (200 mg) in ethanol (30 mL) over 10 % Pd/C (50 mg) was hydrogenated under 15 PSI for 30 min. Hydrogenolysis was then deemed complete

by TLC analysis. The Pd/C was removed by filtration and the filtrate was then concentrated to dryness by rotary evaporation under reduced pressure. The residue was purified by chromatography (gradient from 0:100 to 25:75, methanol:chlorofom). Rotary evaporation of the pure fractions under reduced pressure yielded **133** as the free amine (96 mg, 59%). (NB: It was discovered in a subsequent experiment that hydrogenation in methanol gives rise to fewer impurities.)

^{1}H NMR (DMSO) δ 10.06 (s, 1H), 9.95 (m, 2H), 7.48 (d, 1H, J = 1.89 Hz), 7.43 (bs, 2H), 7.25 (d, 1H, J = 1.75 Hz), 7.19 (d, 1H, J = 1.65 Hz), 7.17 (d, 1H, J = 7.81 Hz), 7.08 (d, 1H, J = 1.79 Hz), 6.96 (d, 1H, J = 1.80 Hz), 6.93 (d, 1H, J = 1.94 Hz), 4.19 (q, 1H, J = 6.63 Hz), 3.86 (m, 9H), 3.76 (s, 3H), 2.80 (t, 2H, J = 7.47 Hz), 2.03-1.78 (m, 2H), 1.42 (s, 9H); ^{13}C NMR (DMSO) δ 160.8, 158.5, 158.3, 122.9, 122.8, 122.5, 122.2, 121.4, 120.7, 118.6, 118.5, 118.3, 108.4, 104.8, 104.2, 78.3, 50.9, 36.3, 36.1, 36.0, 35.9, 28.2; MS (ES$^+$) m/z 599.1 ([M+H]$^{+\bullet}$, 100), 499.1 ([M-BOC+H]$^{+\bullet}$, 10).

Synthesis of 1-Methyl-4-({1-methyl-4-[(1-methyl-1H-pyrrole-2-carbonyl)-amino]-1H-pyrrole-2-carbonyl}-amino)-1H-pyrrole-2-carboxylic acid 134.

134
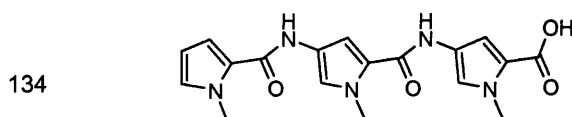
Nitropyrrole dimer **110** (1g, 3.26 mmol) was suspended in DMF (20 mL), in the presence of Pd/C 10% (100 mg) and reduced by hydrogenation under 45 PSI. Separately, commercially available 1-methylpyrrole-2-carboxylic acid (408 mg, 3.26 mmol) was dissolved in anhydrous DMF (20 ml), followed by HOBt (500 mg, 3.26 mmol) and EDCI (626 mg, 3.26 mmol). The mixture was allowed to stir for 5 hours. After completion of the hydrogenation was proved by TLC analysis, Pd/C was removed by filtration, and the filtrate was added to the activated acid solution. The resulting mixture was allowed to stir overnight and the reaction was deemed complete by TLC. It was slowly added to 500 mL of water with vigorous stirring. The resulting precipitate was collected by filtration and immediately saponified following method C. It provided the pure tripyrrole acid **134** as a colourless powder (1.14 g).

^{1}H NMR (DMSO) δ 9.92 (s, 1H), 9.85 (s, 1H), 7.44 (d, 1H, J = 1.84 Hz), 7.24 (d, 1H, J = 1.66 Hz), 7.05 (d, 1H, J = 1.74 Hz), 6.95-6.92 (m, 2H), 6.86 (d, 1H, J = 1.92 Hz),

6.06 (dd, 1H, J = 2.59 Hz, J = 3.82 Hz), 3.88 (s, 3H), 3.85 (s, 3H), 3.83 (s, 3H) ; ^{13}C

NMR (DMSO) δ 161.9, 158.6, 158.4, 128.1, 125.4, 122.6, 122.5, 122.1, 120.2, 119.4,

118.4, 112.6, 108.3, 106.6, 104.6, 36.2, 36.1, 36.0; IR (golden gate) v 1650, 1556, 1413,

1249, 112, 1059, 664 cm^{-1}; MS (ES$^-$) m/z 368.1 ([M-H]$^{-\bullet}$, 100).

Synthesis of Boc protected diaminobutyric hexapyrrole 135.

135
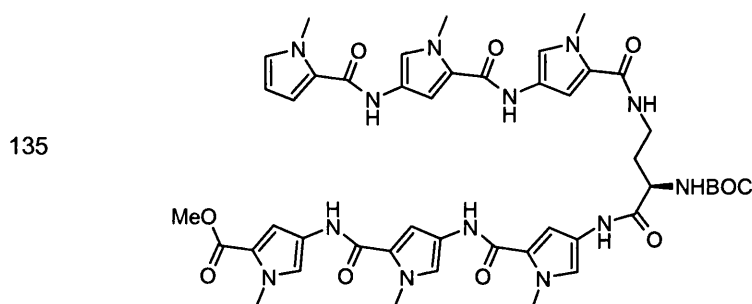
Free amine **133** (87mg) was coupled to carboxylic acid **134** (56 mg) following method A (omitting the Boc deprotection step). The product was used in the next step without further purification. Yield: 138 mg, quantitative. **135**,

^{1}H NMR (DMSO) δ 9.95-9.90 (m, 4H), 9.82 (s, 1H), 7.98 (m, 1H), 7.48 (d, 1H, J = 1.88 Hz), 7.25-7.24 (m, 2H), 7.20 (m, 2H), 7.07-7.02 (m, 3H), 6.96-6.91 (m, 5H), 6.07 (dd, 1H, J = 2.54 Hz, J = 3.87 Hz), 4.11 (q, 1H, J = 7.06 Hz), 3.92-3.82 (m, 18H), 3.76 (s, 3H), 3.30-3.16 (m, 2H), 1.93-1.80 (m, 2H), 1.42 (s, 9H); ^{13}C NMR (DMSO) δ 169.2, 162.3, 160.8, 158.6, 158.5, 155.3, 128.1, 125.4, 122.9, 122.8, 122.5, 122.2, 122.0, 120.7, 118.6, 118.5, 118.4, 112.6, 108.4, 106.6, 104.7, 78.1, 50.9, 36.2, 36.1, 36.0, 35.9, 35.7, 32.2, 30.7, 28.2; MS (ES$^+$) m/z 950.3 ([M+H]$^{+\bullet}$, 100).

Synthesis of hexa pyrrole diaminobutyric acid Alloc THP protected PBD conjugate AT-306.

AT-306
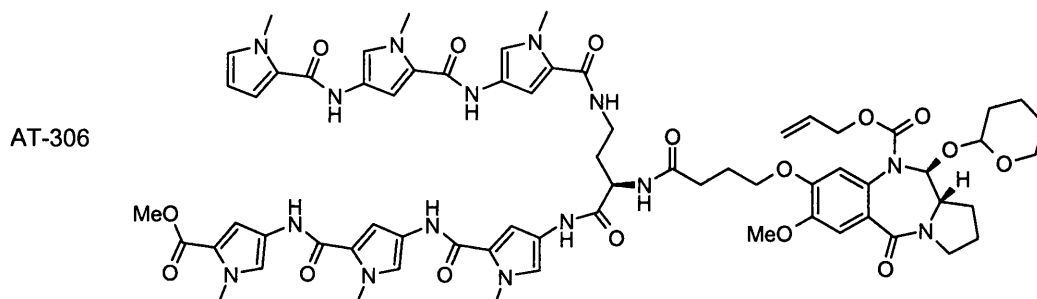
Boc protected polypyrrole **135** (123 mg) was coupled to 4C-Alloc-THP-PBD acid capping unit **57** (65 mg) following method A. The product was purified by chromatography. (gradient from 2:98 to 4.5:95.5, methanol:chlorofom). Evaporation of the pure fractions provided the desired coupled product (100 mg, 57%). (**AT-306**).

^{1}H NMR (DMSO) (mixture of 2 epimers arising from the THP group) δ 10.04 (s, 1H), 9.92 (m, 3H), 9.82 (s, 1H), 8.22 (d, 1H, J = 7.23 Hz), 7.96 (t, 1H, J = 5.87 Hz), 7.48 (d, 1H, J = 1.88 Hz), 7.25-7.20 (m, 4H), 7.11-7.05 (m, 3H), 6.96-6.84 (m, 6H), 6.07 (dd, 1H, J = 2.53 Hz, J = 3.87 Hz), 5.90-5.50 (m, 2H), 5.41-4.92 (m, 3H), 4.73-4.30 (m 3H), 4.10-3.93 (m, 2H), 3.93-3.78 (m, 21H), 3.77-3.70 (m, 4H), 3.50 (m, 2H), 3.38 (m, 2H), 3.29-3.14 (m, 2H), 2.39 (m, 2H), 2.21-1.73 (m, 8H), 1.65 (m, 2H), 1.46 (m, 4H); MS (ES^{+}) m/z 1350.4 ([M+H]$^{+}$, 100).

Synthesis of hexa pyrrole diaminobutyric acid PBD conjugate 136.

AT-307, 136
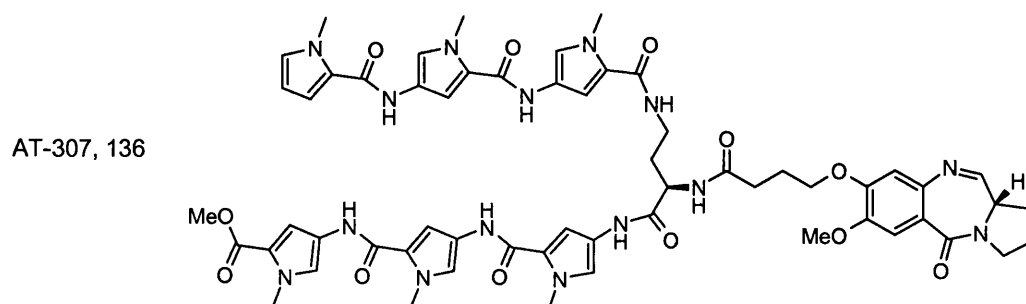
Alloc-THP protected carbinolamine **AT-306** (89 mg) was deprotected following method E. The product was purified by chromatography. (gradient from 3:97 to 6:94,

methanol:chlorofom). Evaporation of the pure fractions provided the desired coupled product (61 mg, 80%). AT-307, **136**

^{1}H NMR (DMSO) δ 10.03 (s, 1H), 9.93 (m, 3H), 9.82 (s, 1H), 8.23 (d, 1H, J = 7.83 Hz), 7.95 (m, 2H), 7.77 (d, 2H, J = 4.40 Hz), 7.48 (d, J = 1.88 Hz, 1H), 7.35 (s, 2H), 7.24 (m, 4H), 7.07 (m, 2H), 6.93 (m, 5H), 6.85 (s, 1H), 6.07 (dd, 1H, J = 1.73Hz, J = 3.89 Hz, 1H), 4.51-4.40 (m, 1H), 4.18-3.99 (m, 2H), 3.94-3.79 (m, 21H), 3.75 (s, 3H) 3.70-3.56 (m, 2H), 3.40-3.20 (m, 3H), 2.39 (t, 2H, J = 7.20 Hz), 2.34-2.16 (m, 1H), 2.08-1.89 (m, 5H), 1.87-1.70 (m, 2H); MS (ES$^+$) m/z 1164.6 ([M+H]$^{+\bullet}$, 50); HRMS (TOF MS ES$^+$) calcd for $C_{58}H_{65}N_{15}O_{12}$ (M+H): 1164.5010. Found: 1164.5023; Purity by analytical HPLC : Luna : 91.4 %; Gemini : 90.2 %.

11.5.2.2 Synthesis of AT-313

Synthesis of 1-Methyl-4-[(1-methyl-1H-pyrrole-2-carbonyl)-amino]-1H-imidazole-2-carboxylic acid methyl ester 137.

137
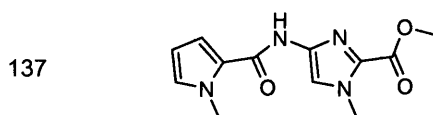
A suspension of imidazole amine **98** (252 mg, 1.62 mmol), commercially available 1-methylpyrrole-2-carboxylic acid (203 g, 1.62 mmol), EDCI (466 mg, 2.43 mmol), and DMAP (40 mg, 0.32 mmol) in dry DMF (5 mL) was allowed to stir overnight at room temperature, followed by stirring for a further 6 h at 60 °C. The reaction mixture was added dropwise to a stirred mixture of ice/water (200 mL) and the resulting suspension was allowed to stir for 30 min. The precipitate was collected by vacuum filtration, washed with water, and dried to provide pure PyImCO2Me **137** (340 mg, 80 %).

^{1}H NMR (DMSO) δ 10.58 (s, 1H), 7.68 (s, 1H), 7.19 (dd, 1H, J = 1.73 Hz, J = 3.73 Hz), 6.99 (s, 1H), 6.05 (dd, 1H, J = 2.52 Hz, J = 3.97 Hz), 3.95 (s, 3H), 3.90 (s, 3H), 3.83 (s, 3H); ^{13}C NMR (DMSO) δ 158.9, 158.7, 137.9, 130.7, 128.9, 124.4, 115.2, 114.0, 106.9, 51.7, 36.4, 35.4; MS (ES$^+$) m/z 262.9 ([M+H]$^{+\bullet}$, 100).

Synthesis of 1-Methyl-4-({1-methyl-4-[(1-methyl-1H-pyrrole-2-carbonyl)-amino]-1H-imidazole-2-carbonyl}-amino)-1H-pyrrole-2-carboxylic acid methyl ester 138.

138
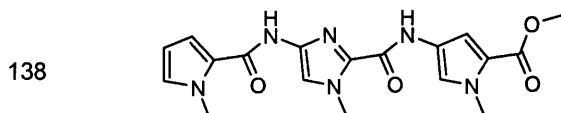
Methyl ester **137** (100 mg, 0.38 mmol) was saponified following method C to provide pure PyImCOOH **143** (82 mg, 86 %). The acid was coupled to the hydrochloride salt of pyrrole amino ester **85** (63 mg, 0.33 mmol) following method A (omitting the Boc deprotection step). The crude product was subjected to flash chromatography (100 % chloroform). Evaporation of the pure fractions yielded the desired coupled product **138** (90 mg, 71 %) , 2 carbon too many (solvent ether or DMF).

^{1}H NMR (DMSO) δ 10.19 (s, 1H), 10.12 (s, 1H), 7.56-7.53 (m, 2H), 7.11 (dd, 1H, J = 1.72 Hz, J = 3.99 Hz), 7.01-6.99 (m, 2H), 6.07 (dd, 1H, J = 2.53 Hz, J = 3.95 Hz), 3.99 (s, 3H), 3.90 (s, 3H), 3.86 (s, 3H), 3.76 (s, 3H); ^{13}C NMR (DMSO) δ 160.7, 158.8, 155.9, 136.1, 133.9, 128.8, 124.5, 122.0, 120.9, 118.8, 114.7, 113.8, 108.6, 106.9, 64.9, 50.9, 36.4, 36.2, 34.9, 15.1; MS (ES$^+$) m/z 385.0 ([M+H]$^{+*}$, 100).

Synthesis of Boc protected diaminobutyric hexa heterocycles 139.

139
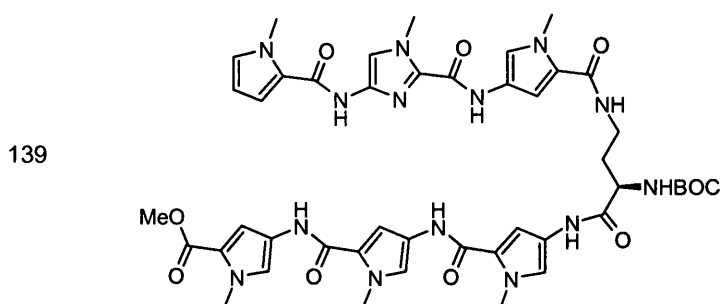
Methyl ester **138** (82 mg, 0.21 mmol) was saponified following method C to provide pure PyImPyCOOH (68 mg, 86 %). The acid was coupled to the free amine **133** (110 mg, 0.18 mmol) following method A (omitting the Boc deprotection step). The crude product was subjected to flash chromatography (gradient elution from 0:100 to 3.5:96.5 methanol:chloroform). Evaporation of the pure fractions yielded the desired coupled product (110 mg, 63 %) **139**.

^{1}H NMR (DMSO) δ 10.21 (s, 1H), 9.93-9.89 (m, 4H), 7.98 (m, 1H), 7.56 (s, 1H), 7.48 (d, 1H, J = 1.63 Hz), 7.25-7.20 (m, 3H), 7.12 (m, 1H), 7.07-6.92 (m, 6H), 6.07 (dd, 1H, J = 2.63 Hz, J = 3.78 Hz), 4.11 (q, 1H, J = 7.11 Hz), 3.99 (s, 3H), 3.91 (s, 3H), 3.86-3.83 (m, 12H), 3.76 (s, 3H), 3.30-3.16 (m, 2H), 1.94-1.78 (m, 2H), 1.42 (s, 9H); ^{13}C NMR (DMSO) δ 160.8, 158.8, 158.4, 158.3, 155.7, 136.1, 134.1, 128.8, 124.5, 123.2, 122.9, 122.8, 122.5, 122.2, 121.1, 120.7, 118.5, 117.9, 114.5, 113.7, 108.4, 106.9, 104.2, 78.1, 50.9, 36.4, 36.1, 36.0, 34.8, 28.2; MS (ES$^+$) m/z 951.1 ([M+H]$^{+*}$, 100).

Synthesis of hexa-heterocycles diaminobutyric acid PBD conjugate 140.

AT-313, 140
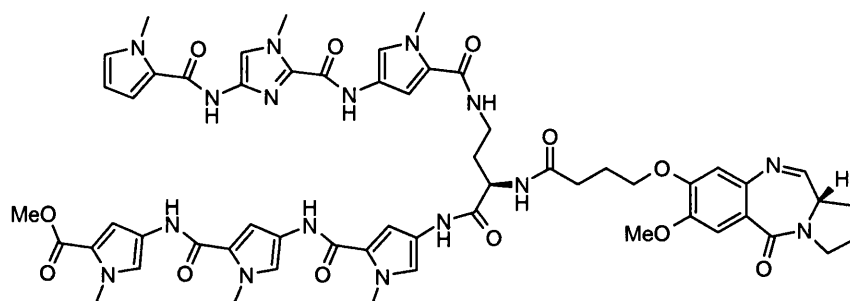
Boc protected amino ester **139** (102 mg, 0.11 mmol) was coupled to 4C-Alloc-THP PBD acid **57** (54 mg, 0.11 mmol) following method A. The crude product was subjected to flash chromatography (gradient elution from 0:100 to 4:96 methanol:chloroform). Rotary evaporation of the pure fractions under reduced pressure yielded the desired coupled product (70 mg, 48 %) AT312.

(57 mg, 0.042 mmol) were immediately deprotected following method E. The crude product was subjected to flash chromatography (gradient elution from 0:100 to 5:95 methanol:chloroform). Rotary evaporation of the pure fractions under reduced pressure yielded the desired biologically active compound AT-313, **140** (30 mg, 61 %).

^{1}H NMR (DMSO) (diimine only) δ 10.21 (s, 1H), 10.03 (s, 1H), 9.93 (m, 2H), 9.88 (s, 1H), 8.23 (d, J = 7.72 Hz, 1H), 7.97 (t, J = 5.66 Hz, 1H), 7.77 (d, J = 4.4 Hz, 1H), 7.56 (s, 1H), 7.48 (d, J = 1.88 Hz, 1H), 7.35 (s, 1H), 7.24 (m, 2H), 7.20 (d, J = 1.72 Hz, 1H), 7.12 (dd, J = 1.69 Hz, J = 3.99 Hz, 1H), 7.07 (d, J = 1.74 Hz, 1H), 6.99 (t, J = 2.02 Hz, 1H), 6.93 (m, 3H), 6.85 (s, 1H), 6.07 (dd, J = 2.52 Hz, J = 3.93 Hz, 1H), 4.51-4.42 (m, 1H), 4.18-4.01 (m, 2H), 3.99 (s, 3H), 3.90 (s, 3H), 3.88-3.84 (m, 12H), 3.82 (s, 3H), 3.76 (s, 3H), 3.70-3.56 (m, 3H), 3.44-3.36 (m, 2H), 2.39 (t, J = 7.24 Hz, 2H), 2.34-2.16

(m, 1H), 2.08-1.89 (m, 5H), 1.89-1.74 (m, 2H) ; ^{13}C NMR (DMSO) δ 171.79, 163.79, 164.13, 163.32, 161.11, 160.77, 158.74, 158.45, 158.36, 155.70, 146.91, 140.56, 136.14, 134.05, 124.52, 123.23, 122.95, 122.86, 122.51, 122.17, 121.47, 121.10, 120.72, 119.75, 118.57, 118.49, 117.90, 114.48, 113.75, 11.26, 110.16, 108.36, 106.94, 104.12, 67.78, 55.60, 53.36, 50.90, 48.56, 46.33, 36.37, 36.12, 36.02, 35.52, 34.84, 31.45, 28.78, 24.71, 23.62 ; MS (ES$^+$) *m/z* 10 (1165.4, M+H), 100 (950.6); HRMS (TOF MS ES$^+$) calcd for $C_{57}H_{64}N_{16}O_{12}$ (M+H): 1165.4962. Found: 1165.4998; Purity by analytical HPLC : Luna : 98.2 %; Gemini : 96.8 %.

11.5.2.3 Synthesis of AT-329 (the starting material BocPyImCO$_2$Me is described in the synthesis of dimer AT-338)

Synthesis of 4-{[4-(3-tert-Butoxycarbonylamino-propionylamino)-1-methyl-1H-pyrrole-2-carbonyl]-amino}-1-methyl-1H-imidazole-2-carboxylic acid methyl ester 142.

The Boc methyl ester **141** (1.5 g, 3.98 mmol) was coupled to Boc β-alanine (828 mg, 4.37 mmol) according to method A (work-up using ethyl acetate (100 mL) instead of chloroform). The crude product was subjected to flash chromatography (gradient elution from 0:100 to 1:99 methanol:chloroform). Rotary evaporation of the pure fractions under reduced pressure yielded the desired coupled product **142** (1.48 g, 83 %).
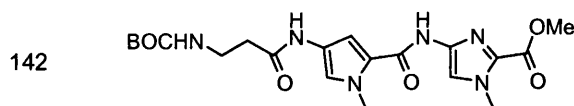
^{1}H NMR (DMSO) δ 10.68 (s, 1H), 9.88 (s, 1H), 7.68 (s, 1H), 7.31 (d, 1H, *J* = 1.72 Hz), 6.96 (d, 1H, *J* = 1.85 Hz), 6.81 (t, 1H, *J* = 5.42 Hz), 3.95 (s, 3H), 3.85 (s, 3H), 3.84 (s, 3H), 3.20 (q, 2H, *J* = 7.03 Hz), 2.42 (t, 2H, *J* = 7.34 Hz), 1.39 (s, 9H); ^{13}C NMR (DMSO) δ 167.6, 158.9, 158.6, 155.5, 137.8, 130.6, 121.9, 121.6, 119.3, 115.4, 104.7, 79.1, 77.6, 51.7, 36.7, 36.3, 35.8, 35.4, 28.2 ; MS (ES$^+$) *m/z* 449.2 ([M+H]$^{+\bullet}$, 100).

Synthesis of 1-Methyl-4-({1-methyl-4-[3-({1-methyl-4-[(1-methyl-1H-pyrrole-2-carbonyl)-amino]-1H-imidazole-2-carbonyl}-amino)-propionylamino]-1H-pyrrole-2-carbonyl}-amino)-1H-imidazole-2-carboxylic acid methyl ester 144.

144
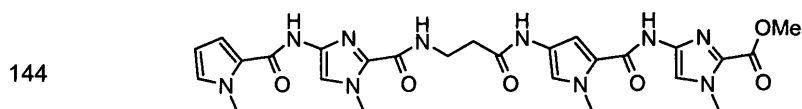
Boc β-alaPyImCO$_2$Me **142** (300 mg, 0.669 mmol) was coupled to PyImCO$_2$H **143** (183 mg, 0.737 mmol) according to method A. The crude product was subjected to flash chromatography (gradient elution from 0:100 to 2:98 methanol:chloroform). Rotary evaporation of the pure fractions under reduced pressure yielded the desired coupled product **144** (230 g, 59 %).

^{1}H NMR (DMSO) δ 10.71 (s, 1H), 10.35 (s, 1H), 9.99 (s, 1H), 7.91 (t, 1H, J = 5.78 Hz), 7.68 (s, 1H), 7.53 (s, 1H), 7.32 (d, 1H, J = 1.75 Hz), 7.13 (dd, 1H, J = 1.70 Hz, J = 3.99 Hz), 6.98 (m, 2H), 6.04 (dd, 1H, J = 2.52 Hz, J = 3.96 Hz), 3.97 (s, 3H), 3.94 (s, 3H), 3.89 (s, 3H), 3.86 (s, 3H), 3.83 (s, 3H), 3.55 (q, 2H, J = 6.18 Hz), 2.57 (t, 2H, J = 6.37 Hz) ; ^{13}C NMR (DMSO) δ 167.9, 158.9, 158.6, 158.5, 158.4, 137.8, 136.2, 133.5, 130.6, 128.8, 124.5, 121.8, 121.7, 119.3, 115.4, 114.0, 113.8, 106.9, 104.7, 51.7, 36.4, 36.3, 35.4, 35.0, 34.9, 34.8 ; MS (ES$^+$) m/z 579.2 ([M+H]$^{+•}$, 100); IR (Golden gate) v 1648, 1529, 1465, 1405, 1248, 1125, 745 cm^{-1}.

**Synthesis of 4-({4-[3-({4-[(4-tert-Butoxycarbonylamino-1-methyl-1H-pyrrole-2-carbonyl)-amino]-1-methyl-1H-imidazole-2-carbonyl}-amino)-propionylamino]-1-methyl-1H-pyrrole-2-carbonyl}-amino)-1-methyl-1H-imidazole-2-carboxylic acid methyl ester 146.**

146
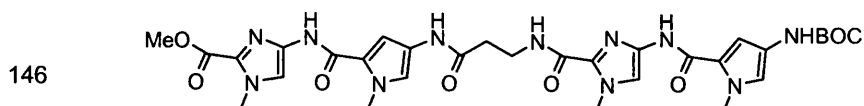
Boc β-alaPyImCO$_2$Me **142** (600 mg, 1.34 mmol) was coupled to BocPyImCO$_2$H **145** (535 mg, 1.47 mmol) according to method A. The crude product was subjected to flash chromatography (gradient elution from 0:100 to 1.5:98.5 methanol:chloroform). Rotary

evaporation of the pure fractions under reduced pressure yielded the desired coupled product (600 mg, 65 %) **146**.

^{1}H NMR (DMSO) δ 10.72 (s, 1H), 10.33 (s, 1H), 10.0 (s, 1H), 9.09 (bs, 1H), 7.94 (t, 1H, J = 5.82 Hz), 7.68 (s, 1H), 7.50 (s, 1H), 7.33 (d, 1H, J = 1.73 Hz), 6.98 (m, 2H), 6.89 (s, 1H), 3.96 (s, 3H), 3.95 (s, 3H), 3.86 (s, 3H), 3.83 (s, 3H), 3.81 (s, 3H), 3.54 (q, 2H, J = 6.31 Hz), 2.57 (t, 2H, J = 6.40 Hz), 1.46 (s, 9H); ^{13}C NMR (DMSO) δ 167.9, 158.9, 158.6, 158.5, 158.4, 152.8, 137.8, 136.2, 133.6, 130.6,122.3, 121.9, 121.8, 121.7, 119.3, 117.9, 115.4, 114.2, 104.8, 104.7, 78.2, 51.7, 36.3, 36.1, 35.4, 35.0, 34.9, 34.8, 28.1; MS (ES$^+$) m/z 693.3 ([M+H]$^{+*}$, 100); IR (Golden gate) v 1654, 1527, 1464, 1403, 1244, 1159, 1128, 1061, 751 cm^{-1}.

Synthesis of MeOImPyβalaImPy-D-Dab(Z)-Boc AT-324.
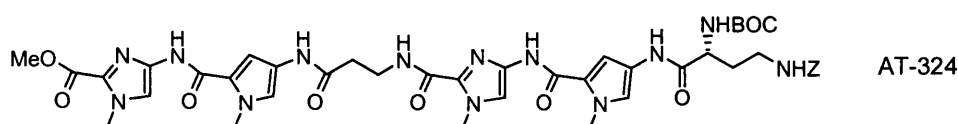
BocPyImβ-alaPyImCO2Me **146** (555 mg, 0.80 mmol) was coupled to Boc-D-Dab(Z)-OH (purchased from Bachem, 338 mg, 0.96 mmol) according to method A. The crude product was subjected to flash chromatography (gradient elution from 0:100 to 2:98 methanol:chloroform). Rotary evaporation of the pure fractions under reduced pressure yielded the desired coupled product (359 mg, 48 %). AT-324.

^{1}H NMR (DMSO) (main rotamer only) δ 10.72 (s, 1H), 10.42 (s, 1H), 10.0 (s, 1H), 9.87 (bs, 1H), 7.93 (t, 1H, J = 5.78 Hz), 7.68 (s, 1H), 7.53 (s, 1H), 7.42-7.27 (m, 6H), 7.21 (m, 2H), 7.06 (d, 1H, J = 7.87 Hz), 6.97 (m, 2H), 5.02 (s, 2H), 4.07 (m, 1H), 3.96 (s, 3H), 3.94 (s, 3H), 3.86 (s, 3H), 3.84 (s, 3H), 3.83 (s, 3H), 3.54 (q, 2H, J = 6.30 Hz), 3.05 (m, 2H), 2.57 (t, 2H, J = 6.34 Hz), 1.70 (m, 2H), 1.39 (s, 9H) ; ^{13}C NMR (DMSO) δ 169.2, 167.9, 158.9, 158.5, 158.4, 156.0, 155.3, 137.8, 137.1, 136.1, 133.6, 130.6, 128.3, 127.8, 121.8, 121.7, 121.5, 119.3, 119.2, 115.4, 114.3, 104.7, 78.0, 65.2, 65.1, 52.3, 51.7, 44.4, 37.5, 36.3, 36.2, 35.4 35.0, 34.9, 34.8, 32.1, 28.2, 14.5 ; MS (ES$^+$) m/z 928.1 ([M+H]$^{+*}$, 100); IR (Golden gate) v 1708, 1659, 1529, 1403, 1367, 1245, 1163, 1129, 1057, 1018, 751 cm^{-1}.

Synthesis of MeOImPyβalaImPy-D-Dab-Boc 147

147
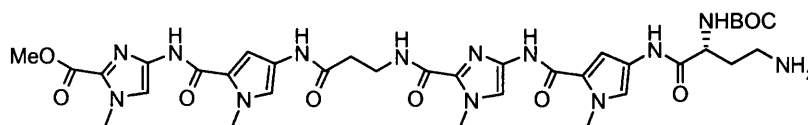
Cbz protected AT-324 (330 mg, 0.355 mmol) was hydrogenated overnight in methanol (50 mL) under 15 PSI over 10% Pd/C (90 mg). Hydrogenolysis was found complete by TLC analysis. The Pd/C was removed by filtration. The filtrate was concentrated to dryness by rotary evaporation under reduced pressure. The residue was purified by chromatography (gradient from 0:100 to 30:70, methanol:chlorofom). Rotary evaporation of the pure fractions under reduced pressure yielded **147** as the free amine. (90 mg, 32 %).

^{1}H NMR (DMSO) δ 10.72 (s, 1H), 10.43 (s, 1H), 10.08-10.03 (m, 2H), 7.92 (t, J = 5.9 Hz, 1H), 7.68 (s, 1H), 7.52 (s, 1H), 7.33-7.29 (m, 2H), 7.19 (d, J = 7.8 Hz, 1H), 6.98 (m, 2H), 4.17 (m, 1H), 3.95 (m, 6H); 3.86-3.78 (m, 9H), 3.57-3.52 (m, 2H), 2.75 (t, J = 7.5 Hz, 2H), 2.57 (t, J = 6.5 Hz, 2H), 1.94-1.80 (m, 2H), 1.39-1.33 (m, 9H); ^{13}C NMR (DMSO, 125 MHz) δ 168.9, 159.8, 159.5, 159.4, 138.7, 137.1, 134.6, 131.7, 122.9, 122.8, 122.7, 122.4, 120.3, 120.1, 116.3, 115.2, 105.8, 80.1, 56.9, 52.6, 37.4, 37.2, 37.1, 36.3, 36.0, 35.8, 32.0, 29.1, 19.4; MS (ES$^+$) m/z 794.2 ([M+H]$^{+\bullet}$, 100).

Synthesis of hairpin MeOImPyβalaImPy-D-Dab-Boc-ImPyβalaImPy 148.

148
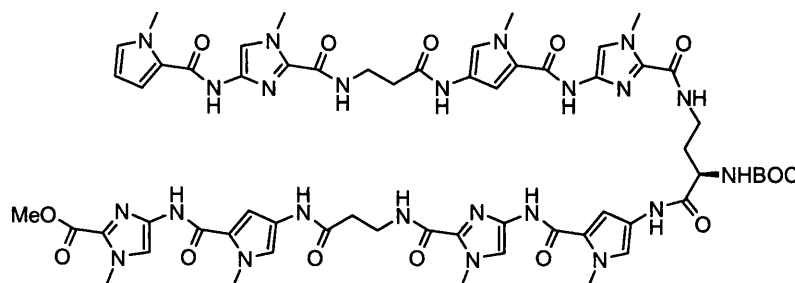
The methyl ester **146** (195 mg, 0.337 mmol) was saponified according to method E. The resulting acid (57.5 mg, 0.102 mmol) was coupled to amine **147** (81 mg, 0.102 mmol) according to method A (omitting the Boc deprotection step). The crude product was subjected to flash chromatography (gradient elution from 0:100 to 8:92

methanol:chloroform, the product started eluting at 6:94). Rotary evaporation of the pure fractions under reduced pressure yielded the desired coupled product (90 mg, 66 %) **148**.

^{1}H NMR (DMSO) δ 10.72 (s, 1H), 10.42-10.34 (m, 3H), 9.99-9.95 (m, 3H), 7.95-7.90 (m, 3H), 7.68 (s, 1H), 7.52-7.50 (m, 3H), 7.32-7.28 (m, 3H), 7.13-7.02 (m, 2H), 6.98-6.92 (m, 4H), 6.04 (m, 1H), 4.17-4.03 (m, 1H), 3.96-3.93 (m, 12H), 3.88-3.82 (m, 15H), 3.57-3.52 (m, 4H), 3.34-3.23 (m, 2H), 2.56 (t, 4H, $J = 6.2$ Hz), 1.97-1.70 (m, 2H), 1.39-1.32 (m, 9H); ^{13}C NMR (DMSO) δ 168.0, 158.9, 158.6, 158.5, 158.4, 155.3, 137.8, 136.2, 136.1, 136.0, 133.6, 133.5, 130.6, 128.8, 124.4, 121.8, 121.6, 119.3, 115.4, 114.3, 114.0, 113.8, 106.9, 104.7, 79.1, 78.1, 51.7, 36.4, 36.3, 35.4, 35.0, 34.9, 34.8, 28.2; HRMS (TOF MS ES$^+$) calcd for $C_{60}H_{73}N_{23}O_{14}$ (M+H): 1340.5780. Found: 1340.5825.

Synthesis of hairpin conjugate MeOImPyβalaImPy-D-Dab-PBD-ImPyβalaImPy 149.

AT-329, 149
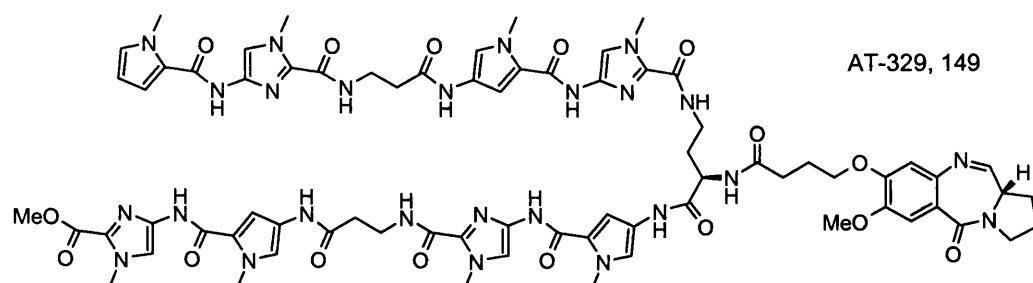
Boc protected amino ester **148** (74 mg, 0.055 mmol) was coupled to 4C-Alloc-THP PBD acid **57** (27.7 mg, 0.055 mmol) following method A. The aqueous work up was complicated by the formation of thick emulsions. The crude product was subjected to flash chromatography (gradient elution from 0:100 to 4:96 methanol:chloroform). Rotary evaporation of the pure fractions under reduced pressure yielded the desired coupled product (32 mg, 33 %) AT328. (29 mg, 0.017 mmol) were immediately deprotected following method E. The crude product was subjected to flash chromatography (gradient elution from 4:96 to 10:90 methanol:chloroform). Rotary evaporation of the pure fractions under reduced pressure yielded the desired biologically active compound AT329, **149** (15.4 mg, 60 %).

^{1}H NMR (DMSO) δ 10.71 (s, 1H), 10.41-10.34 (m, 3H), 10.07 (s, 1H), 9.99 (s, 1H), 8.24 (d, 1H, J = 7.83 Hz), 7.99-7.90 (m, 3H), 8.24 (d, 1H, J = 4.42 Hz), 7.68 (s, 1H), 7.51 (m, 3H), 7.34-7.28 (m, 4H), 7.13 (dd, 1H, J = 1.70 Hz, J = 4.70 Hz), 6.98-6.93 (m, 4H), 6.84 (s, 1H), 6.04 (dd, 1H, J = 2.51 Hz, J = 3.93 Hz), 4.45 (q, 1H, J = 7.31 Hz), 4.17-3.99 (m, 2H), 3.96-3.92 (m, 12H), 3.87-3.82 (m, 18H), 3.67-3.52 (m, 7H), 3.40 (m, 1H), 3.32-3.21 (m, 2H), 2.56 (m, 4H), 2.39-2.34 (m, 2H), 2.31-2.14 (m, 2H), 2.07-1.88 (m, 4H), 1.80 (m, 2H); MS (ES^{+}) m/z 1554.8 ([M+H]$^{+\cdot}$, 10) ; HRMS (TOF MS ES^{+}) calcd for $C_{72}H_{83}N_{25}O_{16}$ (M+H): 1554.6522. Found: 1554.6575; Purity by analytical HPLC : Luna : 95.5 %; Gemini : 88.2 %.

11.5.3 Based on a diaminopropane loop

11.5.3.1 Synthesis of hexa pyrrole conjugate AT-341

Synthesis of (3-{[1-Methyl-4-({1-methyl-4-[(1-methyl-1H-pyrrole-2-carbonyl)-amino]-1H-pyrrole-2-carbonyl}-amino)-1H-pyrrole-2-carbonyl]-amino}-propyl)-carbamic acid tert-butyl ester **150**.
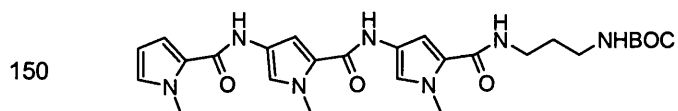
Tripyrrole acid **134** (629 mg, 1.64 mmol) was coupled to commercially available amine (3-amino-propyl)-carbamic acid tert-butyl ester (300 mg, 1.72 mmol) according to method A (omitting the Boc deprotection step). The crude product was quickly purified on a short column of silica gel (2:98 methanol:chloroform). Rotary evaporation of the pure fractions under reduced pressure yielded the desired coupled product (763 mg, 88 %) **150**.

^{1}H NMR (DMSO) δ 9.90 (s, 1H), 9.83 (s, 1H), 7.97 (t, 1H, J = 5.68 Hz), 7.25 (d, 1H, J = 1.79 Hz), 7.20 (d, 1H, J = 1.73 Hz), 7.05 (d, 1H, J = 1.86 Hz), 6.96-6.93 (m, 2H), 6.89 (d, 1H, J = 1.80 Hz), 6.78 (t, 1H, J = 5.44 Hz), 6.08 (dd, 1H, J = 2.57 Hz, J = 3.86 Hz), 3.90 (s, 3H), 3.87 (s, 3H), 3.82 (s, 3H), 3.19 (q, 2H, J = 5.82 Hz), 2.98 (q, 2H, J = 6.63 Hz), 1.60 (p, 2H, J = 6.81 Hz), 1.40 (s, 9H); ^{13}C NMR (DMSO) δ 161.2, 158.6, 158.4, 155.6, 128.1, 125.5, 122.9, 122.8, 122.1, 122.0, 118.4, 117.8, 112.6, 106.6,

104.7, 104.1, 77.5, 37.6, 36.2, 36.0, 35.9, 29.8, 28.2, 18.5; MS (ES$^+$) m/z 526.24 ([M+H]$^{+\bullet}$, 50), 426.21 ([M-BOC+H]$^{+\bullet}$, 100); IR (Golden gate) v 3304, 1689, 1637, 1514, 1465, 1434, 1402, 1365, 1316, 1250, 1205, 1164, 1111, 1062, 1019, 734, 665, 606 cm^{-1}.

Synthesis of BocPyPyPyDapPyPyPy **151**.

151
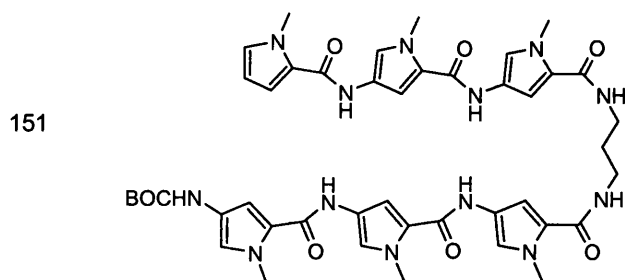
Boc amino tripyrrole **150** (250 mg, 0.475 mmol) was coupled to tripyrrole acid **112** (230 mg, 0.475 mmol) according to method A. The crude product was subjected to flash chromatography (gradient elution from 0:100 to 8:92 methanol:chloroform, the product began to elute at 4:96). Rotary evaporation of the pure fractions under reduced pressure yielded the desired coupled product (85 mg, 20 %) **151**.

^{1}H NMR (DMSO) δ 9.90-9.82 (m, 4H), 9.08 (s, 1H), 8.04 (t, 2H, J = 5.70 Hz), 7.25-7.20 (m, 4H), 7.05 (m, 2H), 6.96-6.85 (m, 6H), 6.07 (dd, 1H, J = 2.54 Hz, J = 3.87 Hz), 3.90-3.81 (m, 18H), 3.25 (q, 4H, J = 6.17 Hz), 1.71 (p, 2H, J = 6.72 Hz), 1.47 (s, 9H); ^{13}C NMR (DMSO) δ 161.3, 158.6, 158.5, 158.4, 152.8, 128.1, 125.4, 122.9, 122.8, 122.7, 122.6, 122.3, 122.1, 122.0, 118.4, 117.8, 116.9, 112.6, 106.6, 104.7, 104.6, 104.0, 103.7, 78.3, 36.2, 36.1, 36.0, 35.9, 29.7, 28.2; MS (ES$^+$) m/z 892.4 ([M+H]$^{+\bullet}$, 80); IR (Golden gate) v 3283, 2940, 1634, 1583, 1518, 1463, 1433, 1401, 1248, 1158, 813, 744 cm^{-1}.

Synthesis of hexa pyrrole conjugate PBD-PyPyPyDapPyPyPy. **152.**

AT-341, 152
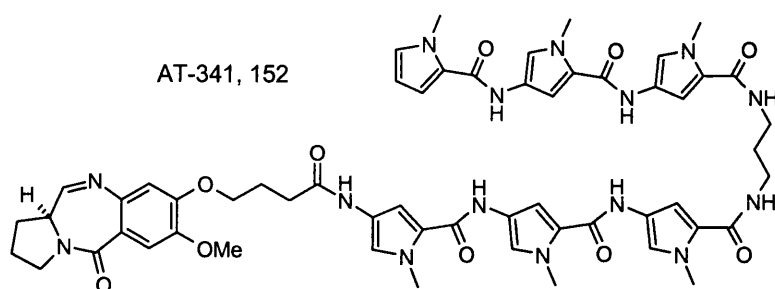
Boc protected **151** (77 mg, 0.086 mmol) was coupled to 4C-Alloc-THP PBD acid **57** (56.3 mg, 0.112 mmol) following method A. The crude product was subjected to flash chromatography (gradient elution from 0:100 to 8:92 methanol:chloroform). Rotary evaporation of the pure fractions under reduced pressure yielded the desired coupled product AT-339 (20 mg, 0.015 mmol, 18 %) which were immediately deprotected following method E. The crude product was subjected to flash chromatography (gradient elution from 4:96 to 9:91 methanol:chloroform). Rotary evaporation of the pure fractions under reduced pressure yielded the desired biologically active compound AT-341, **152** (11 mg, 64 % from AT-339).

^{1}H NMR (DMSO) δ 9.90-9.82 (m, 5H), 8.04 (t, 2H, J = 5.9 Hz), 7.79 (d, 1H, J = 4.4 Hz), 7.36 (s, 1H), 7.25-7.17 (m, 5H), 7.05 (m, 2H), 6.96-6.90 (m, 5H), 6.84 (s, 1H), 6.07 (m, 1H), 4.21-3.99 (m, 2H), 3.95-3.76 (m, 21H), 3.73-3.55 (m, 2H), 3.44-3.37 (m, 1H), 3.27-3.22 (q, 4H, J = 6.9 Hz), 2.46 (t, 2H, J = 7.3 Hz), 2.38-2.17 (m, 2H), 2.08 (p, 2H, J = 7.0 Hz), 2.00-1.82 (m, 4H), 1.70 (p, 2H, J = 6.8 Hz) ; HRMS (TOF MS ES$^+$) calcd for $C_{56}H_{63}N_{15}O_{10}$ (M+H): 1106.4955. Found: 1106.5011; Purity by analytical HPLC : Luna : 96 %; Gemini : 95 %.

11.5.3.1 Synthesis of conjugate PBD-PyImPyDapPyPyPy **155**.

Synthesis of 4-({4-[(4-tert-Butoxycarbonylamino-1-methyl-1H-pyrrole-2-carbonyl)-amino]-1-methyl-1H-imidazole-2-carbonyl}-amino)-1-methyl-1H-pyrrole-2-carboxylic acid methyl ester **153**.
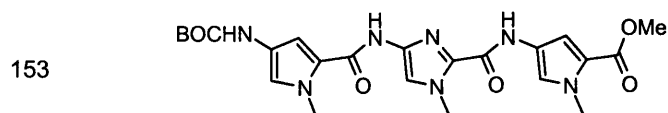
EDCI (1.58 g, 8.22 mmol) was added to BocPyImCO$_2$H **145** (2 g, 5.50 mmol) in anhydrous DMF (5 mL). The insoluble material was observed to disolve as the anhydride was formed. The nitro pyrrole ester **84** (1.01 g, 5.49 mmol) was hydrogenated in ethyl acetate (20 mL) under 45 PSI over 10% Pd/C (100 mg). After 50 min, the hydrogen uptake ceased and the reaction was observed to be complete by TLC. The Pd/C catalyst was removed by filtration and the filtrate was added to the previously prepared anhydride suspension. DMAP (134 mg, 1.09 mmol) was added and the

mixture was allowed to stir for 4 hours, at which time TLC showed reaction to be complete. Completion was observed by TLC. The mixture was diluted with ethyl acetate (100 mL) and washed with water (2 x 50 mL), saturated aqueous $NaHCO_3$ (50 mL), brine (50 mL) and dried ($MgSO_4$). The organic solution was then filtered through a pad of silica gel and evaporated to dryness. The desired product **153** was isolated by trituration with diethyl ether followed by filtration. (1.5 g, 55 %).

^{1}H NMR (DMSO) δ 10.14 (s, 1H), 10.10 (s, 1H), 9.09 (bs, 1H), 7.54 (m, 2H), 7.01 (m, 2H), 6.86 (s, 1H), 3.99 (s, 3H), 3.86-3.83 (m, 6H), 3.76 (s, 3H), 1.47 (s, 9H); ^{13}C NMR (DMSO) δ 160.7, 158.7, 155.9, 152.8, 136.1, 134.0, 122.4, 122.0, 121.9, 120.9, 118.8, 117.9, 114.8, 108.6, 104.7, 78.3, 50.9, 36.2, 34.8, 28.2; MS (ES$^+$) m/z 500.17 ([M+H]$^{+\cdot}$,100); IR v 3393, 1720, 1696, 1668, 1588, 1565, 1468, 1452, 1391, 1368, 1308, 1227, 1209, 1117, 1095, 1061, 998, 897, 820, 797, 775, 762, 744, 672, 625 cm^{-1}.

Synthesis of BocPyImPyDapPyPyPy 154.

154
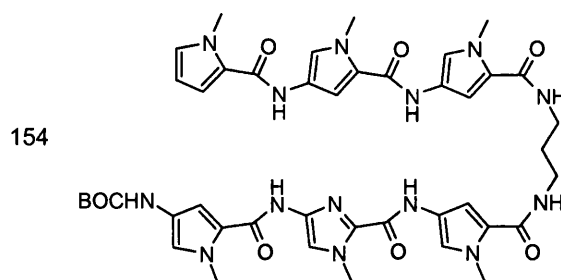
BocPyImPyCO₂Me **153** (320 mg, 0.624 mmol) was saponified according to method E to provide BocPyImPyCO₂H (285 mg, 91 %). It was coupled to Boc amino tripyrrole **153** according to method A (the usual DMF reaction solvent was replaced by a mixture of DCM:DMF 5mL:1mL). The crude product was subjected to flash chromatography (gradient elution from 0:100 to 6:94 methanol:chloroform). Rotary evaporation of the pure fractions under reduced pressure yielded the desired coupled product (214 mg, 42 %). **154**.

^{1}H NMR (DMSO) δ 10.16 (s, 1H), 9.96-9.92 (m, 2H), 9.83 (s, 1H), 9.10 (s, 1H), 8.04 (q, 2H, J = 6.25 Hz), 7.53 (s, 1H), 7.25-7.21 (m, 3H), 7.05-6.88 (m, 7H), 6.07 (dd, 1H, J = 2.54 Hz, J = 3.86 Hz), 3.98 (s, 3H), 3.90-3.83 (m, 15H), 3.25 (q, 4H, J = 6.17 Hz), 1.71 (p, 2H, J = 6.70 Hz), 1.47 (s, 9H); ^{13}C NMR (DMSO) δ 161.3, 161.2, 158.6, 155.7, 128.1, 125.4, 123.3, 122.9, 122.8, 122.4, 122.2, 122.0, 121.2, 118.4, 117.9, 117.8, 112.6, 106.6, 104.8, 104.6, 104.6, 104.1, 36.2, 36.1, 35.9, 34.8, 29.7, 28.2; MS (ES$^+$)

m/z 893.47 ([M+H]$^{+\bullet}$,100); IR (Golden gate) v 3303, 2156, 2018, 1641, 1585, 1529, 1466, 1402, 1248, 1204, 1160, 1111, 996, 901, 749, 665 cm^{-1}.

### Synthesis of conjugate PBD-PyImPyDapPyPyPy. 155.

AT-363, 155
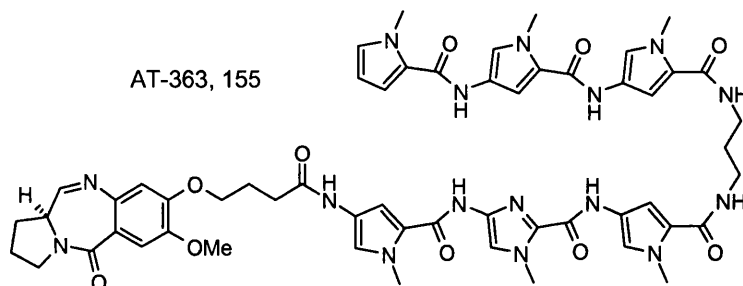
Boc protected **154** (200 mg, 0.224 mmol) was coupled to 4C-Alloc-THP PBD acid **57** (124 mg, 0.247 mmol) following method A. The crude product was subjected to flash chromatography (gradient elution from 0:100 to 6:94 methanol:chloroform). Rotary evaporation of the pure fractions under reduced pressure yielded the desired coupled product (152 mg, 52 %) AT362. (150 mg, 0.116 mmol) were immediately deprotected following method E. The crude product was subjected to flash chromatography (gradient elution from 3:97 to 9:91 methanol:chloroform). Rotary evaporation of the pure fractions under reduced pressure yielded the desired biologically active compound AT-363, **155** (97 mg, 76 %).

^{1}H NMR (DMSO) δ 10.29 (s, 1H), 10.02 (s, 1H), 9.95 (m, 2H), 9.86 (s, 1H), 8.09 (m, 2H), 7.79 (d, 1H, J = 4.42 Hz), 7.56 (s, 1H), 7.35 (s, 1H), 7.29 (s, 1H), 7.26-7.22 (m, 3H), 7.05 (s, 1H), 6.98-6.90 (m, 5H), 6.84 (s, 1H), 6.07 (dd, 1H, J = 2.58 Hz, J = 3.81 Hz), 4.02-3.95 (m, 2H), 3.99 (s, 3H), 3.89-3.83 (m, 18H), 3.75-3.56 (m, 2H), 3.51-3.40 (m, 1H), 3.24 (q, 4H, J = 6.31 Hz), 2.45 (t, 2H, J = 7.31 Hz), 2.38-2.15 (m, 2H), 2.12-1.88 (m, 4H), 1.76-1.63 (m, 2H); HPLC/MS (ES^{+}) *m/z* 1107.50 ([M+H]$^{+\bullet}$, 100); HRMS (TOF MS ES^{+}) calcd for C$_{55}$H$_{62}$N$_{16}$O$_{10}$ (M+H): 1107.4907. Found: 1107.4854; Purity by analytical HPLC : Luna : 96 %; Gemini : 93 %.

11.5.4 Based on an aminobutyric loop

11.5.4.1 Synthesis of PBD hexa pyrrole conjugate AT-373

Synthesis of 4-[(4-{[4-(4-tert-Butoxycarbonylamino-butyrylamino)-1-methyl-1H-pyrrole-2-carbonyl]-amino}-1-methyl-1H-pyrrole-2-carbonyl)-amino]-1-methyl-1H-pyrrole-2-carboxylic acid methyl ester 156.
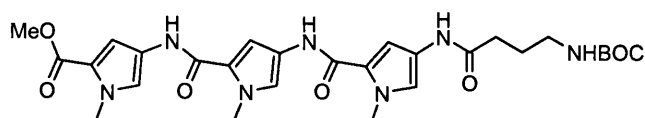
156

BocPyPyPyCO$_2$Me **78** (800 mg, 1.59 mmol) and γ-Boc-amino butyric acid (388 mg, 1.91 mmol) were coupled according to method B. The crude product was subjected to flash chromatography (gradient elution from 0:100 to 2:98 methanol:chloroform). Rotary evaporation of the pure fractions under reduced pressure yielded the desired coupled product **156** (660 mg, 71 %).

^{1}H NMR (DMSO) δ 9.96 (s, 1H), 9.93 (s, 1H), 9.82 (s, 1H), 7.49 (d, 1H, J = 1.89 Hz), 7.26 (d, 1H, J = 1.76 Hz), 7.18 (d, 1H, J = 1.76 Hz), 7.07 (d, 1H, J = 1.80 Hz), 6.93-6.85 (m, 3H), 3.85 (m, 9H), 3.75 (s, 3H), 2.97 (q, 2H, J = 6.42 Hz), 2.24 (t, 2H, J = 7.38 Hz), 1.69 (p, 2H, J = 7.21 Hz), 1.40 (s, 9H); ^{13}C NMR (DMSO) δ 169.1, 160.8, 158.4, 158.3, 155.6, 122.9, 122.6, 122.4, 122.2, 122.0, 120.7, 118.5, 118.4, 118.1, 108.3, 104.7, 103.9, 77.4, 50.9, 36.2, 36.1, 36.0, 33.1, 28.2, 25.8; IR (golden gate) ν 3298, 2946, 1692, 1644, 1579, 1520, 1434, 1402, 1365, 1249, 1202, 1164, 1107, 1059, 1004, 888, 822, 751 cm^{-1}; HPLC/MS (ES$^+$) m/z 584.14 ([M+H]$^{+*}$, 100).

Synthesis of MeoPyPyPyAbaPyPyPyBoc 157.

157
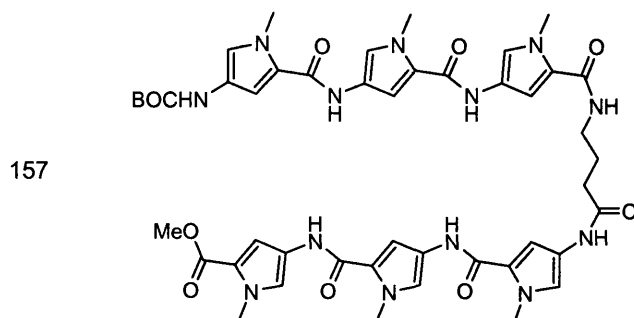
Boc protected amino ester **156** (300 mg, 0.514 mmol), and BocPyPyPyCO2H **112** (274 mg, 0.565 mmol) were coupled together according to method B. The crude product was subjected to flash chromatography (gradient elution from 0:100 to 5:95 methanol:chloroform). Rotary evaporation of the pure fractions under reduced pressure yielded the desired coupled product **157** (120 mg, 24 %).

^{1}H NMR (DMSO) δ 9.94 (s, 1H), 9.92 (s, 1H), 9.89 (s, 1H), 9.87 (s, 1H), 9.85 (s, 1H), 9.10 (s, 1H), 8.06 (t, 1H, J = 5.53 Hz), 7.47 (d, 1H, J = 1.80 Hz), 7.23 (d, 1H, J = 1.70 Hz), 7.21 (d, 1H, J = 1.64 Hz), 7.18 (m, 2H), 7.05 (m, 2H), 6.90-6.83 (m, 5H), 3.83 (m, 18H), 3.73 (s, 3H), 3.21 (q, 2H, J = 6.10 Hz), 2.28 (t, 2H, J = 7.38 Hz), 1.79 (p, 2H, J = 7.21 Hz), 1.47 (s, 9H); IR (golden gate) v 3301, 2952, 1694, 1641, 1581, 1530, 1434, 1401, 1249, 1204, 1157, 1106, 1059, 997, 888, 816, 750, 668 cm^{-1}; HPLC/MS (ES$^+$) m/z 950.59 ([M+H]$^{+*}$, 100).

## Synthesis of MeoPyPyPyAbaPyPyPy-PBD 158.

158, AT-373
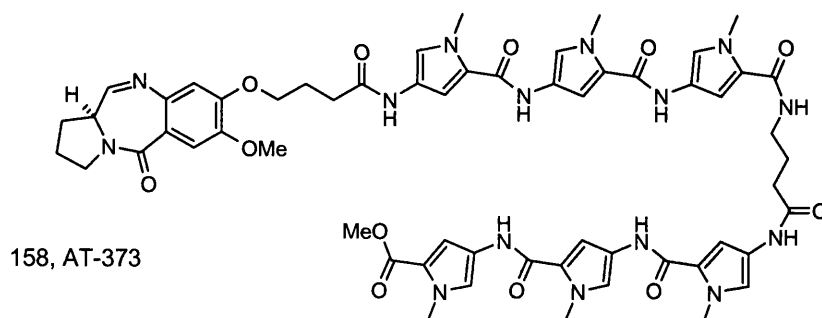
Boc protected **157** (111 mg, 0.117 mmol) was coupled to 4C-Alloc-THP PBD acid **57** (64.5 mg, 0.128 mmol) following method B. The crude product was subjected to flash chromatography (gradient elution from 0:100 to 5:95 methanol:chloroform). Rotary

evaporation of the pure fractions under reduced pressure yielded the desired coupled product AT-371 (75 mg, 47 %, 0.055 mmol) which was immediately deprotected following method E. The crude product was subjected to flash chromatography (gradient elution from 3:97 to 9:91 methanol:chloroform). Rotary evaporation of the pure fractions under reduced pressure yielded the desired biologically active compound AT-373, **158** (60 mg, 93 % from AT-371).

^{1}H NMR (DMSO) δ 9.92 (s, 1H), 9.90 (s, 1H), 9.89 (s, 1H), 9.88 (s, 1H), 9.87 (s, 1H), 9.83 (s, 1H), 8.04 (m, 1H), 7.78 (d, 1H, J = 4.41 Hz), 7.46 (d, 1H, J = 1.89 Hz), 7.34 (s, 1H), 7.23 (m, 2H), 7.18-7.16 (m, 3H), 7.05 (m, 2H), 6.91-6.87 (m, 4H), 6.83 (s, 1H), 4.19-3.99 (m, 2H), 3.85-3.81 (m, 21H), 3.74 (s, 3H), 3.71-3.55 (m, 2H), 3.50-3.35 (m, 1H), 3.22 (q, 2H, J = 6.31 Hz), 2.44 (t, 2H, J = 7.27 Hz), 2.36-2.17 (m, 4H), 2.12-1.88 (m, 4H), 1.87-1.72 (m, 2H); HPLC/MS (ES$^+$) m/z 1165.05 ([M+H]$^{+\cdot}$, 100); HRMS (TOF MS ES$^+$) calcd for $C_{58}H_{65}N_{15}O_{12}$ (M+H):1164.5010. Found: 1164.4954. Purity by analytical HPLC : Luna : 98.9 %; Gemini : 94.2 %.

11.5.4.2 Synthesis of PBD conjugate AT-374

Synthesis of MeoPyPyPyAbaPyImPyBoc 159.

159
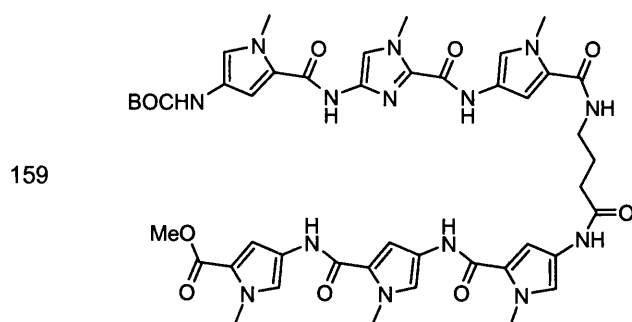
BocPyImPyCO$_2$H (274 mg, 0.564 mmol) was prepared from its methyl ester **153** according to method C. The newly formed acid was coupled to Boc protected amino ester AT367 (300 mg, 0.514 mmol) according to method B. The crude product was subjected to flash chromatography (gradient elution from 0:100 to 5:95

methanol:chloroform). Rotary evaporation of the pure fractions under reduced pressure yielded the desired coupled product **159** (120 mg, 24 %).

^{1}H NMR (DMSO) δ 10.17 (s, 1H), 9.95 (s, 1H), 9.93 (s, 1H), 9.92 (s, 1H), 9.85 (s, 1H), 9.10 (s, 1H), 8.07 (t, 1H, J = 5.48 Hz), 7.51 (s, 1H), 7.47 (d, 1H, J = 1.86 Hz), 7.23 (d, 1H, J = 1.70 Hz), 7.21 (d, 1H, J = 1.79 Hz), 7.17 (d, 1H, J = 1.73 Hz), 7.05 (d, 1H, J = 1.76 Hz), 6.98 (m, 2H), 6.90 (d, 1H, J = 1.93 Hz), 6.87 (m, 2H), 3.96 (s, 3H), 3.83 (m, 15H), 3.73 (s, 3H), 3.22 (q, 2H, J = 6.16 Hz), 2.28 (t, 2H, J = 7.42 Hz), 1.79 (p, 2H, J = 7.14 Hz), 1.45 (s, 9H); IR (golden gate) ν 3287, 2950, 1643, 1529, 1434, 1401, 1247, 1203, 1157, 1108, 1060, 998, 900, 810, 749, 667 cm^{-1}; HPLC/MS (ES$^+$) m/z 951.57 ([M+H]$^{+\cdot}$, 100).

**Synthesis of MeoPyPyPyAbaPyImPy-PBD 160.**

AT-374, 160
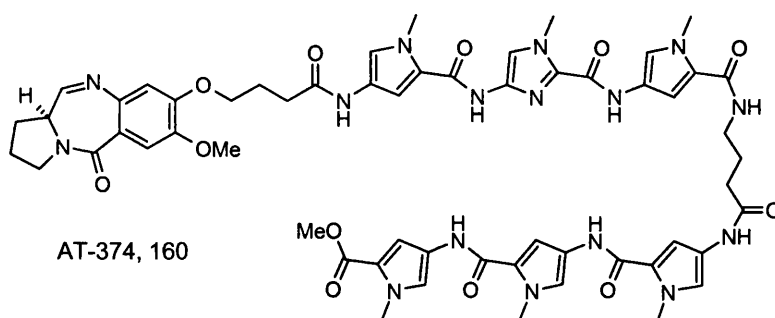
Boc protected **159** (109 mg, 0.115 mmol) was coupled to 4C-Alloc-THP PBD acid **57** (63.3 mg, 0.126 mmol) following method B. The crude product was subjected to flash chromatography (gradient elution from 0:100 to 5:95 methanol:chloroform). Rotary evaporation of the pure fractions under reduced pressure yielded the desired coupled product (55 mg, 35 %) AT372. (55 mg, 0.041 mmol) were immediately deprotected following method E. The crude product was subjected to flash chromatography (gradient elution from 3:97 to 8:92 methanol:chloroform). Rotary evaporation of the pure fractions under reduced pressure yielded the desired biologically active compound AT-374, **160** (38 mg, 80 %).

^{1}H NMR (DMSO) δ 10.22 (s, 1H), 9.91 (s, 1H), 9.90 (s, 1H), 9.89 (s, 1H), 9.88 (s, 1H), 9.82 (s, 1H), 8.05 (m, 1H), 7.77 (d, 1H, J = 4.41 Hz), 7.53 (s, 1H), 7.46 (d, 1H, J = 1.88 Hz), 7.34 (s, 1H), 7.27 (d, 1H, J = 1.72 Hz), 7.22 (m, 2H), 7.17 (d, 1H, J = 1.73 Hz), 7.05 (d, 1H, J = 1.80 Hz), 6.97 (d, 1H, J = 1.78 Hz), 6.93-6.87 (m, 3H), 6.83 (s, 1H),

4.18-4.00 (m, 2H), 3.97 (s, 3H), 3.83-3.81 (m, 18H), 3.74 (s, 3H), 3.70-3.54 (m, 2H), 3.47-3.36 (m, 1H), 3.22 (m, 2H), 2.44 (t, 2H, J = 7.35 Hz), 2.35-2.17 (m, 4H), 2.12-1.99 (m, 2H), 1.98-1.87 (m, 2H), 1.87-1.77 (m, 2H); HPLC/MS (ES$^+$) m/z 1166.05 ([M+H]$^{+*}$, 100); HRMS (TOF MS ES$^+$) calcd for $C_{57}H_{64}N_{16}O_{12}$ (M+H): 1165.4962. Found 1165.4963; Purity by analytical HPLC : Luna : 91.3 %; Gemini : 85.4 %.

11.5.5 Based on a aminobutyric acid loop and cyclised (Cyclin)

11.5.5.1 Synthesis of cyclin 008-AT-087-1, **167**

Synthesis of 4-{[4-(4-tert-Butoxycarbonylamino-butyrylamino)-1-methyl-1H-pyrrole-2-carbonyl]-amino}-1-methyl-1H-pyrrole-2-carboxylic acid 161.

161
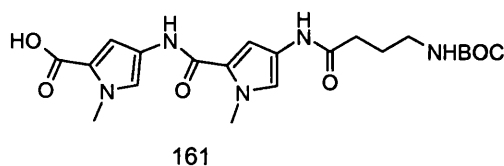
EDCI (1.38 g, 7.19 mmol) was added to a solution of γ-Boc-amino butyric acid (1.32 g, 6.50 mmol) and HOBt (882 mg, 6.53 mmol) in anhydrous DMF (5 mL) and the resulting suspension was allowed to stir for 5 hours. Nitro pyrrole dimer **110** (2.1 g, 6.86 mmol) was hydrogenated in DMF (10 mL) under 45 PSI over Pd/C 10% (200 mg). After 3 hours, the reaction was observed to be complete by TLC analysis. The Pd/C catalyst was removed by filtration and the filtrate was added to the previously prepared activated ester solution. The resulting solution was allowed to stir overnight, after which the reaction was deemed complete by TLC. The solution was diluted with ethyl acetate (150 mL) and washed sequentially with water (200 mL), 10% w/w aqueous citric acid (100 mL), water (200 mL), saturated aqueous NaHCO₃ (100 mL), brine (100 mL) and dried (MgSO₄). Filtration through a pad of silica gel, using ethyl acetate as eluent, followed by rotary evaporation of the solvent under reduced pressure, provided the pure coupled product (2.2 g, 4.76 mmol), which was immediately saponified according to method C to provide acid **161** (1.47 g, 50 %). ^{1}H NMR (DMSO) δ 9.87 (s, 1H), 9.81 (s, 1H), 7.42 (d, 1H, J = 1.84 Hz), 7.15 (d, 1H, J = 1.66 Hz), 6.86-6.83 (m, 3H), 3.82 (s, 6H), 2.96 (q, 2H, J = 6.40 Hz), 2.22 (t, 2H, J = 7.37 Hz), 1.67 (p, 2H, J = 7.07 Hz),

1.38 (s, 9H); ^{13}C NMR (DMSO) δ 169.1, 161.9, 158.3, 155.5, 122.6, 122.5, 122.0, 120.2, 119.4, 118.1, 108.3, 103.9, 77.4, 36.1, 36.0, 33.1, 28.2, 25.8; IR (golden gate) v 1650, 1539, 1435, 1249, 1160, 653 cm^{-1}; MS (ES$^-$) m/z 100 (446.1, M - H).

Synthesis of 1-Allyl-4-[(4-{[4-(4-tert-butoxycarbonylamino-butyrylamino)-1-methyl-1H-pyrrole-2-carbonyl]-amino}-1-methyl-1H-pyrrole-2-carbonyl)-amino]-1H-pyrrole-2-carboxylic acid methyl ester 162.

162
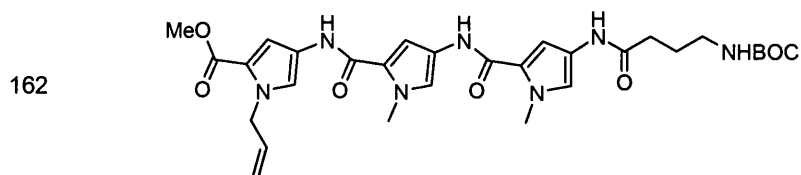
BocPy-allyl-CO₂Me **92** (313 mg, 1.12 mmol) was coupled to acid **161** (500 mg, 1.12 mmol) in anhydrous DCM (10 mL) according to method A. After an overnight reaction period, the crude reaction mixture was loaded on a short column of silica gel. The desired product was eluted with ethyl acetate. Evaporation of the solvent provided pure **162** (540 mg, 80 %).

^{1}H NMR (CDCl₃) δ 9.95 (s, 1H), 9.89 (s, 1H), 9.77 (s, 1H), 7.51 (d, 1H, J = 1.90 Hz), 7.23 (d, 1H, J = 1.74 Hz), 7.15 (d, 1H, J = 1.76 Hz), 7.06 (d, 1H, J = 1.81 Hz), 6.95 (d, 1H, J = 1.93 Hz), 6.87 (d, 1H, J = 1.82 Hz), 6.80 (t, 1H, J = 5.07 Hz), 6.03-5.93 (m, 1H), 5.12-4.91 (m, 4H), 3.85 (s, 3H), 3.83 (s, 3H), 3.73 (s, 3H), 2.95 (q, 2H, J = 6.73 Hz), 2.22 (t, 2H, J = 7.41 Hz), 1.67 (p, 2H, J = 7.22 Hz), 1.38 (s, 9H); ^{13}C NMR (CDCl₃) δ 169.1, 160.5, 158.5, 158.4, 155.6, 135.3, 123.4, 122.7, 122.5, 122.2, 122.0, 119.6, 118.6, 118.1, 117.9, 116.2, 108.8, 104.8, 103.9, 77.4, 50.9, 50.1, 36.0, 33.1, 28.2, 25.8; MS (ES$^+$) m/z 100 (610.16, M + H); IR v 3288, 2949, 1693, 1643, 1574, 1519, 1433, 1397, 1365, 1250, 1208, 1163, 1092, 1059, 994, 821, 774, 642 cm^{-1}.

Synthesis of 4-({4-[(1-Allyl-4-tert-butoxycarbonylamino-1H-pyrrole-2-carbonyl)-amino]-1-methyl-1H-pyrrole-2-carbonyl}-amino)-1-methyl-1H-pyrrole-2-carboxylic acid 163.

163
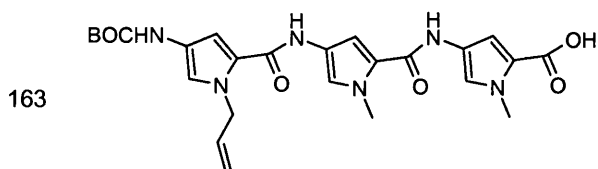
EDCI (251 mg, 1.31 mmol) was added to a stirred solution of BocPy-allyl-CO$_2$H, **93** (316 mg, 1.19 mmol) and HOBt (160 mg, 1.19 mmol) in anhydrous DMF (5 mL) and the resulting reaction mixture was allowed to react for 5 hours.

NitroPyPyCO$_2$Me **110** (400 mg, 1.31 mmol) was hydrogenated in DMF (10 mL) under 45 PSI over 10% Pd/C 10% (100 mg). After 3 hours, the reaction was observed to be complete by TLC analysis. The Pd/C was removed by filtration and the filtrate was added to the previously prepared activated ester solution. The resulting solution was allowed to stir overnight, after which the reaction was observed to be complete by TLC. The solution was diluted with ethyl acetate (150 mL) and washed sequentially with water (200 mL), aqueous citric acid (10% w/w, 100 mL), water (200 mL), saturated aqueous NaHCO$_3$ (100 mL), brine (100 mL) and dried (MgSO$_4$). Filtration and rotary evaporation of the solvent under reduced pressure provided the pure coupled product (430 mg, 4.76 mmol), which was immediately saponified according to method C to provide acid **163** (413 mg, 62 %). ^{1}H NMR (DMSO) δ 9.92 (s, 1H), 9.81 (s, 1H), 9.17 (s, 1H), 7.43 (d, 1H, J = 1.90 Hz), 7.21 (d, 1H, J = 1.70 Hz), 7.06 (d, 1H, J = 1.68 Hz), 6.93 (s, 1H), 6.85 (m, 2H), 6.00-5.92 (m, 1H), 5.07-4.90 (m, 4H), 3.84 (s, 3H), 3.82 (s, 3H), 1.46 (s, 9H); ^{13}C NMR (DMSO) δ 161.9, 158.4, 158.2, 152.8, 136.0, 122.6, 122.5, 122.4, 122.2, 120.2, 119.4, 118.4, 115.7, 108.3, 104.7, 104.0, 78.3, 49.9, 48.6, 36.1, 36.0, 28.2; MS (ES⁻) m/z 100 (509.2, M - H); IR (golden gate) v 1649, 1539, 1396, 1247, 1158, 1059, 995, 666 cm^{-1}.

Synthesis of MeOPyallPyPyabaPyPyPallBoc 164.

164
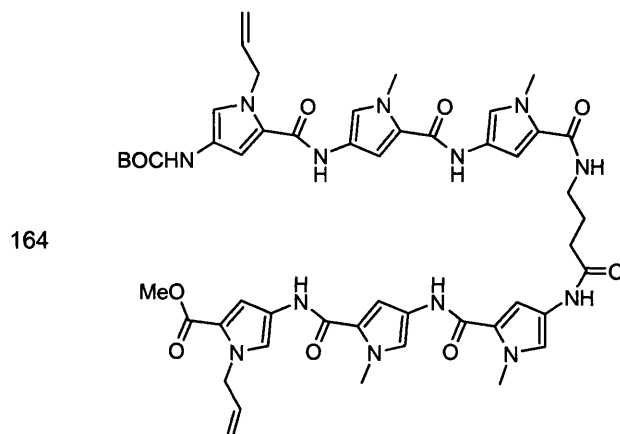
Acid **163** (306 mg, 0.599 mmol) and Boc amino ester **162** (366 mg, 0.600 mmol) were coupled according to method A. The crude product was purified by flash chromatography (gradient elution from 0:100 to 4:96 methanol:chloroform). Rotary evaporation of the pure fractions under reduced pressure provided the desired coupled product **164** (390 mg, 65 %).

^{1}H NMR (CDCl$_3$) δ 9.98 (s, 1H), 9.94 (s, 1H), 9.91 (s, 1H), 9.90 (s, 1H), 9.86 (s, 1H), 9.17 (s, 1H), 8.07 (t, 1H, J = 5.50 Hz), 7.52 (d, 1H, J = 1.91 Hz), 7.25-7.18 (m, 4H), 7.07 (d, 1H, J = 1.80 Hz), 7.05 (d, 1H, J = 1.68 Hz), 6.95-6.84 (m, 5H), 6.03-5.92 (m, 2H), 5.13-4.90 (m, 8H), 3.85-3.80 (m, 12H), 3.73 (s, 3H), 3.22 (q, 2H, J = 6.66 Hz), 2.29 (t, 2H, J = 7.38 Hz), 1.80 (p, 2H, J = 7.18 Hz), 1.46 (s, 9H); MS (ES$^+$) m/z 100 (1002.39, M + H); IR v 3294, 1641, 1582, 1520, 1434, 1398, 1249, 1158, 1095, 1059, 995, 888, 754.

Synthesis of MeOPyPyPyabaPyPyPyBoc 166.

```
|_____(butyl)____|
```


166
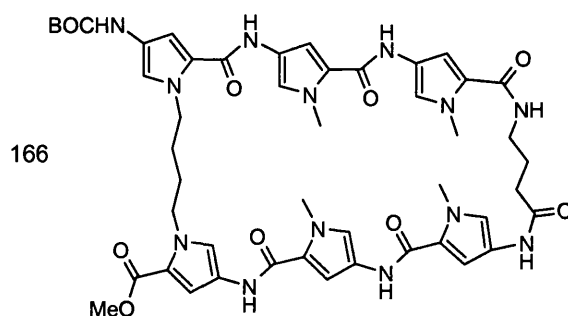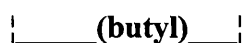
2nd generation Grubbs catalyst (3 mg, 0.003 mmol) was added to a stirred solution of 164 (350 mg, 0.349 mmol) in DCM (300 mL). The reaction was heated at reflux and monitored by TLC analysis. After 2 h, the reaction mixture was treated with further Grubbs catalyst (2 mg) and was heated at reflux for an additional 2 h at which point TLC analysis revealed complete reaction. The DCM was removed by rotary evaporation under reduced pressure and the residue was immediately purified by flash chromatography. (gradient elution from 2:98 to 4.5:95.5 methanol:chloroform). Rotary evaporation of the pure fractions under reduced pressure afforded the macrocycle 165 (160 mg, 47 %).

Unsaturated macrocylce 165 was immediately reduced by hydrogenation under 45 PSI in a mixture of DMF (10 mL) and cetone (30 mL) over 10% Pd/C 10% (200 mg). The reaction vessel was heated to 45 °C and the reaction was observed to be complete by TLC after 6 hours. Pd/C catalyst was removed by filtration and the filtrate was transferred in a round-bottomed flask. The volatiles were removed by rotary evaporation under reduced pressure. The residue was triturated with diethyl ether (20 mL) which was then removed by decantation. The remaining solids were dried under high vacuum to afford the pure product 166 (110 mg, 73 %).

^{1}H NMR (CDCl$_3$) δ 9.88-9.79 (m, 5H), 9.11 (s, 1H), 7.89 (t, 1H, J = 5.30 Hz), 7.42 (d, 1H, J = 1.26 Hz), 7.23-7.13 (m, 4H), 7.04-6.95 (m, 3H), 6.86-6.78 (m, 3H), 6.70 (d, 1H, J = 1.64 Hz), 4.30-4.24 (m, 4H), 3.83-3.79 (m, 12H), 3.74 (s, 3H), 3.22 (m, 2H), 2.28 (t, 2H, J = 7.11 Hz), 1.80 (p, 2H, J = 5.96 Hz), 1.56-1.40 (m, 13H); MS (ES$^+$) m/z 100 (976.3, M + H).

Synthesis of MeOPyPyPyabaPyPyPyPBD 167.

!_____(butyl)___!

008-AT-087-1, 167
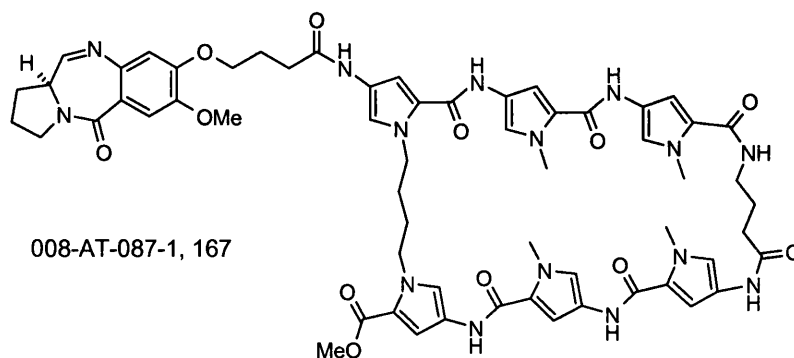
Boc protected **166** (110 mg, 0.113 mmol) was coupled to 4C-Alloc-THP PBD acid **57** (62.2 mg, 0.124 mmol) following method A. The crude product was subjected to flash chromatography (gradient elution from 0:100 to 5:95 methanol:chloroform). Rotary evaporation of the pure fractions under reduced pressure yielded the desired coupled product (66 mg, 0.048 mmol, 42 %) which were immediately deprotected following method E. The crude product was subjected to flash chromatography (gradient elution from 4:96 to 8:92 methanol:chloroform). Rotary evaporation of the pure fractions under reduced pressure yielded the desired biologically active compound 008-AT-087-1, **167** (40 mg, 70 %).

^{1}H NMR (CDCl$_3$) δ 9.88-9.78 (m, 6H), 7.87 (t, 1H, J = 5.30 Hz), 7.75 (d, 1H, J = 4.41 Hz), 7.42 (d, 1H, J = 1.45 Hz), 7.33 (s, 1H), 7.24-7.12 (m, 5H), 7.04 (d, 1H, J = 1.64 Hz), 6.98 (d, 1H, J = 1.58 Hz), 6.86-6.82 (m, 4H), 6.69 (d, 1H, J = 1.71 Hz), 4.35-4.20 (m, 4H), 4.17-3.97 (m, 2H), 3.83-3.79 (m, 15H), 3.73 (s, 3H), 3.68-3.58 (m, 2H), 3.45-3.38 (m, 1H), 3.22 (m, 2H), 2.42 (t, 2H, J = 7.23 Hz), 2.28 (m, 4H), 2.08-1.80 (m, 6H), 1.60-1.40 (m, 4H); MS (ES$^+$) m/z 100 (1190.5, M + H); HRMS (TOF MS ES$^+$) calcd for C$_{60}$H$_{67}$N$_{15}$O$_{12}$ (M+H): 1190.5166. Found: 1190.5217; Purity by analytical HPLC : Luna : 100 %; Gemini : 99.4 %.

12 References

1. Alley, M. C.; Hollingshead, M. G.; Pacula-Cox, C. M.; Waud, W. R.; Hartley, J. A.; Howard, P. W.; Gregson, S. J.; Thurston, D. E.; Sausville, E. A. SJG-136 (NSC 694501), a novel rationally designed DNA minor groove interstrand cross-linking agent with potent and broad spectrum antitumor activity: part 2: efficacy evaluations. *Cancer Res.* **2004**, *64* (18), 6700-6706.

2. Anthony, N. G.; Fox, K. R.; Johnston, B. F.; Khalaf, A. I.; Mackay, S. P.; McGroarty, I. S.; Parkinson, J. A.; Skellem, G. G.; Suckling, C. J.; Waigh, R. D. DNA binding of a short lexitropsin. *Bioorg. Med. Chem. Lett.* **2004**, *14* (5), 1353-1356.

3. Bailly, C.; Colson, P.; Houssier, C.; Houssin, R.; Mrani, D.; Gosselin, G.; Imbach, J. L.; Waring, M. J.; Lown, J. W.; Henichart, J. P. Binding properties and DNA sequence-specific recognition of two bithiazole-linked netropsin hybrid molecules. *Biochemistry* **1992**, *31* (35), 8349-8362.

4. Bailly, C.; Chaires, J. B. Sequence-specific DNA minor groove binders. Design and synthesis of netropsin and distamycin analogues. *Bioconjug. Chem.* **1998**, *9* (5), 513-538.

5. Baird, E. E.; Dervan, P. B. Solid phase synthesis of polyamides containing imidazole and pyrrole amino acids. *Journal of the American Chemical Society* **1996**, *118* (26), 6141-6146.

6. Bando, T.; Narita, A.; Saito, I.; Sugiyama, H. Higly Efficient Sequence-Specific DNA interstrand Cross-Linking by Pyrrole/Imidazole CPI Conjugates. *J. Am. Chem. Soc.* **2002**, (125), 3471-3485.

7. Bando, T.; Narita, A.; Asada, K.; Ayame, H.; Sugiyama, H. Enantioselective DNA alkylation by a pyrrole-imidazole S-CBI conjugate. *J. Am. Chem. Soc.* **2004**, *126* (29), 8948-8955.

8. Bando, T.; Narita, A.; Iwai, A.; Kihara, K.; Sugiyama, H. C-H to N substitution dramatically alters the sequence-specific DNA alkylation, cytotoxicity, and expression of human cancer cell lines. *J. Am. Chem. Soc.* **2004**, *126* (11), 3406-3407.

9. Baraldi, P. G.; Romagnoli, R.; Spalluto, G.; Cozzi, P.; Mongelli, N.; Bianchi, N.; Gambari, R. DNA sequence-recognizing properties of minor groove alkylating agents. Effects of the replacement of N-methylpyrrole by an N-methylimidazole on tallimustine and its own homologue. *Arzneimittelforschung.* **2000**, *50* (3), 309-315.

10. Baraldi, P. G.; Del Carmen, N. M.; Tabrizi, M. A.; De, C. E.; Balzarini, J.; Bermejo, J.; Estevez, F.; Romagnoli, R. Design, synthesis, and biological evaluation of hybrid molecules containing alpha-methylene-gamma-butyrolactones and polypyrrole minor groove binders. *J. Med. Chem.* **2004**, *47* (11), 2877-2886.

11. Barker, P.; Gendler, P.; Rapoport, H. 2-(trichloroacetyl)pyrroles as Intermediates in the Preparation of 2-4-Disubstituted Pyrroles. *J. Org. Chem.* **1978**, *43*, 4849-4853.

12. Barkley, M. D.; Cheatham, S.; Thurston, D. E.; Hurley, L. H. Pyrrolo[1,4]benzodiazepine antitumor antibiotics: evidence for two forms of tomaymycin bound to DNA. *Biochemistry* **1986**, *25* (10), 3021-3031.

13. Belitsky, J. M.; Leslie, S. J.; Arora, P. S.; Beerman, T. A.; Dervan, P. B. Cellular uptake of N-methylpyrrole/N-methylimidazole polyamide-dye conjugates. *Bioorg. Med. Chem.* **2002**, *10* (10), 3313-3318.

14. Berry, J. M.; Howard, P. W.; Kelland, L. R.; Thurston, D. E. Synthesis and biological evaluation of an N10-Psec substituted pyrrolo[2,1-c][1,4]benzodiazepine prodrug. *Bioorg. Med. Chem. Lett.* **2002**, *12* (10), 1413-1416.

15. Best, T. P.; Edelson, B. S.; Nickols, N. G.; Dervan, P. B. Nuclear localization of pyrrole-imidazole polyamide-fluorescein conjugates in cell culture. *Proc. Natl. Acad. Sci. U. S. A* **2003**, *100* (21), 12063-12068.

16. Boger, D. L.; Fink, B. E.; Hedrick, M. P. Total synthesis of distamycin A and 2640 analogues: A solution-phase combinatorial approach to the discovery of new, bioactive DNA binding agents and development of a rapid, high-throughput screen for determining relative DNA binding affinity or DNA binding sequence selectivity. *Journal of the American Chemical Society* **2000**, *122* (27), 6382-6394.

17. bu-Daya, A.; Brown, P. M.; Fox, K. R. DNA sequence preferences of several AT-selective minor groove binding ligands. *Nucleic Acids Res.* **1995**, *23* (17), 3385-3392.

18. Buchmueller, K. L.; Staples, A. M.; Uthe, P. B.; Howard, C. M.; Pacheco, K. A.; Cox, K. K.; Henry, J. A.; Bailey, S. L.; Horick, S. M.; Nguyen, B.; Wilson, W. D.; Lee, M. Molecular recognition of DNA base pairs by the formamido/pyrrole and formamido/imidazole pairings in stacked polyamides. *Nucleic Acids Res.* **2005**, *33* (3), 912-921.

19. Buchmueller, K. L.; Staples, A. M.; Howard, C. M.; Horick, S. M.; Uthe, P. B.; Le, N. M.; Cox, K. K.; Nguyen, B.; Pacheco, K. A.; Wilson, W. D.; Lee, M. Extending the language of DNA molecular recognition by polyamides: unexpected influence of imidazole and pyrrole arrangement on binding affinity and specificity. *J. Am. Chem. Soc.* **2005**, *127* (2), 742-750.

20. Buchmueller, K. L.; Taherbhai, Z.; Howard, C. M.; Bailey, S. L.; Nguyen, B.; O'hare, C.; Hochhauser, D.; Hartley, J. A.; Wilson, W. D.; Lee, M. Design of a Hairpin Polyamide, ZT65B, for Targeting the Inverted CCAAT Box (ICB) Site in the Multidrug Resistant (MDR1) Gene. *Chembiochem.* **2005**, *6* (12), 2305-2311.

21. Chang, A. Y.; Dervan, P. B. Strand selective cleavage of DNA by diastereomers of hairpin polyamide- seco-CBI conjugates. *Journal of the American Chemical Society* **2000**, *122* (20), 4856-4864.

22. Cho, J.; Parks, M. E.; Dervan, P. B. Cyclic polyamides for recognition in the minor groove of DNA. *Proc. Natl. Acad. Sci. U. S. A* **1995**, *92* (22), 10389-10392.

23. Clayden; Greeves; Warren; Wothers *Organic Chemistry;* Oxford University Press: 2001.

24. Cools, J.; Maertens, C.; Marynen, P. Resistance to tyrosine kinase inhibitors: Calling on extra forces. *Drug Resist. Updat.* **2005**.

25. Cooper G. Tumor Suppressor Genes in Human Neoplasms. In *Oncogenes*, Second ed.; Cooper G., Ed.; Jones and Bartlett: 1995; pp 145-155.

26. Cooper, N.; Hagan, D. R.; Tiberghien, A.; Ademefun, T.; Matthews, C. S.; Howard, P. W.; Thurston, D. E. Synthesis of novel C2-aryl pyrrolobenzodiazepines (PBDs) as potential antitumour agents. *Chem. Commun. (Camb.)* **2002**, (16), 1764-1765.

27. Dervan, P. B.; Edelson, B. S. Recognition of the DNA minor groove by pyrrole-imidazole polyamides. *Curr. Opin. Struct. Biol.* **2003**, *13* (3), 284-299.

28. Deziel, R. Mild palladium (0)-catalysed deprotection of allyl esters. A useful application in the synthesis of carbapenems and other beta-lactam derivatives. *Tetrahedron Letters* **1987**, *28* (38), 4371-4372.

29. Dickinson, L. A.; Burnett, R.; Melander, C.; Edelson, B. S.; Arora, P. S.; Dervan, P. B.; Gottesfeld, J. M. Arresting cancer proliferation by small-molecule gene regulation. *Chem. Biol.* **2004**, *11* (11), 1583-1594.

30. Foister, S.; Marques, M. A.; Doss, R. M.; Dervan, P. B. Shape selective recognition of T.A base pairs by hairpin polyamides containing N-terminal 3-methoxy (and 3-chloro) thiophene residues. *Bioorg. Med. Chem.* **2003**, *11* (20), 4333-4340.

31. Foloppe, M. P.; Rault, S.; Thurston, D. E.; Jenkins, T. C.; Robba, M. DNA-binding properties of pyrrolo[2,1-c][1,4]-benzodiazepine N10-C11 amidines. *Eur. J. Med. Chem.* **1996**, *31*, 407-410.

32. Friday, B. B.; Adjei, A. A. K-ras as a target for cancer therapy. *Biochim. Biophys. Acta* **2005**, *1756* (2), 127-144.

33. Fukuyama, T.; Lin, S. C.; Li, L. P. Facile reduction of Ethyl Thiol Ester to Aldehydes - Application to a total synthesis of (+)-Neothramaycin-a Methyl ether. *J. Am. Chem. Soc.* **1990**, *112*, 7050-7051.

34. Goodsell, D.; Dickerson, R. E. Isohelical analysis of DNA groove-binding drugs. *J. Med. Chem.* **1986**, *29* (5), 727-733.

35. Greenberg, W. A.; Baird, E. E.; Dervan, P. B. A comparison of H-Pin and Hairpin Polyamide Motifs for the Recognition of the Minor Groove of DNA. 4 ed.; 1998; pp 796-805.

36. Gregson, S. J.; Howard, P. W.; Corcoran, K. E.; Barcella, S.; Yasin, M. M.; Hurst, A. A.; Jenkins, T. C.; Kelland, L. R.; Thurston, D. E. Effect of C2-exo unsaturation on the cytotoxicity and DNA-binding reactivity of pyrrolo[2,1-c][1,4]benzodiazepines. *Bioorg. Med. Chem. Lett.* **2000**, *10* (16), 1845-1847.

37. Gregson, S. J.; Howard, P. W.; Hartley, J. A.; Brooks, N. A.; Adams, L. J.; Jenkins, T. C.; Kelland, L. R.; Thurston, D. E. Design, synthesis, and evaluation of a novel pyrrolobenzodiazepine DNA-interactive agent with highly efficient cross-linking ability and potent cytotoxicity. *J. Med. Chem.* **2001**, *44* (5), 737-748.

38. Gregson, S. J.; Howard, P. W.; Corcoran, K. E.; Jenkins, T. C.; Kelland, L. R.; Thurston, D. E. Synthesis of the first example of a C2-C3/C2'-C3'-endo unsaturated pyrrolo[2,1-c][1,4]benzodiazepine dimer. *Bioorg. Med. Chem. Lett.* **2001**, *11* (21), 2859-2862.

39. Guiotto, A.; Howard, P. W.; Baraldi, P. G.; Thurston, D. E. Synthesis of novel C7-aryl substituted pyrrolo[2,1-c][1,4]benzodiazepines (PBDs) via pro-N10-Troc protection and Suzuki coupling. *Bioorg. Med. Chem. Lett.* **1998**, *8* (21), 3017-3018.

40. Hanahan, D.; Weinberg, R. A. The hallmarks of cancer. *Cell* **2000**, *100* (1), 57-70.

41. Hartley, J. A.; Souhami, R. L.; Berardini, M. D. Electrophoretic and chromatographic separation methods used to reveal interstrand crosslinking of nucleic acids. *J. Chromatogr.* **1993**, *618* (1-2), 277-288.

42. Hartley, J. A.; Spanswick, V. J.; Brooks, N.; Clingen, P. H.; McHugh, P. J.; Hochhauser, D.; Pedley, R. B.; Kelland, L. R.; Alley, M. C.; Schultz, R.; Hollingshead, M. G.; Schweikart, K. M.; Tomaszewski, J. E.; Sausville, E. A.; Gregson, S. J.; Howard, P. W.; Thurston, D. E. SJG-136 (NSC 694501), a novel rationally designed DNA minor groove interstrand cross-linking agent with potent and broad spectrum antitumor activity: part 1: cellular pharmacology, in vitro and initial in vivo antitumor activity. *Cancer Res.* **2004**, *64* (18), 6693-6699.

43. Hartley, J. M.; Spanswick, V. J.; Gander, M.; Giacomini, G.; Whelan, J.; Souhami, R. L.; Hartley, J. A. Measurement of DNA cross-linking in patients on ifosfamide therapy using the single cell gel electrophoresis (comet) assay. *Clin. Cancer Res.* **1999**, *5* (3), 507-512.

44. Heckel, A.; Dervan, P. B. U-pin polyamide motif for recognition of the DNA minor groove. *Chemistry.* **2003**, *9* (14), 3353-3366.

45. Herman, D. M.; Baird, E. E.; Dervan, P. B. Stereochemical control of the DNA binding affinity, sequence specificity, and orientation preference of chiral hairpin polyamides in the minor groove. *Journal of the American Chemical Society* **1998**, *120* (7), 1382-1391.

46. Herman, D. M.; Baird, E. E.; Dervan, P. B. Tandem Hairpin Motif for Recognition in the Minor Groove of DNA by Pyrrole-Imidazole Polyamides. 5 ed.; 1999; pp 975-983.

47. Herman, D. M.; Turner, J. M.; Baird, E. E.; Dervan, P. B. Cycle polyamide motif for recognition of the minor groove of DNA. *Journal of the American Chemical Society* **1999**, *121* (6), 1121-1129.

48. Hertzberg, R. P.; Hecht, S. M.; Reynolds, V. L.; Molineux, I. J.; Hurley, L. H. DNA sequence specificity of the pyrrolo[1,4]benzodiazepine antitumor antibiotics. Methidiumpropyl-EDTA-iron(II) footprinting analysis of DNA binding sites for anthramycin and related drugs. *Biochemistry* **1986**, *25* (6), 1249-1258.

49. Hurley, L. H.; Gairola, C.; Zmijewski, M. Pyrrolo(1,4)benzodiazepine antitumor antibiotics. In vitro interaction of anthramycin, sibiromycin and tomaymycin with DNA using specifically radiolabelled molecules. *Biochim. Biophys. Acta* **1977**, *475* (3), 521-535.

50. Hurley, L. H.; Allen, C. S.; Feola, J. M.; Lubawy, W. C. In vitro and in vivo stability of anthramycin-DNA conjugate and its potential application as an anthramycin prodrug. *Cancer Res.* **1979**, *39* (8), 3134-3140.

51. Hurley, L. H.; Reck, T.; Thurston, D. E.; Langley, D. R.; Holden, K. G.; Hertzberg, R. P.; Hoover, J. R.; Gallagher, G., Jr.; Faucette, L. F.; Mong, S. M.; . Pyrrolo[1,4]benzodiazepine antitumor antibiotics: relationship of DNA alkylation and sequence specificity to the biological activity of natural and synthetic compounds. *Chem. Res. Toxicol.* **1988**, *1* (5), 258-268.

52. Hurley, L. H.; Boyd, F. L. DNA as a target for drug action. *Trends Pharmacol. Sci.* **1988**, *9* (11), 402-407.

53. James, P. L.; Merkina, E. E.; Khalaf, A. I.; Suckling, C. J.; Waigh, R. D.; Brown, T.; Fox, K. R. DNA sequence recognition by an isopropyl substituted thiazole polyamide. *Nucleic Acids Res.* **2004**, *32* (11), 3410-3417.

54. Kamal, A.; Ramesh, G.; Laxman, N.; Ramulu, P.; Srinivas, O.; Neelima, K.; Kondapi, A. K.; Sreenu, V. B.; Nagarajaram, H. A. Design, synthesis, and evaluation of new noncross-linking pyrrolobenzodiazepine dimers with efficient DNA binding ability and potent antitumor activity. *J. Med. Chem.* **2002**, *45* (21), 4679-4688.

55. Kamal, A.; Ramesh, G.; Srinivas, O.; Ramulu, P.; Laxman, N.; Rehana, T.; Deepak, M.; Achary, M. S.; Nagarajaram, H. A. Design, synthesis, and evaluation of mixed imine-amine pyrrolobenzodiazepine dimers with efficient DNA binding affinity and potent cytotoxicity. *Bioorg. Med. Chem.* **2004**, *12* (20), 5427-5436.

56. Kaneko, T.; Wong, H.; Doyle, T. W.; Rose, W. C.; Bradner, W. T. Bicyclic and tricyclic analogues of anthramycin. *J. Med. Chem.* **1985**, *28* (3), 388-392.

57. Kers, I.; Dervan, P. B. Search for the optimal linker in tandem hairpin polyamides. *Bioorg. Med. Chem.* **2002**, *10* (10), 3339-3349.

58. Khalaf, A. I.; Waigh, R. D.; Drummond, A. J.; Pringle, B.; McGroarty, I.; Skellern, G. G.; Suckling, C. J. Distamycin analogues with enhanced lipophilicity: synthesis and antimicrobial activity. *J. Med. Chem.* **2004**, *47* (8), 2133-2156.

59. Kohn, K. W.; Bono, V. H., Jr.; Kann, H. E., Jr. Anthramycin, a new type of DNA-inhibiting antibiotic: reaction with DNA and effect on nucleic acid synthesis in mouse leukemia cells. *Biochim. Biophys. Acta* **1968**, *155* (1), 121-129.

60. Kohn, K. W.; Spears, C. L. Reaction of anthramycin with deoxyribonucleic acid. *J. Mol. Biol.* **1970**, *51* (3), 551-572.

61. Kopka, M. L.; Goodsell, D. S.; Baikalov, I.; Grzeskowiak, K.; Cascio, D.; Dickerson, R. E. Crystal structure of a covalent DNA-drug adduct: anthramycin bound to C-C-A-A-C-G-T-T-G-G and a molecular explanation of specificity. *Biochemistry* **1994**, *33* (46), 13593-13610.

62. Krutzik, P. O.; Chamberlin, A. R. Rapid solid-phase synthesis of DNA-binding pyrrole-imidazole polyamides. *Bioorg. Med. Chem. Lett.* **2002**, *12* (16), 2129-2132.

63. Kumar, R.; Lown, J. W. Recent developments in novel pyrrolo[2,1-c][1,4]benzodiazepine conjugates: synthesis and biological evaluation. *Mini. Rev. Med. Chem.* **2003**, *3* (4), 323-339.

64. Kumar, R.; Lown, J. W. Design, synthesis and in vitro cytotoxic studies of novel bis-pyrrolo[2,1][1,4] benzodiazepine-pyrrole and imidazole polyamide conjugates. *Eur. J. Med. Chem.* **2005**, *40* (7), 641-654.

65. Langlois, N.; Rojas-Rousseau, A.; Gaspard, C.; Werner, G. H.; Darro, F.; Kiss, R. Synthesis and cytotoxicity on sensitive and doxorubicin-resistant cell lines of new pyrrolo[2,1-c][1,4]benzodiazepines related to anthramycin. *J. Med. Chem.* **2001**, *44* (22), 3754-3757.

66. Lavesa, M.; Fox, K. R. Preferred binding sites for [N-MeCYs(3), N-MeCys(7)]TANDEM determined using a universal footprinting substrate. *Anal. Biochem.* **2001**, *293* (2), 246-250.

67. Leimgruber, W.; Stefanovic, V.; Schenker, F.; Karr, A.; Berger, J. Isolation and characterization of anthramycin, a new antitumor antibiotic. *J. Am. Chem. Soc.* **1965**, *87* (24), 5791-5793.

68. Leimgruber, W.; Batcho, A. D.; Schenker, F. The structure of anthramycin. *J. Am. Chem. Soc.* **1965**, *87* (24), 5793-5795.

69. Martin, C.; Ellis, T.; McGurk, C. J.; Jenkins, T. C.; Hartley, J. A.; Waring, M. J.; Thurston, D. E. Sequence-selective interaction of the minor-groove interstrand cross-linking agent SJG-136 with naked and cellular DNA: footprinting and enzyme inhibition studies. *Biochemistry* **2005**, *44* (11), 4135-4147.

70. Masterson, L. A.; Spanswick, V. J.; Hartley, J. A.; Begent, R. H.; Howard, P. W.; Thurston, D. E. Synthesis and biological evaluation of novel pyrrolo[2,1-c][1,4]benzodiazepine prodrugs for use in antibody-directed enzyme prodrug therapy. *Bioorg. Med. Chem. Lett.* **2006**, *16* (2), 252-256.

71. McHugh, P. J.; Spanswick, V. J.; Hartley, J. A. Repair of DNA interstrand crosslinks: molecular mechanisms and clinical relevance. *Lancet Oncol.* **2001**, *2* (8), 483-490.

72. Melander, C.; Herman, D. M.; Dervan, P. B. Discrimination of A/T sequences in the minor groove of DNA within a cyclic polyamide motif. *Chemistry.* **2000**, *6* (24), 4487-4497.

73. Melander, C.; Burnett, R.; Gottesfeld, J. M. Regulation of gene expression with pyrrole-imidazole polyamides. *J. Biotechnol.* **2004**, *112* (1-2), 195-220.

74. Mico, A.; Margarita R; Parlanti L; Vescovi A; Piancatelli G TEMPO / BAIB oxidation of alcohols to carbonyl compounds. 62 ed.; 1997; pp 6974-6977.

75. Morris, S. J.; Thurston, D. E.; Nevell, T. G. Evaluation of the electrophilicity of DNA-binding pyrrolo[2,1-c][1,4]benzodiazepines by HPLC. *J. Antibiot. (Tokyo)* **1990**, *43* (10), 1286-1292.

76. Mrksich, M.; Parks, M. E.; Dervan, P. B. Hairpin peptide motif. A new class of oligopeptides for sequence-specific recognition in the minor groove of double-helical DNA. *Journal of the American Chemical Society* **1994**, *116* (18), 7983-7988.

77. Neidle, S.; Puvvada, M. S.; Thurston, D. E. The relevance of drug DNA sequence specificity to anti-tumour activity. *Eur. J. Cancer* **1994**, *30A* (4), 567-568.

78. Neidle, S. DNA minor-groove recognition by small molecules. *Nat. Prod. Rep.* **2001**, *18* (3), 291-309.

79. Nguyen, D. H.; Szewczyk, J. W.; Baird, E. E.; Dervan, P. B. Alternative heterocycles for DNA recognition: an N-methylpyrazole/N-methylpyrrole pair specifies for A.T/T.A base pairs. *Bioorg. Med. Chem.* **2001**, *9* (1), 7-17.

80. Nishiwaki, E.; Tanaka, S.; Lee, H.; Shibuya, M. Efficient Synthesis of Oligo-N-methylpyrrolecarboxamides and Related Compounds. 27 ed.; 1988; pp 1945-1952.

81. Olenyuk, B.; Jitianu, C.; Dervan, P. B. Parallel synthesis of H-pin polyamides by alkene metathesis on solid phase. *J. Am. Chem. Soc.* **2003**, *125* (16), 4741-4751.

302

82. Pelton, J. G.; Wemmer, D. E. Structural characterization of a 2:1 distamycin A.d(CGCAAATTGGC) complex by two-dimensional NMR. *Proc. Natl. Acad. Sci. U. S. A* **1989**, *86* (15), 5723-5727.

83. Petrusek, R. L.; Uhlenhopp, E. L.; Duteau, N.; Hurley, L. H. Reaction of anthramycin with DNA. Biological consequences of DNA damage in normal and xeroderma pigmentosum cell. *J. Biol. Chem.* **1982**, *257* (11), 6207-6216.

84. Pierce, J. R.; Nazimiec, M.; Tang, M. S. Comparison of sequence preference of tomaymycin- and anthramycin-DNA bonding by exonuclease III and lambda exonuclease digestion and UvrABC nuclease incision analysis. *Biochemistry* **1993**, *32* (28), 7069-7078.

85. Renneberg, D.; Dervan, P. B. Imidazopyridine/Pyrrole and hydroxybenzimidazole/pyrrole pairs for DNA minor groove recognition. *J. Am. Chem. Soc.* **2003**, *125* (19), 5707-5716.

86. Sagnou, M. J.; Howard, P. W.; Gregson, S. J.; Eno-Amooquaye, E.; Burke, P. J.; Thurston, D. E. Design and synthesis of novel pyrrolobenzodiazepine (PBD) prodrugs for ADEPT and GDEPT. *Bioorg. Med. Chem. Lett.* **2000**, *10* (18), 2083-2086.

87. Shinohara, K.; Narita, A.; Oyoshi, T.; Bando, T.; Teraoka, H.; Sugiyama, H. Sequence-specific gene silencing in mammalian cells by alkylating pyrrole-imidazole polyamides. *J. Am. Chem. Soc.* **2004**, *126* (16), 5113-5118.

88. Smellie, M.; Bose, D. S.; Thompson, A. S.; Jenkins, T. C.; Hartley, J. A.; Thurston, D. E. Sequence-selective recognition of duplex DNA through covalent interstrand cross-linking: kinetic and molecular modeling studies with pyrrolobenzodiazepine dimers. *Biochemistry* **2003**, *42* (27), 8232-8239.

89. Stratton Molecular Biology for Oncologist. second ed.; Yarnold, Stratton, McMillan, Eds.; Chapman and Hall: 1996; pp 16-26.

90. Swalley, S. E.; Baird, E. E.; Dervan, P. B. Effects of [gamma]-turn and [beta]-tail amino acids on sequence-specific recognition of DNA by hairpin polyamides. *Journal of the American Chemical Society* **1999**, *121* (6), 1113-1120.

91. Tercel, M.; Stribbling, S. M.; Sheppard, H.; Siim, B. G.; Wu, K.; Pullen, S. M.; Botting, K. J.; Wilson, W. R.; Denny, W. A. Unsymmetrical DNA cross-linking agents: combination of the CBI and PBD pharmacophores. *J. Med. Chem.* **2003**, *46* (11), 2132-2151.

92. Thurston, D. E.; Hurley, L. H. A Rational Basis for Development of Antitumor Agents in the Pyrrolo[1,4]Benzodiazepine group. *Drugs of the future* **1983**, *8* (11), 957-971.

93. Thurston, D. E.; Langley, D. R. Synthesis and Stereochemistry of Carbinolamine-Containing Pyrrolo[1,4]benzodiazepines by Reductive Cyclisation of *N*-(2-Nitrobenzoyl)pyrrolidine-2-carboxaldehydes. *J. Org. Chem.* **1986**, *51* (705), 705-712.

94. Thurston, D. E. Nucleic acid targeting: therapeutic strategies for the 21st century. *Br. J. Cancer* **1999**, *80 Suppl 1*, 65-85.

95. Thurston, D. E.; Bose, D. S.; Howard, P. W.; Jenkins, T. C.; Leoni, A.; Baraldi, P. G.; Guiotto, A.; Cacciari, B.; Kelland, L. R.; Foloppe, M. P.; Rault, S. Effect of A-ring modifications on the DNA-binding behavior and cytotoxicity of pyrrolo[2,1-c][1,4]benzodiazepines. *J. Med. Chem.* **1999**, *42* (11), 1951-1964.

96. Tiberghien, A. C.; Hagan, D.; Howard, P. W.; Thurston, D. E. Application of the Stille coupling reaction to the synthesis of C2-substituted endo-exo unsaturated pyrrolo[2,1-c][1,4]benzodiazepines (PBDs). *Bioorg. Med. Chem. Lett.* **2004**, *14* (20), 5041-5044.

97. Turner, J. M.; Swalley, S. E.; Baird, E. E.; Dervan, P. B. Aliphatic/aromatic amino acid pairings for polyamide recognition in the minor groove of DNA. *Journal of the American Chemical Society* **1998**, *120* (25), 6219-6226.

98. Ueda, Y.; Kagitani, Y.; Sako, E.; Suyama, T.; Komatsu, N.; Satoh, D. Benzodiazepines, processes for producing them and compositions containing them. UK GB2053894A, 1979.

99. Urbach, A. R.; Szewczyk, J. W.; White, S.; Turner, J. M.; Baird, E. E.; Dervan, P. B. Sequence selectivity of 3-hydroxypyrrole/pyrrole ring pairings in the DNA minor groove. *Journal of the American Chemical Society* **1999**, *121* (50), 11621-11629.

100. Wang, Y. D.; Dziegielewski, J.; Wurtz, N. R.; Dziegielewska, B.; Dervan, P. B.; Beerman, T. A. DNA crosslinking and biological activity of a hairpin polyamide-chlorambucil conjugate. *Nucleic Acids Res.* **2003**, *31* (4), 1208-1215.

101. Wells, G.; Martin, C. R.; Howard, P. W.; Sands, Z. A.; Laughton, C. A.; Tiberghien, A.; Woo, C. K.; Masterson, L. A.; Stephenson, M. J.; Hartley, J. A.; Jenkins, T. C.; Shnyder, S. D.; Loadman, P. M.; Waring, M. J.; Thurston, D. E. Design, Synthesis, and Biophysical and Biological Evaluation of a Series of Pyrrolobenzodiazepine-Poly(N-methylpyrrole) Conjugates. *J. Med. Chem.* **2006**, *49* (18), 5442-5461.

102. White, S.; Szewczyk, J. W.; Turner, J. M.; Baird, E. E.; Dervan, P. B. Recognition of the four Watson-Crick base pairs in the DNA minor groove by synthetic ligands. *Nature* **1998**, *391* (6666), 468-471.

103. Wilkinson, G. P.; Taylor, J. P.; Shnyder, S.; Cooper, P.; Howard, P. W.; Thurston, D. E.; Jenkins, T. C.; Loadman, P. M. Preliminary pharmacokinetic and bioanalytical studies of SJG-136 (NSC 694501), a sequence-selective pyrrolobenzodiazepine dimer DNA-cross-linking agent. *Invest New Drugs* **2004**, *22* (3), 231-240.

104. Wurtz, N. R.; Dervan, P. B. Sequence specific alkylation of DNA by hairpin pyrrole-imidazole polyamide conjugates. *Chem. Biol.* **2000**, *7* (3), 153-161.

105. Xiao, J.; Yuan, G.; Huang, W.; Chan, A. S.; Lee, K. L. A convenient method for the synthesis of DNA-recognizing polyamides in solution. *J. Org. Chem.* **2000**, *65* (18), 5506-5513.

Additional relevant references

1. Bando, T.; Iida, H.; Saito, I.; Sugiyama, H. Sequence-specific DNA interstrand cross-linking by imidazole--pyrrole CPI conjugate. *J. Am. Chem. Soc.* **2001**, *123* (21), 5158-5159.

2. Bando, T.; Iida, H.; Tao, Z. F.; Narita, A.; Fukuda, N.; Yamori, T.; Sugiyama, H. Sequence specificity, reactivity, and antitumor activity of DNA-alkylating pyrrole-imidazole diamides. *Chem. Biol.* **2003**, *10* (8), 751-758.

3. Baraldi, P. G.; Balboni, G.; Romagnoli, R.; Spalluto, G.; Cozzi, P.; Geroni, C.; Mongelli, N.; Rutigliano, C.; Bianchi, N.; Gambari, R. PNU 157977: a new potent antitumour agent exhibiting low in vivo toxicity in mice injected with L1210 leukaemia cells. *Anticancer Drug Des* **1999**, *14* (1), 71-76.

4. Beria, I.; Baraldi, P. G.; Cozzi, P.; Caldarelli, M.; Geroni, C.; Marchini, S.; Mongelli, N.; Romagnoli, R. Cytotoxic alpha-halogenoacrylic derivatives of distamycin A and congeners. *J. Med. Chem.* **2004**, *47* (10), 2611-2623.

5. Boger, D. L.; Dechantsreiter, M. A.; Ishii, T.; Fink, B. E.; Hedrick, M. P. Assessment of solution-phase positional scanning libraries based on distamycin A for the discovery of new DNA binding agents. *Bioorg. Med. Chem.* **2000**, *8* (8), 2049-2057.

6. Boger, D. L.; Tse, W. C. Thiazole orange as the fluorescent intercalator in a high resolution fid assay for determining DNA binding affinity and sequence selectivity of small molecules. *Bioorg. Med. Chem.* **2001**, *9* (9), 2511-2518.

7. Bremer, R. E.; Szewczyk, J. W.; Baird, E. E.; Dervan, P. B. Recognition of the DNA minor groove by pyrrole-imidazole polyamides: comparison of desmethyl- and N-methylpyrrole. *Bioorg. Med. Chem.* **2000**, *8* (8), 1947-1955.

8. Briehn, C. A.; Weyermann, P.; Dervan, P. B. Alternative heterocycles for DNA recognition: the benzimidazole/imidazole pair. *Chemistry.* **2003**, *9* (9), 2110-2122.

9. Cheng, S.; Tarby, C. M.; Comer, D. D.; Williams, J. P.; Caporale, L. H.; Myers, P. L.; Boger, D. L. A solution-phase strategy for the synthesis of chemical libraries containing small organic molecules: a universal and dipeptide mimetic template. *Bioorg. Med. Chem.* **1996**, *4* (5), 727-737.

10. Cheung, A.; Struble, E.; He, J.; Yang, C.; Wang, E.; Thurston, D. E.; Liu, P. Direct liquid chromatography determination of the reactive imine SJG-136 (NSC 694501). *J. Chromatogr. B Analyt. Technol. Biomed. Life Sci.* **2005**, *822* (1-2), 10-20.

11. Cozzi, P.; Mongelli, N. Cytotoxics derived from distamycin A and congeners. *Curr. Pharm. Des* **1998**, *4* (3), 181-201.

12. Cozzi, P. A new class of cytotoxic DNA minor groove binders: alpha-halogenoacrylic derivatives of pyrrolecarbamoyl oligomers. *Farmaco* **2001**, *56* (1-2), 57-65.

13. Dervan, P. B. Design of sequence-specific DNA-binding molecules. *Science* **1986**, *232* (4749), 464-471.

14. Dervan, P. B. Molecular recognition of DNA by small molecules. *Bioorg. Med. Chem.* **2001**, *9* (9), 2215-2235.

15. Dervan, P. B.; Doss, R. M.; Marques, M. A. Programmable DNA binding oligomers for control of transcription. *Curr. Med. Chem. Anti. -Canc. Agents* **2005**, *5* (4), 373-387.

16. Dudouet, B.; Burnett, R.; Dickinson, L. A.; Wood, M. R.; Melander, C.; Belitsky, J. M.; Edelson, B.; Wurtz, N.; Briehn, C.; Dervan, P. B.; Gottesfeld, J. M. Accessibility of nuclear chromatin by DNA binding polyamides. *Chem. Biol.* **2003**, *10* (9), 859-867.

17. Gregson, S. J.; Howard, P. W.; Thurston, D. E. Synthesis of the first examples of A-C8/C-C2 amide-Linked pyrrolo[2,1-c][1,4]benzodiazepine dimers. *Bioorg. Med. Chem. Lett.* **2003**, *13* (14), 2277-2280.

18. Grehn, L.; Ragnarsson, U.; Eriksson, B.; Oberg, B. Synthesis and antiviral activity of distamycin A analogues: substitutions on the different pyrrole nitrogens and in the amidine function. *J. Med. Chem.* **1983**, *26* (7), 1042-1049.

19. Grehn, L.; Ragnarsson, U.; Datema, R. Structure-activity relationships in distamycin A analogues: effect of alkyl groups on the pyrrole nitrogen at the non-amidine end of the molecule combined with methyl elimination in the following ring. *Acta Chem. Scand. B* **1986**, *40* (2), 145-151.

20. Guerra, J. NHC Rhutenium Complexes as Second Generation Grubbs Catalysts. 3 ed.; 2003; pp 423-424.

21. Guichard, S. M.; Macpherson, J. S.; Thurston, D. E.; Jodrell, D. I. Influence of P-glycoprotein expression on in vitro cytotoxicity and in vivo antitumour activity of the novel pyrrolobenzodiazepine dimer SJG-136. *Eur. J. Cancer* **2005**, *41* (12), 1811-1818.

22. Halby, L.; Ryabinin, V. A.; Sinyakov, A. N.; Boutorine, A. S. Functionalized head-to-head hairpin polyamides: Synthesis, double-stranded DNA-binding activity and affinity. *Bioorg. Med. Chem. Lett.* **2005**, *15* (16), 3720-3724.

23. Ham, Y. W.; Boger, D. L. A powerful selection assay for mixture libraries of DNA alkylating agents. *J. Am. Chem. Soc.* **2004**, *126* (30), 9194-9195.

24. Jaramillo, D.; Liu, Q.; drich-Wright, J.; Tor, Y. Synthesis of N-methylpyrrole and N-methylimidazole amino acids suitable for solid-phase synthesis. *J. Org. Chem.* **2004**, *69* (23), 8151-8153.

25. Jones, G. B.; Davey, C. L.; Jenkins, T. C.; Kamal, A.; Kneale, G. G.; Neidle, S.; Webster, G. D.; Thurston, D. E. The non-covalent interaction of pyrrolo[2, 1-c] [1, 4]benzodiazepine-5, 11-diones with DNA. *Anticancer Drug Des* **1990**, *5* (3), 249-264.

26. Kang, G. D.; Howard, P. W.; Thurston, D. E. Synthesis of a novel C2-aryl substituted 1,2-unsaturated pyrrolobenzodiazepine. *Chem. Commun. (Camb.)* **2003**, (14), 1688-1689.

27. Kelly, J. J.; Baird, E. E.; Dervan, P. B. Binding site size limit of the 2:1 pyrrole-imidazole polyamide-DNA motif. *Proc. Natl. Acad. Sci. U. S. A* **1996**, *93* (14), 6981-6985.

28. Kumar, D.; Veldhuyzen, W. F.; Zhou, Q.; Rokita, S. E. Conjugation of a hairpin pyrrole-imidazole polyamide to a quinone methide for control of DNA cross-linking. *Bioconjug. Chem.* **2004**, *15* (4), 915-922.

29. Kumar, R.; Lown, J. W. Design, synthesis and in vitro cytotoxicity studies of novel pyrrolo [2,1][1,4] benzodiazepine-glycosylated pyrrole and imidazole polyamide conjugates. *Org. Biomol. Chem.* **2003**, *1* (19), 3327-3342.

30. Marchini, S.; Cozzi, P.; Beria, I.; Geroni, C.; Capolongo, L.; D'Incalci, M.; Broggini, M. Sequence-specific DNA alkylation of novel tallimustine derivatives. *Anticancer Drug Des* **1998**, *13* (3), 193-205.

31. Marques, M. A.; Doss, R. M.; Urbach, A. R.; Dervan, P. B. Toward an Understanding of the Chemical Etiology for DNA Minor-Groove Recognition by Polyamides. 85 ed.; 2002; pp 4485-4517.

32. Masterson, L. A.; Croker, S. J.; Jenkins, T. C.; Howard, P. W.; Thurston, D. E. Synthesis and biological evaluation of pyrrolo[2,1-c][1,4]benzodiazepine (PBD) C8 cyclic amine conjugates. *Bioorg. Med. Chem. Lett.* **2004**, *14* (4), 901-904.

33. Mongin, F.; Trecourt, F.; Gervais, B.; Mongin, O.; Queguiner, G. First synthesis of caerulomycin B. A new synthesis of caerulomycin C. *J. Org. Chem.* **2002**, *67* (10), 3272-3276.

34. Oyoshi, T.; Kawakami, W.; Narita, A.; Bando, T.; Sugiyama, H. Inhibition of transcription at a coding sequence by alkylating polyamide. *J. Am. Chem. Soc.* **2003**, *125* (16), 4752-4754.

35. Poulin-Kerstien, A. T.; Dervan, P. B. DNA-templated dimerization of hairpin polyamides. *J. Am. Chem. Soc.* **2003**, *125* (51), 15811-15821.

36. Reddy, P. M.; Dexter, R.; Bruice, T. C. DNA sequence recognition in the minor groove by hairpin pyrrole polyamide-Hoechst 33258 analogue conjugate. *Bioorg. Med. Chem. Lett.* **2004**, *14* (14), 3803-3807.

37. Rucker, V. C.; Foister, S.; Melander, C.; Dervan, P. B. Sequence specific fluorescence detection of double strand DNA. *J. Am. Chem. Soc.* **2003**, *125* (5), 1195-1202.

38. Sharma, S. K.; Tandon, M.; Lown, J. W. A general solution- and solid-phase synthetic procedure for incorporating three contiguous imidazole moieties into DNA sequence reading polyamides. *J. Org. Chem.* **2001**, *66* (3), 1030-1034.

39. Thurston, D. E. Advances in the Study of Pyrrolo[2,1-c][1,4]benzodiazepine (PBD) Antitumour Antibiotics. In *Molecular Aspects of Anticancer Drugs-DNA interactions*, Neidle, S., Waring, M. J., Eds.; McMillan: 1993; pp 54-88.

40. Toth, J. L.; Price, C. A.; Madsen, E. C.; Handl, H. L.; Hudson, S. J.; Hubbard, R. B., III; Bowen, J. P.; Kiakos, K.; Hartley, J. A.; Lee, M. Sequence selective recognition of DNA by hairpin conjugates of a racemic seco-cyclopropaneindoline-2-benzofurancarboxamide and polyamides. *Bioorg. Med. Chem. Lett.* **2002**, *12* (16), 2245-2248.

41. Trauger, J. W.; Baird, E. E.; Dervan, P. B. Extended hairpin polyamide motif for sequence-specific recognition in the minor groove of DNA. *Chem. Biol.* **1996**, *3* (5), 369-377.

42. Tse, W. C.; Ishii, T.; Boger, D. L. Comprehensive high-resolution analysis of hairpin polyamides utilizing a fluorescent intercalator displacement (FID) assay. *Bioorg. Med. Chem.* **2003**, *11* (20), 4479-4486.

43. Wang, C. C.; Ellervik, U.; Dervan, P. B. Expanding the recognition of the minor groove of DNA by incorporation of beta-alanine in hairpin polyamides. *Bioorg. Med. Chem.* **2001**, *9* (3), 653-657.

44. Weyermann, P.; Dervan, P. B. Recognition of ten base pairs of DNA by head-to-head hairpin dimers. *J. Am. Chem. Soc.* **2002**, *124* (24), 6872-6878.

45. White, S.; Baird, E. E.; Dervan, P. B. On the pairing rules for recognition in the minor groove of DNA by pyrrole-imidazole polyamides. *Chem. Biol.* **1997**, *4* (8), 569-578.

46. Woods, C. R.; Ishii, T.; Wu, B.; Bair, K. W.; Boger, D. L. Hairpin versus extended DNA binding of a substituted beta-alanine linked polyamide. *J. Am. Chem. Soc.* **2002**, *124* (10), 2148-2152.

47. Woods, C. R.; Faucher, N.; Eschgfaller, B.; Bair, K. W.; Boger, D. L. Synthesis and DNA binding properties of saturated distamycin analogues. *Bioorg. Med. Chem. Lett.* **2002**, *12* (18), 2647-2650.

48. Woods, C. R.; Ishii, T.; Boger, D. L. Synthesis and DNA binding properties of iminodiacetic acid-linked polyamides: characterization of cooperative extended 2:1 side-by-side parallel binding. *J. Am. Chem. Soc.* **2002**, *124* (36), 10676-10682.

49. Wurtz, N. R.; Turner, J. M.; Baird, E. E.; Dervan, P. B. Fmoc solid phase synthesis of polyamides containing pyrrole and imidazole amino acids. *Org. Lett.* **2001**, *3* (8), 1201-1203.

50. Yamamoto, K.; Biswas, K.; Gaul, C.; Danishefsky, S. J. Effects of temperature and concentration in some ring closing metathesis reactions. 44 ed.; 2003; pp 3297-3299.

51. Zhang, Q.; Dwyer, T. J.; Tsui, V.; Case, D. A.; Cho, J.; Dervan, P. B.; Wemmer, D. E. NMR structure of a cyclic polyamide-DNA complex. *J. Am. Chem. Soc.* **2004**, *126* (25), 7958-7966.

52. Zhilina, Z. V.; Ziemba, A. J.; Trent, J. O.; Reed, M. W.; Gorn, V.; Zhou, Q.; Duan, W.; Hurley, L.; Ebbinghaus, S. W. Synthesis and evaluation of a triplex-forming oligonucleotide-pyrrolobenzodiazepine conjugate. *Bioconjug. Chem.* **2004**, *15* (6), 1182-1192.

53. Zhou, Q.; Duan, W.; Simmons, D.; Shayo, Y.; Raymond, M. A.; Dorr, R. T.; Hurley, L. H. Design and synthesis of a novel DNA-DNA interstrand adenine-guanine cross-linking agent. *J. Am. Chem. Soc.* **2001**, *123* (20), 4865-4866.

Appendix A. Bisulphite adducts

Targeting long sequences of DNA entails the use of relatively large molecules. Most of the molecules described in the previous chapter (PBD-polyheterocycles conjugates) possess molecular weights superior to 1000 g/mol. The polyheterocyclic moiety is largely hydrophobic, thus contributing to a major loss of solubility in aqueous systems. This poor solubility causes difficulties when evaluating these molecules in early development stages (*in vitro testing*), and will cause administration problems at latter stages (*in vivo*).

There is therefore a strong impetus for conferring these molecules enhanced water-solubility. Of course, including a tertiary amino tail to the heterocyclic polyamide would address this question effectively, as proved by Peter Dervan's designs. It would mean, however, completely redesigning the synthetic route. Additionally, this strategy is not applicable to PBD polyheterocyclic dimers without major alteration to their designs.

A very attractive alternative solution to this problem, would be to exploit the PBD propensity to form water-soluble bisulphites adducts. (Chapter 2). These adducts are known to be stable and can be lyophilised. Moreover, this strategy has the potential of being applicable to any PBD-conjugates, in just one additional step at the end of the synthesis.

To confirm this hypothesis, two PBD-hairpin polyamide conjugates and one PBD-polyheterocyclic dimer were treated with sodium bisulphite (**Figure 1**).
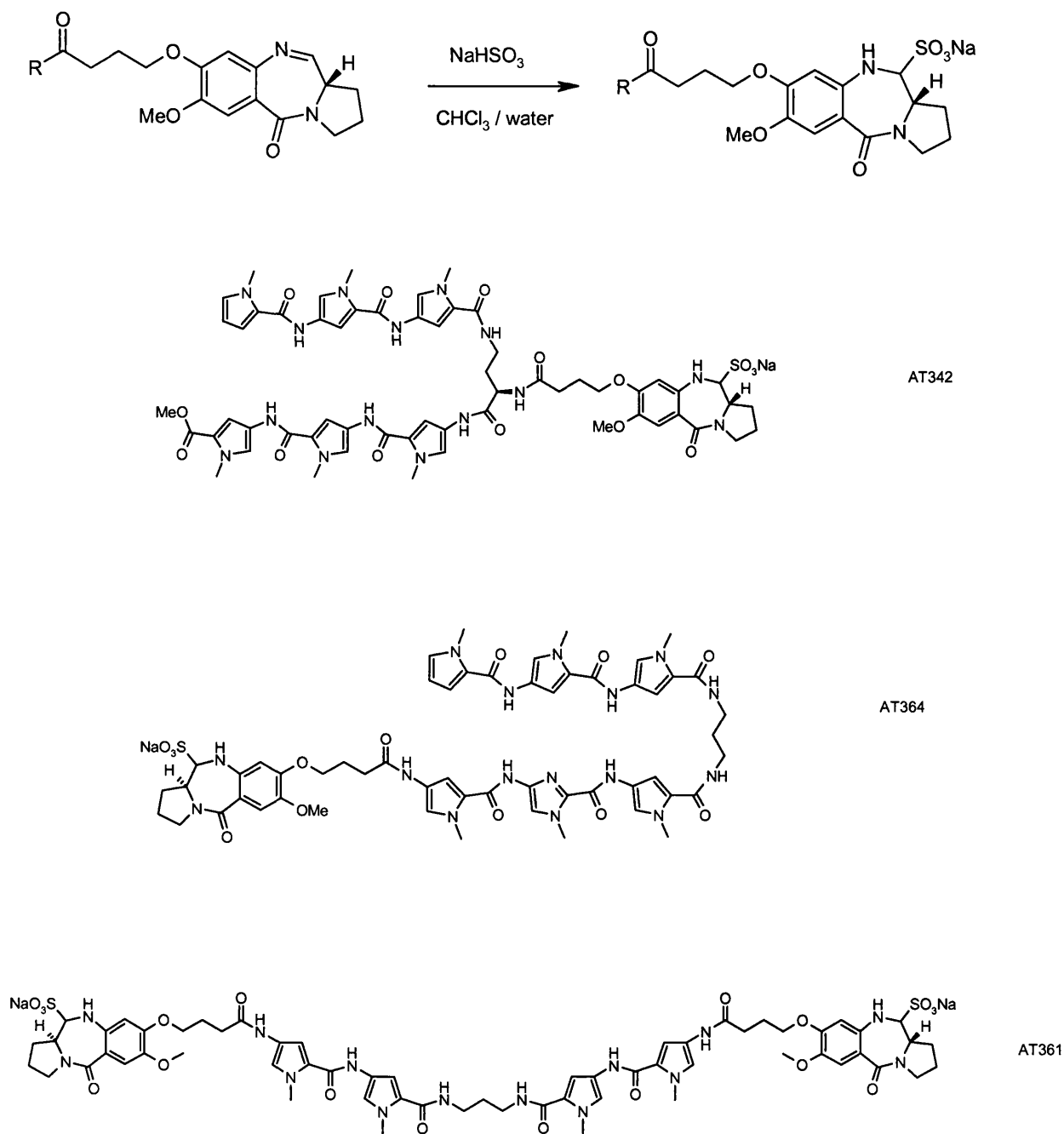
Figure 1: Bisulphite adducts of PBD-polyheterocycle conjugates.

Typically, the PBD-polyheterocyclic conjugates were dissolved in chloroform, followed by overnight stirring with an equivalent aqueous solution of sodium bisulphite. The two
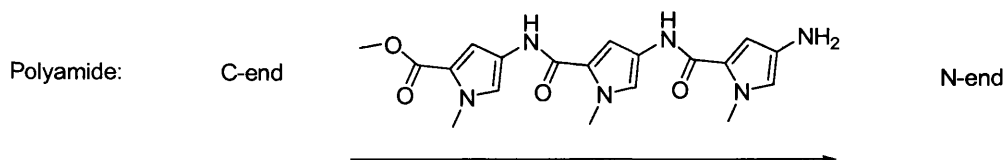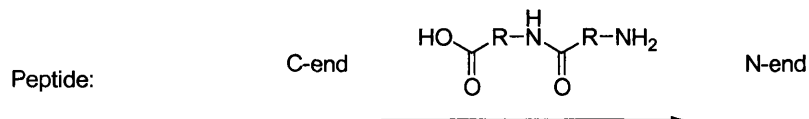
layers were then separated, the organic phase and the organic impurities were discarded, The bisulphite adducts were retrieved by lyophilisation of the aqueous phase.

This method successfully provided adducts of high purity as proved by proton NMR. However, some difficulties were encountered when applying this method to some conjugates of high molecular weight where the lipophilic properties of the polyheterocyclic moiety equalled the hydrophilic properties of the bisulfite adducts. These compounds were found readily prone to form intractable emulsions, preventing a clean separation and isolation of the product. For these conjugates, a monophasic system such as THF, or THF/water will be further investigated.
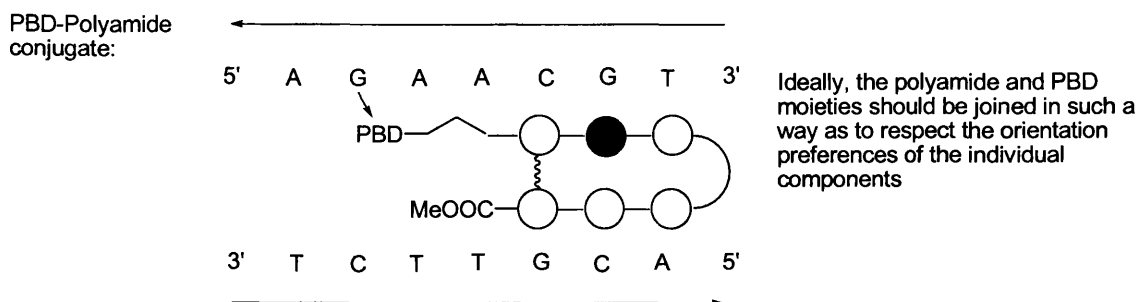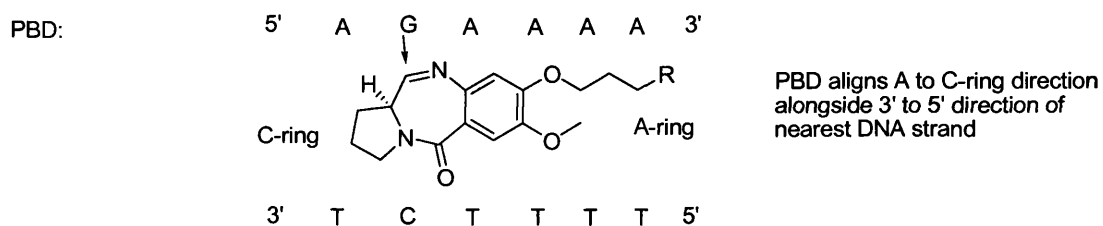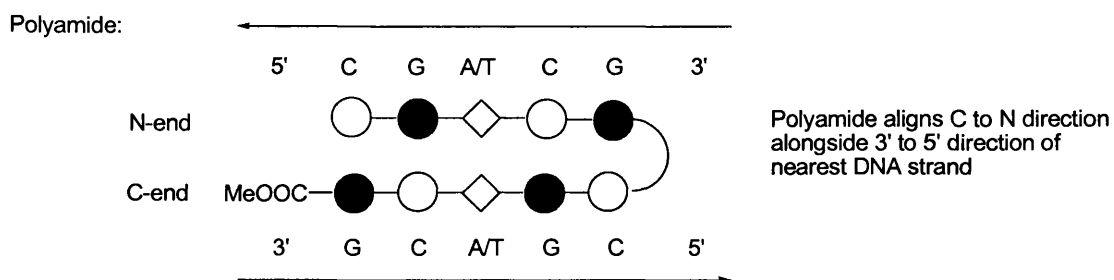
The three bisulphites adducts, AT342, AT361 and AT364 were submitted to biological evaluation alongside their parents compounds. Results are discussed in chapter 8 and 9.

Appendix B: Prefered orientation of polyamides and PBDs

N-end and C-end definition

Peptide: C-end   [chemical structure: HO–C(=O)–R–N(H)–C(=O)–R–NH2]   N-end

Polyamide: C-end   [chemical structure of tri-pyrrole polyamide with MeO ester C-end and NH2 N-end]   N-end

Orientation on DNA

Polyamide:

```
        5'   C    G   A/T   C    G    3'
N-end        ○----●----◇----○----●
C-end  MeOOC-●----○----◇----●----○
        3'   G    C   A/T   G    C    5'
```

Polyamide aligns C to N direction alongside 3' to 5' direction of nearest DNA strand

PBD:

```
        5'   A    G    A    A    A    A    3'
```

[PBD chemical structure with C-ring and A-ring labeled, R substituent]

```
        3'   T    C    T    T    T    T    5'
```

PBD aligns A to C-ring direction alongside 3' to 5' direction of nearest DNA strand

PBD-Polyamide conjugate:

```
        5'   A    G    A    A    C    G    T    3'
             PBD----○----●----○
           MeOOC----○----○----○
        3'   T    C    T    T    G    C    A    5'
```

Ideally, the polyamide and PBD moieties should be joined in such a way as to respect the orientation preferences of the individual components

310

Appendix C: Solid Phase versus Solution Phase chemistry: Advantages and drawbacks.

Peter Dervan's team shifted from solution phase to solid supported chemistry in the 90's. This move is generally described as a significant progress in many of their publications. It was therefore quite natural to consider solid phase chemistry as part of the strategy to synthesise the targets. A careful assessment of the benefits and drawbacks associated with the two sets of methods was conducted.

Solid Supported Chemistry:

Advantages: - Amenable to robotisation and consequently, very fast once optimised.
(days).

          - Direct synthesis from building blocks to final compounds.

Drawbacks: - Require multi-equivalent quantities of building blocks (*i.e.* wasteful)

          - Force a derivatisation on one end of the polyamide, at the point of cleavage from the solid support. (*i.e.* diaminopropane tail in Dervan's design, which does not participate in DNA recognition).

          - Require an analytical and preparative LC/MS equipment.

          - Generate limited quantities of end-material (max : 5 mg). It is generally not sufficient for *in-vivo* or extensive *in-vitro* studies.

          - Monitoring difficulties render the optimisation phase particularly arduous.

Solution phase chemistry:

Advantages: - Alleviate most of the problems encountered on solid phase (equivalence, reaction efficiency, real time monitoring, purification by normal phase chromatography, facile implementation, does not force the introduction of a derivatisation tail through a cleavage step, can generate large quantities of target compounds (100 mg).

- Allows more freedom in the choice of the design, and a faster implementation. This in turn allows the studies of a range of designs.

Drawbacks: - Time-consuming (weeks to months).
                 - Less easily amenable to robotisation.

Based on these considerations and the equipment level of the laboratories at initiation of the project, it was decided to work with solution phase chemistry. This would allow the studies of a variety of design relatively rapidly. In the future, the best designs could be adapted to solid supported chemistry for fast generation of small libraries.